

Severe acute respiratory syndrome coronavirus 2: Host-pathogen interactions and cellular signaling - vol II

Edited by

Vikas Sood and Clement Adebajo Meseko

Published in

Frontiers in Cellular and Infection Microbiology



FRONTIERS EBOOK COPYRIGHT STATEMENT

The copyright in the text of individual articles in this ebook is the property of their respective authors or their respective institutions or funders. The copyright in graphics and images within each article may be subject to copyright of other parties. In both cases this is subject to a license granted to Frontiers.

The compilation of articles constituting this ebook is the property of Frontiers.

Each article within this ebook, and the ebook itself, are published under the most recent version of the Creative Commons CC-BY licence. The version current at the date of publication of this ebook is CC-BY 4.0. If the CC-BY licence is updated, the licence granted by Frontiers is automatically updated to the new version.

When exercising any right under the CC-BY licence, Frontiers must be attributed as the original publisher of the article or ebook, as applicable.

Authors have the responsibility of ensuring that any graphics or other materials which are the property of others may be included in the CC-BY licence, but this should be checked before relying on the CC-BY licence to reproduce those materials. Any copyright notices relating to those materials must be complied with.

Copyright and source acknowledgement notices may not be removed and must be displayed in any copy, derivative work or partial copy which includes the elements in question.

All copyright, and all rights therein, are protected by national and international copyright laws. The above represents a summary only. For further information please read Frontiers' Conditions for Website Use and Copyright Statement, and the applicable CC-BY licence.

ISSN 1664-8714
ISBN 978-2-83251-739-0
DOI 10.3389/978-2-83251-739-0

About Frontiers

Frontiers is more than just an open access publisher of scholarly articles: it is a pioneering approach to the world of academia, radically improving the way scholarly research is managed. The grand vision of Frontiers is a world where all people have an equal opportunity to seek, share and generate knowledge. Frontiers provides immediate and permanent online open access to all its publications, but this alone is not enough to realize our grand goals.

Frontiers journal series

The Frontiers journal series is a multi-tier and interdisciplinary set of open-access, online journals, promising a paradigm shift from the current review, selection and dissemination processes in academic publishing. All Frontiers journals are driven by researchers for researchers; therefore, they constitute a service to the scholarly community. At the same time, the *Frontiers journal series* operates on a revolutionary invention, the tiered publishing system, initially addressing specific communities of scholars, and gradually climbing up to broader public understanding, thus serving the interests of the lay society, too.

Dedication to quality

Each Frontiers article is a landmark of the highest quality, thanks to genuinely collaborative interactions between authors and review editors, who include some of the world's best academicians. Research must be certified by peers before entering a stream of knowledge that may eventually reach the public - and shape society; therefore, Frontiers only applies the most rigorous and unbiased reviews. Frontiers revolutionizes research publishing by freely delivering the most outstanding research, evaluated with no bias from both the academic and social point of view. By applying the most advanced information technologies, Frontiers is catapulting scholarly publishing into a new generation.

What are Frontiers Research Topics?

Frontiers Research Topics are very popular trademarks of the *Frontiers journals series*: they are collections of at least ten articles, all centered on a particular subject. With their unique mix of varied contributions from Original Research to Review Articles, Frontiers Research Topics unify the most influential researchers, the latest key findings and historical advances in a hot research area.

Find out more on how to host your own Frontiers Research Topic or contribute to one as an author by contacting the Frontiers editorial office: frontiersin.org/about/contact

Severe acute respiratory syndrome coronavirus 2: Host-pathogen interactions and cellular signaling - vol II

Topic editors

Vikas Sood — Jamia Hamdard University, India

Clement Adebajo Meseko — National Veterinary Research Institute (NVRI), Nigeria

Citation

Sood, V., Meseko, C. A., eds. (2023). *Severe acute respiratory syndrome coronavirus 2: Host-pathogen interactions and cellular signaling - vol II*. Lausanne: Frontiers Media SA. doi: 10.3389/978-2-83251-739-0

The authors declare that the research was conducted in the absence of any commercial or financial relationships that could be construed as a potential conflict of interest.

Table of contents

- 05 **Editorial: Severe acute respiratory syndrome coronavirus 2: Host-pathogen interactions and cellular signaling - vol II**
Vikas Sood and Clement Adebajo Meseko
- 07 **ACE2 Shedding and the Role in COVID-19**
Jieqiong Wang, Huiying Zhao and Youzhong An
- 14 **Characterization of the Interaction Between SARS-CoV-2 Membrane Protein (M) and Proliferating Cell Nuclear Antigen (PCNA) as a Potential Therapeutic Target**
Érika Pereira Zambalde, Isadora Carolina Betim Pavan, Mariana Camargo Silva Mancini, Matheus Brandemarte Severino, Orlando Bonito Scudero, Ana Paula Morelli, Mariene Ribeiro Amorim, Karina Bispo-dos-Santos, Mariana Marcela Góis, Daniel A. Toledo-Teixeira, Pierina Lorencini Parise, Thais Mauad, Marisa Dolhnikoff, Paulo Hilário Nascimento Saldiva, Henrique Marques-Souza, José Luiz Proenca-Modena, Armando Morais Ventura and Fernando Moreira Simabuco
- 27 **Vaccination Is Associated With Shorter Time to Target Cycle Threshold Value in Patients With SARS-CoV-2 Omicron Variant**
Jiajun Wu, Yong Wei, Feng Shen, Shun Zhu, Yingying Lu, Xue Tian and Pengyu Zhang
- 33 **GDF15 and ACE2 stratify COVID-19 patients according to severity while ACE2 mutations increase infection susceptibility**
Margalida Torrens-Mas, Catalina M. Perelló-Reus, Neus Trias-Ferrer, Lesly Ibargüen-González, Catalina Crespi, Aina Maria Galmes-Panades, Cayetano Navas-Enamorado, Andres Sanchez-Polo, Javier Piérola-Lopetegui, Luis Masmiqel, Lorenzo Socias Crespi, Carles Barcelo and Marta Gonzalez-Freire
- 54 **NOTCH signaling in COVID-19: a central hub controlling genes, proteins, and cells that mediate SARS-CoV-2 entry, the inflammatory response, and lung regeneration**
Piyush Baidara, Md Bodruzzaman Sarker, Alexander P. Earhart, Santi M. Mandal and Adam G. Schrum
- 64 ***Withania somnifera* (L.) Dunal (Ashwagandha) for the possible therapeutics and clinical management of SARS-CoV-2 infection: Plant-based drug discovery and targeted therapy**
Manali Singh, Kuldeep Jayant, Dipti Singh, Shivani Bhutani, Nitesh Kumar Poddar, Anis Ahmad Chaudhary, Salah-Ud-Din Khan, Mohd Adnan, Arif Jamal Siddiqui, Md Imtaiyaz Hassan, Faez Iqbal Khan, Dakun Lai and Shahanavaj Khan
- 87 **Comparison of Intracellular Transcriptional Response of NHBE Cells to Infection with SARS-CoV-2 Washington and New York Strains**
Tiana M. Scott, Antonio Solis-Leal, J. Brandon Lopez, Richard A. Robison, Bradford K. Berges and Brett E. Pickett

- 101 **Choosing a cellular model to study SARS-CoV-2**
Gabriel Augusto Pires De Souza, Marion Le Bideau, Céline Boschi, Nathalie Wurtz, Philippe Colson, Sarah Aherfi, Christian Devaux and Bernard La Scola
- 125 ***In silico* analysis of SARS-CoV-2 genomes: Insights from SARS encoded non-coding RNAs**
Neha Periwal, Urvashi Bhardwaj, Sankritya Sarma, Pooja Arora and Vikas Sood



OPEN ACCESS

EDITED AND REVIEWED BY
Curtis Brandt,
University of Wisconsin-Madison,
United States

*CORRESPONDENCE
Clement Adebajo Meseko
✉ cameseko@yahoo.com

SPECIALTY SECTION
This article was submitted to
Virus and Host,
a section of the journal
Frontiers in Cellular and
Infection Microbiology

RECEIVED 15 January 2023
ACCEPTED 26 January 2023
PUBLISHED 08 February 2023

CITATION
Sood V and Meseko CA (2023) Editorial:
Severe acute respiratory syndrome
coronavirus 2: Host-pathogen interactions
and cellular signaling - vol II.
Front. Cell. Infect. Microbiol. 13:1145235.
doi: 10.3389/fcimb.2023.1145235

COPYRIGHT
© 2023 Sood and Meseko. This is an
open-access article distributed under the
terms of the [Creative Commons Attribution
License \(CC BY\)](#). The use, distribution or
reproduction in other forums is permitted,
provided the original author(s) and the
copyright owner(s) are credited and that
the original publication in this journal is
cited, in accordance with accepted
academic practice. No use, distribution or
reproduction is permitted which does not
comply with these terms.

Editorial: Severe acute respiratory syndrome coronavirus 2: Host-pathogen interactions and cellular signaling - vol II

Vikas Sood¹ and Clement Adebajo Meseko^{2*}

¹Department of Biochemistry, Jamia Hamdard, New Delhi, India, ²Infectious and Transboundary Animal Diseases, National Veterinary Research Institute, Vom, Nigeria

KEYWORDS

COVID-19, SARS-CoV-2, coronaviruses, cellular signaling, host-pathogen interactions

Editorial on the Research Topic

[Severe acute respiratory syndrome coronavirus 2: Host-pathogen interactions and cellular signaling - vol II](#)

The COVID-19 pandemic is caused by SARS-CoV-2, a betacoronavirus in the family Coronaviridae. Coronaviruses are enveloped, positive sense RNA viruses that are capable of infecting a diverse range of animals and humans. Coronaviruses infecting humans including 229E, NL63, OC43, and HKU1 could cause mild respiratory infection. Zoonotic and more pathogenic coronaviruses have emerged from animals in form of severe acute respiratory syndrome (SARS) and Middle East Respiratory Syndrome Coronavirus (MERS-CoV) in Saudi Arabia in 2002 and 2012 respectively. In 2019, SARS-CoV-2 evolved and spread across the globe causing a highly contagious infectious disease and responsible for the death of around 6 million people by the end of 2022. Thus SARS-CoV-2 has emerged as the most serious pandemic crisis since the 1918 pandemic (Agusi et al., 2020). Widespread and persistent circulation of SARS-CoV-2 contributes to host-pathogen interactions and cellular signaling. Consequently, and due to mutations, the virus has evolved rapidly and within three years, several variants have circulated across the globe. Some of those were designated “variants of concern” and predominate at different periods and regions with varying severity ([https://www.who.int/news/item/26-11-2021-classification-of-omicron-\(b.1.1.529\)-sars-cov-2-variant-of-concern](https://www.who.int/news/item/26-11-2021-classification-of-omicron-(b.1.1.529)-sars-cov-2-variant-of-concern)). Continuing emergence of new variants presents challenges for vaccine and antiviral drug development and studies in this special topic provide new information that will be useful for continuing efforts to blunt the impact of the virus. The success of vaccination and chemotherapy depends on a good understanding of the host and the pathogen interactions (Asha et al., 2019). The balance of this interaction determines the susceptibility of SARS-CoV-2 infection. Furthermore, the extent of the host-pathogen interaction affects the virulence or pathogenicity of the SARS-CoV-2 (Casadevall and Pirofski, 1999). In the course of invasion of the host cells, pathogens elicit both humoral and cellular immune responses and metabolic pathways that may contribute to eliminating invading pathogens (Forcados et al.). In addition, multiple cellular signaling pathways are elicited acting to reduce the severity of infection. Infection due to SARS-CoV-2, therefore, may be reduced in its clinical presentation, severity, and even mortality when a positive immune reaction is stimulated by pathogen-host interaction. It is imperative to delineate the

mechanisms of viral entry, infections, and associated host immune response to efficiently manage SARS-CoV-2 infections as investigated in the collection of scientific articles in this special Research Topic. Insights into new aspects of coronavirus biology and pathogenesis will help identify novel cellular pathways that can be targeted for immunity.

In this special collection, Wang et al. reviewed angiotensin-converting enzyme 2 (ACE2), a receptor of SARS-CoV-2 as it mediates viral entry into cells, the spread, and initiation of infection. Soluble ACE2 (sACE2) has also been demonstrated to bind to SARS-CoV-2, and it functions in viral entry into cells and spread suggesting that sACE2 is increased in COVID-19 and correlates with disease severity. Regulating ACE2 shedding and understanding the underlying mechanism between sACE2 and the virus enlightens therapy for COVID-19. The characterization of the interaction between SARS-CoV-2 membrane protein (M) and proliferating cell nuclear antigen (PCNA) as a potential therapeutic target was also discussed by Zambalde et al.. The authors proposed that the transport of PCNA to the cytoplasm and its association with SARS-CoV-2 membrane protein could be a strategy used by the virus to manipulate cell functions and might be considered a target for COVID-19 therapy. For better understanding of downstream molecular signaling pathways induced by SARS-CoV-2 in the lungs of infected individuals, Baindara et al. described and examined the predictions of a model in which NOTCH may represent a central signaling axis in lung infection in COVID-19.

Plant-based drug discovery and targeted therapy is yet another approach that can be explored for discovering reliable, and efficient drugs against infections including SARS-CoV-2. The bioactive compounds of Ashwagandha [*Withania somnifera* (L.) Dunal] may be explored as herbal medicine for the management and treatment of patients infected by SARS-CoV-2 infection (Singh et al., 2022). In a study by Torrens-Mas et al., levels of circulating growth differentiation factor 15 (GDF15) and angiotensin-converting enzyme 2 (ACE2) in plasma of severity-stratified COVID-19 patients and uninfected control patients shows that circulating GDF15 and ACE2 stratify COVID-19 patients according to disease severity. Additionally, ACE2 missense SNPs constitute a risk factor linked to infection susceptibility.

Vaccination responses to the SARS-CoV-2 Omicron variant in the Chinese population were examined by Wu et al. The study was designed to determine whether vaccination could alter the disease course of the SARS-CoV-2 Omicron variant. The authors concluded that vaccination is associated with a shorter time to target cycle threshold value (TtCT) in patients with the SARS-CoV-2 Omicron

variant. A brief research report provided insights from SARS-encoded non-coding RNAs. The authors performed in-silico analysis of SARS-CoV-2 genomes to identify SARS-CoV-2 encoded miRNAs. The study summary identified human and virus-encoded miRNAs that might regulate the pathogenesis of SARS coronaviruses and describe similar non-coding RNA sequences in SARS-CoV-2 that were shown to regulate SARS-induced lung pathology in mice (Periwal et al., 2022). In another study, cellular models to study SARS-CoV-2 and guide scientists venturing into studying the virus in the laboratories to choose the right cellular models were discussed (Pires De Souza et al., 2022). A study led by Scott et al. compared intracellular transcriptional response of NHBE cells to infection with SARS-CoV-2 Washington and New York Strains and suggest that some of the mechanisms associated with more severe disease from these viruses could include virus replication, metal ion usage, host translation shut off, host transcript stability, and immune inhibition.

Overall, this Research Topic highlighted the current research advancements made in the field of SARS-CoV2 Vol II. The structural function and role of ACE receptors in the severity of infection was elucidated. The analysis of host-pathogen interaction is crucial for the development of effective antiviral strategies and vaccines for SARS-CoV-2 and the management of COVID-19.

Author contributions

All authors listed have made a substantial, direct, and intellectual contribution to the work and approved it for publication.

Conflict of interest

The authors declare that the research was conducted in the absence of any commercial or financial relationships that could be construed as a potential conflict of interest.

Publisher's note

All claims expressed in this article are solely those of the authors and do not necessarily represent those of their affiliated organizations, or those of the publisher, the editors and the reviewers. Any product that may be evaluated in this article, or claim that may be made by its manufacturer, is not guaranteed or endorsed by the publisher.

References

- Agusi, E. R., Ijoma, S.I., Nnochin, C.S., Njoku-Achu, N.O., Nwosuh, C.I., Meseko, C.A., et al. (2020). The COVID-19 pandemic and social distancing in Nigeria: ignorance or defiance. *Pan Afr. Med. J.* 35 (Suppl 2), 52. doi: 10.11604/pamj.supp.2020.35.2.23649
- Asha, K., Kumar, P., Sanicas, M., Meseko, C. A., Khanna, M., and Kumar, B. (2019). Advancements in nucleic acid based therapeutics against respiratory viral infections. *J. Clin. Med.* 8 (1), 6. doi: 10.3390/jcm8010006

- Casadevall, A., and Pirofski, L. A. (1999). Host-pathogen interactions: redefining the basic concepts of virulence and pathogenicity. *Infect. Immun.* 67 (8), 3703–3713. doi: 10.1128/IAI.67.8.3703-3713.1999



ACE2 Shedding and the Role in COVID-19

Jieqiong Wang, Huiying Zhao* and Youzhong An*

Department of Critical Care Medicine, Peking University People's Hospital, Beijing, China

OPEN ACCESS

Edited by:

Vikas Sood,
Jamia Hamdard University, India

Reviewed by:

Anirudh K. Singh,
All India Institute of Medical Sciences

Bhopal, India
Samuel Pushparaj Robert Jeyasingh,
Oklahoma State University Oklahoma
City, United States

*Correspondence:

Huiying Zhao
zhaohuiying109@sina.com
Youzhong An
youzhonganicu@163.com

Specialty section:

This article was submitted to
Virus and Host,
a section of the journal
Frontiers in Cellular and
Infection Microbiology

Received: 04 October 2021

Accepted: 21 December 2021

Published: 14 January 2022

Citation:

Wang J, Zhao H and An Y
(2022) ACE2 Shedding and
the Role in COVID-19.
Front. Cell. Infect. Microbiol. 11:789180.
doi: 10.3389/fcimb.2021.789180

Angiotensin converting enzyme 2 (ACE2), a transmembrane glycoprotein, is an important part of the renin-angiotensin system (RAS). In the COVID-19 epidemic, it was found to be the receptor of severe acute respiratory syndrome coronavirus 2 (SARS-COV-2). ACE2 maintains homeostasis by inhibiting the Ang II-AT1R axis and activating the Ang I (1-7)-MasR axis, protecting against lung, heart and kidney injury. In addition, ACE2 helps transport amino acids across the membrane. ACE2 sheds from the membrane, producing soluble ACE2 (sACE2). Previous studies have pointed out that sACE2 plays a role in the pathology of the disease, but the underlying mechanism is not yet clear. Recent studies have confirmed that sACE2 can also act as the receptor of SARS-COV-2, mediating viral entry into the cell and then spreading to the infective area. Elevated concentrations of sACE2 are more related to disease. Recombinant human ACE2, an exogenous soluble ACE2, can be used to supplement endogenous ACE2. It may represent a potent COVID-19 treatment in the future. However, the specific administration concentration needs to be further investigated.

Keywords: soluble angiotensin converting enzyme 2, severe acute respiratory syndrome coronavirus 2, treatment, angiotensin converting enzyme 2, COVID-19

INTRODUCTION

Coronavirus disease 2019 (COVID-19), caused by a novel strain of severe acute respiratory syndrome coronavirus 2 (SARS-COV-2), has become a worldwide pandemic, endangering the health and economy of humans. Angiotensin converting enzyme 2 (ACE2) is the cell membrane receptor of SARS-COV-2, mediating viral entry into cells (Hoffmann et al., 2020). ACE2 has already been identified as a SARS-COV receptor, while the affinity of ACE2 binding to SARS-COV-2 is 10~20-fold higher than that of ACE2 binding with SARS-COV (Wrapp et al., 2020). Although ACE2 anchors onto the cell surface, it is not stable, and can shed from the membrane, which is referred to as ACE2 shedding (Lambert et al., 2005). ACE2 shedding produces soluble ACE2 (sACE2), resulting in loss of the membrane-bound form. Whether ACE2 shedding and increasing sACE2 are physiological or pathological has not been clearly elucidated. Recently, sACE2 has been

Abbreviations: ACE2, Angiotensin Converting Enzyme 2; ADAM17, A Disintegrin and Metalloprotease Domain 17; Ang I, Angiotensin I; Ang I (1-9), Angiotensin I (1-9); Ang II, Angiotensin II; Ang I (1-7), Angiotensin I (1-7); AT1R, Angiotensin II Type 1 Receptor; BALF, bronchoalveolar lavage fluid; CLD, collectrin-like domain; COVID-19, Coronavirus disease 2019; MasR, Mitochondrial assembly receptor; MODS, multiple organ dysfunction syndrome; PD, protease domain; PMA, phorbol ester; RAS, Renin-Angiotensin-System; RBD, receptor binding domain; rhACE2, recombinant human angiotensin converting enzyme 2; sACE2, soluble angiotensin converting enzyme 2; SARS-COV-2, severe acute syndrome coronavirus; Sema4D, Semaphorin 4; TACE, tumor necrosis factor α -converting enzyme; TMPRSS2, transmembrane protease serine 2.

found to facilitate SARS-COV-2 infection in cells (Karthika et al., 2021; Yeung et al., 2021). On the other hand, clinical-grade recombinant human ACE2 (rhACE2), a type of exogenous soluble form of ACE2, binds to SARS-COV-2 in engineered human tissues and inhibits virus infection (Monteil et al., 2020). Therefore, the role sACE2 plays in COVID-19 warrants further study.

In this narrative review, we focus on the generative mechanism of sACE2 and sACE2 in COVID-19 and the therapeutic use of rhACE2 in COVID-19 (Figure 1).

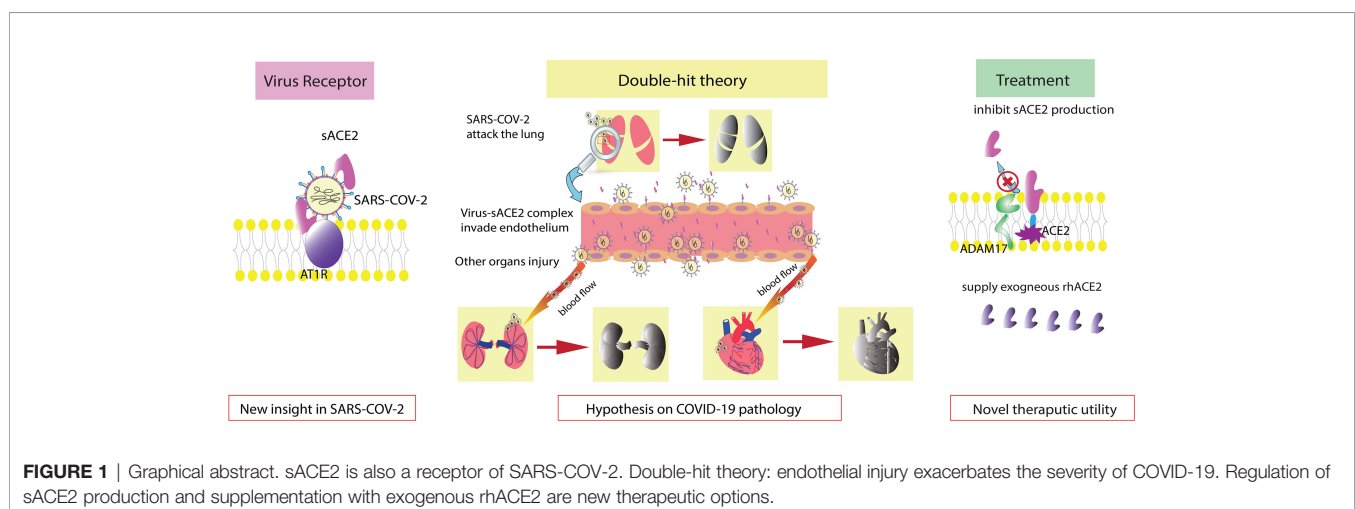
THE STRUCTURE AND FUNCTION OF ACE2

ACE2, discovered in 2000 as the homolog of ACE, is a type I transmembrane glycoprotein that resides on the cell surface (Tipnis et al., 2000). ACE2 is broadly distributed throughout the human body. It is expressed in the kidney, testis, intestine, lung, retina, cardiovascular system, adipose tissue and central nervous system (Hamming et al., 2004; Gheblawi et al., 2020). The human ACE2 gene maps to chromosome Xp22 and contains 18 exons (Tipnis et al., 2000). The ACE2 protein, which has a full length of 805 amino acids, exhibits an extracellular N-terminal claw-like protease domain (PD) and a C-terminal collectrin-like domain (CLD) with a cytosolic tail (Zhang et al., 2001; Gheblawi et al., 2020). The PD of the N-terminus can bind to the receptor binding domain (RBD) of Spike protein both SARS-COV and SARS-COV-2, forming the PD-RBD complex and facilitating virus entry (Li et al., 2003; Hoffmann et al., 2020). The affinity of ACE2 binding to SARS-COV-2 is 10~20-fold higher than that of SARS-COV, which may explain the severity of COVID-19 (Wrapp et al., 2020). Distinct from the virus binding site, the HEXXH zinc binding metalloprotease motif in the N-terminus exerts carboxypeptidase function, which converts angiotensin I (Ang I) to Ang 1-9 or Ang II to Ang I 1-7 (Vickers et al., 2002). In addition, ACE2 cuts the C-terminal residue from three other vasoactive peptides,

neurotensin, kinetensin, and des-Arg bradykinin (Vickers et al., 2002). In contrast, ACE converts Ang I to Ang II and cleaves bradykinin. The counterbalance of ACE-Ang II-angiotensin II type 1 receptor (AT1R) and ACE2-Ang I (1-7)-mitochondrial assembly receptor (MasR) plays an important role in RAS. Increasing and activating the ACE2-Ang I (1-7)-MasR axis reduces cytokine release and protects against organ injury in many human diseases, including cardiovascular disease, obesity, chronic kidney disease, liver diseases and lung injury (Rodrigues Prestes et al., 2017). On the other hand, the intracellular CLD of ACE2 participates in amino acid transport by regulating the epithelial neutral amino acid transporter B0AT1 in the small intestine (Camargo et al., 2009).

sACE2 IS GENERATED FROM ACE2 SHEDDING

Additionally, ADAM17, a disintegrin and metallopeptidase domain 17 (ADAM17)/tumor necrosis factor α -converting enzyme (TACE), cleaves ACE2 from the cell surface, generating a soluble, enzymatically active ectodomain form of the enzyme sACE2. ADAM17-induced ACE2 shedding is activated by phorbol ester (PMA) (Lambert et al., 2005). Lambert et al. confirmed the presence of ectodomain shedding of heterologously expressed ACE2 in HEK293 cells and endogenously expressed ACE2 in Huh7 cells (Lambert et al., 2005). Rice et al. first detected circulating ACE2 in healthy individuals, although the concentration of ACE2 was far lower than that of ACE (Rice et al., 2006). Subsequently, researchers discovered that calmodulin's interaction with the cytoplasmic tail of ACE2 inhibited its shedding, which was independent of PMA-mediated shedding (Lambert et al., 2008; Lai et al., 2009). A study on human epithelial cells indicated that ADAM17 exerted its sheddase function *via* the ectodomain of ACE2 (Jia et al., 2009). It seems that calmodulin and ADAM17 affect ACE2 proteolytic cleavage through two dependent mechanisms. However, Mou et al. found that dissociation of calmodulin from semaphorin 4D



(Sema4D) in platelets was sufficient to trigger ADAM17-dependent Sema4D cleavage (Mou et al., 2013). Whether calmodulin and ADAM-17 apply a similar method to regulate ACE2 shedding or other possible crosstalk between them needs to be further investigated.

On the other hand, transmembrane protease serine 2 (TMPRSS2) competes with ADAM17 in ACE2 cleavage (Shulla et al., 2011; Heurich et al., 2014). In contrast, TMPRSS2 requires arginine and lysine residues within ACE2 amino acids 697 to 716 for receptor cleavage, while ADAM17 acts within sites 652 to 659 (Heurich et al., 2014). In addition, TMPRSS2 primes the virus spike protein of both SARS-CoV and SARS-CoV-2, activating the S protein for membrane fusion (Heurich et al., 2014; Hoffmann et al., 2020). An inhibitor of TMPRSS2 might represent a new therapeutic target in COVID-19.

Although sACE2 is believed to catalyze Ang II hydrolysis, an increasing number of circulating ACE2 attenuates its protective role in many tissues and organs and is even detrimental to many organs, such as the heart (Epelman et al., 2008; Jia et al., 2009; Ramchand et al., 2018; Shao et al., 2019). The physiological and pathological effects of sACE2 on specific organs or tissues are exploring, but the potential mechanism was not determined (Figure 2).

sACE2 IN COVID-19

sACE2 Mediates SARS-CoV-2 Entry Into Cells

ACE2 has been identified as a SARS-CoV-2 receptor on the cell membrane (Hoffmann et al., 2020). What about sACE2, the form that lacks the cytoplasmic region? Recently, two teams demonstrated that sACE2 binds to SARS-CoV-2 and then mediates its entry into cells (Karthika et al., 2021; Yeung et al., 2021). These findings suggest a role of ACE2 shedding and

sACE2 in SARS-CoV-2 infection. Whether it has a beneficial effect or causes harm, remains to be fully understood.

ACE2 is upregulated 199-fold in cells in bronchoalveolar lavage fluid (BALF) from COVID-19 patients (Garvin et al., 2020). In healthy individuals, circulating ACE2 levels are very low and are difficult to detect (Rice et al., 2006). In COVID-19 patients, sACE2 is significantly elevated in the presence of severe complications or pre-existing cardiorenal conditions (Vassiliou et al., 2021; Lundström et al., 2021; Patel et al., 2021; Kragstrup et al., 2021). In addition, monitoring a critically ill COVID-19 patient revealed that sACE2 dramatically increased at the onset of disease (Nagy et al., 2021). These studies suggest that sACE2 is increased in COVID-19, even correlating with the severity of disease. From our perspective, a higher concentration of sACE2 means a higher binding rate with SARS-CoV-2 with increased sACE2-virus complexes. Subsequently, many complexes enter and attack cells and then replicate additional virus, spreading the infection to other sites. On the other hand, the virus-sACE2 complex in the extracellular space can flow toward other areas, causing broad tissue destruction (Rahman et al., 2021).

However, the limitation of the large size of the virus-sACE2 complex may mean that it is unable to cross certain microvessels or spread extensively (Wysocki et al., 2019). ACE2 is expressed by endothelial cells, and the endothelium is considered one of the most damaged areas in COVID-19 (Patel et al., 2016; Amraei and Rahimi, 2020; Varga et al., 2020; Nagy et al., 2021). Thus, we postulated a double-hit theory of SARS-CoV-2. Endothelial cells are the first hit target of SARS-CoV-2. After the endothelium is damaged, an activated inflammatory response induces a cytokine storm, which is also a lethal reaction to COVID-19. Moreover, the impaired endothelial barrier cannot limit the virus-sACE2 complex from traversing across vessels, allowing the complex to infect additional organs and tissues. This contributes to severe complications such as multiple organ dysfunction syndrome (MODS), which we consider to be the second hit. The double-

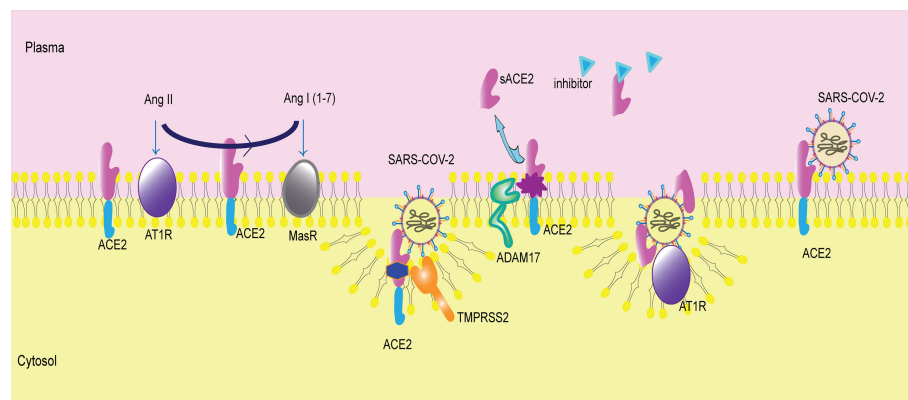


FIGURE 2 | Membrane-bound ACE2 and ACE2 shedding. ACE2 is a membrane receptor. It converts angiotensin II (Ang II) to angiotensin I (1-7) (Ang I(1-7)). Then, Ang II binds to angiotensin type 1 receptor (AT1R), and Ang I(1-7) binds to mitochondrial assembly receptor (MasR). ACE2 is the membrane receptor of SARS-CoV-2. Transmembrane protease serine 2 (TMPRSS2) cleaves ACE2 and mediates viral entry into cells. A disintegrin and metalloprotease domain 17 (ADAM17) catalyzes ACE2 shedding, producing sACE2. The inhibitor of sACE2 is in the plasma, blocking sACE2 activity. sACE2 can bind to SARS-CoV-2 and then facilitate virus entry via AT1R.

hit theory may elucidate the elevated level of sACE2 in COVID-19 patients with severe complications.

Notably, the establishment of double-hit theory is based on the occurrence of viremia. SARS-COV-2 was indicated in blood of COVID-19 patients while the sign was associated with the disease severity (Chen et al., 2020; Fajnzylber et al., 2020; Puelles et al., 2020; Tan et al., 2020; Jacobs et al., 2021; Järhult et al., 2021; Li et al., 2021). Critically ill patients were more prone to have viremia than non-ICU patients and outpatients (Tan et al., 2020; Chen et al., 2020; Jacobs et al., 2021). Li et al. illustrated markers corresponding to gastrointestinal tract, liver and pancreas damage increased in viremic individuals (Li et al., 2021). Like IL-6, IL-2, CCL7, CXCL10/IP-10 and other cytokines also elevated in viremic patients (Tan et al., 2020; Li et al., 2021). Although the rational mechanism between MODS, cytokine storm and viremia have not been demystified, these results may explain why plasma viral load correlates to worsen clinical outcome, disease severity and increasing risk of mortality (Tan et al., 2020; Jacobs et al., 2021; Järhult et al., 2021; Li et al., 2021). In addition, the proteomic analysis uncovered that the appearance of viremia was accompanied by sACE2 elevation in blood and endovascular injury, in favor of circulating of the virus-sACE2 complex through the body (Li et al., 2021).

In addition, biomarkers of endothelial injury and inflammation were increased in the advanced stage of COVID-19 and decreased in the convalescence phase. Notably, the increase in E-selectin and IL-6 was parallel, while sACE2 increased following a two-day delay (Tong et al., 2020; Nagy et al., 2021). This suggests that the inflammatory response initiates increased ACE2 shedding with consequently higher levels of sACE2. Along with the double-hit theory, cytokines that induce ACE2 shedding may participate in the spread of virus throughout the body.

SARS-COV and NL63, two human coronaviruses, have been shown to induce ACE2 shedding (Haga et al., 2008; Glowacka et al., 2010). With respect to SARS-COV-2, research on ACE2 shedding is scarce. We speculate that the elevation of sACE2 levels in the plasma is partially attributed to virus-induced shedding. In parallel, a higher concentration of sACE2 is followed by increased virus-sACE2 complexes and more virus production, which forms positive feedback loop. This feedback contributes to the rapid and aggressive nature of SARS-COV-2, lethally invading the body. If this hypothesis is true, regulating ACE2 shedding, such as through ADAM17, may represent a potential therapeutic target.

sACE2 INHIBITION AND THE VIRUS

An increasing body of evidence suggests that sACE2 elevation occurs during pathogenesis (Roberts et al., 2013; Ramchand et al., 2018; Ramchand et al., 2020), but it is difficult to assess plasma sACE2 levels in healthy people. One possible reason is that an endogenous inhibitor in healthy human plasma perturbs sACE2 enzymatic activity (Lew et al., 2008). The inhibitor identify and its relationship with activators of ACE2 shedding remain an area of active research. We propose that the inhibitor

counterbalances sACE2 activity to maintain homeostasis. Once the concentration of sACE2 becomes sufficiently high, the inhibition is overcome (Lew et al., 2008). The precise concentration of sACE2 at which the inhibition loses efficiency is worthy of investigation. Perhaps the very concentration is the boundary between health and pathology, which could be used in future disease screening. Moreover, sex, geographic ancestry, and BMI are top-level factors determining sACE2 levels (Narula et al., 2020). We need to evaluate and correct for the effects of these factors when determining specific sACE2 levels.

Importantly, existing *in vitro* or organoid experiments ignore that an inhibitor of sACE2 is in human plasma (Lew et al., 2008). Therefore, when the virus enters the human body, will the inhibitor interfere with the interaction between sACE2 and SARS-COV-2? Or can the virus react with the inhibitor? We hypothesize that the inhibitor maintains sACE2 concentrations at physiological ranges due to self-regulation. Perhaps viral infection breaks the balance by initiating more active ACE2 shedding. Given these gaps in knowledge, the network linking sACE2, the inhibitor, and SARS-COV-2 needs to be demystified.

sACE2 IN COVID-19 TREATMENT

Although the interaction between sACE2 and SARS-COV-2 is not fully understood, current knowledge gives us some inspiration for treatment. Exogenous supplementation with rhACE2 competitively inhibits endogenous sACE2 binding to virus. RhACE2 has already been tested in phase 1 and phase 2 clinical trials (Haschke et al., 2013; Khan et al., 2017). A recent study on COVID-19 illustrated that clinical-grade rhACE2 binding to coronavirus in engineered human tissues blocks viral infection (Monteil et al., 2020). One case report of a COVID-19 patient observed an improvement in viremia after a 1-day infusion of rhACE2 (Zoufaly et al., 2020).

On the other hand, ACE2 shedding and internalization of the ACE2-virus complex both lead to the loss of membrane-anchoring ACE2, producing increased Ang II and decreased Ang I (1-7). Then, the balance shifts toward the Ang II-AT1R axis, impairing organs and tissues (Gheblawi et al., 2020). Administration of rhACE2 can convert large amounts of Ang II to Ang I (1-7), guiding the Ang I (1-7)-MasR axis and relieving organ injury. In other words, rhACE2 not only binds to the virus but also ameliorates virus-related complications. In response to rhACE2 treatment, one COVID-19 patient with marked enhancement of Ang I (1-7) and decreased Ang II recovered from lung injury, indicating the dual effect of rhACE2 (Zoufaly et al., 2020). This suggests the feasibility and safety of rhACE2 for the clinical treatment of COVID-19. A clinical trial (NCT04335136) with a larger sample size explored the treatment effect of rhACE2 in COVID-19 patients, which ended in December 2020. We hope the fruits of the trial will bring some new ideas.

With the understanding that sACE2 facilitates SARS-COV-2 cellular entry and exacerbates infection, we question whether the interaction between rhACE2 (a type of sACE2) and virus is beneficial. On the other hand, rhACE2 can be synthesized and designed. Elucidating the mechanism of sACE2 in the pathology

of COVID-19 helps to produce much safer and more effective therapeutic rhACE2. Recently, researchers engineered sACE2 with three mutations, and the novel decoy receptor was named sACE2.v2.4. These designed mutations lead to sACE2.v2.4 having a higher affinity for SARS-CoV-2 than the wild-type ACE2 receptor and the best monoclonal antibody, more potently blocking virus cell entry. In addition, sACE2.v2.4 efficiently neutralized viral infection (Chan et al., 2020; Chan et al., 2021).

Another insightful perspective is that rhACE2 concentrations (~10–200 mg/mL) far beyond the physiological range block SARS-CoV-2 infection, while concentrations near the physiological range (i.e., ng/mL level) facilitate virus cell entry (Yeung et al., 2021). This new idea is in line with the idea that sACE2 binding with virus increases its infectivity. Interestingly, the dose of rhACE2 (0.4 mg/kg) and plasma ACE2 (μg/mL) level in COVID-19 patients did not reach the “treatment concentration”, but they did achieve better outcomes (Monteil et al., 2020). The perspective regarding rhACE2 concentration is based on an *in vitro* cell model (Yeung et al., 2021). In our view, after rhACE2 enters the body, the subsequent reaction between the virus or other factors remains mysterious, which may contribute to the discrepancies in findings. It is difficult to determine the pharmacokinetics and pharmacodynamics of rhACE2, as we cannot distinguish it from endogenous sACE2. Therefore, we are unsure whether rhACE2 binding to SARS-CoV-2 interferes with both the detection of rhACE2 and the protective effect. Therefore, defining the concentration of rhACE2 appropriate for COVID-19 treatment or other clinical practice is vital and warrants deeper study.

DISCUSSION

A topic of interest includes membrane-bound ACE2 being the receptor of SARS-CoV-2. However, the shedding process and

soluble form of ACE2 are active considerations. In this minireview, we focused on the role of sACE2 in COVID-19 and the therapeutic use of rhACE2 in COVID-19. In line with ACE2, sACE2 can bind to SARS-CoV-2, mediating virus entry into cells. In an investigation of COVID-19 patients, sACE2 levels were increased in BALF and serum. Furthermore, levels of sACE2 are positively correlated with disease severity. Based on this observation, we propose a double-hit hypothesis to explain the pathological progress of COVID-19 and emphasize endothelial injury at the onset of COVID-19. Additionally, inflammation may participate in ACE2 shedding, worsening COVID-19-related complications. Understanding the underlying mechanism between sACE2 and virus enlightens therapy for COVID-19. Infusion of rhACE2 exogenously replenishes ACE2, prevents organ injury and potentially improves clinical symptoms. The specific efficacy of rhACE2 in COVID-19 patients is currently undergoing clinical trials. Certainly, the effective dose of rhACE2 for treatment is controversial and warrants careful investigation.

AUTHOR CONTRIBUTIONS

JW, HZ, and YA contributed to the conception of the manuscript. JW and HZ searched the literature and drafted the manuscript. The authors read and approved the final manuscript.

FUNDING

The work was supported by Beijing Municipal Natural Science Foundation, China (Grant No. 7212124). HZ was supported partially by research fund provided by Peking University People's Hospital Research and Development Funds (No. RDY2019-43, derive sepsis phenotypes using electronic medical data and machine learning).

REFERENCES

- Amraei, R., and Rahimi, N. (2020). COVID-19, Renin-Angiotensin System and Endothelial Dysfunction. *Cells* 9 (7), 1652. doi: 10.3390/cells9071652
- Camargo, S. M. R., Singer, D., Makrides, V., Huggel, K., Pos, K. M., Wagner, C. A., et al. (2009). Tissue-Specific Amino Acid Transporter Partners ACE2 and Collectrin Differentially Interact With Hartnup Mutations. *Gastroenterology* 136 (3), 872–882. doi: 10.1053/j.gastro.2008.10.055
- Chan, K. K., Dorosky, D., Sharma, P., Abbasi, S. A., Dye, J. M., Kranz, D. M., et al. (2020). Engineering Human ACE2 to Optimize Binding to the Spike Protein of SARS Coronavirus 2. *Science* 369 (6508), 1261–1265. doi: 10.1126/science.abc0870
- Chan, K. K., Tan, T. J. C., Narayanan, K. K., and Procko, E. (2021). An Engineered Decoy Receptor for SARS-CoV-2 Broadly Binds Protein S Sequence Variants. *Sci. Adv.* 7 (8), eabf1738. doi: 10.1126/sciadv.abf1738
- Chen, X., Zhao, B., Qu, Y., Chen, Y., Xiong, J., Feng, Y., et al. (2020). Detectable Serum Severe Acute Respiratory Syndrome Coronavirus 2 Viral Load (RNAemia) Is Closely Correlated With Drastically Elevated Interleukin 6 Level in Critically Ill Patients With Coronavirus Disease 2019. *Clin. Infect. Dis.* 71 (8), 1937–1942. doi: 10.1093/cid/cia449
- Epelman, S., Tang, W. H. W., Chen, S. Y., Van Lente, F., Francis, G. S., and Sen, S. (2008). Detection of Soluble Angiotensin-Converting Enzyme 2 in Heart Failure: Insights Into the Endogenous Counter-Regulatory Pathway of the Renin-Angiotensin-Aldosterone System. *J. Am. Coll. Cardiol.* 52 (9), 750–754. doi: 10.1016/j.jacc.2008.02.088
- Fajnzylber, J., Regan, J., Coxen, K., Corry, H., Wong, C., Rosenthal, A., et al. (2020). SARS-CoV-2 Viral Load is Associated With Increased Disease Severity and Mortality. *Nat. Commun.* 11 (1), 5493. doi: 10.1038/s41467-020-19057-5
- Garvin, M. R., Alvarez, C., Miller, J. I., Prates, E. T., Walker, A. M., Amos, B. K., et al. (2020). A Mechanistic Model and Therapeutic Interventions for COVID-19 Involving a RAS-Mediated Bradykinin Storm. *Elife* 9, e59177. doi: 10.7554/eLife.59177
- Gheblawi, M., Wang, K., Viveiros, A., Nguyen, Q., Zhong, J.-C., Turner, A. J., et al. (2020). Angiotensin-Converting Enzyme 2: SARS-CoV-2 Receptor and Regulator of the Renin-Angiotensin System: Celebrating the 20th Anniversary of the Discovery of ACE2. *Circ. Res.* 126 (10), 1456–1474. doi: 10.1161/CIRCRESAHA.120.317015
- Glowacka, I., Bertram, S., Herzog, P., Pfeifferle, S., Steffen, I., Muench, M. O., et al. (2010). Differential Downregulation of ACE2 by the Spike Proteins of Severe Acute Respiratory Syndrome Coronavirus and Human Coronavirus NL63. *J. Virol.* 84 (2), 1198–1205. doi: 10.1128/JVI.01248-09
- Haga, S., Yamamoto, N., Nakai-Murakami, C., Osawa, Y., Tokunaga, K., Sata, T., et al. (2008). Modulation of TNF-Alpha-Converting Enzyme by the Spike Protein of SARS-CoV and ACE2 Induces TNF-Alpha Production and

- Facilitates Viral Entry. *Proc. Natl. Acad. Sci. U. S. A.* 105 (22), 7809–7814. doi: 10.1073/pnas.0711241105
- Hamming, I., Timens, W., Bulthuis, M. L. C., Lely, A. T., Navis, G. J., and van Goor, H. (2004). Tissue Distribution of ACE2 Protein, the Functional Receptor for SARS Coronavirus. A First Step in Understanding SARS Pathogenesis. *J. Pathol.* 203 (2), 631–637. doi: 10.1002/path.1570
- Haschke, M., Schuster, M., Poglitsch, M., Loibner, H., Salzberg, M., Bruggisser, M., et al. (2013). Pharmacokinetics and Pharmacodynamics of Recombinant Human Angiotensin-Converting Enzyme 2 in Healthy Human Subjects. *Clin. Pharmacokinet.* 52 (9), 783–792. doi: 10.1007/s40262-013-0072-7
- Heurich, A., Hofmann-Winkler, H., Gierer, S., Liepold, T., Jahn, O., and Pöhlmann, S. (2014). TMPRSS2 and ADAM17 Cleave ACE2 Differentially and Only Proteolysis by TMPRSS2 Augments Entry Driven by the Severe Acute Respiratory Syndrome Coronavirus Spike Protein. *J. Virol.* 88 (2), 1293–1307. doi: 10.1128/JVI.02202-13
- Hoffmann, M., Kleine-Weber, H., Schroeder, S., Krüger, N., Herrler, T., Erichsen, S., et al. (2020). SARS-CoV-2 Cell Entry Depends on ACE2 and TMPRSS2 and Is Blocked by a Clinically Proven Protease Inhibitor. *Cell* 181 (2), 271–280.e8. doi: 10.1016/j.cell.2020.02.052
- Jacobs, J. L., Bain, W., Naqvi, A., Staines, B., Castanha, P. M. S., Yang, H., et al. (2021). SARS-CoV-2 Viremia Is Associated With COVID-19 Severity and Predicts Clinical Outcomes. *Clin. Infect. Dis.* ciab686. doi: 10.1093/cid/ciab686
- Järhult, J. D., Hultström, M., Bergqvist, A., Frithiof, R., and Lipcsey, M. (2021). The Impact of Viremia on Organ Failure, Biomarkers and Mortality in a Swedish Cohort of Critically Ill COVID-19 Patients. *Sci. Rep.* 11 (1), 7163. doi: 10.1038/s41598-021-86500-y
- Jia, H. P., Look, D. C., Tan, P., Shi, L., Hickey, M., Gakhar, L., et al. (2009). Ectodomain Shedding of Angiotensin Converting Enzyme 2 in Human Airway Epithelia. *Am. J. Physiol. Lung Cell. Mol. Physiol.* 297 (1), L84–L96. doi: 10.1152/ajplung.00071.2009
- Karthika, T., Joseph, J., Das, V. R. A., Nair, N., Charulekha, P., Roji, M. D., et al. (2021). SARS-CoV-2 Cellular Entry Is Independent of the ACE2 Cytoplasmic Domain Signaling. *Cells* 10 (7), 1814. doi: 10.3390/cells10071814
- Khan, A., Benthin, C., Zeno, B., Albertson, T. E., Boyd, J., Christie, J. D., et al. (2017). A Pilot Clinical Trial of Recombinant Human Angiotensin-Converting Enzyme 2 in Acute Respiratory Distress Syndrome. *Crit. Care* 21 (1), 234. doi: 10.1186/s13054-017-1823-x
- Kragstrup, T. W., Singh, H. S., Grundberg, I., Nielsen, A. L.-L., Rivelles, F., Mehta, A., et al. (2021). Plasma ACE2 Predicts Outcome of COVID-19 in Hospitalized Patients. *PLoS One* 16 (6), e0252799–e. doi: 10.1371/journal.pone.0252799
- Lai, Z. W., Lew, R. A., Yarski, M. A., Mu, F.-T., Andrews, R. K., and Smith, A. I. (2009). The Identification of a Calmodulin-Binding Domain Within the Cytoplasmic Tail of Angiotensin-Converting Enzyme-2. *Endocrinology* 150 (5), 2376–2381. doi: 10.1210/en.2008-1274
- Lambert, D. W., Clarke, N. E., Hooper, N. M., and Turner, A. J. (2008). Calmodulin Interacts With Angiotensin-Converting Enzyme-2 (ACE2) and Inhibits Shedding of its Ectodomain. *FEBS Lett.* 582 (2), 385–390. doi: 10.1016/j.febslet.2007.11.085
- Lambert, D. W., Yarski, M., Warner, F. J., Thornhill, P., Parkin, E. T., Smith, A. I., et al. (2005). Tumor Necrosis Factor-Alpha Convertase (ADAM17) Mediates Regulated Ectodomain Shedding of the Severe-Acute Respiratory Syndrome-Coronavirus (SARS-CoV) Receptor, Angiotensin-Converting Enzyme-2 (ACE2). *J. Biol. Chem.* 280 (34), 30113–30119. doi: 10.1074/jbc.M505111200
- Lew, R. A., Warner, F. J., Hanchapola, I., Yarski, M. A., Ramchand, J., Burrell, L. M., et al. (2008). Angiotensin-Converting Enzyme 2 Catalytic Activity in Human Plasma Is Masked by an Endogenous Inhibitor. *Exp. Physiol.* 93 (5), 685–693. doi: 10.1113/expphysiol.2007.040352
- Li, W., Moore, M. J., Vasilieva, N., Sui, J., Wong, S. K., Berne, M. A., et al. (2003). Angiotensin-Converting Enzyme 2 Is a Functional Receptor for the SARS Coronavirus. *Nature* 426 (6965), 450–454. doi: 10.1038/nature02145
- Li, Y., Schneider, A. M., Mehta, A., Sade-Feldman, M., Kays, K. R., Gentili, M., et al. (2021). SARS-CoV-2 Viremia Is Associated With Distinct Proteomic Pathways and Predicts COVID-19 Outcomes. *J. Clin. Invest.* 131 (13), e148635. doi: 10.1172/JCI148635
- Lundström, A., Ziegler, L., Havervall, S., Rudberg, A.-S., von Meijenföldt, F., Lisman, T., et al. (2021). Soluble Angiotensin-Converting Enzyme 2 Is Transiently Elevated in COVID-19 and Correlates With Specific Inflammatory and Endothelial Markers. *J. Med. Virol.* 93 (10), 5908–5916. doi: 10.1002/jmv.27144
- Monteil, V., Kwon, H., Prado, P., Hagelkrüys, A., Wimmer, R. A., Stahl, M., et al. (2020). Inhibition of SARS-CoV-2 Infections in Engineered Human Tissues Using Clinical-Grade Soluble Human Ace2. *Cell* 181 (4), 905–913.e7. doi: 10.1016/j.cell.2020.04.004
- Mou, P., Zeng, Z., Li, Q., Liu, X., Xin, X., Wannemacher, K. M., et al. (2013). Identification of a Calmodulin-Binding Domain in Sema4D That Regulates its Exodomain Shedding in Platelets. *Blood* 121 (20), 4221–4230. doi: 10.1182/blood-2012-11-470609
- Nagy, B. Jr., Fejes, Z., Szentkereszty, Z., Sütö, R., Várkonyi, I., Ajzner, É., et al. (2021). A Dramatic Rise in Serum ACE2 Activity in a Critically Ill COVID-19 Patient. *Int. J. Infect. Dis.* 103, 412–414. doi: 10.1016/j.ijid.2020.11.184
- Narula, S., Yusuf, S., Chong, M., Ramasundarahettige, C., Rangarajan, S., Bangdiwala, S. I., et al. (2020). Plasma ACE2 and Risk of Death or Cardiometabolic Diseases: A Case-Cohort Analysis. *Lancet* 396 (10256), 968–976. doi: 10.1016/S0140-6736(20)31964-4
- Patel, S. K., Juno, J. A., Lee, W. S., Wragg, K. M., Hogarth, P. M., Kent, S. J., et al. (2021). Plasma ACE2 Activity is Persistently Elevated Following SARS-CoV-2 Infection: Implications for COVID-19 Pathogenesis and Consequences. *Eur. Respir. J.* 57 (5), 2003730. doi: 10.1183/13993003.03730-2020
- Patel, V. B., Zhong, J.-C., Grant, M. B., and Oudit, G. Y. (2016). Role of the ACE2/Angiotensin 1-7 Axis of the Renin-Angiotensin System in Heart Failure. *Circ. Res.* 118 (8), 1313–1326. doi: 10.1161/CIRCRESAHA.116.307708
- Puelles, V. G., Lütgehetmann, M., Lindenmeyer, M. T., Sperhake, J. P., Wong, M. N., Allweiss, L., et al. (2020). Multiorgan and Renal Tropism of SARS-CoV-2. *N. Engl. J. Med.* 383 (6), 590–592. doi: 10.1056/NEJMc2011400
- Rahman, M. M., Hasan, M., and Ahmed, A. (2021). Potential Detrimental Role of Soluble ACE2 in Severe COVID-19 Comorbid Patients. *Rev. Med. Virol.* 31 (5), 1–12. doi: 10.1002/rmv.2213
- Ramchand, J., Patel, S. K., Kearney, L. G., Matalanis, G., Farouque, O., Srivastava, P. M., et al. (2020). Plasma ACE2 Activity Predicts Mortality in Aortic Stenosis and Is Associated With Severe Myocardial Fibrosis. *JACC Cardiovasc. Imaging* 13 (3), 655–664. doi: 10.1016/j.jcmg.2019.09.005
- Ramchand, J., Patel, S. K., Srivastava, P. M., Farouque, O., and Burrell, L. M. (2018). Elevated Plasma Angiotensin Converting Enzyme 2 Activity is an Independent Predictor of Major Adverse Cardiac Events in Patients With Obstructive Coronary Artery Disease. *PLoS One* 13 (6), e0198144. doi: 10.1371/journal.pone.0198144
- Rice, G. I., Jones, A. L., Grant, P. J., Carter, A. M., Turner, A. J., and Hooper, N. M. (2006). Circulating Activities of Angiotensin-Converting Enzyme, its Homolog, Angiotensin-Converting Enzyme 2, and Neprilysin in a Family Study. *Hypertens. (Dallas Tex: 1979)* 48 (5), 914–920. doi: 10.1161/01.HYP.0000244543.91937.79
- Roberts, M. A., Velkoska, E., Ierino, F. L., and Burrell, L. M. (2013). Angiotensin-Converting Enzyme 2 Activity in Patients With Chronic Kidney Disease. *Nephrol. Dialysis Transplant.: Off. Publ. Eur. Dialysis Transplant. Assoc. - Eur. Renal Assoc.* 28 (9), 2287–2294. doi: 10.1093/ndt/gft038
- Rodrigues Prestes, T. R., Rocha, N. P., Miranda, A. S., Teixeira, A. L., and Simoes-Silva, A. C. (2017). The Anti-Inflammatory Potential of ACE2/Angiotensin-(1-7)/Mas Receptor Axis: Evidence From Basic and Clinical Research. *Curr. Drug Targets* 18 (11), 1301–1313. doi: 10.2174/1389450117666160727142401
- Shao, Z., Schuster, A., Borowski, A. G., Thakur, A., Li, L., and Wilson Tang, W. H. (2019). Soluble Angiotensin Converting Enzyme 2 Levels in Chronic Heart Failure Is Associated With Decreased Exercise Capacity and Increased Oxidative Stress-Mediated Endothelial Dysfunction. *Trans. Res.: J. Lab. Clin. Med.* 212, 80–88. doi: 10.1016/j.trsl.2019.06.004
- Shulla, A., Heald-Sargent, T., Subramanya, G., Zhao, J., Perlman, S., and Gallagher, T. (2011). A Transmembrane Serine Protease Is Linked to the Severe Acute Respiratory Syndrome Coronavirus Receptor and Activates Virus Entry. *J. Virol.* 85 (2), 873–882. doi: 10.1128/JVI.02062-10
- Tan, C., Li, S., Liang, Y., Chen, M., and Liu, J. (2020). SARS-CoV-2 Viremia may Predict Rapid Deterioration of COVID-19 Patients. *Braz. J. Infect. Dis.* 24 (6), 565–569. doi: 10.1016/j.bjid.2020.08.010
- Tipnis, S. R., Hooper, N. M., Hyde, R., Karran, E., Christie, G., and Turner, A. J. (2000). A Human Homolog of Angiotensin-Converting Enzyme. Cloning and Functional Expression as a Captopril-Insensitive Carboxypeptidase. *J. Biol. Chem.* 275 (43), 33238–33243. doi: 10.1074/jbc.M002615200

- Tong, M., Jiang, Y., Xia, D., Xiong, Y., Zheng, Q., Chen, F., et al. (2020). Elevated Expression of Serum Endothelial Cell Adhesion Molecules in COVID-19 Patients. *J. Infect. Dis.* 222 (6), 894–898. doi: 10.1093/infdis/jiaa349
- Varga, Z., Flammer, A. J., Steiger, P., Haberecker, M., Andermatt, R., Zinkernagel, A. S., et al. (2020). Endothelial Cell Infection and Endotheliitis in COVID-19. *Lancet* 395 (10234), 1417–1418. doi: 10.1016/S0140-6736(20)30937-5
- Vassiliou, A. G., Zacharis, A., Keskinidou, C., Jahaj, E., Pratikaki, M., Gallos, P., et al. (2021). Soluble Angiotensin Converting Enzyme 2 (ACE2) Is Upregulated and Soluble Endothelial Nitric Oxide Synthase (eNOS) Is Downregulated in COVID-19-Induced Acute Respiratory Distress Syndrome (ARDS). *Pharm. (Basel)* 14 (7), 695. doi: 10.3390/ph14070695
- Vickers, C., Hales, P., Kaushik, V., Dick, L., Gavin, J., Tang, J., et al. (2002). Hydrolysis of Biological Peptides by Human Angiotensin-Converting Enzyme-Related Carboxypeptidase. *J. Biol. Chem.* 277 (17), 14838–14843. doi: 10.1074/jbc.M200581200
- Wrapp, D., Wang, N., Corbett, K. S., Goldsmith, J. A., Hsieh, C.-L., Abiona, O., et al. (2020). Cryo-EM Structure of the 2019-Ncov Spike in the Prefusion Conformation. *Science* 367 (6483), 1260–1263. doi: 10.1126/science.abb2507
- Wysocki, J., Schulze, A., and Batlle, D. (2019). Novel Variants of Angiotensin Converting Enzyme-2 of Shorter Molecular Size to Target the Kidney Renin Angiotensin System. *Biomolecules* 9 (12), 886. doi: 10.3390/biom9120886
- Yeung, M. L., Teng, J. L. L., Jia, L., Zhang, C., Huang, C., Cai, J.-P., et al. (2021). Soluble ACE2-Mediated Cell Entry of SARS-CoV-2 via Interaction With Proteins Related to the Renin-Angiotensin System. *Cell* 184 (8), 2212–2228.e12. doi: 10.1016/j.cell.2021.02.053
- Zhang, H., Wada, J., Hida, K., Tsuchiyama, Y., Hiragushi, K., Shikata, K., et al. (2001). Collectrin, a Collecting Duct-Specific Transmembrane Glycoprotein, Is a Novel Homolog of ACE2 and Is Developmentally Regulated in Embryonic Kidneys. *J. Biol. Chem.* 276 (20), 17132–17139. doi: 10.1074/jbc.M006723200
- Zoufaly, A., Poglitsch, M., Aberle, J. H., Hoepler, W., Seitz, T., Traugott, M., et al. (2020). Human Recombinant Soluble ACE2 in Severe COVID-19. *Lancet Respir. Med.* 8 (11), 1154–1158. doi: 10.1016/S2213-2600(20)30418-5

Conflict of Interest: The authors declare that the research was conducted in the absence of any commercial or financial relationships that could be construed as a potential conflict of interest.

Publisher's Note: All claims expressed in this article are solely those of the authors and do not necessarily represent those of their affiliated organizations, or those of the publisher, the editors and the reviewers. Any product that may be evaluated in this article, or claim that may be made by its manufacturer, is not guaranteed or endorsed by the publisher.

Copyright © 2022 Wang, Zhao and An. This is an open-access article distributed under the terms of the Creative Commons Attribution License (CC BY). The use, distribution or reproduction in other forums is permitted, provided the original author(s) and the copyright owner(s) are credited and that the original publication in this journal is cited, in accordance with accepted academic practice. No use, distribution or reproduction is permitted which does not comply with these terms.



OPEN ACCESS

Edited by:Vikas Sood,
Jamia Hamdard University, India**Reviewed by:**Henri Gruffat,
Institut National de la Santé et de la
Recherche Médicale (INSERM),
France
Manish SHarma,
Emory University, United States***Correspondence:**Fernando Moreira Simabuco
simabuco@gmail.com
orcid.org/0000-0002-1672-9686**Specialty section:**This article was submitted to
Virus and Host,
a section of the journal
Frontiers in Cellular and
Infection Microbiology**Received:** 05 January 2022**Accepted:** 25 April 2022**Published:** 23 May 2022**Citation:**Zambalde ÉP, Pavan ICB,
Mancini MCS, Severino MB,
Scudero OB, Morelli AP, Amorim MR,
Bispo-dos-Santos K, Góis MM,
Toledo-Teixeira DA,
Parise PL, Mauad T, Dolhnikoff M,
Saldiva PHN, Marques-Souza H,
Proenca-Modena JL, Ventura AM
and Simabuco FM (2022)
Characterization of the Interaction
Between SARS-CoV-2 Membrane
Protein (M) and Proliferating Cell
Nuclear Antigen (PCNA) as a
Potential Therapeutic Target.
Front. Cell. Infect. Microbiol. 12:849017.
doi: 10.3389/fcimb.2022.849017

Characterization of the Interaction Between SARS-CoV-2 Membrane Protein (M) and Proliferating Cell Nuclear Antigen (PCNA) as a Potential Therapeutic Target

Érika Pereira Zambalde¹, Isadora Carolina Betim Pavan², Mariana Camargo Silva Mancini¹,
Matheus Brandemarte Severino¹, Orlando Bonito Scudero³, Ana Paula Morelli¹,
Mariene Ribeiro Amorim⁴, Karina Bispo-dos-Santos⁴, Mariana Marcela Góis¹,
Daniel A. Toledo-Teixeira⁴, Pierina Lorencini Parise⁴, Thais Mauad⁵,
Marisa Dolhnikoff⁵, Paulo Hilário Nascimento Saldiva⁵, Henrique Marques-Souza⁶,
José Luiz Proenca-Modena^{4,7,8}, Armando Moraes Ventura³ and Fernando Moreira Simabuco^{1*}¹ Multidisciplinary Laboratory of Food and Health, School of Applied Sciences, University of Campinas (Unicamp), Limeira, Brazil, ² Laboratory of Signaling Mechanisms, School of Pharmaceutical Sciences, University of Campinas, (Unicamp), Campinas, Brazil, ³ Department of Microbiology, Institute of Biomedical Sciences, University of São Paulo (USP), São Paulo, Brazil, ⁴ Laboratory of Emerging Viruses (LEVE), Department of Genetics, Evolution, Microbiology and Immunology, Institute of Biology, University of Campinas (Unicamp), Campinas, SP, Brazil, ⁵ São Paulo University Medical School, Department of Pathology, University of São Paulo (USP), São Paulo, Brazil, ⁶ Institute of Biology, University of Campinas (Unicamp), Campinas, SP, Brazil, ⁷ Experimental Medicine Research Cluster, University of Campinas (Unicamp), Campinas, Brazil, ⁸ Hub of Global Health (HGH), University of Campinas (Unicamp), Campinas, Brazil

SARS-CoV-2 is an emerging virus from the Coronaviridae family and is responsible for the ongoing COVID-19 pandemic. In this work, we explored the previously reported SARS-CoV-2 structural membrane protein (M) interaction with human Proliferating Cell Nuclear Antigen (PCNA). The M protein is responsible for maintaining virion shape, and PCNA is a marker of DNA damage which is essential for DNA replication and repair. We validated the M-PCNA interaction through immunoprecipitation, immunofluorescence co-localization, and PLA (Proximity Ligation Assay). In cells infected with SARS-CoV-2 or transfected with M protein, using immunofluorescence and cell fractioning, we documented a reallocation of PCNA from the nucleus to the cytoplasm and the increase of PCNA and γ H2AX (another DNA damage marker) expression. We also observed an increase in PCNA and γ H2AX expression in the lung of a COVID-19 patient by immunohistochemistry. In addition, the inhibition of PCNA translocation by PCNA I1 and Verdinexor led to a reduction of plaque formation in an *in vitro* assay. We, therefore, propose that the transport of PCNA to the cytoplasm and its association with M could be a virus strategy to manipulate cell functions and may be considered a target for COVID-19 therapy.

Keywords: SARS-CoV-2, PCNA, M protein, viral-host interaction, DNA damage

INTRODUCTION

The COVID-19 was claimed as a global public health emergency by the World Health Organization (WHO). By April 07th, 2022, more than 495 million cases were confirmed, with more than 6.17 million deaths worldwide (WHO- World Health Organization, 2020). COVID-19 is caused by SARS-CoV-2, an emerging virus from the *Coronaviridae* family of positive single-stranded RNA genome that encodes over 28 proteins, including 16 non-structural proteins (NSP1- NSP16), four structural proteins (spike, membrane, envelope, and nucleocapsid), and eight auxiliary proteins (ORF3a, ORF3b, ORF6, ORF7a, ORF7b, ORF8, ORF9b, and ORF14) (Gordon et al., 2020; Sanche et al., 2020; Wu et al., 2020). The four main structural proteins of the virion are responsible for: cell receptor recognition - spike (S); viral RNA packaging - nucleocapsid (N); and virus assembly - envelope (E) and membrane (M) proteins (Thiel et al., 2003; Chen et al., 2020; Klein et al., 2020).

Nearly two years after the start of the pandemic, no treatment has yet been successful, and the infection mechanisms are still an open question (Song et al., 2020). Many studies have been dedicated to understanding the interactome of SARS-CoV-2 with infected cells (Bouhaddou et al., 2020; Gordon et al., 2020; Li et al., 2021; Stukalov et al., 2021). The interaction between the structural protein M of SARS-CoV-2 and the human protein Proliferating Cell Nuclear Antigen (PCNA) was described with a Significance Analysis of INteractome (SAINT) score of 1.0 (Gordon et al., 2020), indicating a high probability of interaction. In addition, Stukalov et al. (2021) showed increased ubiquitination in specific regions (K13, K14, K77, K80, K248, and K254) of PCNA in cells infected with SARS-CoV-2 when compared to a control group.

M is the most abundant structural protein in the SARS-CoV-2 particle and is highly expressed (Neuman et al., 2011; Wyler et al., 2020; Alharbi and Alrefaei, 2021). M is responsible for giving and maintaining the virion's shape (Hasan and Hossain, 2020), is a three-pass membrane protein with three transmembrane domains and co-localizes with the endoplasmic reticulum (ER), Golgi apparatus, and mitochondrial markers (Hasan and Hossain, 2020; Zhang et al., 2020; Zheng et al., 2020). In addition, the M protein can interact with different coronavirus (CoVs) proteins: the N protein, which helps in viral genome packing (Hurst et al., 2005; Kuo et al., 2016; Lu et al., 2021), and the S protein, for its retention in the ER-Golgi intermediate compartment and its integration into new virions (Opstelten et al., 1995).

It was demonstrated that, in some CoVs, the M protein is highly immunogenic and induces specific T-cell responses after infection (Li et al., 2008). In SARS-CoV-2 infection, M is also targeted by the immune response and plays a critical role in virus-specific B-cell response due to its ability to induce the production of efficient neutralizing antibodies in COVID-19 patients (Pang et al., 2004; Alharbi and Alrefaei, 2021). During SARS-CoV-2 infection, the M protein can directly bind to MAVS (Mitochondrial Antiviral Signaling Protein) to inhibit the innate immune response (Fu et al., 2021). More specifically, the SARS-CoV-2 M protein antagonizes type I and III interferon (IFN)

production by targeting RIG-I/MDA-5 signaling and preventing the multiprotein complex formation of RIG-I, MAVS, TRAF3, and TBK1. This multiprotein complex blocks the activation of IRF3-induced anti-viral immune suppression, facilitating virus replication (Zheng et al., 2020; Fu et al., 2021). Although the M protein binding to MAVS mechanism has been described, other authors suggest that M is mainly involved in ATP biosynthesis and metabolic processes (Bojkova et al., 2020; Li et al., 2021), indicating that it has different functions.

The PCNA is a 36 kDa protein, well-conserved in all eukaryotic species, from yeast to humans (Strzalka and Ziemienowicz, 2011). This protein controls essential cellular processes such as DNA replication and damage repair, transcription, chromosome segregation, and cell-cycle progression (Tsurimoto, 1998; Paunesku et al., 2001; Maga and Hübscher, 2003; Naryzhny et al., 2005; Moldovan et al., 2006; Strzalka and Ziemienowicz, 2011). It has been dubbed the “maestro of the replication fork” (Moldovan et al., 2007). PCNA, as a homotrimer, encircles duplex DNA, forming a ring-shaped clamp (Warbrick, 1998). The PCNA is a scaffolding protein that interacts with several other proteins, mainly involved in DNA replication and repair (Maga and Hübscher, 2003). In most cell types, PCNA is exclusively nuclear, but studies demonstrated that it could go to the cytoplasm. In cancer cells, cytoplasmic PCNA was described as a regulator of the cell metabolism binding to enzymes involved in the glycolysis pathway, regulation of the energy-generating system in mitochondria, cytoskeleton integrity, and other cellular signaling pathways through binding to cytoplasmic and membrane proteins (Naryzhny and Lee, 2010). PCNA is cytosolic in mature neutrophils and acts in immune response, including to virus infection (Witko-Sarsat et al., 2010; Bouayad et al., 2012; Olaisen et al., 2015; Ohayon et al., 2019).

Although many studies indicate the PCNA role in DNA virus infection, its association with RNA viruses is poorly understood. To our knowledge, the only study that observed a function of PCNA in an RNA virus was with the Bamboo Mosaic virus (BaMV), a common virus in plants. In this study, the authors demonstrated that PCNA goes to the cytoplasm and directly binds to the BaMV replication complex, downregulating the replication efficiency of the virus (Lee et al., 2019).

In this study, we validated the M-PCNA interaction and demonstrated that the M protein facilitates the transport of PCNA from the nucleus to the cytoplasm. M expression and SARS-CoV-2 infection were associated with increased phosphorylation of H2AX and an increased PCNA expression. Drugs that block PCNA translocation from nucleus to cytoplasm inhibited virus replication. This indicates a new mechanism in SARS-CoV-2 replication and a potential target for therapy.

MATERIALS AND METHODS

Cell Culture

The VeroE6 (African green monkey, *Cercopithecus aethiops*, kidney) and HEK293T (Human embryonic kidney) cell lines

were cultivated in Dulbecco's modified Eagle (DMEM) (Thermo Scientific #12100-046) medium, supplemented with 10% fetal bovine serum (FBS # 12657029) and 1% penicillin/streptomycin (Gibco #15140-122). Cells were maintained at 37°C in a humidified atmosphere containing 5% carbon dioxide.

Viral Infection

An aliquot of SARS-CoV-2 SP02.2020 (GenBank accession number MT126808) isolate was kindly donated by Dr. Edison Luiz Durigon (Institute of Biomedical Sciences, University of São Paulo). Vero E6 cells were used for virus propagation in the Biosafety Level 3 Laboratory (BSL-3) of the Laboratory of Emerging Viruses (Institute of Biology, State University of Campinas). Viral infections were performed in Vero cells seeded in 24-well plates (5×10^5 cells/well) for the experiments with treatments and immunofluorescence assays, and six-well plates (1×10^6 cells/well) for Western blots. A multiplicity of infection (MOI) of 0.3 was used for all experiments.

Cloning

To do the FLAG-tagged protein expression, a modified pcDNA 3.1 (+) (Thermo Fisher Scientific) was generated by cloning the FLAG peptide coding sequence upstream of the multiple cloning sites, using the *NheI* and *BamHI* restriction sites, and generating the pcDNA-FLAG vector (Oliveira et al., 2013). The full-length of M, N, and E genes were codon-optimized, synthesized (Geneart -Thermo Fisher Scientific), and cloned into pcDNA-FLAG, generating plasmid pFLAG-M, pFLAG-N, and pFLAG-E. The pFLAG-green fluorescent protein (GFP) (Amaral et al., 2016) was used as the control plasmid for the expression of a non-related protein in the immunoprecipitation assays.

Transfection

VeroE6 and HEK293T cells were seeded for 24 hours before transfection. Transfection was performed with Lipofectamine (Thermo Scientific - #20071882) and PLUS reagents (Thermo Scientific - #15338100). The protocol of plasmids' transfection is described by (Amaral et al., 2016). For immunofluorescence, the cells were seeded and transfected in 24-well plates; for western blotting in 6-well plates; and for immunoprecipitation in 100 mm plates.

Immunoprecipitation

For anti-FLAG immunoprecipitation, HEK293T cells cultivated in 100 mm diameter dishes expressing the FLAG-tagged GFP, E, M, and N proteins were washed twice with PBS and harvested by pipetting up and down in PBS after 48 hours. Cells were resuspended in 500 μ L of lysis buffer (50 mM Tris-HCl, pH 7.4, 150 mM NaCl, 1 mM EDTA, 1% Triton X-100) containing protease inhibitor cocktail (Roche). Protein lysates were incubated and shaken on ice for 15 min and centrifuged at $12,000 \times g$ for 10 min at 4°C. Supernatants were collected and protein quantification was performed using a BCA protein assay kit (Thermo Scientific). A total of 2,000 μ g of protein extract was used to perform the immunoprecipitation, so the samples were

diluted with lysis buffer without inhibitors and incubated overnight at 4°C with 30 μ L of anti-FLAG agarose-coupled beads (#A2220, Sigma-Aldrich) under mild agitation. Subsequently, the beads were washed five times with 600 μ L of ice-cold TBS (50 mM Tris-HCl, pH 7.5, 150 mM NaCl) and eluted with 300 ng/L of FLAG peptide (#F4799, Sigma-Aldrich) for four hours under moderate agitation (Pavan et al., 2016). Supernatants were collected and stored at -20°C for immunoblotting analysis.

For reverse immunoprecipitation, in HEK293T cells, the same protocol of protein lysis and quantification were performed. A total of 300 μ g of protein extract was used to perform the immunoprecipitation. The samples were diluted with lysis buffer without inhibitors and incubated overnight at 4°C with anti-PCNA antibody (1:500, #2586, Cell Signaling) under mild agitation. Subsequently, 30 μ L of protein A/G Agarose (#20421, Thermo Scientific) was added to each sample, followed by mild agitation for two hours. Samples were washed five times with a wash buffer (25 mM Tris-HCl, pH 7.5, 150 mM NaCl) and the elution was performed with Laemmli Buffer with SDS 1%. Supernatants were collected and stored at -20°C for immunoblotting analysis.

Immunofluorescence

Sterilized glass coverslips were treated with 6M HCL (Synth) and placed in each well on 24-well plates. Vero E6 cells were seeded at a density of 1×10^5 cells in DMEM with 10% FBS. After the experimental procedures, the wells were washed 1 \times with PBS, permeabilized with ice-cold methanol 100% for 10 minutes, or fixed with paraformaldehyde 4% (PFA - Sigma Aldrich 158127) for 15 minutes. The cells were then permeabilized with PBS-Tween-20 0.1% (PBS-T - Sigma Aldrich P1379) for 10 minutes, blocked with 1% BSA-Tween-20 0.3% for 30 minutes, and incubated overnight with a solution containing the primary antibody in (1:200) 1% BSA-Tween-20 0.3% at 4°C. After a washing step with PBS (three times for 10 minutes each), a solution containing the secondary antibody (1:250) and PBS-Tween20 0.1% was added to each well for one hour in a dark chamber. The wells were then washed three times with PBS (for 10 minutes each), a solution containing Hoechst (Sigma Aldrich - 861405 - 1:1,000) was added for 10 minutes, followed by three times washing with PBS (for 10 minutes each), the glass coverslips were removed from the wells with the aid of tweezers and added to glass slides with 5 μ L of Glycerol (Sigma Aldrich G5516). The primary antibodies used were: PCNA (Cell Signaling #2586), N (Invitrogen #MA5-35943), FLAG (Sigma # F3165). The secondary antibodies used were: Alexa-Fluor-594 Goat anti-Rabbit (Jackson ImmunoResearch #711-585-152), Alexa-Fluor-488 Goat Anti-Mouse (Jackson ImmunoResearch #705-545-003). To quantify the signal on immunofluorescences we used the ImageJ software to transform the images in 8 bit (grayscale), and check-in Set Measurements the options: Area and Integrated density; select an ROI of nuclei area (Hoechst staining) to determinate the fluorescence signal on nuclei; the cytoplasmatic fluorescence signal was obtained by a total cell - nuclei area ROI. Besides that, we computed the signal of the background (region without

cells). Finally, the Corrected Cell Total Fluorescence (CTCF) was calculated by multiplication of the integrated density of gray of nuclei or cytoplasm by their respective areas and subtracting the background signal.

Subcellular Fractioning

Vero E6 cells were seeded at 8×10^6 in a P100 plate and transfected with pFLAG-GFP or pFLAG-M. After 48 hours, the subcellular fractionation was finalized (Baldwin, 1996). Briefly, the cytoplasmic fraction was first isolated from the nuclear solution using a cytoplasmic buffer (10 mM HEPES; 60 mM KCl; 1 mM EDTA; 0.075% NP-40; 1 mM DTT; protease inhibitor 1 \times) (pH=7.6) and centrifuged in 1,400 \times g for 30 minutes. The cytoplasmic supernatants were collected into a new tube. The nuclear pellet was washed with cytoplasmic buffer without NP-40 two times followed by a five-minute centrifugation at 1,000 \times g. The final pellet was resuspended with nuclear buffer (20 mM TrisCl; 420 mM NaCl; 1.5 mM $MgCl_2$; 0.2 mM EDTA; 25% glycerol; protease inhibitor 1 \times) (pH=8.0) and incubated on ice for 10 minutes, and vortexed periodically. Finally, the cytoplasmic and nuclear solutions were centrifuged at 12,000 \times g for 10 minutes and the supernatants were collected into new tubes. The quantification was performed by BCA.

Proximity Ligation Assay (PLA)

For PLA protocol, Vero E6 cells were grown on chambered slides at a confluency of 70% and transfected with pFLAG-M. After 24 hours, cells were fixed with ice-cold methanol for 15 min and permeabilized with 0.1% TritonX-100 in PBS. The next steps faithfully followed the manufacturer's specifications (Duolink[®] *In Situ* – Sigma-Aldrich). Briefly, cells were blocked and stained with primary antibodies (anti-FLAG 1:400 – Sigma F7425 and anti-PCNA 1:400 – Sta Cruz sc-56) and PLA probes (anti-mouse MINUS – DUO92004 and anti-rabbit PLUS – DUO92002). Then, cells were incubated with Ligase for 30 minutes (37°C) and Polymerase for signal amplification for 100 minutes (37°C) (Duolink[®] *In Situ* Orange – DUO92102). For negative controls, cells were stained, missing one of the primary antibodies, or both. After all PLA protocol steps, cells were stained with anti-FLAG 1:400 and anti-rabbit Alexa Fluor 488 1:1,000 (Invitrogen – A-11008) to identify transfected cells. Nuclei were stained with DAPI. After the respective washes, slides were mounted with Fluoromount-G (Invitrogen). The contrast was evenly enhanced in all presented images for better visualization of PLA dots.

Confocal Microscopy

For co-localization analysis, images were taken with a Zeiss LSM 780 NLO confocal microscope coupled to a HeNe (543 nm), an Argon (488 nm) and a Diode (405 nm) lasers (Core Facility for Scientific Research – University of Sao Paulo (CEFAP-USP)). Images were acquired with an objective α Plan-Apochromat 100 \times /NA 1.46 in oil immersion. Fluorescent signal was detected on a 32 channel GaAsP QUASAR detector with the following parameters: Alexa Fluor

594 (578 – 692 nm), Alexa Fluor 488 (491 – 587 nm), DAPI (412 – 491 nm). Pinhole was set to 1 airy unit, and z-stacks were taken with intervals of 340 nm. Presented images show a single representative z-stack. Overlap in signal between different channels was measured with Plot Profile plugin on ImageJ. Images were contrast-enhanced for better visualization.

Western Blotting

The proteins were collected from Vero E6 and HEK293 cells using a cell lysis buffer (50 mM Tris-Cl pH 7.5; 150 mM NaCl, 1 mM EDTA, 1% Triton x-100, and protease and phosphatase inhibitor cocktail). To obtain the lysates, cells were maintained with lysis buffer for 15 minutes on ice and centrifuged at 12,000 \times g for 10 minutes. Samples containing total protein were separated by SDS-PAGE and transferred to nitrocellulose membranes. Membranes were blocked for one hour at room temperature (RT) with 5% non-fat powdered milk dissolved in TBS-Tween-20 (TBS-T) (50 mM Tris-Cl, pH 7.5; 150 mM NaCl; 0.1% Tween-20), incubated overnight (4°C) with primary antibodies and with secondary antibodies against mouse or rabbit IgG conjugated with peroxidase (Amersham) for one hour at RT. The membranes were washed three times with TBS-T, and incubated with the SignalFire ECL Reagent (Cell Signaling Technology) for protein bands visualization. The band's densitometry was performed using ImageJ software v1.53 (National Institutes of Health). The following antibodies were used: anti-PCNA (#2586); anti- γ H2AX (#9718); anti- β -actin (#4967) (Cell Signaling), anti- α -tubulin (CP06) (Calbiochem), anti-N (MA5-35943) (Invitrogen), anti-laminaA/C (#A303-430A) (Bethyl) and anti-FLAG (#A2220) (Sigma).

Immunohistochemistry

Lung tissue sections, obtained *via* Minimally Invasive Autopsies, (COVID-19 case and a control lung tissue of a non-smoker subject) were stained in silanized slides (Sigma Chemical Co. St. Louis, Missouri, EUA). Briefly, the histological sections were deparaffinized in xylene, rehydrated through a graded series of ethanol, and kept in a tri-phosphate buffer (TBS) pH 7.4. After deparaffinization, slides were hydrated for five minutes in graded alcohol series (100%, 95%, 70%, and H₂O) and incubated in Tris-EDTA for 50 minutes at 95°C pH 9.0. The blockage of the endogenous peroxidases was done by hydrogen peroxide 10v (3%).

The slides were then incubated with Ab mix (TBS (1%), BSA (4%), and Tween20 (0.02%)) for 20 minutes at RT followed by treatment overnight at 4°C with anti- γ -H2AX (Cell Signaling #9718S) diluted 1:500 in Ab mix or anti-PCNA diluted 1:1000 (DAKO #M0879). The slides were then washed twice in TBS (1%) and finally incubated for one hour at RT with 1:500 goat anti-rabbit/mouse HRP polymer detection kit – ImmunoHistoprobe Plus (ADVANCED-BIOSYSTEMS) for 30 minutes at 37°C). The diaminobenzidine (DAB) was used as a chromogen (Sigma-Aldrich Chemie, Steinheim, Germany). Finally, the counterstaining was done with Harris Hematoxylin (Merck,

Darmstadt, Germany), and the slides were mounted with a coverslip in Permount (Fischer #SP15-500). The use of this material for research purposes has been previously approved by the Institutional Ethical Board CAAE #30364720.0.0000.0068).

Anti-Viral *In Vitro* Efficacy Assay

Lung tissue sections A plaque assay was performed as described in Kashyap et al. (2021). Briefly, after seeding, Vero E6 (8×10^5 cells per well, 6-well plates) were incubated overnight and infected with 200 PFU per well. PCNA-I1 (Cayman #20454) or Verdinoxor (Cayman #26171) were added at final concentrations of 0.5 μ M or 0.1 μ M and 0.1 μ M or 1 μ M, (Lu and Dong, 2019) in overlays composed of DMEM supplemented with 10% FBS plus carboxymethylcellulose sodium salt (Sigma-Aldrich #C5678) 2%, immediately post-viral adsorption. A MTT cell proliferation assay (Roche #11465007001) was done to verify the toxicity of the drugs (**Supplementary Figure S5**). After four days, cells were fixed with formaldehyde and stained with crystal violet to count plaques.

Statistical Analysis

Data are presented as mean \pm Standard Deviation (SD). Statistical analysis of the data was performed by Student's t-test or ANOVA. P-values of ≤ 0.05 were considered

statistically significant. All experiments were performed in biological duplicates. The odds ratio was calculated to verify if the translocation of the PCNA to the cytoplasm was dependent on the M transfection. A total of 147 cells were analyzed. A value of odds ratio greater than one indicates that the event observed is dependent on the object analyzed.

RESULTS

SARS-CoV-2 Structural Proteins Interact With PCNA in HEK293T Cells

In the study by Gordon et al. (2020), the interactome of the structural and non-structural proteins of SARS-CoV-2 was performed in HEK293T cells (Gordon et al., 2020). The analysis of affinity-purification–mass spectrometry (AP-MS)-based proteomics showed that PCNA interacts with E and M SARS-CoV-2 proteins. In our study, we validated this interaction through an anti-FLAG immunoprecipitation assay (**Figure 1A**). FLAG-tagged GFP, E, M, and N proteins were expressed in HEK293T cells and immunoprecipitated with anti-FLAG antibodies. As a result, we identified that PCNA co-immunoprecipitated with the E and M SARS-CoV-2

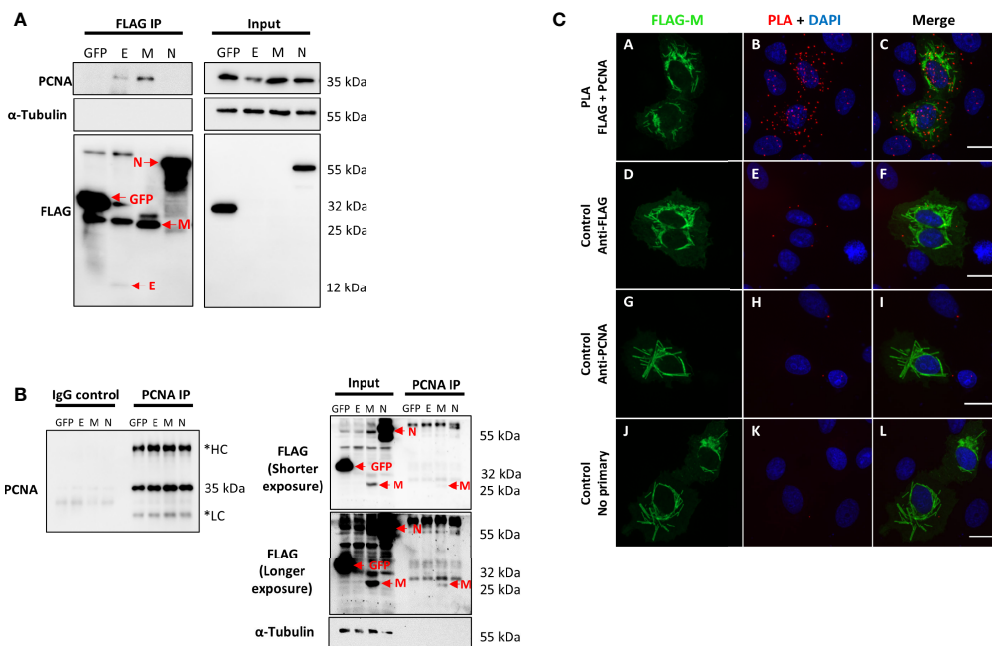


FIGURE 1 | SARS-CoV-2 structural proteins interact with PCNA in HEK293T and Vero E6 cells. FLAG-tagged GFP, E, M, and N proteins (indicated at the top of the panel) were expressed by transfection in HEK293T cells. Immunoprecipitation with anti-FLAG (**A**) or anti-PCNA antibodies (**B**) was performed (indicated on the panel's top). Blots were done with the primary antibodies indicated on the panel's left, and molecular weight markers sizes are indicated on the right. (**A**) PCNA was identified as an interactor of SARS-CoV-2 E and M proteins. (**B**) Immunoprecipitation of endogenous PCNA confirmed that protein M co-immunoprecipitated with PCNA. These data were obtained in one biological replicate. *HC, Heavy Chain; LC, Light chain. Red arrows indicate specific bands. (**C**) Vero E6 cells were transfected with pFLAG-M and submitted to ice-cold methanol fixation after 24h, followed by incubation with the primary antibodies, as indicated on the left, and PLA staining protocol. Panels (**A–C**) show positive PLA dots for FLAG and PCNA staining in transfected cells. Little to no signal is detected in the respective controls omitting one or both primary antibodies [panels (**D–L**)]. Images are representative of two independent experiments. Nuclei were stained with DAPI. All images were taken at 63 \times magnification with a ZEISS Axio Vert.A1 microscope.

proteins but not with the N protein, which is expected since PCNA was not identified as an interactor of N protein (Gordon et al., 2020). Anti-FLAG immunoprecipitation confirmed the interaction between M and PCNA in two independent experiments (**Supplementary Figure S1**). We also confirmed that PCNA and M interact, through a reverse immunoprecipitation assay (**Figure 1B**), in HEK293T cells previously transfected with FLAG-tagged GFP, E, M, and N. We identified that only FLAG-tagged M co-immunoprecipitated with PCNA, revealing a more specific interaction between these proteins. Furthermore, we explored the interaction between FLAG-M and PCNA by proximity ligation assay (PLA). Vero E6 cells expressing FLAG-M were fixed 24 h.p.t. (hours post-transfection) and labeled with primary antibodies against FLAG (rabbit) and PCNA (mouse), followed by PLA probes conjugated to anti-rabbit or anti-mouse. PLA signal is emitted when probes attached to primary antibodies are closer than 40 nm, indicating protein interaction. As negative controls, transfected cells were labeled with only one of the primary antibodies or omitting both. **Figure 1C** (panels A-C and **Supplementary Figure S2**) shows positive PLA dots in transfected cells, while minimal or no signal is seen in the respective controls (**Figure 1C** – panels D-L). Confocal microscopy analysis of the PLA assay also showed that the M-PCNA interaction occurs in the cytoplasm, indicating a possible translocation of the PCNA to the cytoplasm, induced by the M protein (**Supplementary Figure S3**).

SARS-CoV-2 M Expression in Vero E6 Cells Induces PCNA Translocation to the Cytoplasm

To better understand how the interaction of M-PCNA could be acting on the cells, we conducted immunofluorescence (IF) assays in Vero E6 cells expressing FLAG-M. 24 hours after transfection, cells were stained and analyzed by widefield microscopy (**Figure 2A**). Although PCNA did not entirely co-localize to the structures where M is present, we observed that in transfected cells, PCNA presented a more cytosolic pattern when compared to the non-transfected ones, as indicated by plot profile analysis (**Figure 2A** – Arrows 1 and 2). To further investigate this phenomenon, we quantified the fluorescence intensities of nuclear and cytoplasmic PCNA in cells expressing FLAG-M and non-transfected cells. **Figure 2B** shows that in non-transfected cells, PCNA has a propensity to be nuclear, but under FLAG-M expression, the PCNA is translocated to the cytoplasm. We also evaluated the translocation of PCNA to the cytoplasm by odds ratio. The odds ratio for cytoplasmic PCNA with FLAG-M expression was 6.34 (Confidence Interval 95% = 2.83-13.3) compared to non-transfected cells, indicating the correlation of M protein with the translocation of the PCNA to the cytoplasm. In addition, the subcellular fractionation of Vero E6 cells transfected with FLAG-M or FLAG-GFP was carried out (**Figure 2C**). In agreement with IF data, FLAG-M transfected cells showed an evident reduction of PCNA in the nuclear fraction, while it remained nuclear in cells expressing FLAG-GFP (**Figure 2C**).

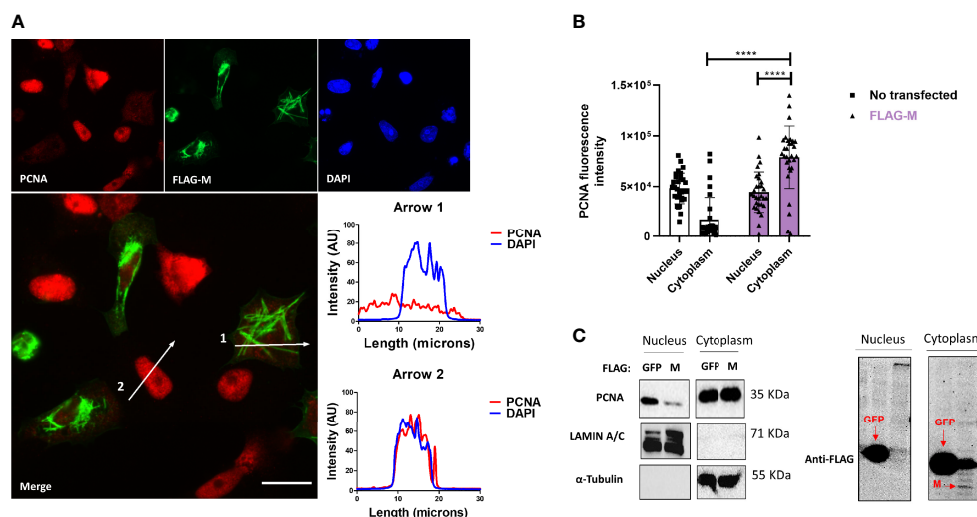


FIGURE 2 | FLAG-M expression promotes PCNA translocation to cytoplasm. **(A)** Vero E6 cells expressing FLAG-M protein, 24h after transfection, were fixed and stained for FLAG-M (green), PCNA (red), and DAPI. Graphs show plot profile intensities for PCNA and DAPI channels in the cross-sections indicated by arrows 1 and 2. Images are representative of two independent experiments. Scale bar 20 μ m. **(B)** PCNA localization was analyzed through fluorescence intensity in non-transfected and FLAG-M transfected cells. Briefly, the nuclei area stained with DAPI was selected manually and the ROI (region of interest) obtained was used to measure PCNA intensities on nucleus and cytoplasm. Fluorescence intensity was quantified in grayscale on ImageJ. This data is representative of two independent experiments. The data represent mean \pm SD (n=30). For statistical analysis, Two-way ANOVA and multiple comparison Bonferroni's tests were used. ****p < 0.0001 were considered statistically significant. **(C)** Vero E6 cells were transfected with vectors to express FLAG-tagged M or GFP proteins, and after 48 hours cellular fractionation followed by Western blotting was performed. LAMIN A/C and α -Tubulin proteins were used as controls for nuclear and cytosolic fractions, respectively. The expression of the transfected proteins is shown in the right panel. Western blot images are representative of one independent experiment.

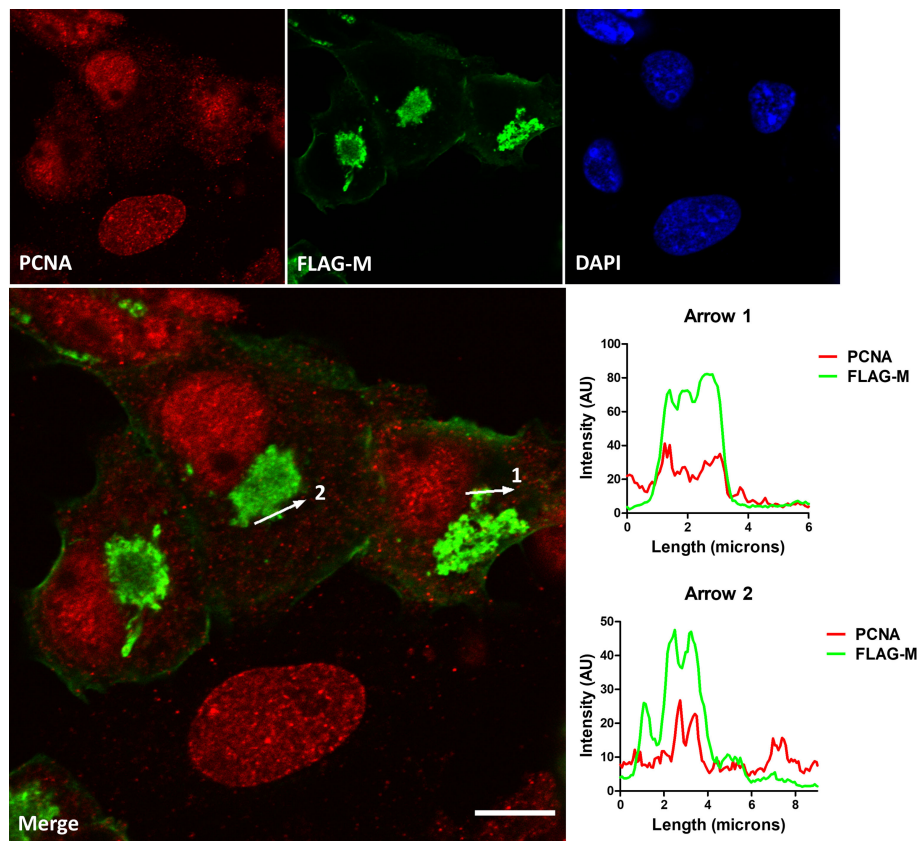


FIGURE 3 | Co-localization of FLAG-M and PCNA by confocal immunofluorescence. Vero E6 cells expressing FLAG-M and stained for PCNA (red) and FLAG-M (green) were analyzed by confocal microscopy. The plot profile of two arrowed areas (arrows 1 and 2) indicates an overlap in signals of both proteins, as shown in the graphs on the right. Images were taken at 100× magnification with a Zeiss LSM-780-NLO microscope. Scale bar 10 μ m.

These results indicate that M protein acts on PCNA translocation from the nucleus to the cytoplasm.

SARS-CoV-2 M Protein Interacts With PCNA in the Cytoplasm of Vero E6 Cells

To confirm the interaction between M and PCNA, we performed confocal immunofluorescence of FLAG-M transfected cells. Plot profile analysis shows an overlap between FLAG-M and PCNA signals, indicating the proximity of the proteins (**Figure 3**). Moreover, as mentioned before, the interaction between FLAG-M and PCNA was detected by PLA (**Figure 1C**), and the co-localization of PLA puncta with FLAG-M was shown by confocal microscopy (**Supplementary Figure S3**). Taken together, these results indicate the ability of M protein in inducing PCNA translocation from the nucleus, and to interact with it in the cytoplasm.

FLAG-M Expression Increases DNA Damage Marker Levels in HEK293T and Vero E6 Cells

PCNA is one of the essential proteins for DNA replication and DNA repair, and it is also known as a DNA damage marker. To address whether M expression could be related to the induction

of DNA damage. We transfected HEK293T and Vero E6 cells with FLAG-M and looked at γ H2AX and PCNA expression levels since both proteins elevated expression is associated with DNA damage. In HEK293T transfected cells, we could observe a slight increase in the levels of PCNA and γ H2AX (**Figure 4A**), but no significant difference was observed in the Vero E6 cell line (**Figure 4B**). Because transfection efficiency could be a limiting factor for detecting inconspicuous events like DNA damage, we also explored γ H2AX levels in transfected Vero E6 cells by immunofluorescence (**Figure 4C**). Comparing the γ H2AX fluorescence intensity in FLAG-M transfected cells with non-transfected cells, we found a significant increase in the phosphorylation level of H2AX, suggesting that M involvement with PCNA may promote DNA damage (**Figure 4D**).

SARS-CoV-2 Infection Induces PCNA Translocation to the Cytoplasm and Promotes DNA Damage

To verify if our findings concerning M protein and the DNA damage markers PCNA and γ H2AX were also reproducible during infection, we evaluated the effect of SARS-CoV-2 infection in Vero E6 cells. Immunofluorescence analysis

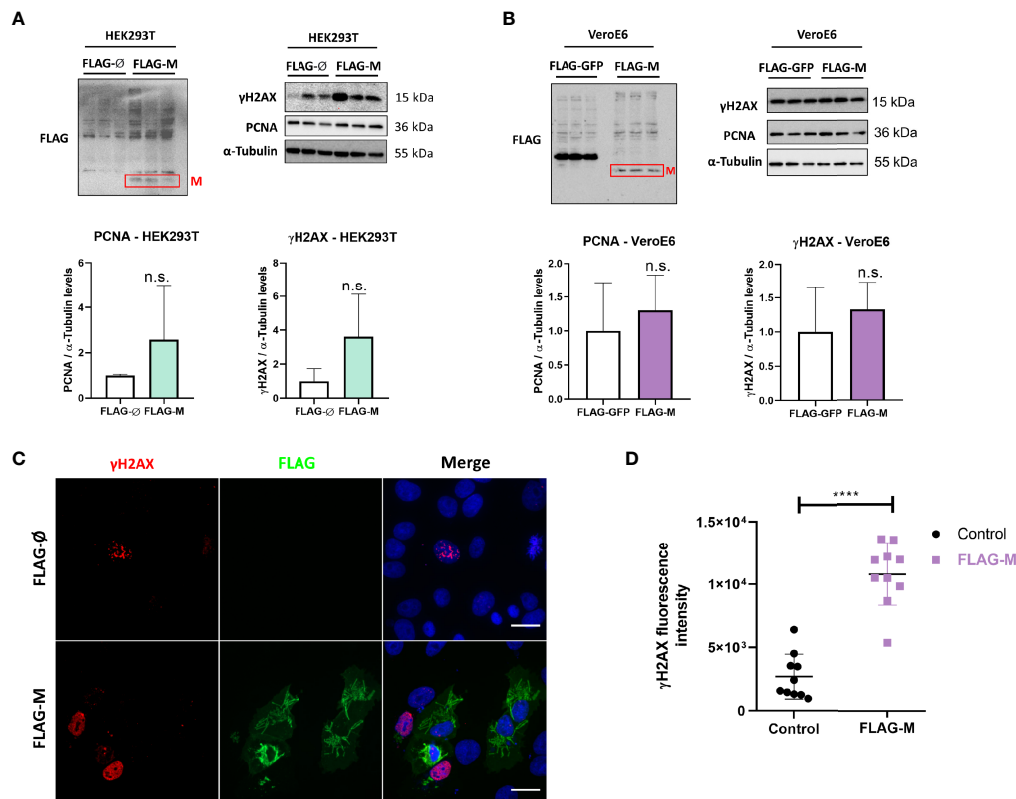


FIGURE 4 | PCNA and γ H2AX levels in transfected cell lines. **(A)** Detection of PCNA and γ H2AX levels in HEK293T cells transfected with pFLAG-M compared to pFLAG (empty vector). **(B)** Detection of PCNA and γ H2AX levels in Vero E6 cells transfected with pFLAG-M compared to pFLAG-GFP. Graphs show a slight increase in normalized protein levels; however, the statistical test does not show significance. Western blotting data in **(A, B)** are representative of one independent experiment. **(C)** Immunofluorescent staining of FLAG-M (green) and γ H2AX (red) in Vero E6 cells 24 hours post-transfection. Images are representative of two independent experiments. Scale bar 20 μ m. **(D)** Fluorescence intensity quantification of γ H2AX levels in FLAG-M transfected versus non-transfected cells. Fluorescence intensities in the nucleus were measured as described in **Figure 2B**. Data represent mean \pm SD in samples from 2 independent experiments ($n = 10$). For statistical analysis, a two-tailed unpaired T-test was conducted. n.s., non-significant, **** $p < 0.0001$ was considered statistically significant.

showed PCNA staining in the cytoplasm of infected cells, with PCNA presenting mainly a nuclear pattern on mock control (**Figure 5A**). The results (**Figures 5B, C**) show a higher intensity of PCNA in the cytoplasm of infected cells with a concomitant reduction in its nuclear signal compared to mock-infected cells. In addition, a higher γ H2AX fluorescence intensity was observed in infected cells compared to non-infected cells, which confirms that the infection promotes DNA damage (**Figures 5D, E**). We also evaluated PCNA and γ H2AX levels by western blotting in HEK293T and Vero E6 infected cells (**Figure 5F**). The effect observed during infection is a higher expression of PCNA and phosphorylation of histone H2AX in both cell lines (**Figures 5G, H**).

We then compared PCNA (top panels) and γ H2AX (bottom panels) expression levels in lung sections obtained from control and COVID-19 patients through immunohistochemistry assay (**Supplementary Figure S4**). Our results indicate high expression of both markers in COVID-19 patient (right panels), suggesting the involvement of both PCNA and γ H2AX in SARS-CoV-2 infection *in vivo*.

Stabilization of PCNA Trimer by PCNA-I1 or Blockage of CRM-1 Transporter by Verdinexor Inhibits SARS-CoV-2 Replication

Our data indicate that PCNA translocates to the cytoplasm after M protein expression or SARS-CoV2 infection. To analyze if this phenomenon plays a role in the replicative cycle of the virus, two inhibitors of this transport were used to prevent the PCNA migration to the cytoplasm and test their possible anti-viral activity. The inhibitor of PCNA (PCNA I1) prevents the transportation of the PCNA to the cytoplasm by stabilizing its trimer form in the nucleus. Verdinexor is a selective inhibitor of nuclear export protein exportin-1 (XPO1), also called Chromosome Region Maintenance 1 (CRM1), and was already described as essential in the PCNA translocation (Bouayad et al., 2012; Perwitasari et al., 2016). Vero E6 cells were tested for PCNAi and Verdinexor toxicity, showing that 10 to 0.1 μ M are safe concentrations for both drugs, since they did not reduce cells viability (**Figure S5**). Vero E6 cells were then infected and submitted to a dose-dependent anti-viral *in vitro* efficacy assay.

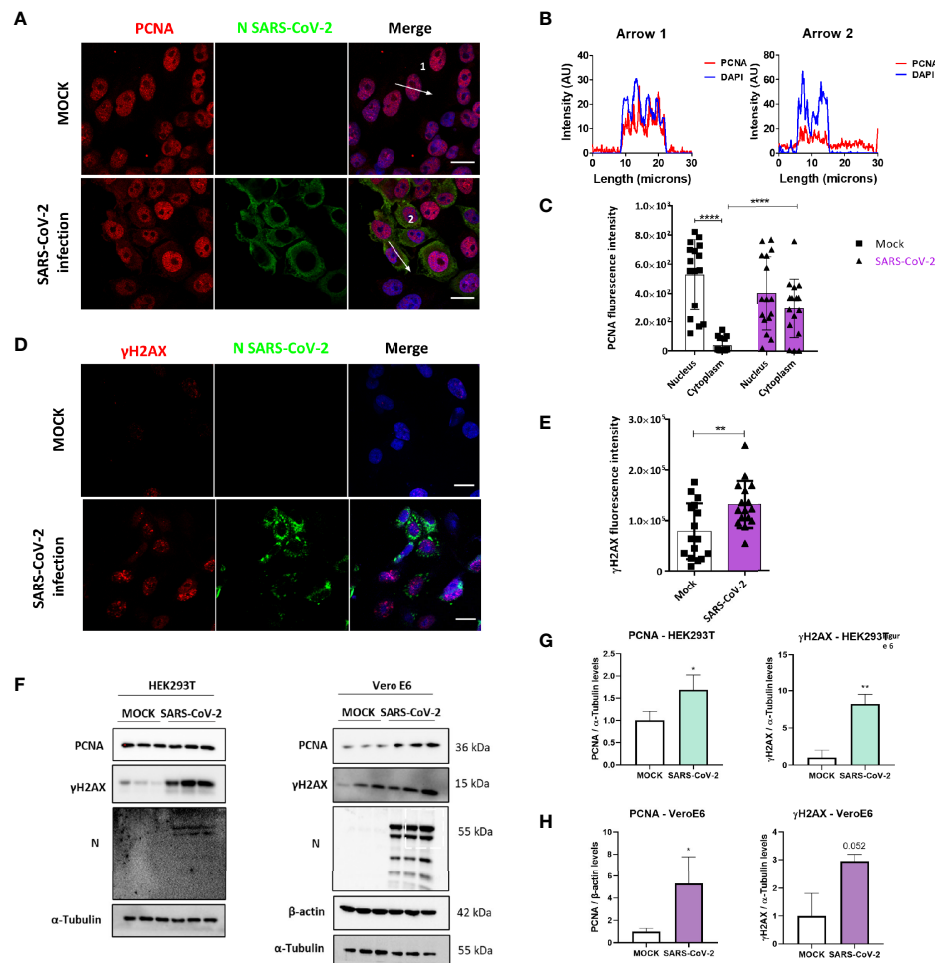


FIGURE 5 | SARS-CoV-2 infection promotes PCNA translocation to the cytoplasm and enhances PCNA and γ H2AX expression. **(A)** Vero E6 cells were infected with SARS-CoV2 (MOI 0.3), and 24 hours post-infection immunofluorescence was performed for N (green) and PCNA (red). Scale bars 20 μ m. **(B)** Plot profile intensities for PCNA and DAPI channels in the cross-sections, indicated by arrows 1 and 2. Images are representative of two independent experiments. Scale bar 20 μ m. **(C)** PCNA localization was analyzed through fluorescence intensity mock versus infected cells, as described in **Figure 2B**. White bars = mock, purple bars = SARS-CoV-2 infection. **(D)** Vero E6 cells were infected with SARS-CoV2 (MOI 0.3), and 24 hours post-infection immunofluorescence was performed for N (green) and γ H2AX (red). Scale bars 20 μ m. **(E)** Fluorescence intensity of γ H2AX in the nucleus was analyzed in mock and infected cells, as described in **Figure 2B**. White bars = mock, purple bars = SARS-CoV-2 infection. **(F)** Western blotting analysis of PCNA and γ H2AX levels in HEK293T and Vero E6 cells infected with SARS-CoV-2 compared to mock. Statistical analysis for normalized expression levels of PCNA and γ H2AX are shown for HEK293T **(G)** and Vero E6 cells **(H)**. Data represent means \pm SD from 1 independent experiment. For fluorescence intensity ($n = 20$), data were analyzed by Two-way ANOVA and multiple comparisons Bonferroni's test. * $p < 0.05$ and **** $p < 0.0001$ were considered statistically significant ** $p < 0.01$.

The results (**Figure 6**) indicate that PCNAi 0.5 μ M and Verdinexor 0.1 μ M have the best effects against SARS-CoV-2, reducing the viral replication roughly by 20% and 15%, respectively, compared to the DMSO.

DISCUSSION

After nearly two years since the start of the COVID-19 pandemic, understanding the underlying mechanisms of SARS-CoV-2 infection and the search for treatment are still in high demand. Large-scale analysis of SARS-CoV-2 human infection interactome

indicated several protein-protein interactions that require further validation (Bouhaddou et al., 2020; Gordon et al., 2020; Li et al., 2021; Stukalov et al., 2021). In this work, we aimed to characterize the interactions of viral proteins and PCNA. According to Gordon et al. (2020), the score of SAINT probability of PCNA for E protein was zero (a low score of interaction probability), and for M was 1.0 (a high score of interaction probability), while PCNA did not appear as an interactor for N protein. Through immunoprecipitation and PLA assays (**Figure 1**), we validated the M-PCNA interaction. The E-PCNA interaction was not detected in the reverse immunoprecipitation (PCNA pull down, **Figure 1B**), and we focused on the M-PCNA interaction.

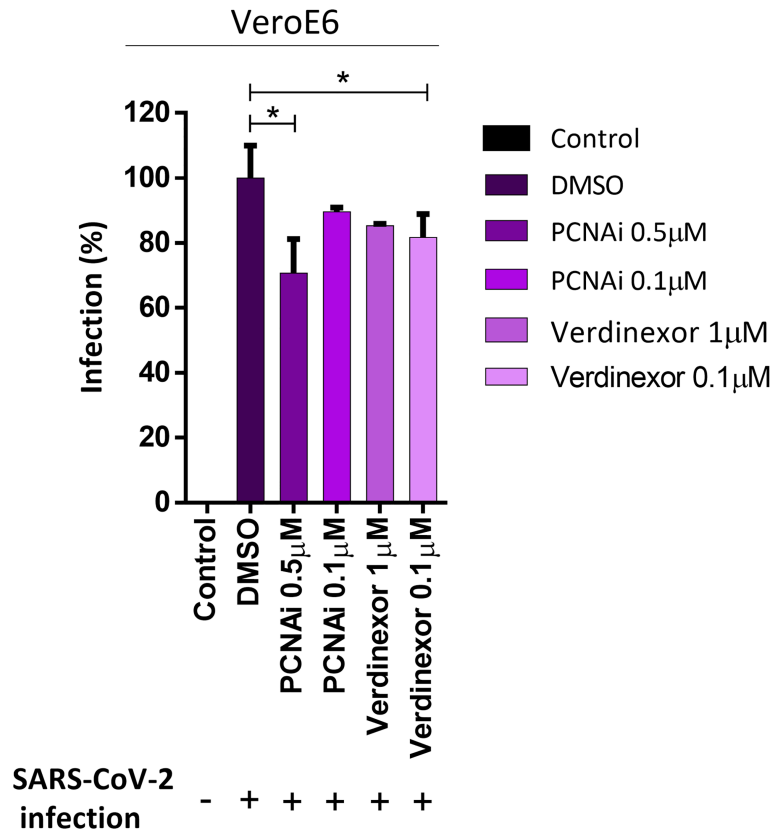


FIGURE 6 | PCNA I1 and Verdinexor inhibit SARS-CoV-2 viral replication *in vitro*. Vero E6 cells were infected with SARS-CoV-2 as described in the anti-viral *in vitro* efficacy assay (see Methods), for one hour, then DMSO, PCNA I1 0.5 and 0.1 µM or Verdinexor 1 and 0.1 µM were added to overlay media one hour after virus adsorption. The viral load was assessed by plaque assay after four days of incubation. This data is representative of two independent experiments. T-test was used for independent comparisons between DMSO versus PCNA I1, and DMSO versus Verdinexor. * $p < 0.05$ were considered statistically significant.

PLA assay indicates that M-PCNA interaction occurs in the cytoplasm (**Figure 1C**), and to better characterize it, we performed a co-localization assay by immunofluorescence and subcellular fractioning. Our data indicate that in M expression (**Figure 2**) or upon SARS-CoV-2 infection (**Figures 5A–C**), PCNA translocates from nucleus to cytoplasm. In agreement with PLA data, upon M expression there is also a partial co-localization among M and PCNA in the cytoplasm documented by confocal microscopy (**Figure 3** and **Supplementary Figure S3**). This can be hypothesized as a need for the virus to have PCNA partially translocated from the nucleus to the cytoplasm, and that M is responsible, at least in part, for this translocation in the context of the viral infection.

PCNA acts as a co-factor for DNA polymerases in normal conditions, being essential for DNA replication (O'Donnell et al., 2013; Siddiqui et al., 2013). PCNA also participates in DNA repair, on the metabolism of DNA, and chromatin by recruiting various enzymes, and not only by acting as a scaffold and localizing these factors, but also activating their enzymatic activities (Choe and Moldovan, 2017). Aside from this, post-translational modifications in PCNA alter its function in different ways (Hoege et al., 2002; Moldovan et al., 2007;

Choe and Moldovan, 2017). The interactome described by Stukalov et al. (2021) demonstrated that higher ubiquitination occurs in specific regions of PCNA in SARS-CoV-2 infection, indicating a regulatory mechanism of PCNA by the virus infection (Stukalov et al., 2021).

In cells transfected with FLAG-M (**Figure 4**) or infected with SARS-CoV-2, we observed an increase of PCNA and γ H2AX (**Figures 5D–H**), and both proteins are associated with DNA repair. We also found a high expression of PCNA and γ H2AX in a COVID-19 patient (**Figure S4**). Li et al. (2021) already reported a high PCNA expression in moderate COVID-19 patients compared to the control group by proteomics analysis (Li et al., 2021). It has been reported that virus infection in human cells can cause DNA damage, inhibiting the association of the DNA polymerase to the DNA stalling and collapsing the replication forks, which results in DNA double-strand breaks (DSB) (Kannouche et al., 2004; Luftig, 2014). This damage activates a stress response, mediated by checkpoint kinases, which help stabilize and restart the replication forks, thus preventing the generation of DNA damage and genomic instability (Zeman and Cimprich, 2014). In this case, one of the strategies of the cells is to trigger the PCNA ubiquitination.

When PCNA is polyubiquitinated, it searches for damaged DNA to assemble the replication complex, with a less specific DNA polymerase (Boehm et al., 2016). This mechanism is known as translesion synthesis (TLS) and is activated to bypass damaged DNA (Kannouche et al., 2004). Thus, the increase of PCNA could be a strategy for the viral infection to maintain cell viability. Also, after DNA damage, several proteins are activated to manage the DNA lesion. One of them is γ H2AX, the phosphorylated form of H2AX, a specific marker of DNA damage that is responsible for recruiting repair proteins to deal with stalled forks (Dickey et al., 2009; Choe et al., 2016), and also increases the expression of p53 and phosphorylation of p53, leading to cell growth inhibition (Dillehay et al., 2014; Dillehay et al., 2015).

PCNA is also found in the cytoplasm of cancer cells. The accumulation of PCNA in the cytoplasm of cancer cells evidenced interactions between PCNA and the proteins in the cytoplasm (Byung and Lee, 2006). PCNA can bind to enzymes of the glycolysis pathway and regulate energy production in the mitochondria; maintain cytoskeleton integrity; and participate in other signaling pathways (Neuman et al., 2011; Bouhaddou et al., 2020). Li et al. (2021) described that SARS-CoV-2 M protein has its activity connected to ATP biosynthesis and metabolic processes (Li et al., 2021). Considering these data, the PCNA translocation from the nucleus to cytoplasm reported here may also be associated with the regulation of metabolism in infected cells to maintain SARS-CoV-2 replication.

Another hypothesis is that cytosolic PCNA, in association with the M protein, could bind to proteins that inhibit the immune response. Several studies pointed out that cytoplasmic PCNA is found in mature neutrophils associated with procaspases, thus preventing neutrophils from apoptosis (Witko-Sarsat et al., 2010). The accumulation of PCNA in the cytoplasm of mature neutrophils is due to the activity of the chromosome region maintenance 1 (CRM1)-dependent nuclear-to-cytoplasmic relocalization during granulocytic (Bouayad et al., 2012). Cytoplasmic PCNA is also associated with Caspase-9 in the SH-SY5Y neuroblastoma cell line, and S-nitrosylation of PCNA at the residues C81 and C162 decreases this interaction, leading to caspase-9 activation (Yin et al., 2015).

Verdinexor is a selective inhibitor of nuclear export (SINE), a molecular drug that binds to CRM-1 and blocks the transport of proteins from the nucleus to the cytoplasm, including PCNA (Bouayad et al., 2012; Widman et al., 2018). The CRM-1 inhibitors have demonstrated activity against over 20 different DNA and RNA viruses, including influenza and respiratory syncytial virus (Perwitasari et al., 2014; Widman et al., 2018; Jorquera et al., 2019). In addition, Selinexor, another SINE, reduced SARS-CoV-2 infection *in vitro* and protected the respiratory system in an *in vivo* model (Kashyap et al., 2021). We found that Verdinexor 0.1 μ M was a safe dose and enough to reduced viral replication by 15% (Figure 6), corroborating the previous SINE study. Nonetheless, SINEs are drugs that could act in the translocation of different proteins, not only in PCNA. We also treated cells with different doses of PCNA inhibitor (PCANI1). This inhibitor stabilizes the PCNA trimer and

prevents the PCNA translocation from the nucleus to the cytoplasm and reallocation inside the nucleus (Lu and Dong, 2019). This inhibits the PCNA action on the replication forks and indirectly leads tumor cells to a higher sensitivity to anticancer DNA damaging drugs (Klein et al., 2020; Wyler et al., 2020). Our results show that PCNA I1 0.5 μ M reduced viral replication by 20% (Figure 6), no difference was seen when the cells were treated with PCNA I1 0.1 μ M. Our results indicate a potential use of PCNA and nuclear translocation inhibitors as treatments for COVID-19.

CONCLUSIONS

The SARS-CoV-2 virus can manipulate many pathways to replicate in the host cell. In this study, we validated the PCNA-M interaction and underlined some of the potential mechanisms regarding this interaction. The increase of the PCNA and γ H2AX levels in the nucleus may prolong cell viability to favor virus replication. On the other hand, the translocation of PCNA and its association with M in the cytoplasm may manipulate the immune response and regulate cell metabolism to favor virus replication. Finally, inhibition of PCNA translocation from the nucleus to cytoplasm reduced the formation of plaques in an *in vitro* assay, indicating a potential therapeutic target. The original data reported here may help to better understand the SARS-CoV-2 replication mechanisms, thus impacting therapeutic strategies for COVID-19 resolution.

DATA AVAILABILITY STATEMENT

The datasets presented in this study can be found in online repositories. The names of the repository/repositories and accession number(s) can be found in the article/Supplementary Material.

ETHICS STATEMENT

The studies involving human participants were reviewed and approved by Institutional Ethical Board CAAE #30364720.0.0000.0068. The patients/participants provided their written informed consent to participate in this study.

AUTHOR CONTRIBUTIONS

Conceptualization, FS and AV; methodology, ÉZ, IP, MM, AM, MS, OS, MG, KS, and MA; software, MS; validation, ÉZ, IP, MM, AM, MS, OS, and MG; formal analysis, ÉZ, FS, HM-S and AV; investigation, ÉZ and FS; resources, FS, JP-M, HM-S, TM, MD, PS, and AV; data curation, ÉZ, MM, MS, FS, HM-S, and AV; writing original draft preparation, ÉZ; writing—review and editing, ÉZ, FS, JP-M, and AV; visualization, ÉZ, IP, MM, AM, MS, OS, MG, KS, MA, DT-T, and PP; supervision, FS, JP-M, HM-S, and AV; project administration, FS and JP-M; funding

acquisition, FS and JP-M. All authors have read and agreed to the published version of the manuscript.

FUNDING

This work was supported by grants from FAEPEX-UNICAMP (2005/20; 2319/20; 2432/20; 2274/20; 2266/20), Fundação de Amparo à Pesquisa do Estado de São Paulo (FAPESP), grant numbers 2020/05346-6, 2018/14818-9, 2020/04558-0 and 2016/00194-8. JP-M is supported by Conselho Nacional de Desenvolvimento Científico e Tecnológico (CNPq) grant no number 305628/2020-8.

REFERENCES

- Alharbi, S. N., and Alrefaei, A. F. (2021). Comparison of the SARS-CoV-2 (2019-NCoV) M Protein With its Counterparts of SARS-CoV and MERS-CoV Species. *J. King Saud. Univ. - Sci.* 33, 101335–101344. doi: 10.1016/j.jksus.2020.101335
- Amaral, C. L., Freitas, L. B., Tamura, R. E., Tavares, M. R., Pavan, I. C. B., Bajgelman, M. C., et al. (2016). S6Ks Isoforms Contribute to Viability, Migration, Docetaxel Resistance and Tumor Formation of Prostate Cancer Cells. *BMC Cancer* 16, 602. doi: 10.1186/s12885-016-2629-y
- Baldwin, (1996). Nuclear & Cytoplasmic Extract Protocol. *Ann. Rev. Immunol.* 14, 649–681. doi: 10.1146/annurev.immunol.14.1.649
- Boehm, E. M., Gildenberg, M. S., and Washington, M. T. (2016). The Many Roles of PCNA in Eukaryotic Dna Replication. *Enzymes* 39, 231–254. doi: 10.1016/b.senz.2016.03.003
- Bojkova, D., Klann, K., Koch, B., Widera, M., Krause, D., Ciesek, S., et al. (2020). Proteomics of SARS-CoV-2-infected Host Cells Reveals Therapy Targets. *Nature* 583, 469–472. doi: 10.1038/s41586-020-2332-7
- Bouayad, D., Pederzoli-Ribeil, M., Mocek, J., Candali, C., Arlet, J. B., Hermine, O., et al. (2012). Nuclear-to-Cytoplasmic Relocalization of the Proliferating Cell Nuclear Antigen (PCNA) During Differentiation Involves a Chromosome Region Maintenance 1 (CRM1)-Dependent Export and is a Prerequisite for PCNA Antiapoptotic Activity in Mature Neutrophils. *J. Biol. Chem.* 287, 33812–33825. doi: 10.1074/jbc.M112.367839
- Bouhaddou, M., Memon, D., Meyer, B., White, K. M., Rezeli, V. V., Correa Marrero, M., et al. (2020). The Global Phosphorylation Landscape of SARS-CoV-2 Infection. *Cell* 182. doi: 10.1016/j.cell.2020.06.034
- Byung, J. K., and Lee, H. (2006). Importin- β Mediates Cdc7 Nuclear Import by Binding to the Kinase Insert II Domain, Which can be Antagonized by Importin- α . *J. Biol. Chem.* 281, 12041–12049. doi: 10.1074/jbc.M512630200
- Chen, N., Zhou, M., Dong, X., Qu, J., Gong, F., Han, Y., et al. (2020). Epidemiological and Clinical Characteristics of 99 Cases of 2019 Novel Coronavirus Pneumonia in Wuhan, China: A Descriptive Study. *Lancet* 395, 30211–30217. doi: 10.1016/S0140-6736(20)30211-7
- Choe, K. N., and Moldovan, G. L. (2017). Forging Ahead Through Darkness: PcnA, Still the Principal Conductor at the Replication Fork. *Mol. Cell* 65, 380–392. doi: 10.1016/j.molcel.2016.12.020
- Choe, K. N., Nicolae, C. M., Constantin, D., Imamura Kawasawa, Y., Delgado-Diaz, M. R., De, S., et al. (2016). HUWE 1 Interacts With PCNA to Alleviate Replication Stress. *EMBO Rep.* 17, 874–886. doi: 10.15252/embr.201541685
- Dickey, J. S., Redon, C. E., Nakamura, A. J., Baird, B. J., Sedelnikova, O. A., and Bonner, W. M. (2009). H2ax: Functional Roles and Potential Applications. *Chromosoma* 118, 683–692. doi: 10.1007/s00412-009-0234-4
- Dillehay, K. L., Lu, S., and Dong, Z. (2014). Antitumor Effects of a Novel Small Molecule Targeting PCNA Chromatin Association in Prostate Cancer. *Mol. Cancer Ther.* 13, 2817–2826. doi: 10.1158/1535-7163.MCT-14-0522
- Dillehay, K. L., Seibel, W. L., Zhao, D., Lu, S., and Dong, Z. (2015). Target Validation and Structure-Activity Analysis of a Series of Novel PCNA Inhibitors. *Pharmacol. Res. Perspect.* 3, 2817–2826. doi: 10.1002/prp2.115
- Fu, Y. Z., Wang, S. Y., Zheng, Z. Q., Huang, Y., Li, W. W., Xu, Z. S., et al. (2021). Sars-CoV-2 Membrane Glycoprotein M Antagonizes the MAVS-mediated Innate Antiviral Response. *Cell. Mol. Immunol.* 18, 613–620. doi: 10.1038/s41423-020-00571-x
- Gordon, D. E., Jang, G. M., Bouhaddou, M., Xu, J., Obernier, K., White, K. M., et al. (2020). A SARS-CoV-2 Protein Interaction Map Reveals Targets for Drug Repurposing. *Nature* 583, 459–468. doi: 10.1038/s41586-020-2286-9
- Hasan, S., and Hossain, M. M. (2020). Analysis of COVID-19 M Protein for Possible Clues Regarding Virion Stability, Longevity and Spreading. doi: 10.31219/osf.io/e7jkc
- Hoeg, C., Pfander, B., Moldovan, G. L., Pyrowolakis, G., and Jentsch, S. (2002). RAD6-Dependent DNA Repair Is Linked to Modification of PCNA by Ubiquitin and SUMO. *Nature* 419, 135–141. doi: 10.1038/nature00991
- Hurst, K. R., Kuo, L., Koetzner, C. A., Ye, R., Hsue, B., and Masters, P. S. (2005). A Major Determinant for Membrane Protein Interaction Localizes to the Carboxy-Terminal Domain of the Mouse Coronavirus Nucleocapsid Protein. *J. Virol.* 79, 13285–13297. doi: 10.1128/jvi.79.21.13285-13297.2005
- Jorquera, P. A., Mathew, C., Pickens, J., Williams, C., Luczo, J. M., Tamir, S., et al. (2019). Verdineor (KPT-335), a Selective Inhibitor of Nuclear Export, Reduces Respiratory Syncytial Virus Replication *In Vitro*. *J. Virol.* 93, e01684–18. doi: 10.1128/jvi.01684-18
- Kannouche, P. L., Wing, J., and Lehmann, A. R. (2004). Interaction of Human DNA Polymerase η With Monoubiquitinated PCNA: A Possible Mechanism for the Polymerase Switch in Response to DNA Damage. *Mol. Cell* 14, 491–500. doi: 10.1016/S1097-2765(04)00259-X
- Kashyap, T., Murray, J., Walker, C. J., Chang, H., Tamir, S., Hou, B., et al. (2021). Selinexor, a Novel Selective Inhibitor of Nuclear Export, Reduces SARS-CoV-2 Infection and Protects the Respiratory System *In Vivo*. *Antiviral Res.* 192, 105115–105123. doi: 10.1016/j.antiviral.2021.105115
- Klein, S., Cortese, M., Winter, S. L., Wachsmuth-Melm, M., Neufeldt, C. J., Cerikan, B., et al. (2020). Sars-CoV-2 Structure and Replication Characterized by *In Situ* Cryo-Electron Tomography. *Nat. Commun.* 11, 5885–5896. doi: 10.1038/s41467-020-19619-7
- Kuo, L., Hurst-Hess, K. R., Koetzner, C. A., and Masters, P. S. (2016). Analyses of Coronavirus Assembly Interactions With Interspecies Membrane and Nucleocapsid Protein Chimeras. *J. Virol.* 90, 4357–4368. doi: 10.1128/jvi.03212-15
- Lee, C.-C., Wang, J.-W., Leu, W.-M., Huang, Y.-T., Huang, Y.-W., Hsu, Y.-H., et al. (2019). Proliferating Cell Nuclear Antigen Suppresses RNA Replication of Bamboo Mosaic Virus Through an Interaction With the Viral Genome. *J. Virol.* 93, e00961–19. doi: 10.1128/jvi.00961-19
- Li, J., Guo, M., Tian, X., Wang, X., Yang, X., Wu, P., et al. (2021). Virus-Host Interactome and Proteomic Survey Reveal Potential Virulence Factors Influencing Sars-CoV-2 Pathogenesis. *Med* 2, 99–112. doi: 10.1016/j.medj.2020.07.002
- Li, C. K., Wu, H., Yan, H., Ma, S., Wang, L., Zhang, M., et al. (2008). T Cell Responses to Whole Sars Coronavirus in Humans. *J. Immunol.* 181, 5490–5500. doi: 10.4049/jimmunol.181.8.5490
- Lu, S., and Dong, Z. (2019). Additive Effects of a Small Molecular PCNA Inhibitor PCNA-11S and DNA Damaging Agents on Growth Inhibition and DNA Damage in Prostate and Lung Cancer Cells. *PloS One* 14, e0223894–0223904. doi: 10.1371/journal.pone.0223894

ACKNOWLEDGMENTS

We acknowledge the students that helped ÉZ during the cell lines infection in the Biosafety Level 3 Laboratory (NB3) and all others that were our backup outside of the lab. We thank the UNICAMP-Task-Force against COVID-19 that facilitated this study.

SUPPLEMENTARY MATERIAL

The Supplementary Material for this article can be found online at: <https://www.frontiersin.org/articles/10.3389/fcimb.2022.849017/full#supplementary-material>

- Luftig, M. A. (2014). Viruses and the DNA Damage Response: Activation and Antagonism. *Annu. Rev. Virol.* 1, 605–625. doi: 10.1146/annurev-virology-031413-085548
- Lu, S., Ye, Q., Singh, D., Cao, Y., Diedrich, J. K., Yates, J. R., et al. (2021). The SARS-CoV-2 Nucleocapsid Phosphoprotein Forms Mutually Exclusive Condensates With RNA and the Membrane-Associated M Protein. *Nat. Commun.* 12, 502–514. doi: 10.1038/s41467-020-20768-y
- Maga, G., and Hübscher, U. (2003). Proliferating Cell Nuclear Antigen (PCNA): A Dancer With Many Partners. *J. Cell Sci.* 116:3051–3060. doi: 10.1242/jcs.00653
- Moldovan, G. L., Pfander, B., and Jentsch, S. (2006). PcnA Controls Establishment of Sister Chromatid Cohesion During S Phase. *Mol. Cell* 23, 723–732. doi: 10.1016/j.molcel.2006.07.007
- Moldovan, G. L., Pfander, B., and Jentsch, S. (2007). PCNA, the Maestro of the Replication Fork. *Cell* 129, 665–679. doi: 10.1016/j.cell.2007.05.003
- Naryzhny, S. N., and Lee, H. (2010). Proliferating Cell Nuclear Antigen in the Cytoplasm Interacts With Components of Glycolysis and Cancer. *FEBS Lett.* 584, 4292–4308. doi: 10.1016/j.febslet.2010.09.021
- Naryzhny, S. N., Zhao, H., and Lee, H. (2005). Proliferating Cell Nuclear Antigen (PCNA) may Function as a Double Homotrimer Complex in the Mammalian Cell. *J. Biol. Chem.* 280, 13888–13894. doi: 10.1074/jbc.M500304200
- Neuman, B. W., Kiss, G., Kunding, A. H., Bhella, D., Baksh, M. F., Connelly, S., et al. (2011). A Structural Analysis of M Protein in Coronavirus Assembly and Morphology. *J. Struct. Biol.* 174, 11–22. doi: 10.1016/j.jsb.2010.11.021
- O'Donnell, M., Langston, L., and Stillman, B. (2013). Principles and Concepts of DNA Replication in Bacteria, Archaea, and Eukarya. *Cold Spring Harb. Perspect. Biol.* 5, a010108–010115. doi: 10.1101/cshperspect.a010108
- Ohayon, D., De Chiara, A., Dang, P. M. C., Thiebtemont, N., Chatfield, S., Marzaoli, V., et al. (2019). Cytosolic PCNA Interacts With p47phox and Controls NADPH Oxidase NOX2 Activation in Neutrophils. *J. Exp. Med.* 216, 2669–2687. doi: 10.1084/jem.20180371
- Olaisen, C., Müller, R., Nedal, A., and Otterlei, M. (2015). PCNA-Interacting Peptides Reduce Akt Phosphorylation and TLR-mediated Cytokine Secretion Suggesting a Role of PCNA in Cellular Signaling. *Cell. Signal.* 27, 1478–1487. doi: 10.1016/j.cellsig.2015.03.009
- Oliveira, A. P., Simabuco, F. M., Tamura, R. E., Guerrero, M. C., Ribeiro, P. G. G., Libermann, T. A., et al. (2013). Human Respiratory Syncytial Virus N, P and M Protein Interactions in HEK-293T Cells. *Virus Res.* 177, 108–112. doi: 10.1016/j.virusres.2013.07.010
- Opstelten, D. J. E., Raamsman, M. J. B., Wolfs, K., Horzinek, M. C., and Rottier, P. J. M. (1995). Envelope Glycoprotein Interactions in Coronavirus Assembly. *J. Cell Biol.* 131, 339–349. doi: 10.1083/jcb.131.2.339
- Pang, H., Liu, Y., Han, X., Xu, Y., Jiang, F., Wu, D., et al. (2004). Protective Humoral Responses to Severe Acute Respiratory Syndrome-Associated Coronavirus: Implications for the Design of an Effective Protein-Based Vaccine. *J. Gen. Virol.* 85, 3109–3113. doi: 10.1099/vir.0.80111-0
- Paunescu, T., Mittal, S., Protić, M., Oryhon, J., Korolev, S. V., Joachimiak, A., et al. (2001). Proliferating Cell Nuclear Antigen (PCNA): Ringmaster of the Genome. *Int. J. Radiat. Biol.* 77, 1007–1021. doi: 10.1080/09553000110069335
- Pavan, I. C. B., Yokoo, S., Granato, D. C., Meneguello, L., Carnielli, C. M., Tavares, M. R., et al. (2016). Different Interactomes for P70-S6K1 and P54-S6K2 Revealed by Proteomic Analysis. *Proteomics* 16:2650–2666. doi: 10.1002/pmic.201500249
- Perwitasari, O., Johnson, S., Yan, X., Howerth, E., Shacham, S., Landesman, Y., et al. (2014). Verdineor, a Novel Selective Inhibitor of Nuclear Export, Reduces Influenza A Virus Replication *In Vitro* and *In Vivo*. *J. Virol.* 88, 10228–10243. doi: 10.1128/jvi.01774-14
- Perwitasari, O., Johnson, S., Yan, X., Register, E., Crabtree, J., Gabbard, J., et al. (2016). Antiviral Efficacy of Verdineor *In Vivo* in Two Animal Models of Influenza A Virus Infection. *PLoS One* 11, e0167221–0167232. doi: 10.1371/journal.pone.0167221
- Sanche, S., Lin, Y. T., Xu, C., Romero-Severson, E., Hengartner, N., and Ke, R. (2020). Research High Contagiousness and Rapid Spread of Severe Acute Respiratory Syndrome Coronavirus 2. *Emerg. Infect. Dis.* 26, 1470–1477. doi: 10.3201/eid2607.200282
- Siddiqui, K., On, K. F., and Diffley, J. F. X. (2013). Regulating DNA Replication in Eukarya. *Cold Spring Harb. Perspect. Biol.* 5, a012930–012939. doi: 10.1101/cshperspect.a012930
- Song, Y., Zhang, M., Yin, L., Wang, K., Zhou, Y., Zhou, M., et al. (2020). 106080–106086. Covid-19 Treatment: Close to a Cure? A Rapid Review of Pharmacotherapies for the Novel Coronavirus (SARS-Cov-2). *Int. J. Antimicrob. Agents* 56, 1060807–106086. doi: 10.1016/j.ijantimicag.2020.106080
- Strzalka, W., and Ziemienowicz, A. (2011). Proliferating Cell Nuclear Antigen (PCNA): A Key Factor in DNA Replication and Cell Cycle Regulation. *Ann. Bot.* 107, 1127–1140. doi: 10.1093/aob/mcq243
- Stukalov, A., Girault, V., Grass, V., Karayel, O., Bergant, V., Urban, C., et al. (2021). Multilevel Proteomics Reveals Host Perturbations by SARS-CoV-2 and SARS-Cov. *Nature* 594 (7862), 246–252. doi: 10.1038/s41586-021-03493-4
- Thiel, V., Ivanov, K. A., Putics, Á., Hertzog, T., Schelle, B., Bayer, S., et al. (2003). Mechanisms and Enzymes Involved in SARS Coronavirus Genome Expression. *J. Gen. Virol.* 84, 2305–2315. doi: 10.1099/vir.0.19424-0
- Tsurimoto, T. (1998). PCNA, a Multifunctional Ring on DNA. *Biochim. Biophys. Acta - Gene Struct. Expr.* 1443, 23–39. doi: 10.1016/S0167-4781(98)00204-8
- Warbrick, E. (1998). PCNA Binding Through a Conserved Motif. *BioEssays* 20, 195–199. doi: 10.1002/(SICI)1521-1878(199803)20:3<195::AID-BIES2>3.0.CO;2-R
- WHO. World Health Organization (2020). Who. Coronavirus Disease (COVID-2019) Situation Reports.
- Widman, D. G., Gornisiewicz, S., Shacham, S., and Tamir, S. (2018). *In Vitro* Toxicity and Efficacy of Verdineor, an Exportin 1 Inhibitor, on Opportunistic Viruses Affecting Immunocompromised Individuals. *PLoS One* 13, e0200043–0200053. doi: 10.1371/journal.pone.0200043
- Witko-Sarsat, V., Mocek, J., Bouayad, D., Tamassia, N., Ribeil, J. A., Candali, C., et al. (2010). Proliferating Cell Nuclear Antigen Acts as a Cytoplasmic Platform Controlling Human Neutrophil Survival. *J. Exp. Med.* 207, 2631–2645. doi: 10.1084/jem.20092241
- Wu, A., Peng, Y., Huang, B., Ding, X., Wang, X., Niu, P., et al. (2020). Genome Composition and Divergence of the Novel Coronavirus (Ncov) Originating in China. *Cell Host Microbe* 27, 325–328. doi: 10.1016/j.chom.2020.02.001
- Wyler, E., Mösbauer, K., Franke, V., Diag, A., Gottula, L. T., Arsie, R., et al. (2020). Bulk and Single-Cell Gene Expression Profiling of SARS-CoV-2 Infected Human Cell Lines Identifies Molecular Targets for Therapeutic Intervention. *bioRxiv*. doi: 10.1101/2020.05.05.079194
- Yin, L., Xie, Y., Yin, S., Lv, X., Zhang, J., Gu, Z., et al. (2015). The S-nitrosylation Status of PCNA Localized in Cytosol Impacts the Apoptotic Pathway in a Parkinson's Disease Paradigm. *PLoS One* 10, e0117546–0117550. doi: 10.1371/journal.pone.0117546
- Zeman, M. K., and Cimprich, K. A. (2014). Causes and Consequences of Replication Stress. *Nat. Cell Biol.* 16, 2–9. doi: 10.1038/ncb2897
- Zhang, J., Cruz-cosme, R., Zhuang, M. W., Liu, D., Liu, Y., Teng, S., et al. (2020). A Systemic and Molecular Study of Subcellular Localization of SARS-CoV-2 Proteins. *Signal Transduction Targeting Ther.* 5, 269–275. doi: 10.1038/s41392-020-00372-8
- Zheng, Y., Zhuang, M. W., Han, L., Zhang, J., Nan, M. L., Zhan, P., et al. (2020). Severe Acute Respiratory Syndrome Coronavirus 2 (SARS-CoV-2) Membrane (M) Protein Inhibits Type I and III Interferon Production by Targeting RIG-I/MDA-5 Signaling. *Signal Transduction Targeting Ther.* 5, 299–306. doi: 10.1038/s41392-020-00438-7

Conflict of Interest: The authors declare that the research was conducted in the absence of any commercial or financial relationships that could be construed as a potential conflict of interest.

Publisher's Note: All claims expressed in this article are solely those of the authors and do not necessarily represent those of their affiliated organizations, or those of the publisher, the editors and the reviewers. Any product that may be evaluated in this article, or claim that may be made by its manufacturer, is not guaranteed or endorsed by the publisher.

Copyright © 2022 Zambalde, Pavan, Mancini, Severino, Scudero, Morelli, Amorim, Bispo-dos-Santos, Góis, Toledo-Teixeira, Parise, Mauad, Dolnikoff, Saldiva, Marques-Souza, Proença-Modena, Ventura and Simabuco. This is an open-access article distributed under the terms of the Creative Commons Attribution License (CC BY). The use, distribution or reproduction in other forums is permitted, provided the original author(s) and the copyright owner(s) are credited and that the original publication in this journal is cited, in accordance with accepted academic practice. No use, distribution or reproduction is permitted which does not comply with these terms.



Vaccination Is Associated With Shorter Time to Target Cycle Threshold Value in Patients With SARS-CoV-2 Omicron Variant

Jiajun Wu, Yong Wei*, Feng Shen, Shun Zhu, Yingying Lu, Xue Tian and Pengyu Zhang

Department of COVID-19 for Temporary Centralized Isolation and Treatment, Shanghai General Hospital, Shanghai Jiao Tong University School of Medicine, Shanghai, China

OPEN ACCESS

Edited by:

Clement Adebajo Meseko,
National Veterinary Research Institute
(NVR), Nigeria

Reviewed by:

Dania AlQasrawi,
Mayo Clinic Florida, United States
Melvin Sanicas,
Clover Biopharmaceuticals,
Switzerland

*Correspondence:

Yong Wei
weiyong202@qq.com

Specialty section:

This article was submitted to
Virus and Host,
a section of the journal
Frontiers in Cellular and
Infection Microbiology

Received: 13 May 2022

Accepted: 07 June 2022

Published: 06 July 2022

Citation:

Wu J, Wei Y, Shen F, Zhu S, Lu Y,
Tian X and Zhang P (2022) Vaccination
Is Associated With Shorter Time to
Target Cycle Threshold Value in
Patients With SARS-CoV-2
Omicron Variant.
Front. Cell. Infect. Microbiol. 12:943407.
doi: 10.3389/fcimb.2022.943407

Background: Limited data are available on the responses to vaccination for severe acute respiratory syndrome coronavirus 2 (SARS-CoV-2) Omicron variant in the Chinese population. This study aimed to investigate whether vaccination could alter the disease course of SARS-CoV-2 Omicron variant.

Methods: A retrospective cohort included 142 patients who had no or mild symptoms and were admitted to our department for centralized isolation after being locally infected with SARS-CoV-2 Omicron variant from March 4 to 30, 2022, in Shanghai, China.

Results: Of the 142 subjects with the mean age of 43.1 years, 53.5% were male and 90.8% had been vaccinated before the infection. Comparing the vaccinated with the unvaccinated patients, there was no difference in patient characteristics, but patients with vaccination had shorter time to target cycle threshold value (TtCT) (vaccinated vs. unvaccinated, 12.6 ± 3.4 vs. 14.8 ± 4.7 days, $P = 0.039$). There was no difference in TtCT between heterogeneous and homologous vaccination. Of subjects with homologous vaccination, 43.1% were vaccinated with CoronaVac (Sinovac Life Science), 47.2% with Sinopharm BBIBP-CorV, 4.9% with Sinopharm WIBP, 3.3% with CanSinoBio, and 1.6% with Zhifei Longcom. No difference in TtCT was observed among different vaccines. Comparing two-dose primary vaccination with three-dose booster vaccination, we found no difference in TtCT either.

Conclusion: Vaccination is associated with shorter TtCT in patients with SARS-CoV-2 Omicron variant.

Keywords: omicron variant, SARS-COV-2, vaccination, cycle threshold, inactivated vaccines

INTRODUCTION

The novel severe acute respiratory syndrome coronavirus 2 (SARS-CoV-2) has spread worldwide for more than 2 years. It threatens our health and lives and seriously disrupts the daily life. The SARS-CoV-2 keeps mutating, resulting in a number of variants (Cui et al., 2019; Yang et al., 2022). The Omicron variant BA.2 is the newest variant and has become dominant in the SARS-CoV-2

outbreak in Shanghai, China, on March 2022. SARS-CoV-2 Omicron BA.2 shows an increase in its transmissibility and becomes less virulent than the Delta SARS-CoV-2 variant, apparently with less involvement of the lower respiratory tract, milder symptoms, and fewer probability of hospitalizations (Menni et al., 2022; Davies et al., 2022).

Although the SARS-CoV-2 vaccines currently have been reported to reduce the incidence of severe cases after infection (Tanriover et al., 2021), it is unclear whether vaccination could alter the natural history of SARS-CoV-2 Omicron variant infection, especially for SARS-CoV-2 vaccines made in China. Nucleic acid detection has been the primary laboratory diagnostic method for SARS-CoV-2. Both N and ORF genes of SARS-CoV-2 show significant curve, which is specific for SARS-CoV-2-positive patients. They are of great clinical significance for the cycle threshold (CT) value of above 35 of the two genes tested by fluorescent quantitative polymerase chain reaction (PCR) is the discharge criteria for mild patients with SARS-CoV-2 in China. Hence, this study was performed to investigate the effect of SARS-CoV-2 vaccines on the time to target CT value (TtCT) greater than 35 for both N gene and ORF gene.

METHODS

Study Design and Data Source

This is a retrospective cohort study including 142 patients who were locally infected with SARS-CoV-2 Omicron variant on March 2022 in Shanghai, China. They had no or mild symptoms and were admitted to our department for centralized isolation. At admission, the demographic and health information of all patients were collected and saved in the electronic medical records. The SARS-CoV-2 vaccination history of each patient was inquired in detail, including vaccination date, names of vaccine manufacturer, and times of vaccination. This study was conducted in accordance with the Declaration of Helsinki, and its ethical approval was obtained from the Ethics Committee of Shanghai General Hospital, Shanghai Jiao Tong University School of Medicine, Shanghai, China. All participants were informed of the nature and objectives of the study. Informed consent was obtained from each enrolled subject.

Nucleic Acid Amplification Test of SARS-CoV-2

After nasopharyngeal swab samples were collected, they were shifted to the laboratories immediately and the PCR tests started within 2 h. Real-time fluorescent reverse transcriptase-PCR was used to detect different viral RNA sequences of SARS-CoV-2, including open reading frame (ORF1ab), nucleocapsid (N), and envelope (E) genes. All PCR tests were performed in laboratories of Shanghai Public Health Clinical Center Affiliated to Fudan University, using the SARS-CoV-2 RNA detection kit (Bioperfectus Technologies Co., Ltd., Jiangsu, China) with the SLAN Real-time PCR system following the manufacturer's instructions. In brief, the total volume of the reaction mixture

was 25 μ l, and it contained 5 μ l of RNA template. The reaction conditions were as follows: reverse transcription at 50°C for 10 min; cDNA pre-denaturation at 97°C for 1 min; denaturation at 97°C for 5 s (45 cycles); then annealing and elongation (with fluorescence monitoring) at 58°C for 30 s; and a final step at 25°C for 10 min. The CT value of each target gene was reported.

The patient received the first nucleic acid amplification test (NAAT) on the second day after admission and the second NAAT on the seventh day after admission. If the CT value was ≥ 35 , then the patient continued to receive the next NAAT in the next day. If the CT value was < 35 , then the patient received NAAT every other day. Two weeks after admission, NAAT was performed every day.

Definition and Variables

The latest Diagnosis and Treatment Plan of SARS-CoV-2 (Trial Version 9) was released by the National Health Commission of the People's Republic of China on March 2022, and the discharge criteria for mild cases were revised as the CT values ≥ 35 of N gene and ORF gene tested by NAAT (fluorescent quantitative PCR with limit value 40) for two consecutive samples with over 24-h interval. In the world, it is generally judged as negative when the CT value exceeds 35. In China, it is judged as negative when the CT value exceeds 40, so as to powerfully reduce the risk of SARS-CoV-2 transmission. The CT value of the new scheme was reduced from 40 to 35, which is limited to the criteria for being out of quarantine and discharge for mild cases after treatment. The adjustment of CT value for discharge is of great significance to improve the allocation of medical resources in China but does not mean that the positive diagnostic criteria for SARS-CoV-2 have changed. TtCT was defined as the duration from the date when the infection of SARS-CoV-2 was first confirmed by NAAT to the date when the patient got two consecutive CT values greater than 35 for both N gene and ORF gene of SARS-CoV-2 with an interval of more than 24 h. Homologous vaccination is defined as multiple injections with the same vaccines and heterogeneous vaccination is defined as multiple injections with different kinds of vaccines.

Hypertension was defined as systolic blood pressure (SBP) ≥ 140 mmHg, diastolic blood pressure (DBP) ≥ 90 mmHg, or current antihypertensive therapy. Diabetes mellitus was defined as having a previous diagnosis of diabetes mellitus, receiving oral hypoglycemic agents or insulin treatment, or having a fasting plasma glucose ≥ 126 mg/dl (7.0 mmol/L) or a hemoglobin A1c level $\geq 6.5\%$. The history of coronary heart disease (CHD) was made primarily according to clinical symptoms of angina pectoris, ECG manifestations of myocardial ischemia, and coronary stenosis showed by contrast-enhanced coronary computed tomography angiography or percutaneous coronary angiography. Stroke was defined as a history of cerebral thromboembolism or bleeding manifested by brain computed tomography or magnetic resonance imaging. Renal dysfunction was defined as the estimated glomerular filtration rate (eGFR) < 60 ml/min/1.73 m² at baseline or having a history of chronic renal failure.

Statistics

For numerical variables, the mean (standard deviation) was used for statistical description, and the t-test or ANOVA was

TABLE 1 | Patient characteristics.

| Variables | Total N = 142 | Vaccinated N = 129 | Unvaccinated N = 13 | P* |
|------------------------------------|------------------|-----------------------|------------------------|-------|
| Age, years old | 43.1 ± 13.5 | 42.9 ± 13.1 | 46.0 ± 16.9 | 0.423 |
| Sex male, n (%) | 76 (53.6) | 69 (53.5) | 7 (53.8) | 0.980 |
| Hypertension, n (%) | 20 (14.1) | 18 (14.0) | 2 (15.4) | 1.000 |
| Coronary heart disease, n (%) | 1 (0.7) | 0 (0.0) | 1 (7.7) | 0.092 |
| Heart failure, n (%) | 0 (0.0) | 0 (0.0) | 0 (0.0) | 1.000 |
| Stroke, n (%) | 0 (0.0) | 0 (0.0) | 0 (0.0) | 1.000 |
| Chronic lung disease, n (%) | 0 (0.7) | 1 (0.8) | 0 (0.0) | 1.000 |
| Diabetes, n (%) | 4 (2.8) | 4 (3.1) | 0 (0.0) | 1.000 |
| Renal dysfunction, n (%) | 0 (0.0) | 0 (0.0) | 0 (0.0) | 1.000 |
| Malignant tumor, n (%) | 1 (0.7) | 0 (0.0) | 1 (7.7) | 0.092 |
| Smoking, n (%) | 21 (14.8) | 19 (14.7) | 2 (15.4) | 1.000 |
| Body mass index, kg/m ² | 23.8 ± 4.1 | 23.9 ± 4.1 | 22.9 ± 4.0 | 0.394 |
| Times of NAATs | 4.2 ± 2.4 | 4.1 ± 2.3 | 5.0 ± 3.1 | 0.186 |

*P indicated P values when comparing the vaccinated with the unvaccinated. NAAT, nucleic acid amplification test.

performed for inter-group comparison. Categorical data were presented as absolute value and percentage, and they were compared between groups with the chi-square test. All statistical analyses were performed with SPSS 13.0. Two-tailed P-value of less than 0.05 was considered of statistical significance.

RESULTS

Demographics and Clinical Data of the Enrolled Subjects

The 142 patients were locally infected with SARS-CoV-2 Omicron variant from March 4 to 30, 2022, in Shanghai, China. Sixty-nine (53.5%) of them were male, and the mean age was 43.1 years (SD, 13.5). The 90.8% of them had been vaccinated before infection. Comparing the vaccinated with the unvaccinated patients, we found no difference in patient characteristics (Table 1).

Difference in TtCT Between the Vaccinated and Unvaccinated Individuals

Compared with patients who did not receive vaccination, patients with vaccination had shorter TtCT (vaccinated vs. unvaccinated, 12.6 ± 3.4 vs. 14.8 ± 4.7 days, P = 0.039) (Figure 1).

Details of SARS-CoV-2 Vaccination for Selected Patients

Overall, we have identified 129 patients with SARS-CoV-2 infection after vaccination, of which 69 (53.5%) of them were male and the mean age was 42.9 years (SD, 13.1) (Table 1). Of them, six patients had undergone heterologous vaccination, and the other 123 patients had undergone homologous vaccination (Figure 2A). There was no difference in TtCT between heterogeneous and homologous vaccination (Figure 2B).

For subjects with homologous vaccination, they all were vaccinated with inactivated COVID-19 vaccines produced by the five Chinese manufacturers, such as Sinovac Life Science, Beijing Bio-Institute of Biological Products (BBIBP), Wuhan Institute of Biological Products (WIBP), CanSinoBio, and

Zhifei Longcom. Patients vaccinated with CoronaVac (Sinovac Life Science) accounted for 43.1%, Sinopharm BBIBP-CorV for 47.2%, Sinopharm WIBP for 4.9%, CanSinoBio for 3.3%, and Zhifei Longcom for 1.6% (Figure 2C). No difference in TtCT was observed among different vaccines (Figure 2D).

When comparing two-dose primary vaccination with three-dose booster vaccination, we found no difference in TtCT for both CoronaVac (Figure 2E) and Sinopharm BBIBP-CorV (Figure 2F) respectively.

DISCUSSION

The main findings of this study are as follows: 1) Vaccination is associated with shorter TtCT in patients with SARS-CoV-2 Omicron variant; 2) inactivated vaccines produced by different manufacturers in China have similar effects on TtCT; and 3)

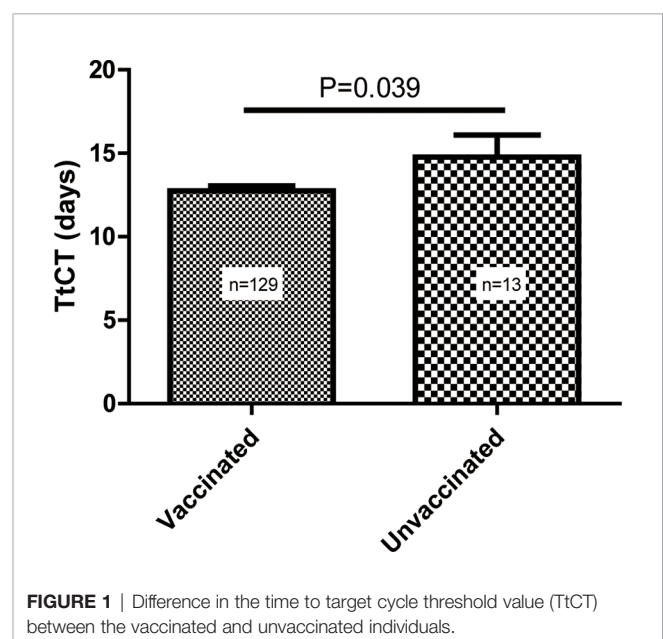


FIGURE 1 | Difference in the time to target cycle threshold value (TtCT) between the vaccinated and unvaccinated individuals.

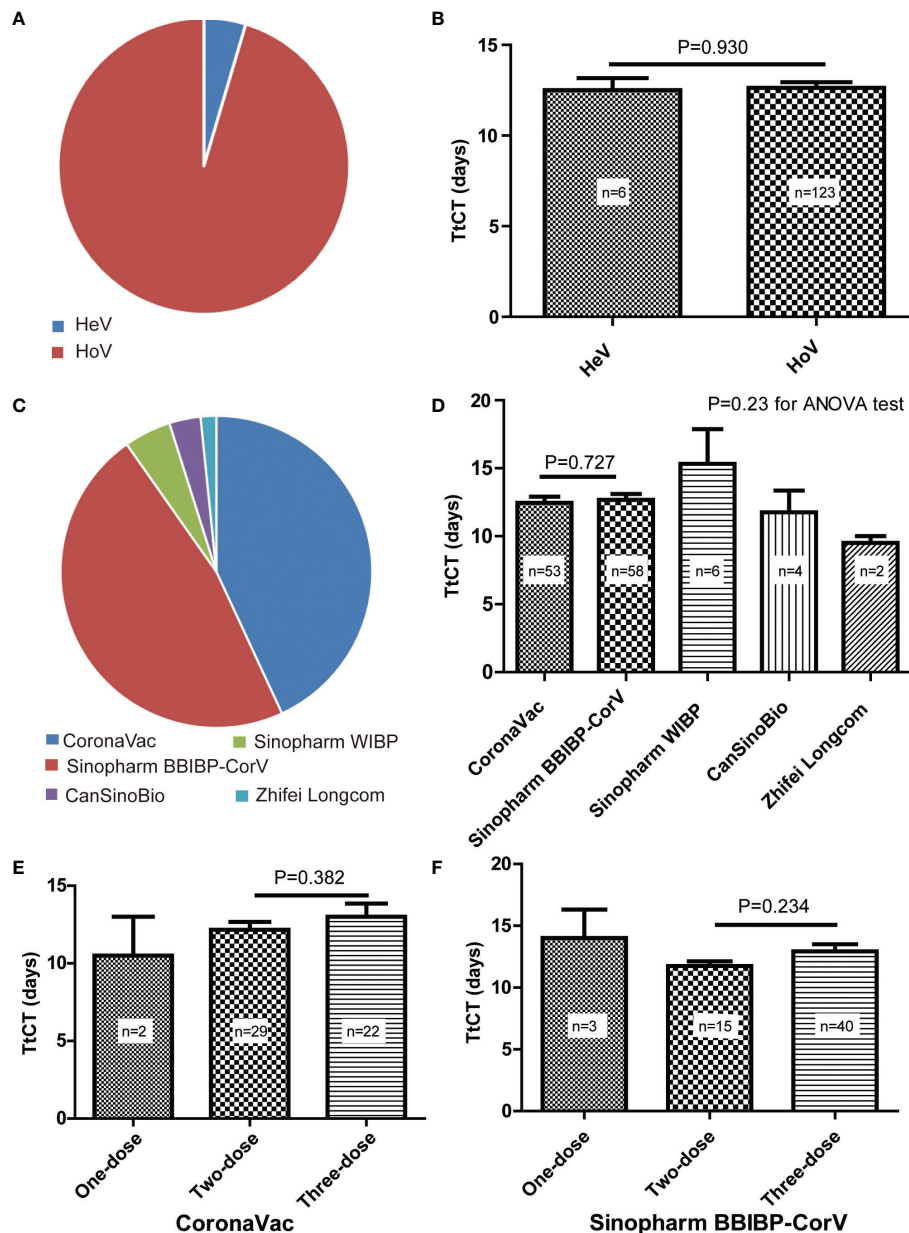


FIGURE 2 | Details of SARS-CoV-2 vaccination for selected patients. **(A)** Proportions of heterogeneous vaccination (HeV) and homologous vaccination (HoV). **(B)** Comparison of the time to target cycle threshold value (TtCT) between HeV and HoV. **(C)** Proportions of different vaccines for homologous vaccination. **(D)** Comparison of TtCT among different vaccines for homologous vaccination. **(E)** Comparison of TtCT between the two-dose primary vaccination and the three-dose booster vaccination of CoronaVac. **(F)** Comparison of TtCT between two-dose primary vaccination and three-dose booster vaccination of Sinopharm BBIBP-CorV.

compared with the two-dose primary vaccination, the three-dose booster vaccination does not appear to reduce TtCT.

Currently, vaccination has been verified to be the most effective way to prevent SARS-CoV-2, irrespective of the mRNA or the inactivated vaccines (Fan et al., 2021). Although the SARS-CoV-2 vaccines currently used could not powerfully prevent infection, it significantly reduced the incidence of severe cases after infection. Two inactivated SARS-CoV-2 vaccines, CoronaVac and BBIBP-CorV, were developed in China and were reported to reduce the risk

of symptomatic SARS-CoV-2 with rare serious adverse events (Al Kaabi et al., 2021; Tanriover et al., 2021). Although these two vaccines have been widely used in China, their phase 3 trials were not performed in China, for there were few individuals infected with SARS-CoV-2 after the second half of 2020 in China due to the Chinese dynamic clearance strategy and strict adherence to public health measures. It was impossible to complete the enrollment at that moment in China. Thus, actually, less is known about their effectiveness in the Chinese population. In addition, there is a lack of

knowledge about their roles in protection against SARS-CoV-2 Omicron variant in China. This study shows that the vaccinated patients had shorter TtCT than the unvaccinated ones, indicating the inactivated vaccines keep working effectively against SARS-CoV-2 Omicron variant in the Chinese population. The mutations are causing numbers of SARS-CoV-2 variants that confer escape from antibodies (Kontopodis et al., 2022). There is no guarantee that the disease caused by subsequent mutations will be less severe and that the previous vaccines are still effective. Hence, it is of great significance to pay continuous efforts to evaluate the effectiveness of the previous vaccines against the new SARS-CoV-2 variants. As the SARS-CoV-2 continues to evolve, humans must be ready to develop new vaccines at any time.

A meta-analysis of different vaccines at phase 3 indicated that mRNA vaccines conferred a lesser risk of SARS-CoV-2 infection and showed more relevance to serious adverse events than viral vector and inactivated vaccines (Fan et al., 2021). A higher humoral response rate was also observed after using the mRNA vaccine compared with the inactivated vaccine (Lu et al., 2022; Ciampi et al., 2022). This suggests that there are great differences in the safety and effectiveness of different kinds of vaccines. For vaccines of the same kind but developed by different manufacturers, it is unclear whether such difference also exists. This retrospective cohort showed that most individuals suffered from this wave of SARS-CoV-2 pandemic in Shanghai, China, had been vaccinated with CoronaVac (Sinovac Life Science) accounting for 43.1% and Sinopharm BBIBP-CorV accounting for 47.2%. Our data indicated that there was no difference in TtCT between these two inactivated vaccines. This may suggest that the homogeneity of these two vaccines is good in the Chinese population.

The inactivated SARS-CoV-2 vaccines have been widely used in a two-dose schedule (Tanriover et al., 2021; Tanriover et al., 2021). A third vaccine booster dose appears to induce a significant increase in binding and neutralizing antibodies, which may improve protection against infection (Costa Clemens et al., 2022).

REFERENCES

- Al Kaabi, N., Zhang, Y., Xia, S., Yang, Y., Al Qahtani, M. M., Abdulrazzaq, N., et al. (2021). Effect of 2 Inactivated SARS-CoV-2 Vaccines on Symptomatic COVID-19 Infection in Adults: A Randomized Clinical Trial. *JAMA* 326 (1), 35–45. doi: 10.1001/jama.2021.8565
- Ciampi, E., Uribe-San-Martin, R., Soler, B., Garcia, L., Guzman, J., Pelayo, C., et al. (2022). Safety and Humoral Response Rate of Inactivated and mRNA Vaccines Against SARS-CoV-2 in Patients With Multiple Sclerosis. *Mult. Scler. Relat. Disord.* 59, 103690. doi: 10.1016/j.msard.2022.103690
- Costa Clemens, S. A., Weckx, L., Clemens, R., Almeida Mendes, A. V., Ramos Souza, A., Silveria, M. B. V., et al. (2022). Heterologous Versus Homologous COVID-19 Booster Vaccination in Previous Recipients of Two Doses of CoronaVac COVID-19 Vaccine in Brazil (RHH-001): A Phase 4, non-Inferiority, Single Blind, Randomised Study. *Lancet* 399 (10324), 521–529. doi: 10.1016/S0140-6736(22)00094-0
- Cui, J., Li, F., and Shi, Z. L. (2019). Origin and Evolution of Pathogenic Coronaviruses. *Nat. Rev. Microbiol.* 17 (3), 181–192. doi: 10.1038/s41579-018-0118-9
- Davies, M. A., Kassanjee, R., Rosseau, P., Morden, E., Johnson, L., Solomon, W., et al. (2022). Outcomes of Laboratory-Confirmed SARS-CoV-2 Infection in the Omicron-Driven Fourth Wave Compared With Previous Waves in the

However, our results show that the booster vaccination does not appear to reduce TtCT compared with the two-dose primary vaccination. Therefore, we hypothesize that the booster vaccination may increase antibody titer in a short time, but such effect would gradually decline. It is also unknown whether it is necessary to take the fourth or fifth dose. Hence, a randomized controlled trial is expected to evaluate whether the three-dose booster vaccination is superior to the two-dose primary vaccination.

In conclusion, vaccination is associated with shorter TtCT in patients with SARS-CoV-2 Omicron variant. It indicates that the inactivated vaccines keep working effectively against SARS-CoV-2 Omicron variant in Chinese population.

DATA AVAILABILITY STATEMENT

The raw data supporting the conclusions of this article will be made available by the authors, without undue reservation.

ETHICS STATEMENT

The studies involving human participants were reviewed and approved by Ethics Committee of Shanghai General Hospital, Shanghai Jiao Tong University School of Medicine, Shanghai, China. The patients/participants provided their written informed consent to participate in this study.

AUTHOR CONTRIBUTIONS

Conceptualization: YW; methodology: YW and JW; formal analysis: YW; investigation: YW, JW, FS, SZ, YL, XT, and PZ; writing: YW. All authors contributed to the article and approved the submitted version.

Western Cape Province, South Africa. *Trop. Med. Int. Health* 27(6), 564–573. doi: 10.1111/tmi.13752

- Fan, Y. J., Chan, K. H., and Hung, I. F. (2021). Safety and Efficacy of COVID-19 Vaccines: A Systematic Review and Meta-Analysis of Different Vaccines at Phase 3. *Vaccines (Basel)* 9 (9), 989. doi: 10.3390/vaccines9090989
- Kontopodis, E., Pierros, V., Stravopodis, D. J., and Tsangaris, D. G. T. (2022). Prediction of SARS-CoV-2 Omicron Variant Immunogenicity, Immune Escape and Pathogenicity, Through the Analysis of Spike Protein-Specific Core Unique Peptides. *Vaccines (Basel)* 10 (3), 357. doi: 10.3390/vaccines10030357
- Lu, L., Chen, L. L., Zhang, R. R., Chang, O. T., Chan, J. M., Tam, A. R., et al. (2022). Boosting of Serum Neutralizing Activity Against the Omicron Variant Among Recovered COVID-19 Patients by BNT162b2 and CoronaVac Vaccines. *EBioMedicine* 79, 103986. doi: 10.1016/j.ebiom.2022.103986
- Menni, C., Valdes, A. M., Polidori, L., Antonelli, M., Penamakuri, S., Nogal, A., et al. (2022). Symptom Prevalence, Duration, and Risk of Hospital Admission in Individuals Infected With SARS-CoV-2 During Periods of Omicron and Delta Variant Dominance: A Prospective Observational Study From the ZOE COVID Study. *Lancet* S0140-6736 (22), 00327–00320. doi: 10.1016/S0140-6736(22)00327-0
- Tanriover, M. D., Doğanay, H. L., Akova, M., Güner, H. R., Azap, A., Akhan, S., et al. (2021). Efficacy and Safety of an Inactivated Whole-Virion SARS-CoV-2

Vaccine (CoronaVac): Interim Results of a Double-Blind, Randomised, Placebo-Controlled, Phase 3 Trial in Turkey. *Lancet* 398 (10296), 213–222. doi: 10.1016/S0140-6736(21)01429-X

Yang, Z., Zhang, S., Tang, Y. P., Zhang, S., Xu, D. Q., Yue, S. J., et al. (2022). Clinical Characteristics, Transmissibility, Pathogenicity, Susceptible Populations, and Re-Infectivity of Prominent COVID-19 Variants. *Aging Dis.* 13 (2), 402–422. doi: 10.14336/AD.2021.1210

Conflict of Interest: The authors declare that the research was conducted in the absence of any commercial or financial relationships that could be construed as a potential conflict of interest.

Publisher's Note: All claims expressed in this article are solely those of the authors and do not necessarily represent those of their affiliated organizations, or those of the publisher, the editors and the reviewers. Any product that may be evaluated in this article, or claim that may be made by its manufacturer, is not guaranteed or endorsed by the publisher.

Copyright © 2022 Wu, Wei, Shen, Zhu, Lu, Tian and Zhang. This is an open-access article distributed under the terms of the Creative Commons Attribution License (CC BY). The use, distribution or reproduction in other forums is permitted, provided the original author(s) and the copyright owner(s) are credited and that the original publication in this journal is cited, in accordance with accepted academic practice. No use, distribution or reproduction is permitted which does not comply with these terms.



OPEN ACCESS

EDITED BY

Vikas Sood,
Jamia Hamdard University, India

REVIEWED BY

Grégory Dubourg,
IHU Mediterranée Infection, France
Devin Wahl,
Colorado State University,
United States

*CORRESPONDENCE

Marta Gonzalez-Freire
marta.gonzalezfreire@ssib.es
Carles Barcelo
carles.barcelo@ssib.es

[†]These authors have contributed
equally to this work and share
first authorship

[‡]These authors have contributed
equally to this work and share
last authorship

SPECIALTY SECTION

This article was submitted to
Virus and Host,
a section of the journal
Frontiers in Cellular and
Infection Microbiology

RECEIVED 13 May 2022

ACCEPTED 27 June 2022

PUBLISHED 22 July 2022

GDF15 and ACE2 stratify COVID-19 patients according to severity while ACE2 mutations increase infection susceptibility

Margalida Torrens-Mas^{1†}, Catalina M. Perelló-Reus^{2†},
Neus Trias-Ferrer¹, Lesly Ibargüen-González²,
Catalina Crespi³, Aina Maria Galmes-Panades^{1,4},
Cayetano Navas-Enamorado¹, Andres Sanchez-Polo¹,
Javier Piérola-Lopetegui⁵, Luis Masmiquel⁶, Lorenzo
Socias Crespi⁷, Carles Barcelo^{2*‡}
and Marta Gonzalez-Freire^{1*‡}

¹Translational Research in Aging and Longevity Group (TRIAL group), Health Research Institute of the Balearic Islands (IdISBa), Palma de Mallorca, Spain, ²Translational Pancreatic Cancer Oncogenesis Group, Health Research Institute of the Balearic Islands (IdISBa), Palma de Mallorca, Spain, ³Cell Culture and Flow Cytometry Facility, Health Research Institute of the Balearic Islands (IdISBa), Palma de Mallorca, Spain, ⁴Physical Activity and Sport Sciences Research Group (GICAFE), Institute for Educational Research and Innovation (IRIE), University of the Balearic Islands, Palma de Mallorca, Spain, ⁵Microscopy Facility, Health Research Institute of the Balearic Islands (IdISBa), Palma de Mallorca, Spain, ⁶Vascular and Metabolic Pathologies Group, Health Research Institute of the Balearic Islands (IdISBa), Palma de Mallorca, Spain, ⁷Intensive Care Unit, Health Research Institute of the Balearic Islands (IdISBa), Son Llatzer University Hospital, Palma de Mallorca, Spain

Coronavirus disease 19 (COVID-19) is a persistent global pandemic with a very heterogeneous disease presentation ranging from a mild disease to dismal prognosis. Early detection of sensitivity and severity of COVID-19 is essential for the development of new treatments. In the present study, we measured the levels of circulating growth differentiation factor 15 (GDF15) and angiotensin-converting enzyme 2 (ACE2) in plasma of severity-stratified COVID-19 patients and uninfected control patients and characterized the *in vitro* effects and cohort frequency of ACE2 SNPs. Our results show that while circulating GDF15 and ACE2 stratify COVID-19 patients according to disease severity, ACE2 missense SNPs constitute a risk factor linked to infection susceptibility.

KEYWORDS

GDF5, ACE2, inflammation, mutations, COVID-19

Introduction

In December 2019, several cases of pneumonia emerged in Wuhan, China, which were caused by a novel coronavirus initially named 2019-nCoV (Zhu et al., 2020). Due to its phylogenetic proximity to SARS-CoV, this new coronavirus was renamed as ‘SARS-CoV-2’ by the International Committee on Taxonomy of Viruses (Coronaviridae Study Group of the International Committee on Taxonomy of Viruses, 2020). This virus rapidly spread around the world due to its high transmissibility and the presence of asymptomatic subjects, which led to the declaration of a global pandemic by the World Health Organization. COVID-19 shows a very heterogeneous disease presentation, and clinical symptoms may differ with age and sex. Disease severity has been associated with older age, male sex, and comorbidities such as hypertension, diabetes, obesity, cardiovascular disease, chronic obstructive pulmonary disease, and lung, liver, and kidney disease (Huang C et al., 2020; Chen et al., 2020; Sanyaolu et al., 2020). Severe or fatal cases of COVID-19 usually present with increased levels of pro-inflammatory cytokines and chemokines, known as cytokine storm (de la Rica et al., 2020), low albumin levels (de la Rica et al., 2020), as well as decreased lymphocyte counts and platelets, elevated levels of C-Reactive Protein (CRP), procalcitonin, D-dimer, lactate dehydrogenase, and ferritin, among others (Guan et al., 2020; Zhou et al., 2020; Malik et al., 2021). Similarly, recent studies report that GDF15 levels, a member of the transforming growth factor- β (TGF- β) superfamily, are increased in COVID-19 patients who require hospitalization, and its levels are associated with viremia, hypoxemia, and worse clinical outcome (Notz et al., 2020; Myhre et al., 2020; Luis García de Guadiana et al., 2021). It is known that GDF15 levels are upregulated by inflammation, cancer, cardiovascular and metabolic diseases (Adela and Banerjee, 2015; Wischhusen et al., 2020). Also, circulating GDF15 levels show a high correlation with age and are primarily expressed under conditions of inflammation and oxidative stress (Doerstling et al., 2018). On the other hand, a predisposing genetic background may contribute to the wide clinical variability of COVID-19. To date, genetic markers of susceptibility to COVID-19 have not yet been identified.

The most well-known and evaluated mechanism of SARS-CoV-2 infection is the binding and uptake of viral particle through the ACE2 receptor, a type 1 integral membrane glycoprotein. The spike protein of the SARS-CoV-2 virus mediates its entry into the host cell through its interaction with ACE2. Transmembrane protease serine 2 (TMPRSS2) also participates in the cleavage of the spike protein, facilitating the entry. Both ACE2 and TMPRSS2 are highly expressed in different tissues and cell types, including the type II alveolar epithelial cells (Sungnak et al., 2020; Li et al., 2020). It has been observed that ACE2 expression in this type of cells

increases with age, which could contribute to the severity of COVID-19 symptoms among elderly patients (Pinto et al., 2020; Inde et al., 2021). For instance, plasma levels of ACE2 have been found elevated in kidney disease and cardiovascular disease (Narula et al., 2020). Recent studies show that ACE2 plasma levels are increased in COVID-19 patients compared to healthy subjects (Lundström et al., 2021; van Lier et al., 2021).

The emergence of SARS-CoV-2 variants-of-concern from last semester of 2021, accounted for vast majority of reported worldwide COVID-19 positivity. Such variants represent a public health challenge during the COVID-19 pandemic due to their ability to increase viral transmission and disease severity. Several mechanisms might account for increased variant transmissibility, especially mutations involved in enhanced spike protein binding affinity for the ACE2 receptor (Ramanathan et al., 2021). Therefore, coding variants within ACE2 could have the potential to alter SARSCoV-2 binding and possible infection responses in different individuals based on host genetics (Novelli et al., 2020; Benetti et al., 2020; Yildirim et al., 2021; Vadgama et al., 2022).

Based in all the above, the aims of this study were: i) to analyze whether GDF15 and ACE2 levels correlate with a worse COVID-19 prognosis as well as with other inflammatory and cellular markers of damage and senescence, and ii) to determine if different SNPs variants within ACE2 were associated to disease severity.

For this, circulating levels of both proteins, as well as RNA and DNA, were analyzed from plasma and buffy coats samples obtained from COVID-19 patients and in a uninfected control group matched by age and sex.

Methods

Patient population

This study included blood samples from 72 subjects: 47 COVID-19 samples were obtained from the Biobank Unit located in the Hospital Universitario Son Espases (HUSE), in Palma de Mallorca and 25 uninfected patients (control group), matched by age and sex, obtained from the Blood and Tissue Bank of the Balearic Islands. COVID-19 patients were classified based on disease severity into two groups: those requiring intensive care unit (ICU) admission for more than 24 h and died (n=21), and those requiring only low care intensity hospitalization and recovered (n=26) (non-ICU). The SARS-CoV-2 infection was confirmed by a positive result of a real time RT-PCR from nasal or pharyngeal swabs. Blood and buffy coat samples were obtained from the patients and stored at -80°C at the Biobank Unit. Clinical data of the individuals included in this study include age, sex, smoking habit, comorbidities, and inflammatory and coagulation

markers (PCR, ferritin, and D dimer). Not all the subjects had complete clinical data available.

Determination of ACE2 and GDF15 circulating levels

Circulating levels of ACE2 from plasma samples were quantified using the Human ACE2 SimpleStep ELISA® Kit (#ab235649, Abcam) following the manufacturer's instructions. Briefly, plasma samples were diluted 1:2 with the Sample Diluent NS and plated with the Antibody cocktail. Plates were incubated overnight at 4°C with gentle rocking. The following day, plates were washed, the TMB Development Solution was incubated for 10 min and the Stop Solution was added. An endpoint reading was performed at 450 nm in the Biotek Synergy H1 microplate reader. All samples were assayed in duplicate.

GDF15 circulating levels were measured using the Human GDF15 Quantikine® ELISA Kit (#DGD150, R&D Systems). Plasma samples were diluted 1:4 with the Calibrator Diluent and plated and incubated overnight at 4°C with gentle rocking. The next day, after washing the plates, Human GDF15 Conjugate was incubated by shaking for 1 h at room temperature. Then, the Substrate Solution was incubated for 30 min at room temperature in the dark and the Stop Solution was added. An endpoint reading was performed at 450 nm with a wavelength correction set at 540 nm in the Biotek Synergy H1 microplate reader. All samples were assayed in duplicate.

RNA and DNA isolation

RNA and DNA from plasma samples and buffy coats were extracted using TRI Reagent® BD (#T3809, Sigma-Aldrich) following the manufacturer's protocol. RNA and DNA quantity and quality were evaluated using a Nanodrop 1000 spectrophotometer (Thermo Scientific) set at 260 and 280 nm. Samples were stored at -80°C until further use.

RT-qPCR

For each sample, 200 ng of the total RNA isolated from plasma, or 1 µg of the total RNA extracted from the buffy coats were reversed transcribed to cDNA at 37°C for 50 min. The reaction mixture contained 250 mM Tris-HCl (pH 8.3), 375 mM KCl, 15 mM MgCl₂, 2.5 µM random hexamers, 500 µM of each dNTP, 20 U RNase inhibitor, 10 mM DTT, and 200 U M-Mlv reverse transcriptase. Each cDNA was diluted 1/10 with free RNase water and frozen at -20°C until further use. PCR reactions were performed on a LightCycler® 480 System. Genes, primers, and annealing temperatures are specified in [Supplementary Table 1](#). Reaction mix contained 7.5 µL SYBR TB

Green® Premix Ex Taq™ (RR420A, Takara) with 0.5 µM forward and reverse primers and 2.5 µL of each cDNA sample. The amplification program consisted of a denaturation step at 95°C for 5 min, followed by 45 cycles with a denaturation step (10 s, 95°C), an annealing step (10 s, temperature depending on primers), and an elongation step (12 s, 72°C). A negative control was run in each assay. The relative expression levels of each gene were calculated using the $\Delta\Delta C_t$ method and normalized to GAPDH expression.

Circulating mtDNA levels determination

Circulating levels of mtDNA were quantified using 5 ng of the isolated DNA from plasma samples. A mitochondrial gene (cytochrome C oxidase subunit III, COX3) and a nuclear gene (GAPDH) were amplified in a qPCR reaction. The reaction program for COX3 amplification consisted of a denaturation step of 95°C for 3 min, and 45 cycles of 95°C for 10 s and 55°C for 30 s. The levels of mtDNA were estimated using the $\Delta\Delta C_t$ method and normalized to 18S expression. All primers are specified in [Supplementary Table 1](#).

Analysis of mtDNA oxidation

Oxidation of mtDNA was performed as described previously in ([Cordani et al., 2018](#)) using the DNA extracted from buffy coats. Briefly, 5 ng of total DNA were used to amplify two different regions of mtDNA which are sensitive to oxidative damage. Oxidation of the G nucleotide diminishes the efficiency of the PCR reaction. Oxidation levels were estimated with the C_t ratio of these two regions and normalized by mtDNA levels determined as reported before. All primers are specified in [Supplementary Table 2](#).

Telomere length

Telomere length was analyzed as described by Joglekar et al ([Joglekar et al., 2020](#)) using the DNA isolated from buffy coats. Briefly, two PCR reaction were performed using 25 ng of total DNA, amplifying a telomere region and a single-copy gene (human beta globin, HBG). All primers are specified in [Supplementary Table 1](#).

Generation of SARS-CoV-2 pseudovirus

pcDNA3.1 plasmids encoding for Spike SARS-CoV-2 variants Alpha (B.1.1.7), Beta (B.1.351), Delta (B.1.617.2) and Epsilon (B.1.427/B.1.429) variants-of-concern (VOCs) were obtained from Dr. Thomas Peacock (Barclay lab, Imperial

College London, UK). *psPAX2* was a gift from Dr Didier Trono (Addgene plasmid # 12260); *pLV-mCherry* was a gift from Dr Pantelis Tsoulfas (Addgene plasmid # 36084); *pcDNA3 mCherry* was a gift from Dr Scott Gradia (Addgene plasmid # 30125); *pcDNA3.1(+)*eGFP was a gift from Dr Jeremy Wilusz (Addgene plasmid # 129020); *pcDNA3.1-SARS2-Spike* was a gift from Dr Fang Li (Addgene plasmid # 145032); *pcDNA3.1-ACE2-GFP* was a gift from Dr Utpal Pajvani (Addgene plasmid # 154962). *pcDNA3.1-GFP-ACE2* expressing *ACE2* SNPs were synthesized by GenScript. To generate SARS-Cov-2 pseudovirus, Human embryonic kidney 293 (HEK 293, ATCC[®] CRL-1573[™]) cells were seeded in a 10 cm²-plate at 4.5×10⁶ cells/plate, in DMEM (ThermoFisher Scientific, #11995073) supplemented with 10% FBS and 1x Normocin (*In vivo* gen, #ant-nr-1) and grown overnight at 37°C, 85% rel humidity, 5% CO₂. Next day, HEK 293 cells were then cotransfected with 15 µg of *psPAX2* : *pcDNA3.1SpikeVOCs* : *pLV-mCherry* at ratio 1:1:1 (i.e. 5:5:5 µg) using Lipofectamin[™] 3000 transfection reagent (ThermoFisher Scientific, #L3000015). Pseudoviruses harvested from the supernatant at 48 h 72h post-transfection were filtered (0.44 µm, Millipore Sigma, #SLHA033SS) concentrated with 50kDa-PES (ThermoFisher Scientific, #88540) at 20 min a 14,000g RT and stored at -80°C.

Pseudovirus entry assay

A549 cells (ATCC[®] CCL-185) seeded in 6-multiwell plates at 0.23 × 10⁶ cells/well in DMEM (10% FBS and 1x Normocin), and grown overnight at 37°C, 85% rel humidity 5% CO₂. Next day, cells were transfected with either *pcDNA3.1(+)*eGFP (control) or *pcDNA3.1-GFP-ACE2* expressing the *ACE2* SNPs. To test the effect of *ACE2* SNPs on pseudovirus entry, at 24h posttransfection cells were infected with 0.25 mL concentrated pseudoviruses + 0.25 mL DMEM (10% FBS and 1x Normocin) overnight at 37°C, 85% rel humidity, 5% CO₂. Next day, 1 ml of fresh DMEM was added (10% FBS and 1x Normocin). To measure the mCherry signal (a proxy for virus uptake), at 48h postinfection, medium was removed and cells were detached using TrypLE (ThermoFisher, #12605036) washed in DPBS (ThermoFisher, #14190250) and incubated for 5 min RT with 4',6-diamidino-2-phenylindole (DAPI) at a final concentration of 0.1 µg/mL. Viable (DAPI negative) double positive eGFP/mCherry cells were measured using a BD FACSAria Fusion cell Sorter (BD Bioscience). 10,000 total events were recorded for every sample. Samples with less than 5,000 total events were discarded. Flow cytometer data was analyzed using BD Bioscience Flow cytometry analysis software. Briefly, cell population was defined using FSH/SCC gating and the percentage of positive cells was calculated using a manually defined cutoff based on log10 fluorescence intensity histograms of the corresponding channel on a non-infected population.

Microscope imaging

In order to assess overall protein localization of *ACE2* variants, A549 cells grown at 40000 cells/well in 8-well cell culture chamber (Sarstedt, #94.6170.802) were transfected with 1,5 µL Lipofectamine 3000[®] (Thermo Scientific, #L3000015) following the manufacturer's protocol. At 48h post transfection, cells were fixed with 4% paraformaldehyde in PBS for 10 minutes at room temperature (RT) and washed twice with PBS. Then, they were permeabilized with 0.1% Triton X-100- PBS for 15 min and incubated with 2% BSA in PBST (PBS+ 0.1% Tween 20) for 1 h at RT to block nonspecific binding. Chambers were incubated with either anti-*ACE2* (1:100; MA5-32307; Thermo Scientific) or anti-*ACE2* (1:50; MAB933; R&D Systems) in PBST containing 0,1% BSA ON at 4°C, washed twice in PBS and incubated with Alexa-Fluor647-labeled anti-rabbit (1:2000; ab150079; Abcam) or anti-mouse (1:2000; ab150115, Abcam) for 1h at RT. Images were acquired with Cell Observer-Zeiss.

Identification and selection of *ACE2* polymorphisms

We queried multiple genomic databases including gnomAD (Karczewski et al., 2020), RotterdamStudy (Ikram et al., 2017), UK's 100k Genomes Project (100KGP) (Consortium GER, 2019) as the main sources of aggregated data for *ACE2* protein altering variations in populations groups across the world. These databases display summary statistics and aggregate variant data from the identified exome and genome data. Aggregation of data from disparate sources and platforms has been made possible by uniform joint variant calling using a standardized BWA-Picard-GATK pipeline (Van der Auwera et al., 2013). We only considered non-synonymous allele variants with high allelic frequency (>1.00.e-4) and allele count >20. Then we selected variants within the human *ACE2*-claw S-protein RBD-binding interface as described in previous studies that could potentially increase or decrease the binding affinity of *ACE2* to the S-protein and thereby alter the ability of the virus to infect the host cell. Finally, we aimed to investigate which *ACE2* variants were associated with clinical outcome to shortlist the candidates to study in detail. Two different studies identified 5 *ACE2* variants as potentially predisposing genetic background to the observed interindividual clinical variability (Benetti et al., 2020; Vadgama et al., 2022). We finally shortlisted the 5 variants fulfilling this triple requirement of being abundant, involving critical residues in RBD interface and being potentially clinically relevant.

ACE2 polymorphism genotyping

cDNA obtained from circulating mRNA was analyzed to detect selected *ACE2* SNPs. Three different PCR reactions were

designed to cover the regions comprising the studied *ACE2* SNPs. Primers were designed to obtain amplicons of 0.2–0.8 kb and specificity was confirmed by PrimerBLAST (Ye et al., 2012). PCRs were performed with GoTaq® G2 Flexi DNA Polymerase (Promega; M7805). PCR conditions were optimized by the Promega PCR design software (<https://www.promega.es/resources/tools/biomath/tm-calculator/>).

PCR1 amplified the region corresponding to residues Ser3 to Met249 (743 bp). Primers Forward 5' AAGCTCTTCTGGCTCCTTC3', Reverse 5' TCATCAACTTTGCCCTCACA3'. Cycling conditions were as follows: 95°C for 5 minutes, followed by 40 cycles (94°C for 30s, 67°C for 30s, 72°C for 1 min) with a final extension at 72°C during 10 min.

PCR2 amplified the region corresponding to residues Phe308 to Arg621 (944 bp). Primers Forward 5' ATTCAAGGAGGCCGAGAAGT3', Reverse 5' TCCTCACTTTGATGCTTTGG3'. Cycling conditions were as follows: 95°C for 5 minutes, followed by 40 cycles (94°C for 30s, 63°C for 30s, 72°C for 1 min) with a final extension at 72°C during 10 min.

PCR3 amplified the region corresponding to residues Val670 to Val752 (250 bp). Primers Forward 5' TGTGCGAGTGGCTAATTTGA3', Reverse 5' CACTCCCATCACAACTCCAA3'. Cycling conditions were as follows: 95°C for 5 minutes, followed by 40 cycles (94°C for 30s, 65°C for 30s, 72°C for 30s) with a final extension at 72°C during 10 min.

Agarose gel electrophoresis was performed in order to confirm specificity. PCR product was purified by clean-up (FAGCK001, Favorgen) and further sequenced by Macrogen. Alignment of sequencing reads against reference *ACE2* (NM_021804) and SNP genotyping was attained by the SnapGene® Software (snapgene.com). **Supplementary Figure 2**

Statistical analysis

Descriptive characteristics were summarized as means and standard deviations (SDs) or as numbers and percentages (%). One-way analysis of variance (ANOVA), Chi-square tests (χ^2), and Fisher's exact test were used to assess differences across 3 groups of participants: ICU; non-ICU and controls, for continuous and categorical variables respectively. Non-normally distributed continuous data were compared using the Mann-Whitney-Wilcoxon test or the Kruskal-Wallis H-test. The relationships between variables were studied using Spearman or Pearson correlations. Linear regression modeling was used to quantify the associations of *ACE2* genotypes on GDF15 and *ACE2*. Analyses were adjusted for: age, sex, and group. Correlation coefficients were performed to determine correlations between GDF15 and changes on biochemical parameters among COVID-19 infected patients. To test potential associations between the studied parameters, a Principal Component Analysis (PCA) was computed. Statistical analyses were performed using R Studio version

3.5.2 of the R programming language (R Project for Statistical Computing; R Foundation, Vienna, Austria). and Stata v17.0 program. *P*-values <0.05 were deemed as statistically significant.

Study approval

This study was conducted in agreement with the Good Clinical Practice principles and the Declaration of Helsinki for ethical research. Ethical approval for this project (IB 4165/20 PI, 6 April 2020) was obtained from the ethics committee of the Balearic Islands and waived the requirement for informed consent, due to the emergency situation.

Results

Demographic and clinical characteristics.

Demographic data, comorbidities, and inflammation markers of the individuals included in this study are shown in **Table 1**. A total of 72 subjects were included in the study, 46% males, with an average age of 69 years (range 28–88 years). SARS-CoV-2 infection was diagnosed by a real-time RT-PCR. There were no differences in age or sex among the three groups ($p > 0.05$). All the ICU patients died. The most frequent comorbidities were hypertension (51%), type 2 diabetes mellitus (38%), smokers (38%), or others (59%). Inflammatory markers such as ferritin, CRP, and D-dimer were significantly higher in the ICU group that died, compared to the non-ICU and control group.

Circulating levels of GDF15 and *ACE2*

Plasma levels of both GDF15 and *ACE2* were measured using ELISA (**Figures 1A, B**). ICU patients showed higher levels of GDF15 when compared to non-ICU patients and control group (3846.84 pg/mL vs 1620.29 pg/mL and 1073.6 pg/mL, respectively; $P < 0.001$; **Figure 1A**). However, there was no difference between the non-ICU and the uninfected control group ($P > 0.05$). *ACE2* circulating levels (**Figure 1B**) were increased in the ICU group compared with the non-ICU and control groups (10107.36 pg/mL vs 7172.9 pg/mL and 7708.5 pg/mL, respectively). ICU patients showed significantly higher levels than the non-ICU patients ($P = 0.02$). Interestingly, the ratio between the levels of GDF15 and the levels of *ACE2* (**Figure 1C**) was also significantly higher in the ICU patients compared to the non-ICU and control groups ($P = 0.010$ and $P < 0.001$, respectively). This ratio was also increased in non-ICU patients compared to the control group ($P = 0.006$). Finally, we found a positive correlation, although not statistically significant, between the levels of GDF15 and *ACE2* (**Figure 2**), ($r = 0.204$, $P = 0.087$).

TABLE 1 Baseline characteristics of the sample population.

| | Total (n=72) | ICU (n=21) | non-ICU (n=26) | Control group (n=25) | p-value |
|-----------------------------|-------------------------------|---------------------------------|-------------------------------|-------------------------------|---------|
| Age (years) | 69.51(10.31) [62-72] | 71.2 (13.87) [65-78] | 71.84 (7.38) [69-75] | 65.84 (8.78) [62-69] | 0.081 |
| Males (%) | 33 (46%) | 10 (48%) | 13 (50%) | 10 (40%) | 0.759 |
| Mortality (%) | 21 (29.16%) | 21 (100%) | 0 (0%) | 0(0%) | <0.001* |
| Comorbidities | | | | | |
| Hypertension | 29/57 (51%) | 6/11 (54%) | 15/26 (58%) | 8/20 (40%) | 0.475 |
| Type 2 diabetes | 22/57 (38%) | 6/11 (54%) | 11/26 (42%) | 5/20 (25%) | 0.236 |
| Obesity | 7/57 (12%) | 2/11 (18%) | 3/26 (42%) | 2/20 (10%) | 0.792 |
| COPD | 3/57 | 3/11 (27%) | 0/26 (0%) | 0/20 (0%) | 0.001* |
| Dyslipidemia | 18/57 (31%) | 4/11 (36%) | 14/26 (54%) | 0/20 (0%) | <0.001* |
| Other | 33/56 (59%) | 7/11 (64%) | 14/26 (54%) | 12/19 (63%) | 0.772 |
| Smokers | 22/57 (38%) | 5/11 (45%) | 17/26 (65%) | 0/20 (0%) | <0.001* |
| Inflammation markers | | | | | |
| Ferritin (ng/mL) | 651.64 (1068.24) [327-976] | 1332.79 (1350.07) [682-1984] | 133.93 (176.17) [61-207] | – | <0.001* |
| CRP (mg/dL) | 39.93 (78.40) [16-64] | 89.65 (98.31) [42-137] | 0.56 (0.82) [0.22-0.91] | – | <0.001* |
| D-Dimer (ng/mL) | 907.98 (2057.98) [275-1541] | 1761.25 (2810.61) [446-3077] | 166.00 (160.64) [97-235] | – | <0.001* |
| GDF15 (pg/mL) | 2079.88 (1594.51) [6606-9838] | 3846.84 (1473.42) [3176-4518] | 1620.29 (972.05) [1228-2013] | 1073.60 (844.13) [725-1422] | <0.001* |
| ACE2 (pg/mL) | 8221.84 (6826.93) [6606-9838] | 10107.36 (5337.96) [7678-12537] | 7172.9 (9243.67) [3439-10906] | 7708.50 (4407.88) [5847-9570] | 0.011* |

Data are presented as mean, standard deviation (), rank [], or percentage (%). *Statistically significant difference. Some patients' inflammation markers or comorbidities were not available. In this case, total number of patients with available data is shown in each row.

Association between the levels of GDF15 and ACE2, with age, sex, and inflammatory markers

As expected, circulating GDF15 was positively associated with age ($r=0.482$, $P<0.001$, Figure 3A). However, ACE2 levels were not associated with age ($r=-0.003$, $P=0.982$, Figure 3B). No differences were found in the circulating levels of GDF15 (Figure 4A) and ACE2 (Figure 4B) with sex ($P>0.05$). Since ACE2 is the functional receptor of SARS-CoV-2, we checked whether there were differences in the ACE2 mRNA by RT-qPCR (Figure 5). ICU patients showed higher levels of ACE2 expression compared to non-ICU and control groups ($P=0.006$ and $P=0.003$, respectively). Interestingly, ACE2 expression levels did not correlate with ACE2 protein levels measured by ELISA (data not shown).

We next analyzed the association between the levels of GDF15 and ACE2 with ferritin, D-dimer and CRP, classical markers of inflammation. Only COVID-19 patients had data on inflammatory markers. As expected, the levels of both GDF15 (Figure 6A) and ACE2 (Figure 6B) were positively correlated with the levels of ferritin, D-dimer, and CRP (GDF15: $r=0.561$, $r=0.688$, $r=0.497$, respectively, $P<0.001$; ACE2: $r=0.386$ and $P=0.009$, $r=0.350$ and $P=0.021$, $r=0.381$ and $P=0.012$, respectively).

Since hypoxia is one of the main pathophysiological causes of mortality in patients with COVID-19 and the release of damaged mitochondrial DNA (*mtDNA*) is related to the increase of the systemic inflammatory response, we sought to determine the circulating levels of hypoxia inducible factor 1 A (*HIF1A*) mRNA, a transcription factor that normally is upregulated during hypoxic and inflammatory conditions, and circulating levels of *mtDNA*, measured as the ratio between nuclear to mitochondrial DNA. Unexpectedly, we did not find differences neither in the expression levels of *mtDNA* or *HIF1A* (Figures 7A, B respectively).

We performed principal component analysis (PCA) with all the markers above plus GDF15, ACE2, age, and sex (Figure 8). These analyses showed a clear distinction between ICU, non-ICU patients and the control group, revealing a clear effect of SARS-CoV-2 infected patients compared to uninfected subjects.

We had complete clinical data from blood routine analysis (Supplementary Table 3) as well as buffy coats from the non-UCI group, we decided to test if the levels of GDF15 and ACE2 were correlated with those parameters. We also extracted RNA and DNA from buffy coats and measured known markers of senescence and oxidative damage, such as *p16*, *p21*, telomere length, *mtDNA/nDNA* ratio and *mtDNA* oxidation. In the <xr id="sf4">Supplemental Table 4</xr> we show the correlation

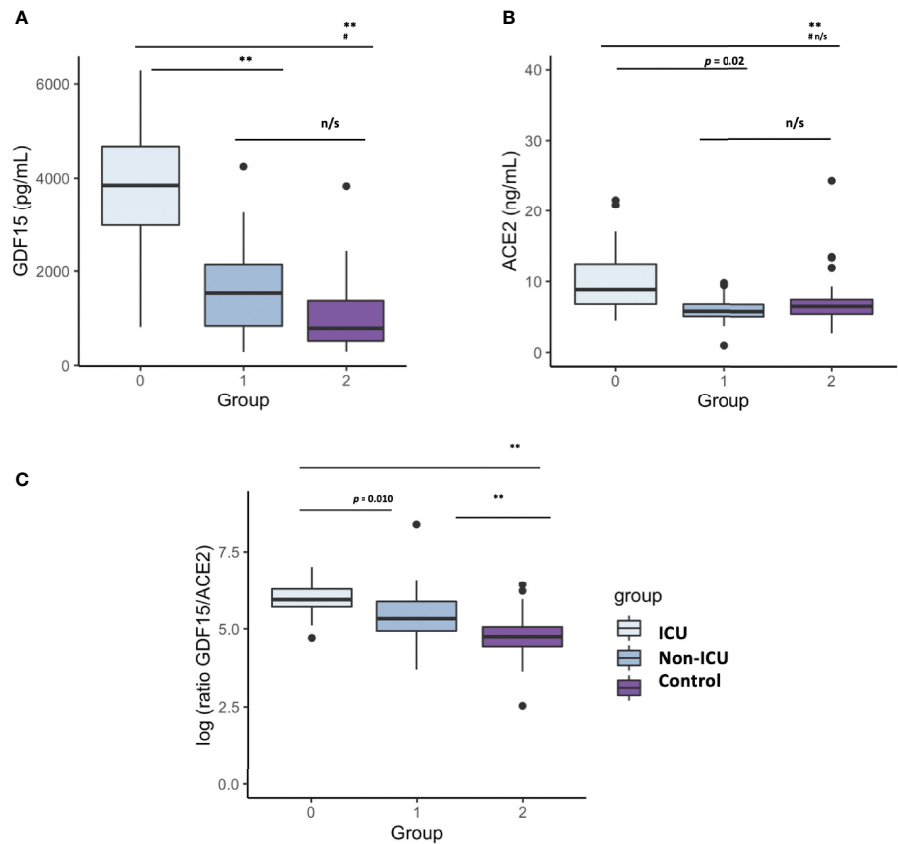


FIGURE 1
Differences in circulating GDF15 and ACE2 levels in COVID-19 patients and an uninfected control group. **(A)** GDF15 levels; **(B)** ACE2 levels; **(C)** ratio GDF15/ACE2; The box plots represent the maximum and minimum levels (whiskers), the upper and lower quartiles, and the median. The length of each box represents the interquartile range. Dots represent outliers. Statistical significance between groups was determined using the ANOVA test. ** $p < 0.001$, * $p < 0.001$ UCI vs Control, n/s (non significant); GDF15 (Growth differentiation factor 15); ACE2 (angiotensin-converting enzyme 2).

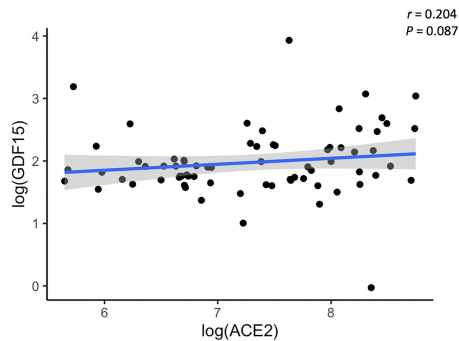


FIGURE 2
Representative scatterplot showing the association between GDF15 and ACE2 levels. Results of the 72 subjects are shown. Each dot represents an individual value. The solid blue line represents the regression line. The grey shade represents the confidence interval.

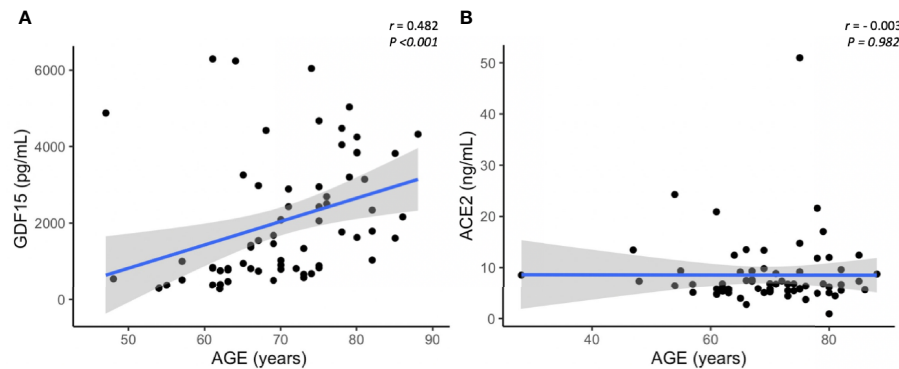


FIGURE 3

Representative scatterplots showing the association between GDF15 and ACE2 levels with age. GDF15 is positive associated with age (A), while ACE2 is not correlated with age (B). Each dot represents an individual value. The solid blue line represents the regression line. The grey shade represents the confidence interval.

coefficient between all the variables described above, GDF15 and ACE2. Interestingly, both circulating GDF15 and ACE2 were positively correlated with glucose, urea, creatinine, and N-terminal (NT)-pro hormone BNP (NT-proBNP) ($P < 0.01$). Circulating GDF15 was negatively correlated to the platelets levels ($r = -0.557$, $P < 0.05$) and the levels of *mtDNA* oxidation ($r = -0.495$, $P < 0.05$). With regards to mRNA expression data, the expression levels of *ACE2* in plasma were also correlated with the neutrophil and the ratio lymphocyte to neutrophils ($r = 0.478$, $p < 0.05$; $r = 0.629$, $P < 0.01$ respectively), while the expression levels of *ACE2* in buffy coats were only associated with the eosinophils levels ($r = 0.542$, $P < 0.05$). Finally, the protein and mRNA expression levels of *ACE2* in plasma were highly positive correlated with the expression of *HIF1A* in buffy coats ($r = 0.637$, $P < 0.05$), while the levels of *ACE2* in buffy coats were correlated with the expression of *HIF1A* in plasma ($r = 0.704$, $P < 0.01$).

Differential SARS-CoV-2 infection dependent on COVID-19 variant-of-concern and ACE2 expression

Since ACE2 circulating levels were increased in the ICU group compared to the non-ICU and control group, both at mRNA and protein levels (Figures 5, 1B), we then tested the effect of full length ACE2 expression on the infection capacity of SARS-CoV-2. To this end, we developed an infection model based on SARS-CoV-2 pseudotyped lentivirus (pseudovirus) expressing Spike protein and encapsulating a mCherry reporter. We tested infection with this approach in human alveolar lung A549 cells, as a COVID-19 human infection model to recapitulate airway infection (Figure 9A). We found untransfected A549 to be non-permissive to SARS-CoV-2 pseudoinfection (Figure 9B) due to the low expression of the endogenous viral receptor ACE2 (Supplementary Figure 1). This

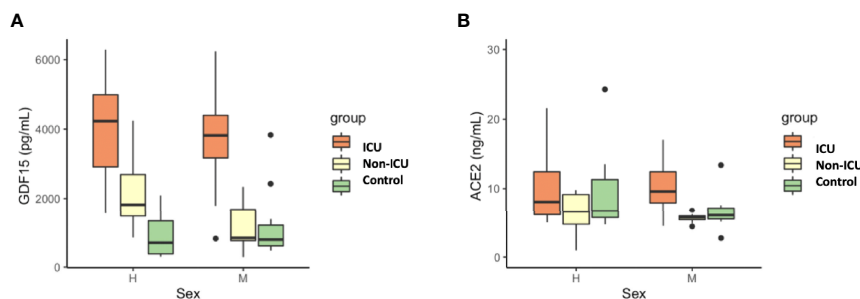


FIGURE 4

Differences in circulating GDF15 (A) and ACE2 levels (B) by sex in COVID-19 patients and the uninfected control group. No differences were found by sex in GDF15 and ACE levels. The box plots represent the maximum and minimum levels (whiskers), the upper and lower quartiles, and the median. The length of each box represents the interquartile range. Dots represent outliers. Statistical significance between groups was determined using the ANOVA test.

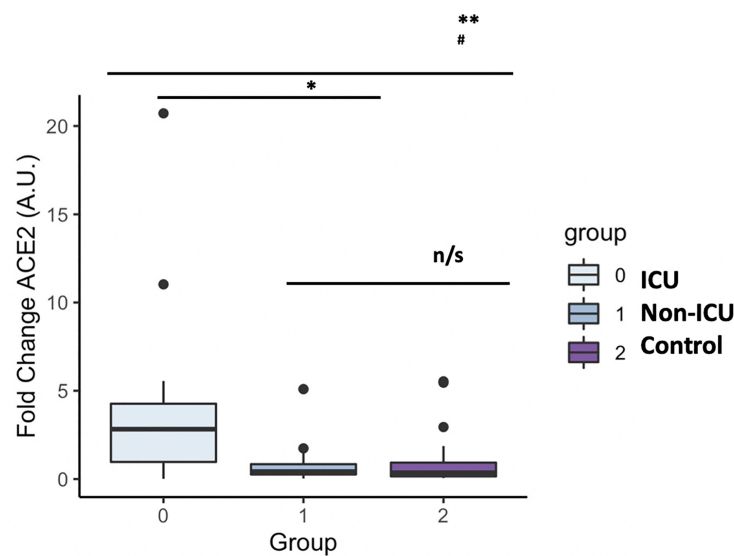


FIGURE 5

ACE2 mRNA levels in COVID-19 patients and the uninfected control group. The box plots represent the maximum and minimum levels (whiskers), the upper and lower quartiles, and the median. The length of each box represents the interquartile range. Dots represent outliers. Statistical significance between groups was determined using the ANOVA test. ** $p < 0.001$, # $p < 0.001$ UCI vs Control, n/s (non significant); ACE2 (angiotensin-converting enzyme 2).

eliminates the interference of endogenous ACE2 when overexpressing *ACE2* variants and facilitates the interpretation of results when performing pseudovirus entry studies. Exogenous expression of GFP-*ACE2* enabled SARS-CoV-2 pseudovirus to effectively infect the cells with mCherry reporter as determined by Fluorescent Activated Cell Sorter (FACS) (Figure 9B).

Finally, in order to test whether the main variants of concern (VOC) circulating the last semester of 2021 [B.1.1.7 (Alpha), B.1.351 (Beta), P.2 (Zeta) and B.1.617.2 (Delta)] infected ACE2-expressing cells with differential efficiency, we expressed the different full-length Spike protein corresponding to the VOCs (Wuhan-1, Alpha, Beta, Delta and Zeta) in the lentiviral pseudovirus model described above and infected the A549 transiently expressing full length *ACE2* described above.

We found significant increased infectivity in the Delta variant as compared to the origin variant Wuhan-1 ($P < 0.016$). Alpha, Beta and Zeta showed a modest non-significant increased infectivity as compared to Wuhan-1 (Figure 9C).

ACE2 polymorphisms K26R, P389 and N720D promote SARS-CoV-2 infection in all VOCs

Given that host genetics and ethnicity predisposition to COVID-19 is now recognized to be relevant to COVID-19

susceptibility and severity, we reasoned that it is very likely that there exists *ACE2* variants in human populations that may modulate its affinity to SARS-CoV-2 S-protein and thereby render individuals more resistant or susceptible to the virus. To investigate this, we shortlisted the *ACE2* non-synonymous variants fulfilling the triple requirement of 1) high allelic frequency [$>10^{-4}$ (gnomAD)], 2) involved critical residues in the ACE2-claw S-protein RBD-binding interface (Hussain et al., 2020; Suryamohan et al., 2021) and 3) being potentially clinically relevant especially in Mediterranean populations (Benetti et al., 2020; Vadgama et al., 2022) (Figure 10A). Therefore we 5 shortlisted three common c.2158A>G p.(N720D), c.77A>G p.(K26R), and c.631G>A p.(G211R) SNPs and two rare variants, namely, c.1051C>G p.(L351V) and c.1166C>A p.(P389H) (Figure 10A). Intriguingly, these variants are overrepresented in the Mediterranean and European populations ($P < 0.001$) but are extremely rare in the Asian population (Consortium GER, 2019; Benetti et al., 2020; Vadgama et al., 2022). We analyzed the impact of the shortlisted *ACE2* non-synonymous variants on SARS-CoV-2 infection using the Pseudovirus infection model described above. We found that upon similar expression of the *ACE2* variants (Supplementary Figure 1A), SARS-CoV-2 pseudovirus containing Wuhan-1 Spike was able to infect A549 cells more efficiently in K26R ($P = 0.0008$), P389H ($P = 0.0012$) and N720D ($P = 0.0059$) as compared to the wild-type (WT) *ACE2* (Figure 10B). Conversely, we found that the variant G112R

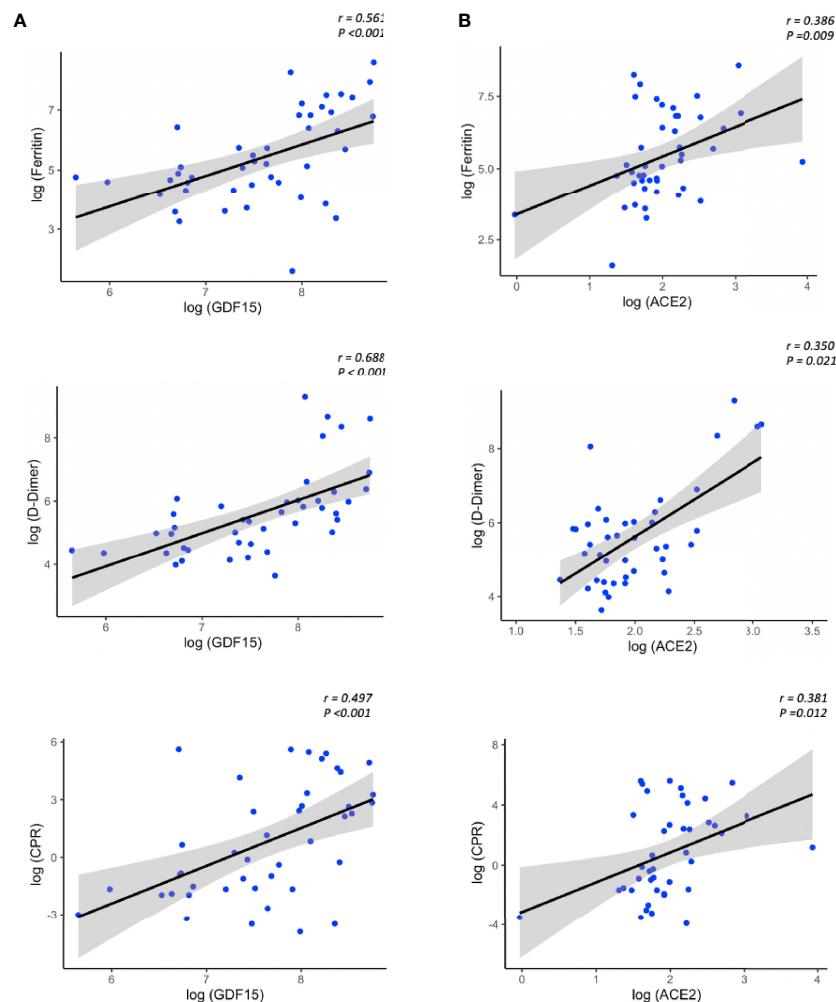


FIGURE 6

Representative scatterplots (spearman correlations) showing the association between GDF15 (A) and ACE2 levels (B) with classical inflammatory markers. The solid line represents the regression line. The grey shade represents the confidence interval.

exhibited a moderate protective effect on infection ($P=0.027$). No significant differences were observed in L351V variant ($P=0.768$) compared to WT, therefore this variant was not further studied (Figure 10B). We obtained similar results when pseudotyping with Alpha, Beta, Delta or Zeta VOC (Figure 10C). This increased infectivity strongly suggests that bearing K26R, P389H or N720D ACE2 variants could constitute a predisposing genetic background for severe COVID-19.

ACE2 polymorphisms K26R, P389H and N720D are risk factor for severe COVID-19

Given the potential impact of shortlisted ACE2 variants in SARS-CoV-2 infection and its overrepresentation in

Mediterranean populations (Benetti et al., 2020; Vadgama et al., 2022), we analyzed the presence of these variants in severity-stratified groups from our cohort in order to get an insight on the role of ACE2 variants on interindividual severity and susceptibility to COVID-19. We found a differential distribution among groups (Figure 11 and Table 2). Notably, and in line with our *in vitro* observations, we found that the “infection-promoting” variants K26R, P389H and N720D were enriched in COVID-positive (non-ICU and ICU groups) as compared to matched uninfected controls (Fisher’s exact test $P = 0.001$; OR= 5.097; RR=3.439 at 95% CI) (Figure 11B and Table 3), suggesting that they constitute a risk factor for COVID-19 patients. Conversely, “infection-protective” G211R variant had a modest protective effect (Fisher’s exact test $P < 0.001$; OR=0.01327; RR= 0.2295 at 95% CI) (Table 3). While these associations need to be confirmed in larger sample sizes, they

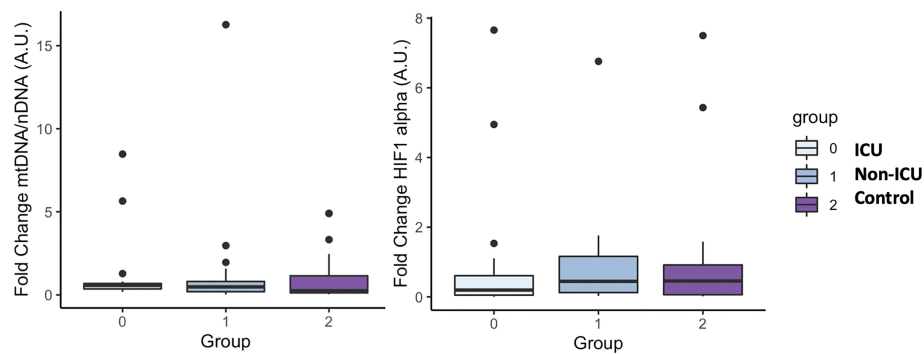


FIGURE 7

mtDNA and HIF1 alpha mRNA levels in COVID-19 patients and the uninfected control group. The box plots represent the maximum and minimum levels (whiskers), the upper and lower quartiles, and the median. The length of each box represents the interquartile range. Dots represent outliers. Statistical significance between groups was determined using the ANOVA test. No difference were found in mtDNA and HIF1 alpha mRNA levels among groups.

strongly suggest that these variants could play a central role in COVID-19 susceptibility.

Influence of *ACE2* polymorphisms on inflammation markers

We then analyzed whether the different *ACE2* polymorphisms may influence the levels of inflammation markers. First, we tested if the presence or absence of the different variants could affect the levels of GDF15 or *ACE2*. Interestingly, we did not find differences in the circulating

protein levels of GDF15 and *ACE2* when taken the 72 samples as a whole (Supplementary Figure 3). However, the P389H, G211R, and L351V variants were associated with a decrease in the levels of circulating *ACE2* mRNA, while the individuals bearing the N720D variant showed increased levels of circulating *ACE2* mRNA (Supplementary Figure 4). Second, we repeated the analysis comparing ICU vs non-ICU group, and we found that the levels of GDF15 and *ACE2* were similar in the ICU patients carrying the different mutations compared to the non-ICU group (Figure 12). Then, we decided to repeat the same analysis, but classifying our sample population in 4 genotypes based on the presence or absence of

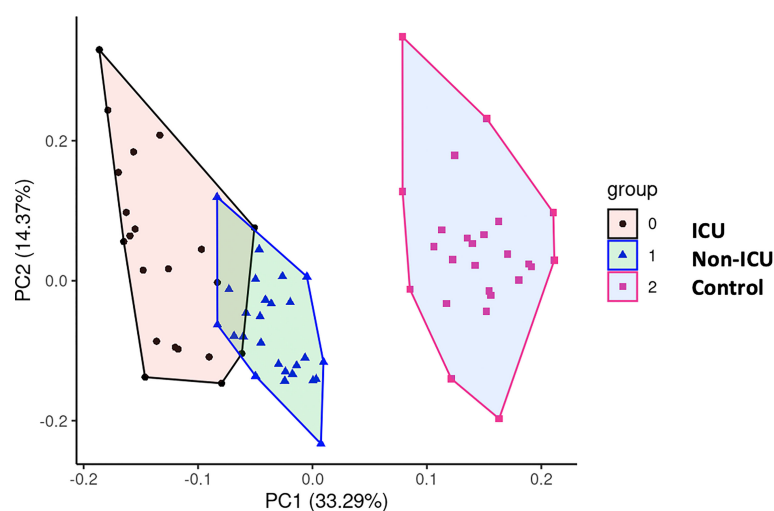


FIGURE 8

Principal Component Analysis (PCA). To test potential associations between the studied parameters, a PCA was computed, showing a clear distinction between COVID-19 patients and uninfected control subjects.

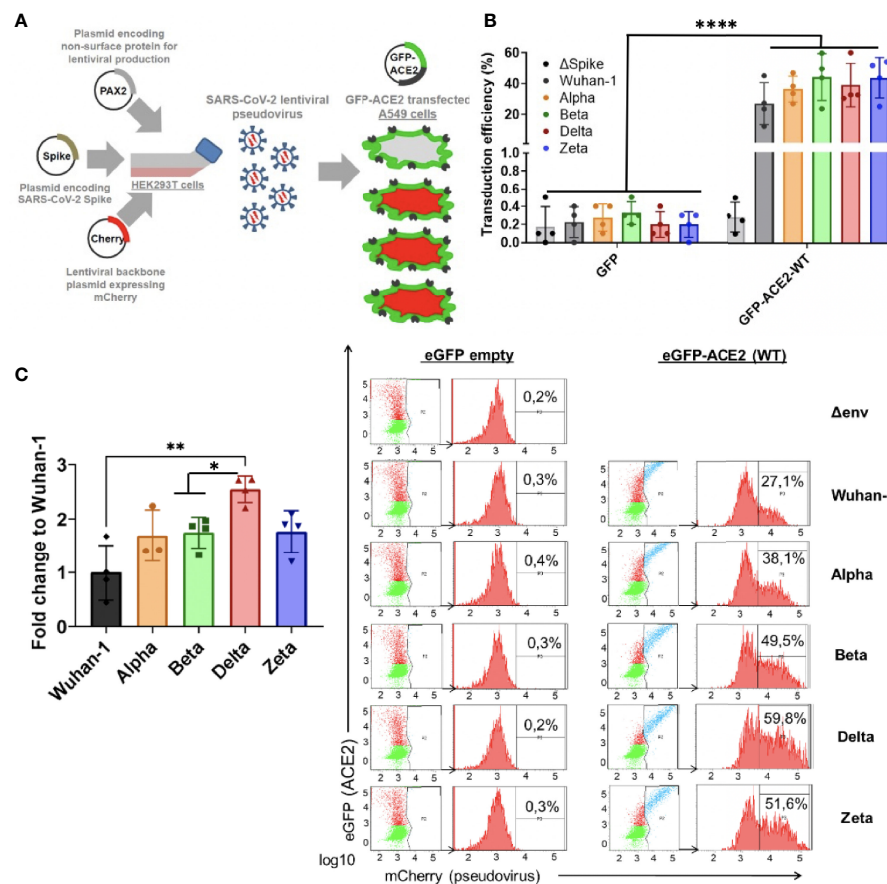


FIGURE 9

Differential SARS-CoV-2 infection is dependent on COVID19 variant-of-concern and ACE2 expression. **(A)** SARS-CoV-2 cell entry assay strategy: Lentiviral-based replication-defective pseudovirus were generated in HEK293T cells from lentiviral parental genes, SARS-CoV-2 Spike and encapsulating a mCherry reporter. Since the entry steps of the SARS-CoV-2 pseudovirions are governed by the coronavirus Spike protein at their surface, they enter cells in a similar fashion to native counterparts. A549 airway cells were transfected with exogenous GFP-hACE2 enabling SARS-CoV-2 pseudovirus to effectively infect the cells with mCherry reporter. Double-positive GFP/mCherry cells were quantified by flow cytometry to assess viral infection capacity. **(B,C)** Following the strategy described in A, A549 cells expressing GFP-hACE2 were assayed for cell entry by SARS-CoV-2 pseudovirus expressing either empty vector (Δ Spike) or Spike protein corresponding to origin variant (Wuhan-1) or variants-of-concern Alpha, Beta, Delta or Zeta. A representative flow cytometry experiment is shown. Bars demonstrate mean and Standard Error of Mean while each data point represents a unique experiment; **** $P < 0.0001$; ** $P < 0.01$; * $P < 0.1$ by two-tailed t-test.

the different variants. Genotype 0 corresponding to subjects that did not carry any variant; Genotype 1, subjects that carry at least one promoting variant; Genotype 2, subjects that carry at least one protective variant; Genotype 3, subjects that carry at least one promoting and one protective variant (Supplementary Table 5; Figure 13). We only found differences in the levels of the ACE2 mRNA ($P < 0.05$).

Finally, in linear regression models, adjusting for age, sex, and group (ICU, non-ICU, and Control group) we did not find any association between the ACE2 genotypes with GDF15 and ACE2 levels (Supplementary Table 6) suggesting a separate role of these markers in COVID-19 susceptibility and severity.

Discussion

Despite the fact that the majority of the population is already vaccinated against SARS-CoV-2 and the rate of mortality has been reduced, vaccination is not enough to defeat the virus. COVID-19 infection rate remains high, and treatment of severe cases has become a great challenge. Therefore, early recognition of the sensitivity and severity of COVID-19 is essential for the development of new treatments. In the present study, we measured the levels of circulating GDF15 and ACE2 in plasma of patients with COVID-19 who were admitted to the ICU and died and admitted to the ICU who recovered, as well as in an uninfected matched control group. We also characterized the *in*

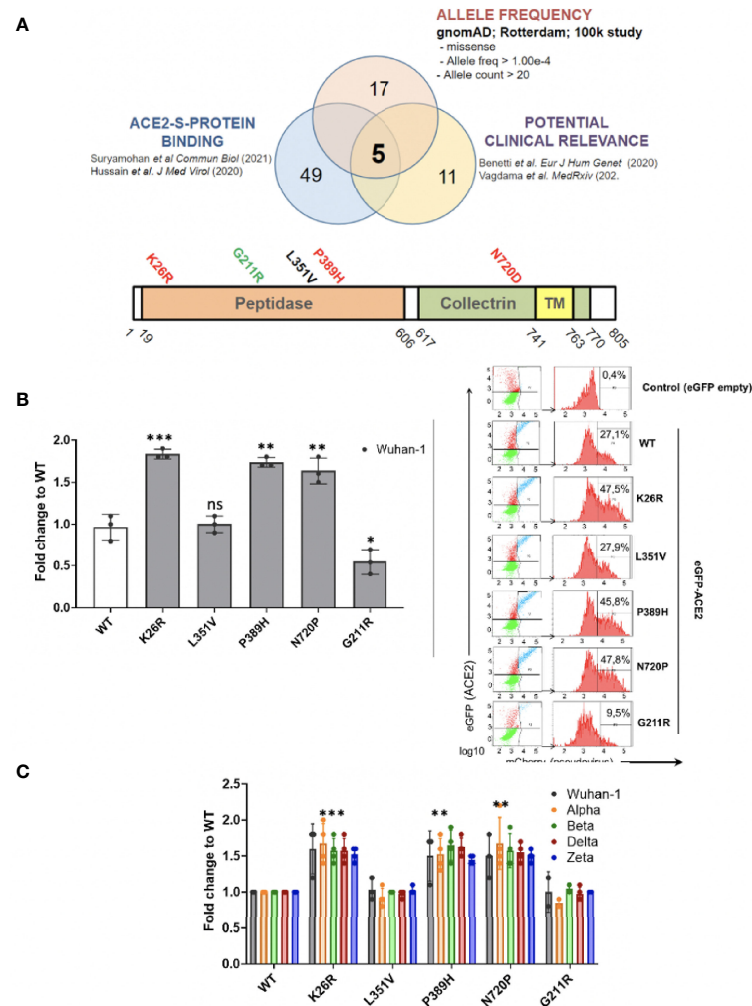


FIGURE 10

ACE2 polymorphisms K26R, P389 and N720D promote SARS-CoV-2 infection in all VOCs. (A) Studying the effect of ACE2 SNPs. Non-synonymous ACE2 single nucleotide polymorphism were selected among those fulfilling the triple criteria of high allelic frequency (Allele freq > 1.00e-4; Allele count > 20); involved in ACE2-claw S-protein RBD-binding interface and previously associated to clinical outcome. (B, C) Following the strategy described in Fig 9A, A549 cells expressing either GFP-ACE2 either WT or polymorphisms were assayed for cell entry by SARS-CoV-2 pseudovirus expressing either empty vector (Δ Spike) or Spike protein corresponding to origin variant (Wuhan-1) or variants-of-concern Alpha, Beta, Delta or Zeta. A representative flow cytometry experiment is shown. Bars demonstrate mean and Standard Error of Mean while each data point represents a unique experiment; ***P < 0.001, **P < 0.01, *P < 0.1, ns P > 0.1 to WT by two-tailed t-test.

vitro effects and frequency of 5 ACE2 SNPs overrepresented in Southern European populations and associated with COVID-19 disease (Benetti et al., 2020; Vagdama et al., 2022).

We found that both circulating GDF15 and ACE2 levels were higher in patients admitted to the ICU who died, compared to those who recovered from the disease and the control group. Our results are consistent with recent studies that have found that increased circulating levels of GDF15 and ACE2 are associated with a poor prognosis in patients with COVID-19 (Notz et al., 2020; Myhre et al., 2020; Luis García de Guadiana et al., 2021; Lundström et al., 2021; van Lier et al., 2021). On the other hand, we also found significant changes in ACE2 gene

expression levels in COVID-19 patients compared to uninfected controls, as well as among COVID-19 patients. Previous studies have shown that ACE2 is highly expressed in infected tissues with SARS-CoV-2 compared to normal tissues (Li et al., 2020; Gheware et al., 2022).

It is well established that both the occurrence and severity of COVID-19 increase with age, and the presence of comorbidities such as hypertension, diabetes, obesity, and cardiovascular disease conditions also largely related to the production of GDF15 (Doerstling et al., 2018; Wischhusen et al., 2020). In the present study, and as we expected, we found an association between the GDF15 levels and age while we did not find

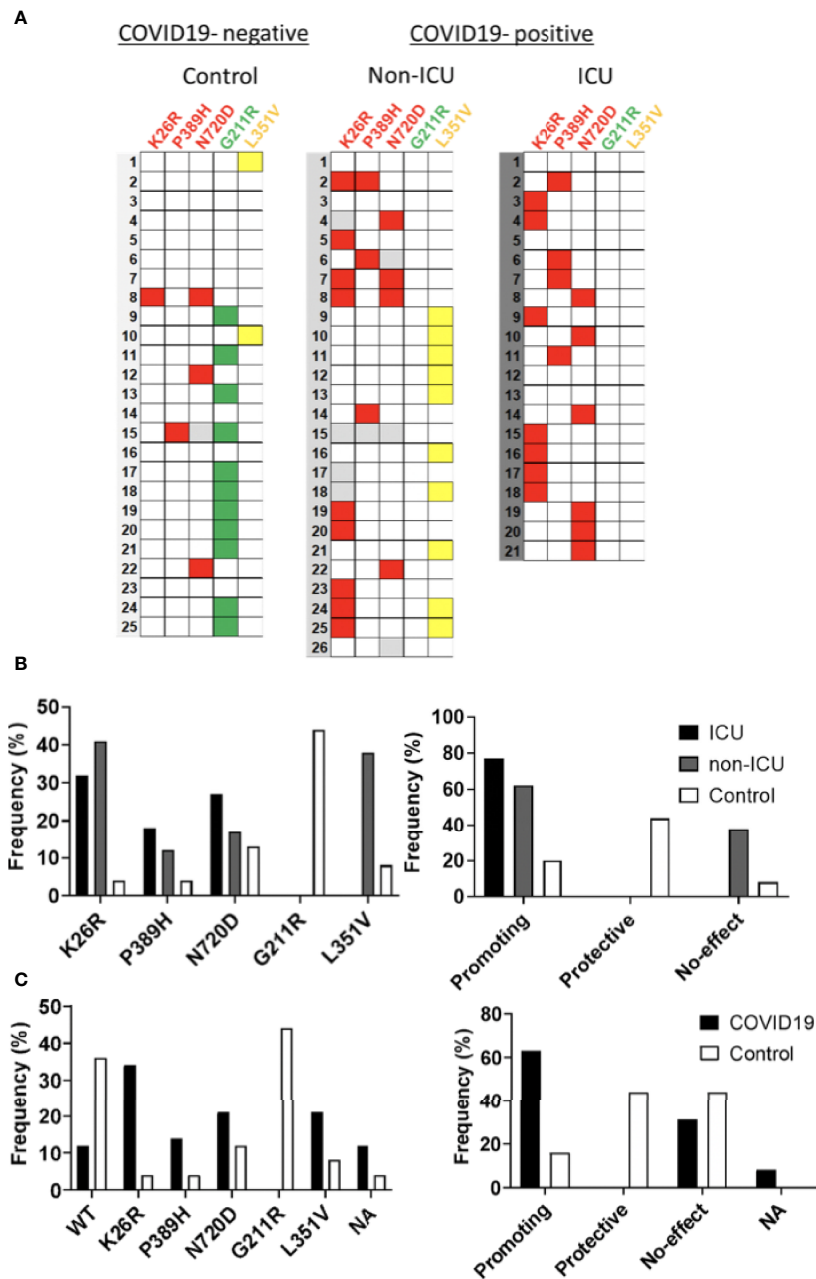


FIGURE 11
Infection-promoting ACE2 SNPs are a risk factor for COVID19 susceptibility. **(A)** Heatmap showing the distribution of ACE2 variants in the hospitalization severity groups. Coloured squares indicate the presence of the ACE2 variants. Red: Promoting; Green: Protective; Yellow: No-effect. **(B)** Frequencies of ACE2 SNPs among hospitalization severity groups. Bars represent frequencies of the SNP in each group **(C)** Frequencies of ACE2 SNPs among susceptibility groups.

differences in ACE2 levels with age. Recently, Tanaka et al. characterized the plasma proteomic signature in humans in different age ranges and found that GDF15 had the strongest positive association with age (Tanaka et al., 2018). In addition, GDF15 was found to be one of the proteins in the secretory senescence-associated phenotype (SASP) protein repertoire,

indicating the possibility that GDF15 modulates and/or predicts cellular senescence (Ha et al., 2019; Schafer et al., 2020).

Regarding gender, there were no differences in circulating GDF15 nor ACE2 levels in our studied population, although slightly higher levels were observed in men, but not statistically significant. Other studies have shown that ACE2 levels were

TABLE 2 ACE2 SNP distribution of the sample population.

| | Total (n=72) | ICU (n=21) | Non-ICU (n=26) | Control group (n=25) | Chi-square p-value |
|------------|--------------|------------|----------------|----------------------|--------------------|
| K26R | 17/68 | 7/21 | 9/22 | 1/25 | 0.0081 |
| P389H | 8/71 | 4/21 | 3/25 | 1/25 | 0.2718 |
| N720D | 13/68 | 6/21 | 4/23 | 3/24 | 0.3795 |
| G211R | 11/72 | 0/21 | 0/26 | 11/25 | < 0.001 |
| L351V | 12/72 | 0/21 | 10/26 | 2/25 | < 0.001 |
| Promoting | 34/72 | 17/21 | 13/26 | 4/25 | 0.003 |
| Protective | 11/72 | 0/21 | 0/26 | 11/25 | < 0.001 |

higher in men than in women (Sama et al., 2020). Regarding the association of ACE2 levels and age, the data available in the literature are limited. AlGhatrif et al. found that ACE2 levels show a curvilinear association with age in healthy people, with a positive association among participants younger than 55 years and a negative association in participants older than 55 (AlGhatrif et al., 2021). A recent study found that ACE2 levels increase with age in patients with acute respiratory failure who required mechanical ventilation (Baker et al., 2021).

Elevated levels of classic inflammatory markers, such as CRP, ferritin, and D-dimer, are associated with a worse prognosis in patients with COVID-19 (Huang I et al., 2020). We found that both, GDF15 and ACE2 levels, were positively correlated with those markers. In COVID-19, possible mechanisms behind systemic clinical findings include dysregulated iron homeostasis, resulting in oxidative stress and an inflammatory response. Dysregulation of iron homeostasis and higher iron levels may support the progression of viral infections (Schmidt, 2020). Also, it seems that GDF15 has a fundamental role in the regulation of iron metabolism through the modulation of hepcidin so that the deregulation of plasma levels of GDF15 could directly affect iron homeostasis (Wang

et al., 2017). Our data are consistent with previous studies (van Lier et al., 2021; Teng et al., 2021). Interestingly, both circulating GDF15 and ACE2 were positively correlated with glucose, urea, creatinine, and NT-proBNP. GDF15 has been recently recognized as a metabolic regulator, due to its role in regulating appetite and metabolism and obesity through its receptor (Miyake et al., 2021).

GDF15 is closely related to inflammation. GDF15 is a known marker of mitochondrial dysfunction, and due to its function as hormone-cytokine may play an important role in the regulation of cellular oxygenation and the inflammatory response, all of which are key mechanisms in the pathophysiology of COVID-19. Recently, circulating mtDNA has been proposed as a marker of disease severity and inflammation in COVID-19 (Scozzi et al., 2021). Changes in circulating mtDNA quantity and quality are associated with inflammation, and poorer outcomes in age related diseases, such as insulin resistance, cancer, neurodegenerative conditions, and cardiovascular disease (Gonzalez-Freire et al., 2020; Valdés-Aguayo et al., 2021). Unfortunately, we did not find differences in circulating mtDNA in our population, although COVID-19 patients presented higher levels compared to the uninfected control patients.

TABLE 3 Infection-promoting ACE2 polymorphisms are risk factor for COVID19 susceptibility in a 72-patient cohort.

| | Control (n=25) | COVID-19 patients (n=47) | Relative risk [95% CI] | Odds ratio [95% CI] | Fisher's exact test p-value |
|------------|----------------|--------------------------|---------------------------|----------------------------|-----------------------------|
| K26R | 1/25 | 16/43 | 8.00 [1.168-54.79] | 14.22 [1.752-115.5] | 0.0028 |
| P389H | 1/25 | 7/46 | 3.048 [0.4741-19.59] | 4.308 [0.4985-37.23] | 0.2455 |
| N720D | 3/24 | 10/47 | 1.655 [0.5801-4.719] | 2.059 [0.5801-4.719] | 0.3553 |
| G211R | 11/25 | 0/47 | 0.2295 [0.1449-0.3635] | 0.01327 [0.0007-0.2394] | <0.0001 |
| L351V | 2/25 | 10/47 | 2.3 [0.6234-8.486] | 3.108 [0.6242-15.48] | 0.1958 |
| Promoting | 5/25 | 33/47 | 3.439 [1.346-8.790] | 5.097 [1.719-15.11] | 0.0014 |
| Protective | 11/25 | 0/47 | 0.2295 [0.1449-0.3635] | 0.01327 [0.0007-0.2394] | <0.0001 |

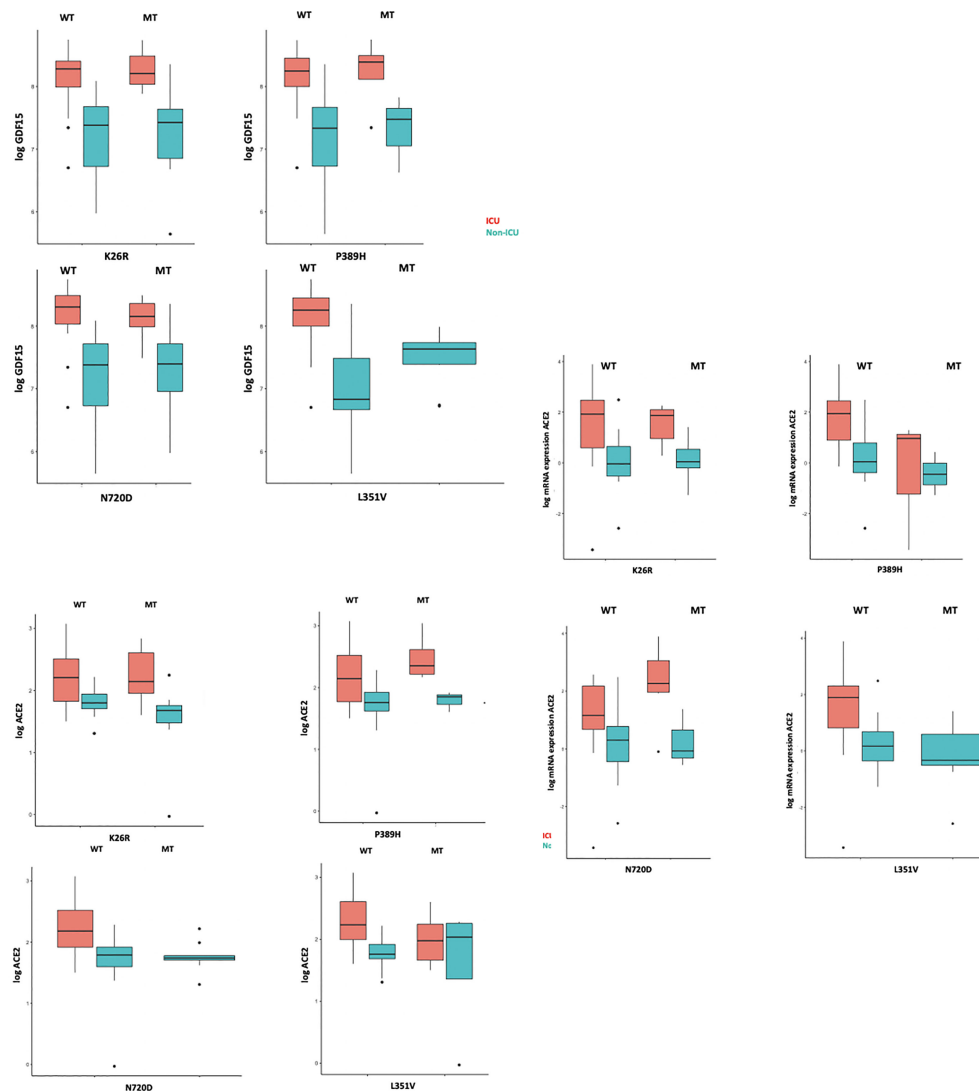


FIGURE 12
GDF15 and ACE2 levels among ICU and non-ICU COVID-19 patients and ACE2 genotypes.

GDF15 is upregulated in situations of hypoxia and tissue damage (Ahmed et al., 2022). However, knowledge of its pathophysiological function at the molecular level is still limited and more studies are needed. It has recently been discovered that the α -type glial cell-derived neurotrophic factor family receptor (*GFRAL*), expressed exclusively in the brain, could be key to the molecular mechanism of GDF15 and its relationship with pathological states (Rochette et al., 2020). A recent study has shown that GDF15 can promote human rhinovirus-associated lung inflammation in mice, leading to severe respiratory viral infections (Wu et al., 2018). In contrast, GDF15 has also been proposed as a central mediator of tissue tolerance induced by inflammation, by protecting

against bacterial and viral infections, as well as sepsis, in mouse models (Luan et al., 2019).

ACE2 is a membrane-bound enzyme and therefore measurement of circulating levels of ACE2 is complex. ACE2 is cleaved from the plasma membrane through ADAM17-mediated regulated removal (Bartolomé et al., 2021). Therefore, elevated plasma ACE2 levels could also result from increased lysis of ACE2-expressing cells as a consequence of more severe COVID-19 infection (Kragstrup et al., 2021). Contrary to what we expected, we found no association between the levels of GDF15 and the levels of ACE2 in plasma. However, a previous study GDF15 levels were positively associated with ACE2 levels in patients with atrial fibrillation (Wallentin et al., 2020).

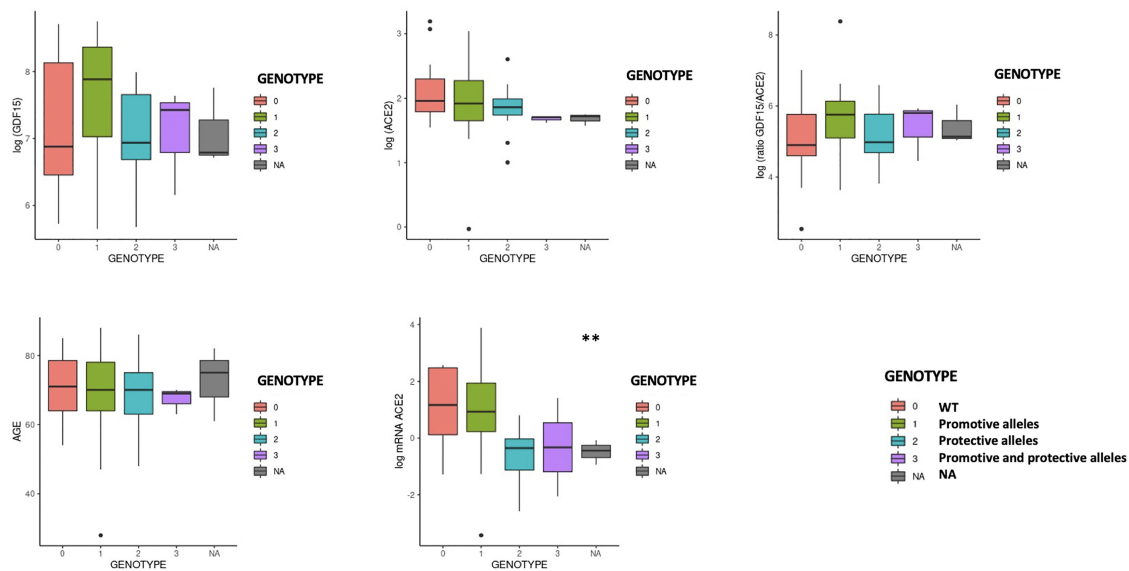


FIGURE 13

GDF15 and ACE2 levels by protective or promotive genotypes. Genotype 0 corresponding to subjects that did not carry any variant; Genotype 1, subjects that carry at least one promoting variant; Genotype 2, subjects that carry at least one protective variant; Genotype 3, subjects that carry at least one promoting and one protective variant (Supplementary Table 5; Figure 13). We only found differences in the levels of the ACE2 mRNA ($P < 0.05$).

Based on the all the above, we believe that both GDF15 and ACE2 could provide valuable information on the pathophysiology of COVID-19. More studies are needed to elucidate the role that these biomarkers play in the progression of SARS-CoV-2 infection.

Host genetics is known to play an important role in susceptibility to other viral infectious diseases, including SARS-CoV, HIV and influenza (Wang et al., 2019). Previous studies like the one led by “The COVID19 Host Genetics Initiative” (Niemi et al., 2021) support the notion that some genetic variants, most notably at the ABO and PPP1R15A loci, in addition to SLC6A20 have a direct effect on susceptibility to infection rather than COVID19 severity. In contrast, variants at DPP9, FOXP4 or TYK2 loci with reported effects on several autoimmune-related diseases (Kichaev et al., 2019) or inflammatory-related loci (e.g. CXCR6, LZTFL1, IFNAR2 and OAS1/OAS2/OAS3 loci) and specially the 3p21.31 locus have been described to have an huge impact on COVID19 severity (Niemi et al., 2021).

The most well-known and evaluated mechanism of SARS-CoV-2 infection is the binding and uptake of viral particles through ACE2 receptor, a type 1 integral membrane glycoprotein (Zamorano Cuervo and Grandvaux, 2020). Based on the premise that a predisposing genetic background may contribute to the wide clinical variability of COVID-19, we set out to investigate whether variations in ACE2 might modulate susceptibility to SARS-CoV-2 and influence severity. We queried multiple genomic databases comprising the main sources of

aggregated data for ACE2 protein altering variations in populations groups across the world to considered non-synonymous allele variants with high allelic frequency ($>1.00.e-4$) and allele count >20 . Then we selected variants within the human ACE2-claw S-protein RBD-binding interface as described in previous studies (Hussain et al., 2020; Suryamohan et al., 2021) that could potentially increase or decrease the binding affinity of ACE2 to the S-protein and thereby alter the ability of the virus to infect the host cell. Then, we considered the ACE2 variants previously described potentially predisposing genetic background to the observed individual clinical variability (Benetti et al., 2020; Vadgama et al., 2022). Finally, five ACE2 variants fulfilled this triple requirement. Notably, these variants have not been reported in the Asian population and are rare in non-South European populations (Benetti et al., 2020; Vadgama et al., 2022). Given their rarity in other populations, we cannot exclude that these variants can partially account for the clinical outcome observed in the Spanish population (Benetti et al., 2020). Using a pseudovirus infection approach similar to the previously reported (Letko et al., 2020; Ou et al., 2020) we recapitulated airway infection in human alveolar lung A549 cells. This cell line does not express detectable levels of ACE2, thus being an excellent model to test the effects of ectopic ACE2 containing particular SNPs. With this approach, we found that variants K26R, P389H and N720D promoted a significant increase in infection while G211R diminished the infection being potentially

protective. Variant N720D lies in a residue located close to the cleavage sequence of TMPRSS2, likely affecting the cleavage dependent virion intake (Suryamohan et al., 2021). Variant K26R was previously reported to increase affinity for S-protein by biochemical assays (Suryamohan et al., 2021) while G211R was predicted *in silico* to affect S-protein and ACE2 interaction (Benetti et al., 2020). In our model, variant L351V showed no significant difference in infection in contrast to the previous results by crystal structure (Benetti et al., 2020).

We also studied the presence of the 5 specific SNPs in *ACE2* coding regions using human plasma circulating mRNA. Transcription of *ACE2* produces different mRNA transcript variants responsible for translation into different protein isoforms (Harmer et al., 2002; Nikiforuk et al., 2021) that could be regulated by COVID-19 infection in a cytokine-specific manner (Albini et al., 2021). Therefore, we reasoned that patient genotyping from mRNA could better reflect the *ACE2* variants expressed in those patients. In fact, previous studies have shown that SNPs could be detected with high precision in transcriptome sequencing approaches as compared to DNA-seq procedures (Deelen et al., 2015; Jehl et al., 2021). This has led to the emergence of transcriptome or RNA sequencing as a potential alternative approach to variant detection within protein coding regions, since the transcriptome of a given tissue represents a quasi-complete set of transcribed genes (mRNAs) and other noncoding RNAs which also bypasses the need for exome enrichment (Ku et al., 2012; Lopera Maya et al., 2020). Using this approach, we identified the presence of the 5 shortlisted SNPs involved *in vitro* in a differential susceptibility in the 72-patient cohort. Notably, infection-promoting variants K26R, P389H and N720D were a risk factor for Severe COVID-19 Hospitalized groups as compared to wild-type *ACE2*. Conversely, infection inhibiting variant G211R showed a protective effect as compared to wild-type *ACE2*. Interestingly G211R exhibited a gender bias, being significantly enriched in women. This is in agreement with the gender effect in COVID-19 susceptibility showed by others (Yildirim et al., 2021; Vadgama et al., 2022).

Our data suggest that *ACE2* SNPs could stratify patients according to infection susceptibility in complete agreement with our pseudoviral infection model. Therefore, it is plausible to think that the effect of allelic variability on *ACE2* conformation would at least partially account for the interindividual clinical differences and likely modulate clinical susceptibility. This finding reinforces the hypothesis that at least some of the identified variants or the cumulative effect of few of them could confer a different susceptibility to virus cell entry and consequently to disease onset. This fundamental knowledge paves the way to perform a precision medicine screening -e.g. by blood sample genotyping of *ACE2* variants- in order to identify COVID19 infection susceptibility groups. Host genomic information like this may facilitate stratification and

targeting of care and vaccination, and enable the identification of people who may be at higher risk of harm. Genetic information might also enable targeting therapeutic interventions to those more likely to develop severe illness or protecting them from adverse reactions. Information from those less susceptible to infection with SARS-CoV-2 may be valuable in identifying potential therapies (Milne, 2020).

Our study has limitations. First the study population is small, including patients from Hospital Son Llatzer and Hospital Son Espases, two of the main hospitals in the Balearic Health System. There might be a selection bias when identifying factors that differ between patients with COVID-19, although COVID-19 patients were matched for age and sex as well with the control group. Second, we did not include a control uninfected ICU group which could have strengthen our findings. Third, it is a retrospective study conducted in an emergency situation, and in which not all the clinical characteristics of the patients were recorded. Third, some patients had elevated biomarker data in some laboratory measurements, as well as in GDF15 and *ACE2* levels, and we did not exclude them from the analysis due to small sample size and because those numbers were physiological and not due to technical errors. Finally, the study is cross-sectional and no causal inferences can be made. Despite the limitations, our study provides convincing evidence that in patients with COVID-19, the levels of GDF15 and *ACE2* could be associated with increased inflammation and disease severity while *ACE2* missense SNPs might be linked to infection susceptibility.

In conclusion, critically ill patients with COVID-19 present higher levels of GDF15 and *ACE2*, as well as acute inflammation. These two proteins might be of importance because of its association with disease severity in patients infected with SARS-CoV-2. Our results suggest that certain genetic variations in *ACE2* might modulate susceptibility to SARS-CoV-2 infection and influence severity. More studies are needed to elucidate the role of GDF15 and *ACE2* in COVID-19.

Data availability statement

The original contributions presented in the study are included in the article/supplementary material, further inquiries can be directed to the corresponding author/s.

Ethics statement

The studies involving human participants were reviewed and approved by ethics committee of the Balearic Islands. The ethics committee waived the requirement of written informed consent for participation.

Author contributions

Conceptualization and methodology, MG-F and CB; MT-M, CP-R, NT-F, LI-G, AG-P, CNE, and CB performed experiments, analyzed the data and wrote—original draft preparation; LS, AS-P, JP-L, CC, and LM collected and contributed data. Writing—review and editing, MG-F, CB, MT-M, CMPR, ASP, and LM; supervision, MGF and CB; Project administration and funding acquisition, MG-F and CB. All authors have read and agreed to the published version of the manuscript. MT-M and CMPR share co-first authorship; MG-F and CB are the co-corresponding authors. All authors contributed to the article and approved the submitted version.

Funding

This research was supported by the Miguel Servet program (MS19/00201 and MS19/00100) (MG-F and CB), Instituto de Salud Carlos III (ISCIII), Madrid; Fondo extraordinario COVID—ISCIII (COV20/00571) (CB); Fundació LaMaratóTV3 (167-C-2021 51); the Margalida Comas Program (PD/050/2020), Comunidad Autonoma de las Islas Baleares (MT-M); the FOLIUM fellowship program (FOLIUM 19/01), Impost turisme sostenible/Govern de les Illes Balears (AP-G and CPR); the TECH fellowship program, Impost turisme sostenible/Govern de les Illes Balears (TECH19/03) (LI-G). And the LIBERI 2022 program.

Acknowledgments

We would like to thank Dr Gabriel Bretones and Prof Carlos López-Otín (Universidad de Oviedo, Spain) for kindly providing psPAX2 pLV-mCherry vectors and protocol for pseudovirus production. We thank Dr Thomas Peacock and Prof Wendy Barclay (Imperial College London, UK) for kindly providing SARS-CoV-2 VOC vectors. We thank Victoria Elizabeth Cano Garcia, from the HUSE Biobank, for providing the patient samples and demographic characteristics.

Conflict of interest

The authors declare that the research was conducted in the absence of any commercial or financial relationships that could be construed as a potential conflict of interest.

Publisher's note

All claims expressed in this article are solely those of the authors and do not necessarily represent those of their affiliated

organizations, or those of the publisher, the editors and the reviewers. Any product that may be evaluated in this article, or claim that may be made by its manufacturer, is not guaranteed or endorsed by the publisher.

Supplementary material

The Supplementary Material for this article can be found online at: <https://www.frontiersin.org/articles/10.3389/fcimb.2022.942951/full#supplementary-material>

SUPPLEMENTARY TABLE 1

Primer sequences and annealing temperatures.

SUPPLEMENTARY TABLE 2

Primer sequences and annealing temperatures for assessment of mtDNA oxidation.

SUPPLEMENTARY TABLE 3

Clinical and Biochemical Characteristics of non-ICU group

SUPPLEMENTARY TABLE 4

Correlation coefficient between GDF15, ACE2 and changes on biochemical parameters among non-ICU COVID19 patients.

SUPPLEMENTARY TABLE 5

ACE2 genotypes frequency among the study population.

SUPPLEMENTARY TABLE 6

Association between ACE2 genotypes with circulating levels of GDF15 and ACE2

SUPPLEMENTARY FIGURE 1

ACE2 polymorphisms exhibit similar fashion when expressed in A549 cells. A549 cells were transfected with either GFP-ACE2 WT, GFP-ACE2 polymorphisms or GFP alone. Then, ACE2 protein expression was analyzed by A) Western Blot with MA5-32307 antibody B) Immunocytochemistry (red) with either MA5-32307 antibody (left panel) or MAB933 antibody (right panel). Nuclei was stained with DAPI (blue). Transfected cells contain GFP (green). CT: secondary antibody control to detect unspecific binding. Images were acquired with Cell Observer-Zeiss. Scale bar: 50 μ m

SUPPLEMENTARY FIGURE 2

ACE2 missense SNPs genotyping. cDNA was obtained by RT-PCR from circulating mRNA of the patients. Then, PCR1, PCR2 and PCR3 were performed in order to amplify the regions comprising the studied SNPs. PCR products were sequenced and aligned against reference ACE2 (NM_021804). PCR1: residues from Ser3 to Met249 (743 bp), PCR2: residues Phe308 to Arg621 (944 bp), PCR3: residues from Val670 to Val752 (250 bp) A) Agarose gel electrophoresis with the PCR products of several patients was performed to confirm specificity. B) Representative image of the alignment of the sequenced (forward and reverse) PCR products against reference ACE2 using SnapGene® Software. In particular, the image corresponds to the PCR2 of the non-ICU patient 10 that presents the L351V variant.

SUPPLEMENTARY FIGURE 3

Frequency distribution of ACE2 genotypes by sex. (A) 'promoting' alleles; (B) 'Protective' alleles; (C) 'WT' alleles.

SUPPLEMENTARY FIGURE 4

GDF15 and ACE2 levels across ACE2 variants.

References

- Adela, R., and Banerjee, S. K. (2015). GDF-15 as a target and biomarker for diabetes and cardiovascular diseases: a translational prospective. *J. Diabetes Res.* 2015, 490842. doi: 10.1155/2015/490842
- Ahmed, D. S., Isnard, S., Berini, C., Lin, J., Routy, J. P., and Royston, L. (2022). Coping with stress: the mitokine GDF-15 as a biomarker of COVID-19 severity. *Front. Immunol.* 13, 820350. doi: 10.3389/fimmu.2022.820350
- Albini, A., Calabrone, L., Carlini, V., Benedetto, N., Lombardo, M., Bruno, A., et al. (2021). Preliminary evidence for IL-10-Induced ACE2 mRNA expression in lung-derived and endothelial cells: implications for SARS-CoV-2 ARDS pathogenesis. *Front. Immunol.* 12, 718136. doi: 10.3389/fimmu.2021.718136
- AlGhatrif, M., Tanaka, T., Moore, A. Z., Bandinelli, S., Lakatta, E. G., and Ferrucci, L. (2021). Age-associated difference in circulating ACE2, the gateway for SARS-CoV-2, in humans: results from the InCHIANTI study. *GeroScience* 43 (2), 619–627. doi: 10.1007/s11357-020-00314-w
- Baker, S. A., Kwok, S., Berry, G. J., and Montine, T. J. (2021). Angiotensin-converting enzyme 2 (ACE2) expression increases with age in patients requiring mechanical ventilation. *PLoS One* 16 (2), e0247060. doi: 10.1371/journal.pone.0247060
- Bartolomé, A., Liang, J., Wang, P., Ho, D. D., and Pajvani, U. B. (2021). Angiotensin converting enzyme 2 is a novel target of the γ -secretase complex. *Sci. Rep.* 11 (1), 9803. doi: 10.1038/s41598-021-89379-x
- Benetti, E., Tita, R., Spiga, O., Ciolfi, A., Birolo, G., Bruselles, A., et al. (2020). ACE2 gene variants may underlie interindividual variability and susceptibility to COVID-19 in the Italian population. *Eur. J. Hum. Genet.* 28 (11), 1602–1614. doi: 10.1038/s41431-020-0691-z
- Chen, N., Zhou, M., Dong, X., Qu, J., Gong, F., Han, Y., et al. (2020). Epidemiological and clinical characteristics of 99 cases of 2019 novel coronavirus pneumonia in wuhan, China: a descriptive study. *Lancet* 395 (10223), 507–513. doi: 10.1016/S0140-6736(20)30211-7
- Consortium GER (2019). *100,000 Genomes project the national genomics research and healthcare knowledgebase amendment to the 100,000 genomes project protocol v4*. Available at: genomicsengland.co.uk (Accessed May 4, 2022).
- Cordani, M., Butera, G., Dando, I., Torrens-Mas, M., Butturini, E., Pacchiana, R., et al. (2018). Mutant p53 blocks SESN1/AMPK/PGC-1 α /UCP2 axis increasing mitochondrial O₂- production in cancer cells. *Br. J. Cancer*, 1–15. doi: 10.1038/s41416-018-0288-2
- Coronaviridae Study Group of the International Committee on Taxonomy of Viruses (2020). The species severe acute respiratory syndrome-related coronavirus: classifying 2019-nCoV and naming it SARS-CoV-2. *Nat. Microbiol.* 5 (4), 536–544. doi: 10.1038/s41564-020-0695-z
- Deelen, P., Zhernakova, D. V., de Haan, M., van der Sijde, M., Bonder, M. J., Karjalainen, J., et al. (2015). Calling genotypes from public RNA-sequencing data enables identification of genetic variants that affect gene-expression levels. *Genome Med.* 7 (1):30. doi: 10.1186/s13073-015-0152-4
- de la Rica, R., Borges, M., and Gonzalez-Freire, M. (2020). COVID-19: in the eye of the cytokine storm. *Front. Immunol.* 11, 2313.
- de la Rica, R., Borges, M., Aranda, M., Del Castillo, A., Socias, A., Payeras, A., et al. (2020). Low albumin levels are associated with poorer outcomes in a case series of COVID-19 patients in Spain: a retrospective cohort study. *Microorganisms* 8 (8), 1106. doi: 10.3390/microorganisms8081106
- Doerflinger, S., Hedberg, P., Öhrvik, J., Leppert, J., and Henriksen, E. (2018). Growth differentiation factor 15 in a community-based sample: age-dependent reference limits and prognostic impact. *Ups J. Med. Sci.* 123 (2), 86. doi: 10.1080/03009734.2018.1460427
- Ghware, A., Ray, A., Rana, D., Bajpai, P., Nambirajan, A., Arulselvi, S., et al. (2022). ACE2 protein expression in lung tissues of severe COVID-19 infection. *Sci. Rep.* 12 (1), 4058. doi: 10.1038/s41598-022-07918-6
- Gonzalez-Freire, M., Moore, A. Z., Peterson, C. A., Kosmac, K., McDermott, M. M., Sufit, R. L., et al. (2020). Associations of peripheral artery disease with calf skeletal muscle mitochondrial DNA heteroplasmy. *J. Am. Heart Assoc.* 9 (7), e015197. doi: 10.1161/JAHA.119.015197
- Guan, W. J., Ni, Z. Y., Hu, Y., Liang, W. H., Ou, C. Q., He, J. X., et al. (2020). Clinical characteristics of coronavirus disease 2019 in China. *N. Engl. J. Med.* 382 (18), 1708–1720. doi: 10.1056/NEJMoa2002032
- Ha, G., De Torres, F., Arouche, N., Benzoubir, N., Ferratge, S., Hatem, E., et al. (2019). GDF15 secreted by senescent endothelial cells improves vascular progenitor cell functions. *PLoS One* 14 (5), e0216602. doi: 10.1371/journal.pone.0216602
- Harmer, D., Gilbert, M., Borman, R., and Clark, K. L. (2002). Quantitative mRNA expression profiling of ACE 2, a novel homologue of angiotensin converting enzyme. *FEBS Lett.* 532 (1–2), 107–110. doi: 10.1016/S0014-5793(02)03640-2
- Huang, C., Wang, Y., Li, X., Ren, L., Zhao, J., Hu, Y., et al. (2020). Clinical features of patients infected with 2019 novel coronavirus in wuhan, China. *Lancet* 395 (10223), 497–506. doi: 10.1016/S0140-6736(20)30183-5
- Huang, I., Pranata, R., Lim, M. A., Oehadian, A., and Alisjahbana, B. (2020). C-reactive protein, procalcitonin, d-dimer, and ferritin in severe coronavirus disease-2019: a meta-analysis. *Ther. Adv. Respir. Dis.* 14, 1753466620937175. doi: 10.1177/1753466620937175
- Hussain, M., Jabeen, N., Raza, F., Shabbir, S., Baig, A. A., Amanullah, A., et al. (2020). Structural variations in human ACE2 may influence its binding with SARS-CoV-2 spike protein. *J. Med. Virol.* 92 (9), 1580–1586. doi: 10.1002/jmv.25832
- Ikram, M. A., Jabeen, N., Raza, F., Shabbir, S., Baig, A. A., Amanullah, A., et al. (2020). The Rotterdam study: 2018 update on objectives, design and main results. *Eur. J. Epidemiol.* 32 (9), 807–850. doi: 10.1007/s10654-017-0321-4
- Inde, Z., Croker, B. A., Yapp, C., Joshi, G. N., Spetz, J., Fraser, C., et al. (2021). Age-dependent regulation of SARS-CoV-2 cell entry genes and cell death programs correlates with COVID-19 severity. *Sci. Adv.* 7 (34):eabf8609. doi: 10.1126/SCIADV.ABF8609
- Jehl, F., Degalez, F., Bernard, M., Lecerf, F., Lagoutte, L., Désert, C., et al. (2021). RNA-Seq data for reliable SNP detection and genotype calling: interest for coding variant characterization and cis-regulation analysis by allele-specific expression in livestock species. *Front. Genet.* 12, 655707. doi: 10.3389/fgene.2021.655707
- Joglekar, M. V., Satoor, S. N., Wong, W. K. M., Cheng, F. Ma, RCW, and Hardikar, A. A. (2020). An optimised step-by-step protocol for measuring relative telomere length. *Methods Protoc.* 3 (2), 27. doi: 10.3390/mps3020027
- Karczewski, K. J., Francioli, L. C., Tiao, G., Cummings, B. B., Alfoldi, J., Wang, Q., et al. (2020). The mutational constraint spectrum quantified from variation in 141,456 humans. *Nature* 581 (7809), 434–443. doi: 10.1038/s41586-020-2308-7
- Kichaev, G., Bhatia, G., Loh, P. R., Gazal, S., Burch, K., Freund, M. K., et al. (2019). Leveraging polygenic functional enrichment to improve GWAS power. *Am. J. Hum. Genet.* 104 (1), 65–75. doi: 10.1016/j.ajhg.2018.11.008
- Kragstrup, T. W., Singh, H. S., Grundberg, I., Nielsen, A. L., Rivelles, F., Mehta, A., et al. (2021). Plasma ACE2 predicts outcome of COVID-19 in hospitalized patients. *PLoS One* 16 (6), e0252799. doi: 10.1371/journal.pone.0252799
- Ku, C. S., Wu, M., Cooper, D. N., Naidoo, N., Pawitan, Y., Pang, B., et al. (2012). Exome versus transcriptome sequencing in identifying coding region variants. *Expert Rev. Mol. Diagn.* 12 (3), 241–251. doi: 10.1586/erm.12.10
- Letko, M., Marzi, A., and Munster, V. (2020). Functional assessment of cell entry and receptor usage for SARS-CoV-2 and other lineage B betacoronaviruses. *Nat. Microbiol.* 5 (4), 562–569. doi: 10.1038/s41564-020-0688-y
- Li, M. Y., Li, L., Zhang, Y., and Wang, X. S. (2020). Expression of the SARS-CoV-2 cell receptor gene ACE2 in a wide variety of human tissues. *Infect. Dis. Poverty* 9 (1), 45. doi: 10.1186/s40249-020-00662-x
- Lopera Maya, E. A., an der Graaf, A., Lanting, P., van der Geest, M., Fu, J., Swertz, M., et al. (2020). Lack of association between genetic variants at ACE2 and TMPRSS2 genes involved in SARS-CoV-2 infection and human quantitative phenotypes. *Front. Genet.* 11, 613. doi: 10.3389/fgene.2020.00613
- Luan, H., Wang, A., Hilliard, B. K., Carvalho, F., Rosen, C. E., Ahasic, A. M., et al. (2019). GDF15 is an inflammation-induced central mediator of tissue tolerance. *Cell* 178 (5), 1231–1244.e11. doi: 10.1016/j.cell.2019.07.033
- García de Guadiana Romualdo, L., Mulero, M. D. R., Olivo, M. H., Rojas, C. R., Arenas, V. R., Morales, M. G., et al. (2021). Circulating levels of GDF-15 and calprotectin for prediction of in-hospital mortality in COVID-19 patients: a case series. *J. Infect.* 82 (2), e40–e42. doi: 10.1016/j.jinf.2020.08.010
- Lundström, A., Ziegler, L., Havervall, S., Rudberg, A. S., von Meijenföldt, F., Lisman, T., et al. (2021). Soluble angiotensin-converting enzyme 2 is transiently elevated in COVID-19 and correlates with specific inflammatory and endothelial markers. *J. Med. Virol.* 93 (10), 5908–5916. doi: 10.1002/jmv.27144
- Malik, P., Patel, U., Mehta, D., Patel, N., Kelkar, R., Akrmah, M., et al. (2021). Biomarkers and outcomes of COVID-19 hospitalisations: systematic review and meta-analysis. *BMJ Evidence-Based Med.* 26 (3), 107–108. doi: 10.1136/bmjebm-2020-111536
- Milne, R. (2020). Societal considerations in host genome testing for COVID-19. *Genet. Med.* 22 (9), 1464–1466. doi: 10.1038/s41436-020-0861-y
- Miyake, M., Zhang, J., Yasue, A., Hisanaga, S., Tsugawa, K., Sakaue, H., et al. (2021). Integrated stress response regulates GDF15 secretion from adipocytes, preferentially suppresses appetite for a high-fat diet and improves obesity. *iScience* 24 (12), 103448. doi: 10.1016/j.isci.2021.103448
- Myhre, P. L., Prebensen, C., Strand, H., Roysland, R., Jonassen, C. M., Rangberg, A., et al. (2020). Growth differentiation factor 15 provides prognostic information superior to established cardiovascular and inflammatory biomarkers in unselected patients hospitalized with COVID-19. *Circulation* 142 (22), 2128–2137. doi: 10.1161/CIRCULATIONAHA.120.050360
- Narula, S., Yusuf, S., Chong, M., Ramasundarahettige, C., Rangarajan, S., Bangdiwala, S. I., et al. (2020). Plasma ACE2 and risk of death or cardiometabolic

diseases: a case-cohort analysis. *Lancet (London England)* 396 (10256), 968–976. doi: 10.1016/S0140-6736(20)31964-4

Niemi, M. E. K., Karjalainen, J., Liao, R. G., Neale, B., Daly, M., Ganna, A., et al. (2021). Mapping the human genetic architecture of COVID-19. *Nature* 600 (7889), 472–477. doi: 10.1038/s41586-021-03767-x.

Nikiforuk, A. M., Kuchinski, K. S., Twa, D. D. W., Lukac, C. D., Sbihi, H., Basham, C. A., et al. (2021). The contrasting role of nasopharyngeal angiotensin converting enzyme 2 (ACE2) transcription in SARS-CoV-2 infection: A Cross-Sectional Study of People Tested for COVID-19 in British Columbia, Canada. *EBioMedicine* 66, 103316. doi: 10.1016/j.ebiom.2021.103316

Notz, Q., Schmalzing, M., Wedekind, F., Schlesinger, T., Gernert, M., Herrmann, J., et al. (2020). Pro- and anti-inflammatory responses in severe COVID-19-induced acute respiratory distress syndrome—an observational pilot study. *Front. Immunol.* 11, 581338. doi: 10.3389/fimmu.2020.581338

Novelli, A., Biancolella, M., Borgiani, P., Cocciaferro, D., Colona, V. L., D'Apice, M. R., et al. (2020). Analysis of ACE2 genetic variants in 131 Italian SARS-CoV-2-positive patients. *Hum. Genomics* 14 (1), 29. doi: 10.1186/s40246-020-00279-z.

Ou, X., Liu, Y., Lei, X., Li, P., Mi, D., Ren, L., et al. (2020). Characterization of spike glycoprotein of SARS-CoV-2 on virus entry and its immune cross-reactivity with SARS-CoV. *Nat. Commun.* 11 (1), 620. doi: 10.1038/s41467-020-15562-9

Pinto, B. G. G., Oliveira, A. E. R., Singh, Y., Jimenez, L., Gonçalves, A. N. A., Ogawa, R. L. T., et al. (2020). ACE2 expression is increased in the lungs of patients with comorbidities associated with severe COVID-19. *J. Infect. Dis.* 222 (4), 556–563. doi: 10.1093/infdis/jiaa332

Ramanathan, M., Ferguson, I. D., Miao, W., and Khavari, P. A. (2021). SARS-CoV-2 B.1.1.7 and B.1.351 spike variants bind human ACE2 with increased affinity. *Lancet Infect. Dis.* 21 (8), 1070. doi: 10.1016/2021.02.22.432359

Rochette, L., Zeller, M., Cottin, Y., and Vergely, C. (2020). Insights into mechanisms of GDF15 and receptor GFRAL: therapeutic targets. *Trends Endocrinol. Metab.* 31 (12), 939–951. doi: 10.1016/j.tem.2020.10.004

Sama, I. E., Ravera, A., Santema, B. T., van Goor, H., Ter Maaten, JM, Cleland, J. G. F., et al. (2020). Circulating plasma concentrations of angiotensin-converting enzyme 2 in men and women with heart failure and effects of renin-angiotensin-aldosterone inhibitors. *Eur. Heart J.* 41 (19), 1810–1817. doi: 10.1093/eurheartj/ehaa373

Sanyaolu, A., Okorie, C., Marinkovic, A., Patidar, R., Younis, K., Desai, P., et al. (2020). Comorbidity and its impact on patients with COVID-19. *SN Compr. Clin. Med.* 2 (8), 1069–1076. doi: 10.1007/s42399-020-00363-4

Schafer, M. J., Zhang, X., Kumar, A., Atkinson, E. J., Zhu, Y., Jachim, S., et al. (2020). The senescence-associated secretome as an indicator of age and medical risk. *JCI Insight* 5 (12), e133668. doi: 10.1172/jci.insight.133668

Schmidt, S. M. (2020). The role of iron in viral infections. *Front. Biosci. - Landmark* 25 (5), 893–911. doi: 10.2741/4839

Scozzi, D., Cano, M., Ma, L., Zhou, D., Zhu, J. H., O'Halloran, J. A., et al. (2021). Circulating mitochondrial DNA is an early indicator of severe illness and mortality from COVID-19. *JCI Insight* 6 (4):e143299. doi: 10.1172/jci.insight.143299

Sungnak, W., Huang, N., Bécavin, C., Berg, M., Queen, R., Litvinukova, M., Talavera-López, C., et al. (2020). SARS-CoV-2 entry factors are highly expressed in nasal epithelial cells together with innate immune genes. *Nat. Med.* 26 (5), 681–687. doi: 10.1038/s41591-020-0868-6

Suryamohan, K., Diwanji, D., Stawiski, E. W., Gupta, R., Miersch, S., Liu, J., Chen, C., et al. (2021). Human ACE2 receptor polymorphisms and altered susceptibility to SARS-CoV-2. *Commun. Biol.* 4 (1), 475. doi: 10.1038/s42003-021-02030-3

Tanaka, T., Biancotto, A., Moaddel, R., Moore, A. Z., Gonzalez-Freire, M., Aon, M. A., et al. (2018). Plasma proteomic signature of age in healthy humans. *Aging Cell* 17 (5), 1–13. doi: 10.1111/ace1.12799

Teng, X., Zhang, J., Shi, Y., Liu, Y., Yang, Y., He, J., et al. (2021). Comprehensive profiling of inflammatory factors revealed that growth differentiation factor-15 is an indicator of disease severity in COVID-19 patients. *Front. Immunol.* 12, 662465. doi: 10.3389/fimmu.2021.662465

Vadgama, N., Kreymerman, A., Campbell, J., Shamardina, O., Brugger, C., Research Consortium, G. E., et al. (2022). SARS-CoV-2 susceptibility and ACE2 gene variations within diverse ethnic backgrounds. *Front. Genet.* 13. doi: 10.3389/fgene.2022.888025

Valdés-Aguayo, J. J., Garza-Veloz, I., Vargas-Rodríguez, J. R., Martínez-Vázquez, M. C., Avila-Carrasco, L., Bernal-Silva, S., et al. (2021). Peripheral blood mitochondrial DNA levels were modulated by SARS-CoV-2 infection severity and its lessening was associated with mortality among hospitalized patients with COVID-19. *Front. Cell. Infect. Microbiol.* 11, 754708. doi: 10.3389/fcimb.2021.754708

Van der Auwera, G. A., Carneiro, M. O., Hartl, C., Poplin, R., Del Angel, G., Levy-Moonshine, A., et al. (2013). From FastQ data to high-confidence variant calls: the genome analysis toolkit best practices pipeline. *Curr. Protoc. Bioinforma* 43 (1110), 11.10.1–11.10.33. doi: 10.1002/0471250953.bi1110s43

van Lier, D., Kox, M., Santos, K., van der Hoeven, H., Pillay, J., and Pickkers, P. (2021). Increased blood angiotensin converting enzyme 2 activity in critically ill COVID-19 patients. *ERJ Open Res.* 7 (1), 00848–02020. doi: 10.1183/23120541.00848-2020

Wallentin, L., Lindbäck, J., Eriksson, N., Hijazi, Z., Eikelboom, J. W., Ezekowitz, MD, et al. (2020). Angiotensin-converting enzyme 2 (ACE2) levels in relation to risk factors for COVID-19 in two large cohorts of patients with atrial fibrillation. *Eur. Heart J.* 41 (41), 4037–4046. doi: 10.1093/eurheartj/ehaa697

Wang, C., Fang, Z., Zhu, Z., Liu, J., and Chen, H. (2017). Reciprocal regulation between hepcidin and erythropoiesis and its therapeutic application in erythroid disorders. *Exp. Hematol.* 52, 24–31. doi: 10.1016/j.exphem.2017.05.002

Wang, D., Eraslan, B., Wieland, T., Hallström, B., Hopf, T., Zolg, D. P., et al. (2019). A deep proteome and transcriptome abundance atlas of 29 healthy human tissues. *Mol. Syst. Biol.* 15 (2), e8503. doi: 10.15252/msb.20188503

Wischhusen, J., Melero, I., and Fridman, W. H. (2020). Growth/differentiation factor-15 (GDF-15): from biomarker to novel targetable immune checkpoint. *Front. Immunol.* 11, 951. doi: 10.3389/fimmu.2020.00951

Wu, Q., Jiang, D., Schaefer, N. R., Harmacek, L., O'Connor, B. P., Eling, T. E., et al. (2018). Overproduction of growth differentiation factor 15 promotes human rhinovirus infection and virus-induced inflammation in the lung. *Am. J. Physiol. Lung Cell. Mol. Physiol.* 314 (3), L514–L527. doi: 10.1152/ajplung.00324.2017

Ye, J., Coulouris, G., Zaretskaya, I., Cutcutache, I., Rozen, S., Madden, T. L., et al. (2012). Primer-BLAST: A tool to design target-specific primers for polymerase chain reaction. *BMC Bioinf.* 13, 134. doi: 10.1186/1471-2105-13-134

Yildirim, Z., Sahin, O. S., Yazar, S., and Bozok Cetintas, V. (2021). Genetic and epigenetic factors associated with increased severity of covid-19. *Cell Biol. Int.* 45 (6), 1158–1174. doi: 10.1002/cbin.11572

Zamorano Cuervo, N., and Grandvaux, N. (2020). ACE2: evidence of role as entry receptor for sars-cov-2 and implications in comorbidities. *Elife* 9, e61390.

Zhou, F., Yu, T., Du, R., Fan, G., Liu, Y., Liu, Z., et al. (2020). Clinical course and risk factors for mortality of adult inpatients with COVID-19 in wuhan, china: a retrospective cohort study. *Lancet* 395 (10229), 1054–1062. doi: 10.1016/S0140-6736(20)30566-3

Zhu, N., Zhang, D., Wang, W., Li, X., Yang, B., Song, J., et al. (2020). A novel coronavirus from patients with pneumonia in china, 2019. *N. Engl. J. Med.* 382 (8), 727–733. doi: 10.1056/NEJMoa2001017

Citation: Torrens-Mas M, Perelló-Reus CM, Trias-Ferrer N, Ibarra-González L, Crespi C, Galmes-Panades AM, Navas-Enamorado C, Sanchez-Polo A, Piérola-Lopetegui J, Masmiquel L, Crespi LS, Barcelo C and Gonzalez-Freire M (2022) GDF15 and ACE2 stratify COVID-19 patients according to severity while ACE2 mutations increase infection susceptibility. *Front. Cell. Infect. Microbiol.* 12:942951. doi: 10.3389/fcimb.2022.942951

Copyright © 2022 Torrens-Mas, Perelló-Reus, Trias-Ferrer, Ibarra-González, Crespi, Galmes-Panades, Navas-Enamorado, Sanchez-Polo, Piérola-Lopetegui, Masmiquel, Crespi, Barcelo and Gonzalez-Freire. This is an open-access article distributed under the terms of the Creative Commons Attribution License (CC BY). The use, distribution or reproduction in other forums is permitted, provided the original author(s) and the copyright owner(s) are credited and that the original publication in this journal is cited, in accordance with accepted academic practice. No use, distribution or reproduction is permitted which does not comply with these terms.



OPEN ACCESS

EDITED BY

Vikas Sood,
Jamia Hamdard University, India

REVIEWED BY

Manish Sharma,
Emory University, United States
Yongfen Xu,
Institut Pasteur of Shanghai, Chinese
Academy of Sciences (CAS), China

*CORRESPONDENCE

Piyush Baindara
pbaindara@health.missouri.edu
Santi M. Mandal
mandalsm@gmail.com
Adam G. Schrum
schruma@health.missouri.edu

SPECIALTY SECTION

This article was submitted to
Virus and Host,
a section of the journal
Frontiers in Cellular and
Infection Microbiology

RECEIVED 26 April 2022

ACCEPTED 11 July 2022

PUBLISHED 04 August 2022

CITATION

Baindara P, Sarker MB, Earhart AP,
Mandal SM and Schrum AG (2022)
NOTCH signaling in COVID-19: a
central hub controlling genes,
proteins, and cells that mediate SARS-
CoV-2 entry, the inflammatory
response, and lung regeneration.
Front. Cell. Infect. Microbiol. 12:928704.
doi: 10.3389/fcimb.2022.928704

COPYRIGHT

© 2022 Baindara, Sarker, Earhart,
Mandal and Schrum. This is an open-
access article distributed under the
terms of the [Creative Commons
Attribution License \(CC BY\)](#). The use,
distribution or reproduction in other
forums is permitted, provided the
original author(s) and the copyright
owner(s) are credited and that the
original publication in this journal is
cited, in accordance with accepted
academic practice. No use,
distribution or reproduction is
permitted which does not comply with
these terms.

NOTCH signaling in COVID-19: a central hub controlling genes, proteins, and cells that mediate SARS-CoV-2 entry, the inflammatory response, and lung regeneration

Piyush Baindara^{1*}, Md Bodruzzaman Sarker^{1,2},
Alexander P. Earhart¹, Santi M. Mandal^{3*}
and Adam G. Schrum^{1,2,4,5*}

¹Department of Molecular Microbiology & Immunology, School of Medicine, University of Missouri, Columbia, MO, United States, ²Division of Animal Sciences, College of Agriculture, Food and Natural Resources, University of Missouri, Columbia MO, United States, ³Central Research Facility, Indian Institute of Technology Kharagpur, Kharagpur, India, ⁴Department of Surgery, School of Medicine, University of Missouri, Columbia, MO, United States, ⁵Department of Biomedical, Biological, & Chemical Engineering, College of Engineering, University of Missouri, Columbia, MO, United States

In the lungs of infected individuals, the downstream molecular signaling pathways induced by Severe Acute Respiratory Syndrome Coronavirus 2 (SARS-CoV-2) are incompletely understood. Here, we describe and examine predictions of a model in which NOTCH may represent a central signaling axis in lung infection in Coronavirus Disease 2019 (COVID-19). A pathway involving NOTCH signaling, furin, ADAM17, and ACE2 may be capable of increasing SARS-CoV-2 viral entry and infection. NOTCH signaling can also upregulate IL-6 and pro-inflammatory mediators induced to hyperactivation in COVID-19. Furthermore, if NOTCH signaling fails to turn down properly and stays elevated, airway regeneration during lung healing can be inhibited—a process that may be at play in COVID-19. With specific NOTCH inhibitor drugs in development and clinical trials for other diseases being conducted, the roles of NOTCH in all of these processes central to both infection and healing merit contemplation if such drugs might be applied to COVID-19 patients.

KEYWORDS

ADAM, ACE2, furin, Notch, SARS-CoV-2, COVID-19, gamma-secretase inhibitor (GSI)

Introduction

SARS-CoV-2 infection has been reported to cause various pathologies in respiratory, cardiovascular, gastrointestinal, and central nervous systems with a prominent cause of death being Acute Respiratory Distress Syndrome (ARDS) secondary to COVID-19 (Long et al., 2020; Paybast et al., 2020; Holliday et al., 2021; Hu et al., 2021a). Cellular entry of SARS-CoV-2 is mediated by its spike protein upon interaction with the human receptor ACE2 (Walls et al., 2020). Protease activities that affect viral entry include those of furin, which cleaves spike protein and facilitates entry. In SARS-CoV-2 target cells, ADAM17 can induce ectodomain shedding of ACE2 inhibiting viral engagement and entry, while TMPRSS2 cleaves ACE2 but enhances SARS-CoV-2 infection, highlighting that regulation of ACE2 cleavage and shedding is a complex process incompletely understood (Hoffmann et al., 2020; Zipeto et al., 2020; Wang et al., 2022).

Greater understanding of host signaling pathways important for infection might point toward novel viral or host targets with therapeutic potential for COVID-19. NOTCH signaling is highly evolutionarily conserved and plays a role as master regulator of various biological functions in health and disease (Shang et al., 2016). In terms of viral pathogenesis, NOTCH signaling has previously been shown to regulate different processes in infection by Epstein-Barr virus, influenza virus, respiratory syncytial virus, human papillomavirus, hepatitis B virus, and human immunodeficiency virus (Hayward, 2004; Breikaa and Lilly, 2021). Recently, up-regulation of NOTCH signaling was implicated by transcriptional signatures obtained from the lungs of SARS-CoV-2-infected rhesus macaques (Rosa et al., 2021). In the present study, we describe and examine predictions of a model where NOTCH signaling may represent a central hub controlling genes, proteins, and cells in SARS-CoV-2 infection, and in the resulting processes of inflammation and tissue regeneration in the lung.

Rizzo's model where NOTCH impacts SARS-CoV-2 infection and inflammation

Expressed at the surface membrane, four human NOTCH receptors (NOTCH 1-4) can be engaged by Jagged-1, Jagged-2, and Delta-like ligands (Dll)1, 3, and 4 (Aster et al., 2017; Sprinzak and Blacklow, 2021). Recently, we were highly interested in a model that was proposed, described, and illustrated by Paola Rizzo and colleagues (Rizzo et al., 2020), placing NOTCH as a candidate regulatory pathway in SARS-CoV-2 infection and inflammation. Here, we first concisely summarize main points of the Rizzo model,

building on illustrations inspired from that seminal publication. Next, we extend the model to potential roles for NOTCH in adaptive immunity and tissue regeneration in the lung. With key elements of the model described, we test predictions of the model accessing publicly available single-cell gene expression data from human lungs. In the polygenic, multi-ligand, post-translationally regulated NOTCH family system, so many different colors of response are theoretically possible; yet, we will allow an oversimplified framework tool assignment of “NOTCH good” versus “NOTCH bad” to represent predicted net effects on disease outcome upon NOTCH pathway activation. Finally, we consider the extent to which drug-mediated NOTCH inhibition should be contemplated for severe COVID-19 that is unresponsive to other therapies.

NOTCH bad #1

First, for cells directly infected by SARS-CoV-2, the NOTCH pathway might promote viral entry (Figure 1). Beginning at the cell surface of a potential target of SARS-CoV-2, NOTCH activation by ligand engagement leads to the sequential proteolytic cleavage of NOTCH by protease ADAM10 or ADAM17, and then by the gamma-secretase complex (Qiu et al., 2015; Breikaa and Lilly, 2021; Sprinzak and Blacklow, 2021). Liberated NOTCH intracellular domain (NICD) translocates to the nucleus where it joins CBF-1/RBP-Jk/Suppressor of hairless/Lag-1 (CSL) and mastermind-like (MAML) in a transcriptional complex inducing expression of many target genes, including furin and miRNA-145 (Rizzo et al., 2020). As a protein convertase, furin cleaves immature NOTCH protein to its mature heterodimeric form prior to surface expression (van Tetering and Vooijs, 2011), and also cleaves SARS-CoV-2 spike protein in a process required for its efficient cellular entry during infection (Peacock et al., 2021; Wu and Zhao, 2021). Therefore, by increasing furin levels, NOTCH signaling might promote positive-feedback of more NOTCH surface expression and concomitantly increase viral spike cleavage and cellular entry.

NOTCH signaling might also make more cell surface ACE2 available for SARS-CoV-2 docking. ADAM17 is a main convertase involved in the proteolytic cleavage and ectodomain shedding of ACE2 during SARS-CoV-2 infection (Palau et al., 2020). At the mRNA level, ADAM17 expression can be inhibited when NOTCH upregulates miRNA-145 (Doberstein et al., 2013). Thus, it is possible that NOTCH could reduce ADAM17 levels, resulting in increased non-cleaved, surface-retained ACE2 available for spike-mediated viral entry.

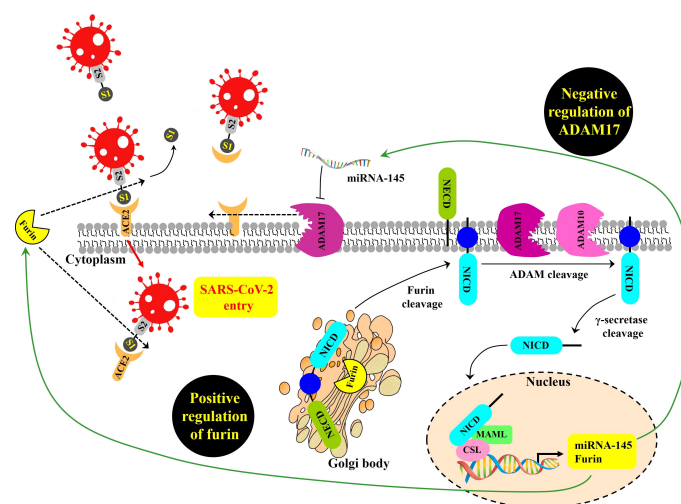


FIGURE 1

Proposed NOTCH signaling pathway effects on SARS-CoV-2 infection, modeled from Rizzo et al. (2020). SARS-CoV-2 entry is mediated by the binding of the viral spike (S) glycoprotein to ACE2 and proteolytic cleavage at the S1/S2 site of the S glycoprotein by the host protease furin. ADAM17 regulates ACE2 levels on the plasma membrane by promoting ACE2 shedding. NOTCH signaling is a positive regulator of furin and a negative regulator of ADAM17 transcript, the latter due to induction of miRNA-145. GSIs are NOTCH inhibitors that may represent a possible therapeutic strategy to inhibit viral entry into cells by reducing furin and increasing ADAM17-mediated ACE2 shedding. NOTCH precursor is cleaved by furin in the Golgi apparatus to form a heterodimer of NOTCH extracellular domain (NECD), plus the remaining cleavage product containing within the NOTCH intracellular domain (NICD). This cleavage-induced heterodimer is exported to surface expression. Upon productive ligand engagement, NOTCH is cleaved by ADAM10 or ADAM17 and later cleaved by the gamma-secretase complex. Afterwards, liberated NICD translocates into the nucleus and interacts with the transcription factor CSL and the transcriptional co-activator MAML to regulate the transcription of NOTCH target genes, including furin, and miRNA-145.

NOTCH bad #2

In the immune response to SARS-CoV-2 infection, excessive NOTCH signaling may promote IL-6 and inflammatory pathways that can exacerbate morbidity and severity of COVID-19 (Figure 2). Hyperactivation of innate immune cells and products contribute to cytokine storm (Hu et al., 2021b) and disease severity in the lung airway, gastrointestinal tract, and myocardial and neurological tissues (Najjar et al., 2020; Pezzini and Padovani, 2020). IL-6 is a major cytokine involved in the immunopathophysiology of COVID-19, a characteristic biomarker of cytokine storm and a therapeutic target to reduce inflammation and disease symptoms (Campochiaro and Dagna, 2020; Grifoni et al., 2020; Santa Cruz et al., 2021). Additionally, COVID-19-induced cytokine storm syndrome often includes high IL-6 receptor, TNF- α , granulocyte-colony stimulating factor and other immune products (Zhang et al., 2020).

NOTCH1 can directly bind to the IL-6 promoter to activate its transcription (Wongchana and Palaga, 2012). In turn, IL-6 increases the expression of NOTCH ligands such as DLL1 and DLL4, enacting a potential positive feedback loop (Yang et al., 2015; Hildebrand et al., 2018; Rizzo et al., 2020). NOTCH signaling also triggers the production of iNOS and numerous cytokines including IL-4, IL-13, plus other inducers of JNK and

ERK MAP kinase pathways that can ultimately influence downstream T cell differentiation (Qu et al., 2017; Wang et al., 2018; Segal et al., 2019). TNF- α has also been reported to induce expression of NOTCH1 and NOTCH4 (Quillard et al., 2010) and high serum TNF- α levels are associated with increased mortality in severe COVID-19 (Mortaz et al., 2021). In a recent cohort study, TNF- α inhibitor monotherapy was found to reduce risk in severe COVID-19 patients (Izadi et al., 2021). These observations are consistent with a contributing role for NOTCH in the inflammatory response known to promote severity in COVID-19.

NOTCH good #1

NOTCH activation can influence peripheral CD4 T helper cell responses (Adler et al., 2003; Eagar et al., 2004; Osborne and Minter, 2007), thus potentially aiding adaptive immune protection, memory generation, and antibody production for sterilizing immunity in the long run. The expression of this potentially positive effect might be observed subsequent to the more dangerous, early, hyper-innate immune signaling imbalance (Figure 2) that precedes the zenith of a fully mounted adaptive immune protective response. But this illustrates one means by which NOTCH signaling in certain

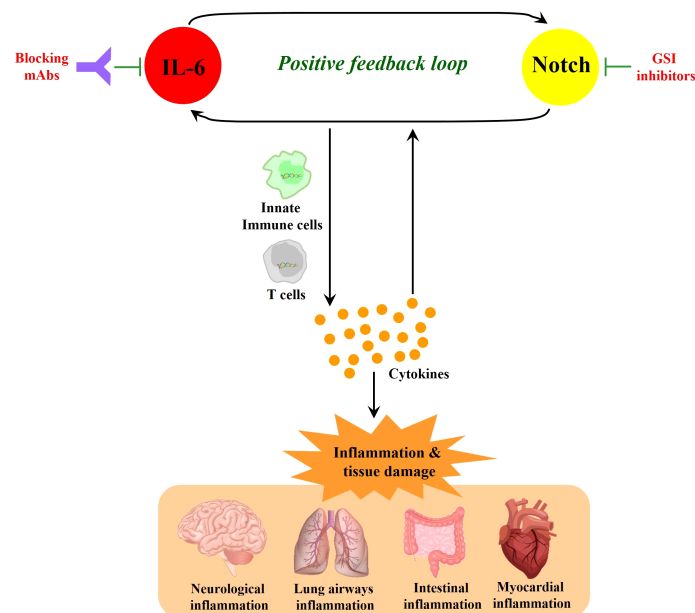


FIGURE 2

NOTCH signaling induces IL-6 in a positive-feedback loop. NOTCH signaling promotes the production of inflammatory cytokines including IL-6. In turn, IL-6 increases the expression of NOTCH ligands (such as DLL1 and DLL4), which can further amplify NOTCH signaling. This NOTCH : IL-6 positive-feedback loop can promote innate immune cell and adaptive immune T cell activation together with further amplified inflammatory cytokine elaboration. When these processes are highly active without sufficient downregulation in a resolution phase, they can cause inflammatory tissue damage and continued cycles of IL-6 and NOTCH upregulation and activation. While monoclonal antibodies (mAbs) that block IL-6 or its receptor represent promising therapeutic modalities, GSIs block NOTCH signaling as candidate drugs in clinical trials for other diseases, and these latter compounds could be contemplated when severe COVID-19 may be unresponsive to other therapies. In sum, it is suggested that targeting the positive feedback loop between NOTCH and IL-6 could be a potential therapeutic strategy that may have application against COVID-19.

specific cells, like T cells, perhaps at the right time in the response kinetic, may be predicted to promote a positive effect against SARS-CoV-2 infection.

NOTCH good #2

In homeostasis and healing post-injury, NOTCH signaling is essential for tissue regeneration in lung and it is thus conceivable this principle may apply to ARDS in COVID-19. The proximal-distal axis of the human respiratory tract consists of a variety of lung epithelial cells (Figure 3). The trachea, bronchi, and bronchioles are proximal regions of the respiratory system that are made up of basal cells, goblet cells, ciliated cells, club cells, and neuroendocrine cells. Basal cells reside in both cartilaginous and smaller airways that include bronchioles. The alveolar or distal regions consist of flattened alveolar type I cells (AT1) and cuboidal alveolar type II cells (AT2) (Kiyokawa and Morimoto, 2020). NOTCH signaling promotes proliferation and dissemination of basal cells necessary for healing and regeneration of other lung cell types to restore functional airways (Kotton and Morrissey, 2014).

NOTCH bad #3

Excessive NOTCH signaling inhibits regeneration of cell types necessary for airway function (Figure 3). Subsequent to NOTCH signaling, its tightly regulated inhibition is critical for normal maintenance of airway cell subsets and their regeneration during healing. Upon alveolar epithelial injury, NOTCH signaling in AT2 cells becomes downregulated by a non-canonical ligand of NOTCH (Dlk1), facilitating AT2 to AT1 transition, and leading to alveolar repair (Finn et al., 2019). NOTCH inhibition is required to promote diverse cell differentiation in airway replenishment and restoration while avoiding lung fibrosis during healing (Wasnick et al., 2019). Continuous or excessive NOTCH activation can perturb the balance of cell differentiation during regeneration, promoting basal cell proliferation and goblet cell development at the expense of other diverse airway cell types. In the proximal airways, excessive NOTCH activation can promote goblet cell hyperplasia accompanied by high cytokine levels (Danahay et al., 2015). In the distal area, continuous NOTCH blocks the trans-differentiation of basal cells into alveolar cells (Kiyokawa and Morimoto, 2020), while inhibiting AT2 to AT1 transition,

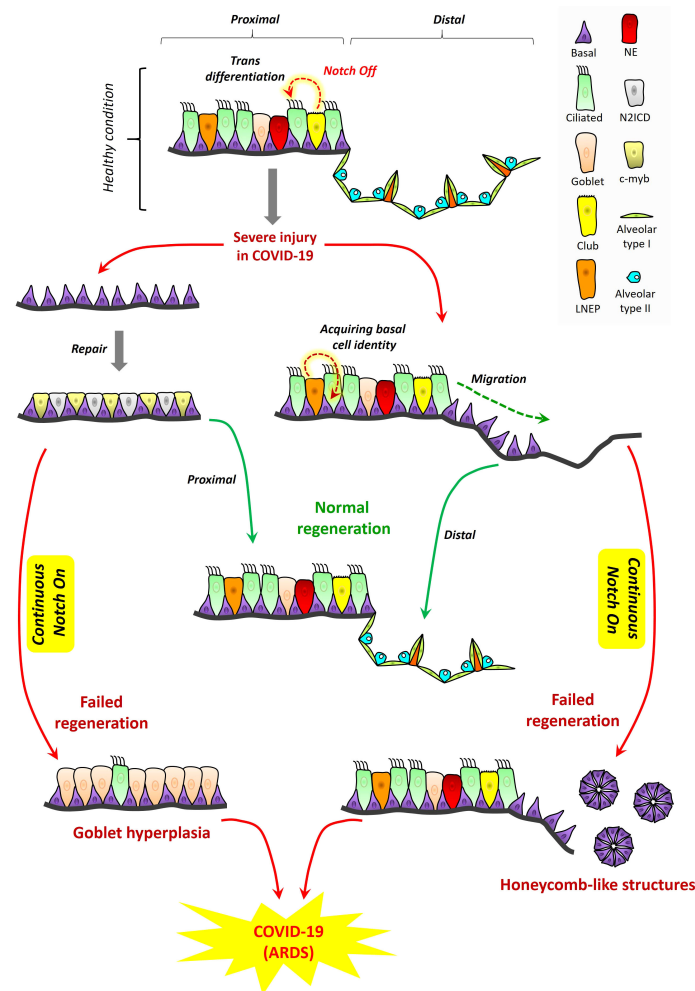


FIGURE 3

Proposed role for NOTCH in lung regeneration in COVID-19: tissue structure in the proximal and distal respiratory tract. A variety of lung epithelial cells exist along the proximal-distal axis. In proximal regions, there are five major cell populations, which include basal cells (purple), goblet cells (light pink), ciliated cells (green), club cells (yellow), and neuroendocrine cells (red). LNEPs (lineage-negative epithelial progenitor cells) are shown in light orange color. In alveolar regions, there are mainly two types of epithelial cells, flattened alveolar type I cells (light green) and cuboidal alveolar type II cells (indigo). Septa are shown in dark orange color. Cell loss in the proximal respiratory tract due to injury triggers the expansion of basal cells and their direct segregation into N2ICD (club progenitor, light grey) and c-myb (ciliated progenitor, light yellow) cells. However, continuous NOTCH activation during COVID-19 along with cytokine storm may result in goblet cell hyperplasia which could exacerbate disease pathogenesis and contribute to ARDS. LNEPs acquire basal cell identity and migrate towards the damaged area of the distal respiratory tract. NOTCH blocks the trans-differentiation of basal cells into alveolar cells and thus NOTCH inhibition is necessary for normal regeneration. However, continuous NOTCH activation may occur in COVID-19 and this could result in abnormal regeneration with basal cell excess and honeycomb-like structures that may contribute to ARDS and disease severity.

resulting in failure to regenerate the alveolus, an outcome sometimes marked by honeycomb cysts and basal cell excess (Vaughan et al., 2015; Reyfman et al., 2019).

Some published observations support the notion that these patterns of NOTCH activation and inhibition may be at play in COVID-19, at least in subsets of patients with underlying chronic lung conditions. SARS-CoV-2 shows gradient infectivity from proximal to distal regions of the respiratory tract that follows ACE2 expression patterns, with ciliated cells and AT2 cells being primary targets (Hou et al., 2020) in

addition to goblet cells (Osan et al., 2020). As infection progresses, SARS-CoV-2 cell tropism expands to infect a greater array of airway epithelial cells including club and basal cells (Ryu and Shin, 2021). It has been previously proposed that goblet cell hyperplasia could occur in COVID-19 and other viral infections known to induce high mucus production (Mehedi, 2020; Cortez and Schultz-Cherry, 2021). An *in vitro* model of airway epithelium derived from healthy or COPD subjects suggested that goblet cell hyperplasia may have been involved in SARS-CoV-2 infection and COVID-19 disease progression

(Osan et al., 2020). Other case studies of COVID-19 patients with pulmonary fibrosis reported the presence of honeycomb-like structures with speculation these might impact infection or recovery (Combet et al., 2020; Zou et al., 2021). One case report of COVID-19 showed, among the pathological changes in lung epithelium, the presence of plugged bronchioles with mucus and goblet cell hyperplasia (Yin et al., 2021). It seems reasonable to suggest that NOTCH's role in lung regeneration is likely to be important in patients who have underlying chronic lung conditions among the highest risk of ARDS secondary to severe COVID-19. To propose that a similar role may be important in the general patient population may be logical, but we are unaware of empirical evidence that directly assesses this concept to date. Therefore, we hypothesize a model where it is conceivable that known rules of NOTCH signaling and downregulation might be at play in COVID-19, where excessive NOTCH activity might inhibit healthy regeneration and increase ARDS severity in COVID-19.

Testing predictions of the model using publicly available single-cell gene expression data

We reviewed publicly accessible single-cell (sc)RNA-seq data from healthy human lungs (Vieira Braga et al., 2019), assuming these data would represent gene expression patterns of critical cell types early in or near the start of SARS-CoV-2 infection. The first goal was to determine if the model in Figure 1 could be rejected, unless single cell types could be found to co-express the key genes in cis required for the model to remain sustainable. Supplemental figures each include gene expression data on two pages: (a) epithelial airway cell types and (b) non-epithelial cell types including leukocytes.

First, we assessed whether NOTCH genes were expressed by cell types that could impact SARS-CoV-2 infection. NOTCH1 and NOTCH2 were expressed by basal, alveolar, club, goblet, and ciliated cells, as well as numerous non-epithelial cells (Figures S1, S2), although NOTCH1 was relatively greater in the airway than parenchyma in basal2 cells, with an opposite trend for NOTCH2 which favored parenchyma over airway expression in basal1 cells. NOTCH3 expression was largely in basal2, club, and goblet cells with little non-epithelial expression (Figure S3). NOTCH4 was mostly expressed by basal1 cells in lung airways along with some ciliated cell expression (Figure S4). We observed that another human-specific gene, NOTCH2NL, was mostly expressed by goblet cells in lung airways followed by type1 alveolar cells in the lung parenchyma (Figure S5). Similarly, we checked the expression pattern of NOTCH receptors in different cell types. We observed that NOTCH ligand dll1 was expressed mostly by basal cells in lung parenchyma and lung airways, along with club and ciliated cell expression in airways (Figure S6), while dll3 and dll4 showed

sparse expression (Figures S7, S8). Other NOTCH receptors, Jag1 and Jag2, were found highly expressed by airway epithelial cell types, with Jag1 expression was also well-represented in leukocytes (Figures S9, S10). Additionally, all the components of the gamma-secretase complex (PSENEN, PSEN1, PSEN2, NCSTN, APH1A, and APH1B) were expressed in lung airways, lung parenchyma, and leukocytes (Figures S11–S16). These observations showed that genes relevant to NOTCH signaling have widespread representation in expression levels present in cell types relevant to SARS-CoV-2 infection in the lung.

Next, we checked the gene expression profiles of ACE2, furin, TMPRSS2, ADAM17, and ADAM10. ACE2 was concentrated in goblet and ciliated2 cells, with expression also among ciliated1, club, basal, and alveolar cells (Figure S17). Furin and TMPRSS2 expression was observed in all epithelial subsets weighted toward parenchyma and furin also displayed clear expression in non-epithelial subsets, including leukocytes (Figures S18, S19). ADAM17 and ADAM10 showed expression in all epithelial and non-epithelial subsets (Figures S20, S21). Because these data show that the same cell types can co-express NOTCH, ACE2, furin, TMPRSS2, and ADAM proteases, it validates the possibility that these gene products could act in cis and affect each other as required by the model (Figure 1).

Elements of the model in Figures 2, 3, are less reliant on predictions of gene expression in single cell types in cis and rather involve signaling and/or differentiation between cell types. In lung epithelial cell types, IL-6 showed sparse but clear expression spread across all subsets, while greater relative expression was seen in leukocytes and other non-epithelial cells (Figure S22). Expression of receptors for IL-6 (IL-6R and IL6ST) was observed across all cell types (Figures S23, S24), indicating that a feedback loop between IL-6 responsiveness and NOTCH signaling remains a possible feature which might contribute to the inflammatory response during COVID-19.

Contemplating NOTCH-based inhibitor drugs for severe, COVID-19 that is unresponsive to other treatments

We visualized a molecular interaction network connecting NOTCH signaling with SARS-CoV-2 (Figure 4). Inhibition of NOTCH signaling, NOTCH : IL-6 positive feedback loop, or downstream molecules in these pathways might be hypothesized to decrease SARS-CoV-2 infection, downregulate the inflammatory response, and/or favor lung regeneration.

NOTCH represents a complicated pathway. At the molecular level, it is polygenic, multi-ligand, and post-translationally regulated. At the cell and tissue level, it has multiple different effects including opposing effects on many different cell types in development, activation, differentiation, proliferation, and regeneration. Therefore, it is possible that

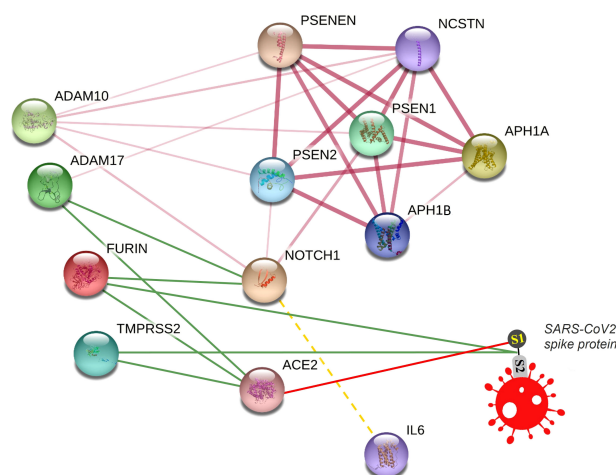


FIGURE 4

Connecting NOTCH and SARS-CoV-2 in a molecular interaction network. This network is partially generated by STRING v11. All STRING-generated edges are shown in pink (light or dark), while other edges are drawn manually. Gamma secretase complex is represented by different subunits including APOE1A, APOE1B, PSEN1, PSEN2, PSENEN, and NCSTN. Other proteins included are NOTCH1, FURIN, ADAM17, ADAM10, TMPRSS2, and ACE2. The SARS-CoV2 spike protein is drawn manually. Interaction edges of some proteases (ADAM17, FURIN, TMPRSS2) with NOTCH and ACE2 are indicated by green lines, while binding of SARS-CoV-2 spike protein with its receptor ACE2 is indicated by a red line. The transcriptional (not protein) interaction of NOTCH and IL-6 is indicated by a dashed yellow line.

pharmacologic targeting of NOTCH could generate unwanted on-target, off-disease side-effects. However, it is also true that other pathways targeted in therapy, for example, those involving cortisol or corticosteroid, may also interact with and potentially effect a similar list of processes in multiple cell types and tissues. Yet with the right timing and at the right dose, corticosteroid improves outcomes of severe COVID-19 and is administered as part of standard care (Li et al., 2021). We wonder if NOTCH-based inhibitor drugs should be considered as clinical trial candidates for severe COVID-19 when patient subset risk or other factors make outcomes unresponsive to current established therapies.

Still, prior to discussing specific NOTCH inhibitor treatment ideas, more deliberation is provided here to consider the extent to which this could be foreseen as beneficial versus potentially harmful. In the present study, we counted issues where a net effect of NOTCH signaling could be predicted to be “bad” or “good”. Despite the oversimplification of this scoring tool, there is a pattern worth noting: the two processes scored as “good” are deemphasized in acute, severe disease, whereas the three processes scored as “bad” occur during acute, severe disease, and are here hypothesized to play a causal role contributing to severity. Therefore, if the present model were correct, then inhibition of NOTCH signaling in severe, COVID-19 that is unresponsive to other therapies might (a) decrease furin expression, decrease NOTCH expression, increase ADAM17 expression, and thus decrease new avenues of SARS-CoV-2 infection; (b) decrease inflammation by inhibiting NOTCH : IL-6 positive feedback loop; and (c) favor regeneration of alveoli

and healing of respiratory apparatus. In contrast, predictable negative side-effects of NOTCH inhibition in this scenario could include (d) inhibiting CD4 helper T cells, which eventually are needed for adaptive immunity including optimal antibody generation from helped B cells; and (e) inhibiting a basic pathway required for lung tissue regeneration by precursor cells. Regarding (d), other treatments such as corticosteroid can have a similar effect and thus timing and dosage are critical in order to maximize benefit while minimizing this risk. Regarding (e), this might be an acceptable risk, perhaps briefly during intensive care, if NOTCH inhibition might provide the break that is needed to boost alveolar regeneration, even if more distal precursor cells were to be temporarily inhibited. Upon identifying these specific issues where NOTCH impacts SARS-CoV-2-mediated disease in the lungs, we propose that NOTCH inhibitory drug strategies are worth contemplating for severe COVID-19 that may be unresponsive to other therapies.

The data and studies summarized here could suggest a strategy for a subset of patients for whom a targeted NOTCH-based diagnostic assay could be developed and tested for technical efficacy as well as relevance to disease severity. Gamma secretase inhibitor (GSI) drugs have been developed to the point of various clinical trials for other indications (Espinoza and Miele, 2013; Yuan et al., 2015). We suggest that GSIs, provided for a finite period, might be beneficial for the treatment of severe COVID-19 that is unresponsive to other therapies. Regarding the route of administration, perhaps nebulization for direct delivery to the lungs may maximally target the infection and regeneration

pathways discussed herein, while systemic delivery might have a more far-reaching effect to inhibit the NOTCH : IL-6 positive feedback loop in immune cells, and might also be predicted to cause more on-target, off-disease side-effects.

Concluding remarks

We present a model where NOTCH may be a central hub regulating the processes of infection, inflammation, and lung regeneration in COVID-19. In outlining specific aspects of this model with prior knowledge documentation, and testing some predictions using public sc-RNA-seq data, we did not reject the model and found gene expression characteristics in the lung to be largely compatible. NOTCH activation might cause an increase in SARS-CoV-2 cell entry and infection, exacerbate inflammation in a NOTCH : IL-6 positive feedback loop, and inhibit functional airway regeneration. It is conceivable that NOTCH inhibitory drug candidates, such as GSIs, might improve these outcomes in severe COVID-19 that is unresponsive to other therapies.

Data availability statement

Publicly available datasets were analyzed in this study. This data can be found here: Lung Cell Atlas (<https://asthma.cellgeni.sanger.ac.uk/>).

Ethics statement

The present work uses publicly available human gene expression data.

Author contributions

PB, MBS, AE, and AS collected, analyzed, and/or interpreted data. PB and AS wrote the manuscript. PB, SM, and AS led

ideation, hypothesis generation, and conclusions. All authors contributed to the article and approved the submitted version.

Funding

This work was supported by University of Missouri Biomedical Innovation recruitment funds and NIH grant R01GM103841 (AGS).

Acknowledgment

We thank Kimberly G. Laffey, PhD, and Zachary M. Holliday, MD, for the critical review of this manuscript.

Conflict of interest

The authors declare that the research was conducted in the absence of any commercial or financial relationships that could be construed as a potential conflict of interest.

Publisher's note

All claims expressed in this article are solely those of the authors and do not necessarily represent those of their affiliated organizations, or those of the publisher, the editors and the reviewers. Any product that may be evaluated in this article, or claim that may be made by its manufacturer, is not guaranteed or endorsed by the publisher.

Supplementary material

The Supplementary Material for this article can be found online at: <https://www.frontiersin.org/articles/10.3389/fcimb.2022.928704/full#supplementary-material>

References

- Adler, S. H., Chiffolleau, E., Xu, L., Dalton, N. M., Burg, J. M., Wells, A. D., et al. (2003). Notch signaling augments T cell responsiveness by enhancing CD25 expression. *J. Immunol.* 171, 2896–2903. doi: 10.4049/jimmunol.171.6.2896
- Aster, J. C., Pear, W. S., and Blacklow, S. C. (2017). The varied roles of notch in cancer. *Annu. Rev. Pathol. Mech. Dis.* 12, 245–275. doi: 10.1146/annurev-pathol-052016-100127
- Breikaa, R. M., and Lilly, B. (2021). The notch pathway: A link between COVID-19 pathophysiology and its cardiovascular complications. *Front. Cardiovasc. Med.* 8. doi: 10.3389/fcvm.2021.681948
- Campochiaro, C., and Dagna, L. (2020). The conundrum of interleukin-6 blockade in COVID-19. *Lancet Rheumatol* 2, e579–e580. doi: 10.1016/S2665-9913(20)30287-3
- Combet, M., Pavot, A., Savale, L., Humbert, M., and Monnet, X. (2020). Rapid onset honeycombing fibrosis in spontaneously breathing patient with COVID-19. *Eur. Respir. J.* 56, 2001808. doi: 10.1183/13993003.01808-2020
- Cortez, V., and Schultz-Cherry, S. (2021). The role of goblet cells in viral pathogenesis. *FEBS J.* 288, 7060–7072. doi: 10.1111/febs.15731
- Danahay, H., Pessotti, A. D., Coote, J., Montgomery, B. E., Xia, D., Wilson, A., et al. (2015). Notch2 is required for inflammatory cytokine-driven goblet cell metaplasia in the lung. *Cell Rep.* doi: 10.1016/j.celrep.2014.12.017
- Doberstein, K., Steinmeyer, N., Hartmetz, A. K., Eberhardt, W., Mittelbronn, M., Harter, P. N., et al. (2013). MicroRNA-145 targets the metalloprotease ADAM17 and is suppressed in renal cell carcinoma patients. *Neoplasia* 15, 218–30. doi: 10.1593/neo.121222

- Eagar, T. N., Tang, Q., Wolfe, M., He, Y., Pear, W. S., and Bluestone, J. A. (2004). Notch 1 signaling regulates peripheral T cell activation. *Immunity* 20, 407–415. doi: 10.1016/S1074-7613(04)00081-0
- Espinoza, I., and Miele, L. (2013). Notch inhibitors for cancer treatment. *Pharmacol. Ther.* 139, 95–110. doi: 10.1016/j.pharmthera.2013.02.003
- Finn, J., Sottoriva, K., Pajcini, K. V., Kitajewski, J. K., Chen, C., Zhang, W., et al. (2019). Dlk1-mediated temporal regulation of notch signaling is required for differentiation of alveolar type II to type I cells during repair. *Cell Rep.* 26, 2942–2954.e5. doi: 10.1016/j.celrep.2019.02.046
- Grifoni, E., Valoriani, A., Cei, F., Lamanna, R., Gelli, A. M. G., Ciambotti, B., et al. (2020). Interleukin-6 as prognosticator in patients with COVID-19. *J. Infect.* 81, 452–82. doi: 10.1016/j.jinf.2020.06.008
- Hayward, S. D. (2004). Viral interactions with the notch pathway. *Semin. Cancer Biol.* 14, 387–396. doi: 10.1016/j.semcancer.2004.04.018
- Hildebrand, D., Uhle, F., Sahin, D., Krauser, U., Weigand, M. A., and Heeg, K. (2018). The interplay of notch signaling and STAT3 in TLR-activated human primary monocytes. *Front. Cell. Infect. Microbiol.* 8, 241. doi: 10.3389/fcimb.2018.00241
- Hoffmann, M., Kleine-Weber, H., and Pöhlmann, S. (2020). A multibasic cleavage site in the spike protein of SARS-CoV-2 is essential for infection of human lung cells. *Mol. Cell* 78, 779–784.e5. doi: 10.1016/j.molcel.2020.04.022
- Holliday, Z. M., Earhart, A. P., Alnijoumi, M. M., Kravac, A., Allen, L. A. H., and Schrum, A. G. (2021). Non-randomized trial of dornase Alfa for acute respiratory distress syndrome secondary to covid-19. *Front. Immunol.* 12. doi: 10.3389/fimmu.2021.714833
- Hou, Y. J., Okuda, K., Edwards, C. E., Martinez, D. R., Asakura, T., Dinno, K. H., et al. (2020). SARS-CoV-2 reverse genetics reveals a variable infection gradient in the respiratory tract. *Cell* 182, 429–446.e14. doi: 10.1016/j.cell.2020.05.042
- Hu, B., Guo, H., Zhou, P., and Shi, Z. L. (2021a). Characteristics of SARS-CoV-2 and COVID-19. *Nat. Rev. Microbiol.* 19, 141–154. doi: 10.1038/s41579-020-00459-7
- Hu, B., Huang, S., and Yin, L. (2021b). The cytokine storm and COVID-19. *J. Med. Virol.* 93, 250–256. doi: 10.1002/jmv.26232
- Izadi, Z., Brenner, E. J., Mahil, S. K., Dand, N., Yiu, Z. Z. N., Yates, M., et al. (2021). Association between tumor necrosis factor inhibitors and the risk of hospitalization or death among patients with immune-mediated inflammatory disease and COVID-19. *JAMA Netw. Open* 4, e2129639. doi: 10.1001/jamanetworkopen.2021.29639
- Kiyokawa, H., and Morimoto, M. (2020). Notch signaling in the mammalian respiratory system, specifically the trachea and lungs, in development, homeostasis, regeneration, and disease. *Dev. Growth Differ.* 62, 67–79. doi: 10.1111/dgd.12628
- Kotton, D. N., and Morrissey, E. E. (2014). Lung regeneration: Mechanisms, applications and emerging stem cell populations. *Nat. Med.* 20, 822–832. doi: 10.1038/nm.3642
- Li, H., Yan, B., Gao, R., Ren, J., and Yang, J. (2021). Effectiveness of corticosteroids to treat severe COVID-19: A systematic review and meta-analysis of prospective studies. *Int. Immunopharmacol.* 100, 108121. doi: 10.1016/j.intimp.2021.108121
- Long, B., Brady, W. J., Koyfman, A., and Gottlieb, M. (2020). Cardiovascular complications in COVID-19. *Am. J. Emerg. Med.* 38, 1504–1507. doi: 10.1016/j.ajem.2020.04.048
- Mehedi, M. (2020). Goblet cells in SARS-CoV-2 pathogenesis. *Am. J. Biomed. Sci. Res.* 11, 102–104. doi: 10.34297/ajbsr.2020.11.001596
- Mortaz, E., Tabarsi, P., Jamaati, H., Dalil Roofchayee, N., Dezfali, N. K., Hashemian, S. M. R., et al. (2021). Increased serum levels of soluble TNF- α receptor is associated with ICU mortality in COVID-19 patients. *Front. Immunol.* 12. doi: 10.3389/fimmu.2021.592727
- Najjar, S., Najjar, A., Chong, D. J., Pramanik, B. K., Kirsch, C., Kuzniecky, R. I., et al. (2020). Central nervous system complications associated with SARS-CoV-2 infection: integrative concepts of pathophysiology and case reports. *J. Neuroinflamm.* 17, 231. doi: 10.1186/s12974-020-01896-0
- Osan, J. K., Talukdar, S. N., Feldmann, F., DeMontigny, B. A., Jerome, K., Bailey, K. L., et al. (2020). Goblet cell hyperplasia increases SARS-CoV-2 infection in COPD. *bioRxiv*, 12. doi: 10.1101/2020.11.11.379099
- Osborne, B. A., and Minter, L. M. (2007). Notch signalling during peripheral T-cell activation and differentiation. *Nat. Rev. Immunol.* 7, 64–75. doi: 10.1038/nri1998
- Palau, V., Riera, M., and Soler, M. J. (2020). ADAM17 inhibition may exert a protective effect on COVID-19. *Nephrol. Dial. Transplant.* 35, 1071–1072. doi: 10.1093/ndt/gfaa093
- Paybast, S., Emami, A., Koosha, M., and Baghalha, F. (2020). Novel coronavirus disease (COVID-19) and central nervous system complications: What neurologists need to know. *Acta Neurol. Taiwan* 29, 24–31.
- Peacock, T. P., Goldhill, D. H., Zhou, J., Baillon, L., Frise, R., Swann, O. C., et al. (2021). The furin cleavage site in the SARS-CoV-2 spike protein is required for transmission in ferrets. *Nat. Microbiol.* 6, 899–909. doi: 10.1038/s41564-021-00908-w
- Pezzini, A., and Padovani, A. (2020). Lifting the mask on neurological manifestations of COVID-19. *Nat. Rev. Neurol.* 16, 636–644. doi: 10.1038/s41582-020-0398-3
- Qiu, H., Tang, X., Ma, J., Shaverdashvili, K., Zhang, K., and Bedogni, B. (2015). Notch1 autoactivation via transcriptional regulation of furin, which sustains Notch1 signaling by processing Notch1-activating proteases ADAM10 and membrane type 1 matrix metalloproteinase. *Mol. Cell. Biol.* 35, 3622–3632. doi: 10.1128/mcb.00116-15
- Quillard, T., Devallière, J., Coupel, S., and Charreau, B. (2010). Inflammation dysregulates notch signaling in endothelial cells: Implication of Notch2 and Notch4 to endothelial dysfunction. *Biochem. Pharmacol.* 80, 2032–2041. doi: 10.1016/j.bcp.2010.07.010
- Qu, S.Y., Lin, J. J., Zhang, J., Song, L. Q., Yang, X. M., and Wu, C.G. (2017). Notch signaling pathway regulates the growth and the expression of inflammatory cytokines in mouse basophils. *Cell. Immunol.* 318, 29–34. doi: 10.1016/j.cellimm.2017.05.005
- Reyfan, P. A., Walter, J. M., Joshi, N., Anekalla, K. R., McQuattie-Pimentel, A. C., Chiu, S., et al. (2019). Single-cell transcriptomic analysis of human lung provides insights into the pathobiology of pulmonary fibrosis. *Am. J. Respir. Crit. Care Med.* 199, 1517–1536. doi: 10.1164/rccm.201712-2410OC
- Rizzo, P., Viececi Dalla Sega, F., Fortini, F., Marracino, L., Rapezzi, C., and Ferrari, R. (2020). COVID-19 in the heart and the lungs: could we “Notch” the inflammatory storm? *Basic Res. Cardiol.* 115, 31. doi: 10.1007/s00395-020-0791-5
- Rosa, B. A., Ahmed, M., Singh, D. K., Choreño-Parra, J. A., Cole, J., Jiménez-Álvarez, L. A., et al. (2021). IFN signaling and neutrophil degranulation transcriptional signatures are induced during SARS-CoV-2 infection. *Commun. Biol.* 4, 290. doi: 10.1038/s42003-021-01829-4
- Ryu, G., and Shin, H. W. (2021). Sars-cov-2 infection of airway epithelial cells. *Immune Netw.* 21, 1–16. doi: 10.4110/in.2021.21.e3
- Santa Cruz, A., Mendes-Frias, A., Oliveira, A. I., Dias, L., Matos, A. R., Carvalho, A., et al. (2021). Interleukin-6 is a biomarker for the development of fatal severe acute respiratory syndrome coronavirus 2 pneumonia. *Front. Immunol.* 12. doi: 10.3389/fimmu.2021.613422
- Sega, F. V. D., Fortini, F., Aquila, G., Campo, G., Vaccarezza, M., and Rizzo, P. (2019). Notch signaling regulates immune responses in atherosclerosis. *Front. Immunol.* 10, 1130. doi: 10.3389/fimmu.2019.01130
- Shang, Y., Smith, S., and Hu, X. (2016). Role of notch signaling in regulating innate immunity and inflammation in health and disease. *Protein Cell* 7, 159–174. doi: 10.1007/s13238-016-0250-0
- Sprinzak, D., and Blacklow, S. C. (2021). Biophysics of notch signaling. *Annu. Rev. Biophys.* 50, 157–189. doi: 10.1146/annurev-biophys-101920-082204
- van Tetering, G., and Vooijs, M. (2011). Proteolytic cleavage of notch: “HIT and RUN”. *Curr. Mol. Med.* 11, 255–269. doi: 10.2174/156652411795677972
- Vaughan, A. E., Brumwell, A. N., Xi, Y., Gotts, J. E., Brownfield, D. G., Treutlein, B., et al. (2015). Lineage-negative progenitors mobilize to regenerate lung epithelium after major injury. *Nature* 517, 621–625. doi: 10.1038/nature14112
- Vieira Braga, F. A., Kar, G., Berg, M., Carpaij, O. A., Polanski, K., Simon, L. M., et al. (2019). A cellular census of human lungs identifies novel cell states in health and in asthma. *Nat. Med.* 25, 1153–1163. doi: 10.1038/s41591-019-0468-5
- Walls, A. C., Park, Y. J., Tortorici, M. A., Wall, A., McGuire, A. T., and Veesler, D. (2020). Structure, function, and antigenicity of the SARS-CoV-2 spike glycoprotein. *Cell*. doi: 10.1016/j.cell.2020.02.058
- Wang, R., Li, Y., Tsung, A., Huang, H., Du, Q., Yang, M., et al. (2018). INOS promotes CD24+CD133+ liver cancer stem cell phenotype through a TACE/ADAM17-dependent notch signaling pathway. *Proc. Natl. Acad. Sci. U. S. A.* 115, E10127–E10136. doi: 10.1073/pnas.1722100115
- Wang, J., Zhao, H., and An, Y. (2022). ACE2 shedding and the role in COVID-19. *Front. Cell. Infect. Microbiol.* 11. doi: 10.3389/fcimb.2021.789180
- Wasnick, R. M., Korfei, M., Piskulak, K., Henneke, I., Wilhelm, J., Mahavadi, P., et al. (2019). Restored alveolar epithelial differentiation and reversed human lung fibrosis upon notch inhibition. *bioRxiv*. doi: 10.1101/580498
- Wongchana, W., and Palaga, T. (2012). Direct regulation of interleukin-6 expression by notch signaling in macrophages. *Cell. Mol. Immunol.* 9, 155–162. doi: 10.1038/cmi.2011.36
- Wu, Y., and Zhao, S. (2021). Furin cleavage sites naturally occur in coronaviruses. *Stem Cell Res.* 50, 102115. doi: 10.1016/j.scr.2020.102115
- Yang, Z., Guo, L., Liu, D., Sun, L., Chen, H., Deng, Q., et al. (2015). Acquisition of resistance to trastuzumab in gastric cancer cells is associated with activation of IL-6/STAT3/Jagged-1/Notch positive feedback loop. *Oncotarget* 6, 5072–5087. doi: 10.18632/oncotarget.3241

Yin, W., Cao, W., Zhou, G., Wang, L., Sun, J., Zhu, A., et al. (2021). Analysis of pathological changes in the epithelium in COVID-19 patient airways. *ERJ Open Res.* 7, 00690–02020. doi: 10.1183/23120541.00690-2020

Yuan, X., Wu, H., Xu, H., Xiong, H., Chu, Q., Yu, S., et al. (2015). Notch signaling: An emerging therapeutic target for cancer treatment. *Cancer Lett* 369, 20–7. doi: 10.1016/j.canlet.2015.07.048

Zhang, C., Wu, Z., Li, J.-W., Zhao, H., and Wang, G.-Q. (2020). The cytokine release syndrome (CRS) of severe COVID-19 and interleukin-6 receptor (IL-6R)

antagonist tocilizumab may be the key to reduce the mortality. *Int. J. Antimicrob. Agents* 55, 105954. doi: 10.1016/j.ijantimicag.2020.105954

Zipeto, D., Palmeira, J., da, F., Argañaraz, G. A., and Argañaraz, E. R. (2020). ACE2/ADAM17/TMPRSS2 interplay may be the main risk factor for COVID-19. *Front. Immunol.* 11. doi: 10.3389/fimmu.2020.576745

Zou, J. N., Sun, L., Wang, B. R., Zou, Y., Xu, S., Ding, Y. J., et al. (2021). The characteristics and evolution of pulmonary fibrosis in COVID-19 patients as assessed by AI-assisted chest HRCT. *PLoS One* 16, e0248957. doi: 10.1371/journal.pone.0248957



OPEN ACCESS

EDITED BY

Vikas Sood,
Jamia Hamdard University, India

REVIEWED BY

Danish Javed,
All India Institute of Medical Sciences
Bhopal, India
Nawab John Dar,
The University of Texas Health Science
Center at San Antonio, United States
Dharmendra Maurya,
Bhabha Atomic Research Centre
(BARC), India

*CORRESPONDENCE

Shahanavaj Khan
sdkhan@ksu.edu.sa
Dakun Lai
dklai@uestc.edu.cn
Nitesh Kumar Poddar
niteshkumar.poddar@
jaipur.manipal.edu

SPECIALTY SECTION

This article was submitted to
Virus and Host,
a section of the journal
Frontiers in Cellular and
Infection Microbiology

RECEIVED 01 May 2022

ACCEPTED 11 July 2022

PUBLISHED 15 August 2022

CITATION

Singh M, Jayant K, Singh D, Bhutani S,
Poddar NK, Chaudhary AA, Khan S,
Adnan M, Siddiqui AJ, Hassan MI,
Khan FI, Lai D and Khan S (2022)
Withania somnifera (L.) Dunal
(Ashwagandha) for the possible
therapeutics and clinical management
of SARS-CoV-2 infection: Plant-based
drug discovery and targeted therapy.
Front. Cell. Infect. Microbiol. 12:933824.
doi: 10.3389/fcimb.2022.933824

COPYRIGHT

© 2022 Singh, Jayant, Singh, Bhutani,
Poddar, Chaudhary, Khan, Adnan,
Siddiqui, Hassan, Khan, Lai and Khan.
This is an open-access article
distributed under the terms of the
Creative Commons Attribution License
(CC BY). The use, distribution or
reproduction in other forums is
permitted, provided the original
author(s) and the copyright owner(s)
are credited and that the original
publication in this journal is cited, in
accordance with accepted academic
practice. No use, distribution or
reproduction is permitted which does
not comply with these terms.

Withania somnifera (L.) Dunal (Ashwagandha) for the possible therapeutics and clinical management of SARS-CoV-2 infection: Plant-based drug discovery and targeted therapy

Manali Singh^{1,2}, Kuldeep Jayant³, Dipti Singh², Shivani Bhutani¹,
Nitesh Kumar Poddar^{4*}, Anis Ahmad Chaudhary⁵,
Salah-Ud-Din Khan⁶, Mohd Adnan⁷, Arif Jamal Siddiqui⁷,
Md Imtaiyaz Hassan⁸, Faez Iqbal Khan^{9,10}, Dakun Lai^{10*}
and Shahanavaj Khan^{11,12,13*}

¹Department of Biotechnology, Invertis University, Bareilly, Uttar Pradesh, India, ²Department of Biochemistry, C.B.S.H, G.B Pant University of Agriculture and Technology, Pantnagar, Uttarakhand, India, ³Department of Agricultural and Food Engineering, IIT Kharagpur, West Bengal, Kharagpur, India, ⁴Department of Biosciences, Manipal University Jaipur, Jaipur, Rajasthan, India, ⁵Department of Biology, College of Science, Imam Mohammad Ibn Saud Islamic University, Riyadh, Saudi Arabia, ⁶Department of Biochemistry, College of Medicine, Imam Mohammad Ibn Saud Islamic University (IMSIU), Riyadh, Saudi Arabia, ⁷Department of Biology, College of Science, University of Hail, Hail, Saudi Arabia, ⁸Center for Interdisciplinary Research in Basic Sciences, Jamia Millia Islamia, New Delhi, India, ⁹Department of Biological Sciences, School of Science, Xi'an Jiaotong-Liverpool University, Suzhou, China, ¹⁰School of Electronic Science and Engineering, University of Electronic Science and Technology of China, Chengdu, China, ¹¹Department of Health Sciences, Novel Global Community Educational Foundation 7 Peterlee Place, Hebersham, NSW, Australia, ¹²Department of Medical Lab Technology, Indian Institute of Health and Technology (IIHT), Deoband, Saharanpur, UP, India, ¹³Department of Pharmaceutics, College of Pharmacy, King Saud University, Riyadh, Saudi Arabia

Coronavirus disease 2019 (COVID-19) pandemic has killed huge populations throughout the world and acts as a high-risk factor for elderly and young immune-suppressed patients. There is a critical need to build up secure, reliable, and efficient drugs against the infection of severe acute respiratory syndrome coronavirus 2 (SARS-CoV-2) virus. Bioactive compounds of Ashwagandha [*Withania somnifera* (L.) Dunal] may implicate as herbal medicine for the management and treatment of patients infected by SARS-CoV-2 infection. The aim of the current work is to update the knowledge of SARS-CoV-2 infection and information about the implication of various compounds of medicinal plant *Withania somnifera* with minimum side effects on the patients' organs. The herbal medicine *Withania somnifera* has an excellent antiviral activity that could be implicated in the management and treatment of flu and flu-like diseases connected with SARS-CoV-2. The analysis was performed by systematically re-evaluating the published articles related to the infection of SARS-CoV-2 and the herbal medicine *Withania somnifera*. In the current review, we have provided the important information and data of

various bioactive compounds of *Withania somnifera* such as Withanoside V, Withanone, Somniferine, and some other compounds, which can possibly help in the management and treatment of SARS-CoV-2 infection. *Withania somnifera* has proved its potential for maintaining immune homeostasis of the body, inflammation regulation, pro-inflammatory cytokines suppression, protection of multiple organs, anti-viral, anti-stress, and anti-hypertensive properties. Withanoside V has the potential to inhibit the main proteases (Mpro) of SARS-CoV-2. At present, synthetic adjuvant vaccines are used against COVID-19. Available information showed the antiviral activity in Withanoside V of *Withania somnifera*, which may explore as herbal medicine against to SARS-CoV-2 infection after standardization of parameters of drug development and formulation in near future.

KEYWORDS

SARS-CoV-2, ACE2 receptors, *Withania somnifera*, Ashwagandha, COVID-19, targeted therapy

1 Introduction

The infection of severe acute respiratory syndrome coronavirus 2 (SARS-CoV-2) has caused coronavirus disease 2019 (COVID-19). SARS-CoV-2 is a highly pathogenic virus that has spread very quickly throughout the globe. Many drugs and herbal compounds have been used for the management of this pandemic. Some important compounds of *Withania somnifera* may also have an antiviral activity, which may involve the management and treatment of SARS-CoV-2 infection. During the outbreak of COVID-19 in December 2019, Wuhan, the capital of the Hubei region and the most critical transportation center in China, witnessed harsh pneumonia-like symptoms. With its proximal origin on 31 December 2019, China informed the occurrence of an unknown disease to World Health Organization (WHO) and the Huanan seafood market was closed on 11 January 2020. The virus was recognized as a coronavirus on 7 January 2020, and it has more than 95% similarity with bat coronavirus and more than 70% homology related to SARS-CoV (World Health Organization, 2020). The first death was detected on 11 January 2020 after a daily rise in COVID-19 cases globally (Qin and Hernández, 2020).

Abbreviations: SARS-CoV-2, Severe acute respiratory syndrome coronavirus 2; CoV, Coronavirus; WHO, World Health Organization; RNA, Ribonucleic acid; ORF1, Open reading frame 1; ACE2, Angiotensin-converting enzyme 2; GI, Gastrointestinal; SARS, Severe acute respiratory syndrome; IFN, Interferon; IgG, Immunoglobulin G; JAK, Janus kinase; TMPRSS2, Transmembrane protease serine 2; CMK, Chloromethyl ketone; FDA, Food and Drug Administration; RdRp, RNA-dependent RNA polymerases; HIV, Human immunodeficiency virus; NK cell, Natural killer cell; PCNA, Proliferating cell nuclear antigen; GABA, Gamma-aminobutyric acid.

A huge wave of infection of Omicron variant of SARS-CoV-2 is experienced throughout the world. The world is experiencing a huge wave of infection with the Omicron variant of SARS-CoV-2. The report of Institute for Health Metrics and Evaluation (IHME) on 17 January 2022 showed that about 125 million cases of Omicron infections observed in a single day throughout the world, which is more than 10-fold of the peak of the wave of Delta variant in April 2021 (IHME, 2022; Murray, 2022). Although the cases of Omicron has increased with compared with previous SARS-CoV-2 variants, the world infection-detection rate has decreased worldwide from 20% to 5% (IHME, 2022).

SARS-CoV-2 has been spread from animals to humans and from humans to humans and may cause respiratory, neurological, enteric, and renal symptoms (Swelum et al., 2020). The SARS-CoV-2 has several important proteins that help the virus in attachment, replication, and multiplication in host cells. Various factors such as host receptor, age of patients, and viral proteins have been connected with the transmission of SARS-CoV-2 in humans. These factors play an essential role in the transmission, infection, and multiplication of viruses. Recent studies showed the critical role of these factors in the infection of SARS-CoV-2 in the human and intermediate host (Zhao et al., 2020; Jackson et al., 2022) (Figure 1).

2 Genome and crucial proteins of SARS-CoV-2

The coronaviruses are a diverse group of enveloped positive-strand RNA viruses. The virus CoV-2 contains single-stranded positive senses ~30-kb RNA genomes that encode approximately

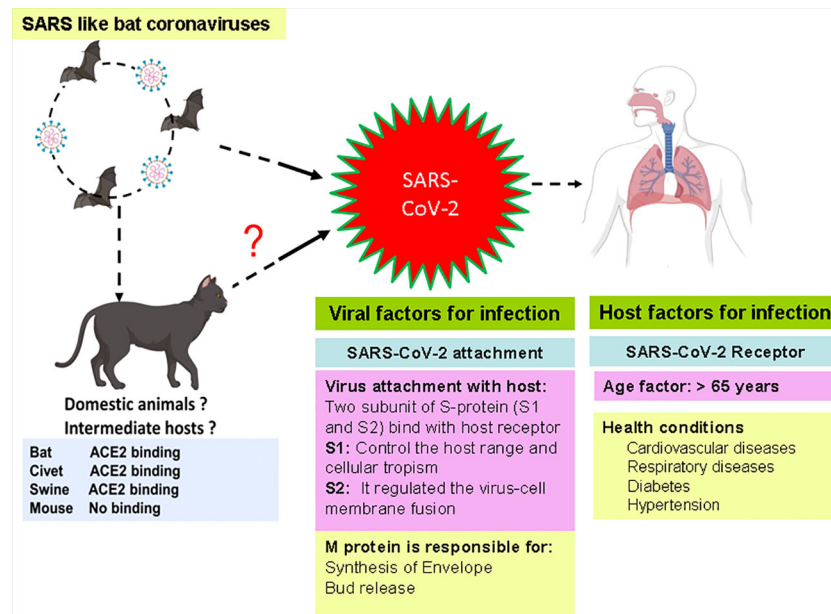


FIGURE 1
Factors connected with the infection of SARS-CoV-2 in human.

29 proteins. The 5'-end of the RNA is polyadenylated, whereas capping at the 3'-end increases the virus's life span. The CoV-2 virus contains 6–11 open reading frames (ORFs), which encoded polypeptides having 9,680 amino acids (Guo et al., 2020). The ORF-1 encodes 16 nonstructural proteins (nsps), which comprises about 67% of the genome. The remaining ORFs encode structural proteins and other accessory proteins of the virus. The SARS-CoV-2 genome lacks the hemagglutinin-esterase gene. Nevertheless, it contains two flanking untranslated regions (UTRs) of 265 and 358 nucleotides long at 5'-end and 3'-end, respectively. The nsps comprises two viral cysteine proteases [papain-like protease (nsp3) and chymotrypsin-like protease], 3C-like, or main protease (nsp5), helicase (nsp13), and RNA-dependent RNA polymerase (nsp12), which involved in the process of replication and transcription of SARS-CoV-2 (Gao et al., 2020).

Four variants—Alpha CoV, Beta CoV, Gamma CoV, and Delta CoV of CoV-2—have been identified due to high rate of mutation in RNA virus. Recently, a new variant, Omicron, is also discovered in many countries. The possible adaptive mutations in the genome of SARS-CoV-2 may responsible to made it more pathogenic and hard for the development of vaccine and drug (Xu et al., 2020). This virus can circulate to several hosts by the loosely attached receptor binding domain with the virus (Raj et al., 2013). The virus entered into host cells that moderated to the host receptors through spike glycoprotein S; it is a major target for neutralization antibodies. Studies showed that the

virus enters through the respiratory mucosa with the help of the receptor named ACE2 (angiotensin-converting enzyme 2) (Cheng and Shan, 2019; Balkrishna et al., 2020). S contains two functional subunits (S1 and S2 subunits) responsible for attaching the virus to the host cell receptor. According to structure, N- and C-terminal domains of the S1-fold are recommended as independent domains. Each of the N-terminal domains or the C-terminal domains can serve as a receptor-binding domain. CoV S protein is typically class 1 viral protein and proteases. The S protein of the virus is cleaved by the host proteases, and the subunits of the virus S protein remain present in a noncovalent form until the fusion of viral particle occurs. As a result, coronavirus entry into susceptible cells is a complicated process that needs the concerted action of receptor binding and proteolytic treating of the S protein to upgrade virus-cell fusion.

Cleavage is essential for the establishment of the fusion property of S protein. The availability of these proteases on target cells highly determines whether viruses enter the host cells through endocytosis or plasma membrane. Proteases remain evasive, which promotes the entry of the virus into host cells. The study showed that SARS-CoV encoded S protein with 23 N-linked glycosylation sites (Rota et al., 2003). It is predicted that these 12 N-linked glycosylation sites play an essential role in attaching viruses to host cell receptors (Krokhin et al., 2003). ACE2 works like a port for coronavirus entry, which invades our infected cells and replicates. It is mainly found in our lungs and

helps enter the virus into the host cells, but it also occurs in our GI tracts, heart, blood vessels, and muscles. The entry of SARS-CoV-2 triggers the infection in healthy cells and may accelerate the death rates. SARS-CoV-2 and another SARS-related coronavirus directly interact with ACE2 (Figure 2).

3 Mode of infection and multiplication of SARS-CoV-2

The lung is the main target of SARS-CoV-2 infection, where the virus penetrates the infecting cells of host through binding with ACE2 (Seth et al., 2020). Although infection of SARS-CoV-2 commences in the proximal part of airways, more severe and occasionally fatal symptoms of the disease appeared in the alveolar type 2 cells of the distal lung (Mulay et al., 2021). The study also showed other symptoms such as fever, cold, gastrointestinal (GI) problem, nausea, vomiting and diarrhea upon hospital admission (Li et al., 2020). SARS-CoV-2 enters the respiratory tract and starts replicating in the epithelial cells of enteric tracts. The binding of SARS-CoV-2 with ACE2 induces the conformational changes in the S1 protein subunit, which helps in the exposure of S2 subunit. Depending on the entrance route chosen by the SARS-CoV-2, the S2 subunit is cleaved by different proteases and helps in the penetration of host cell. Fusion of SARS-CoV-2 with cell membrane of host cell generates a fusion pore by which RNA of the virus is delivered into the cytoplasm of infecting host cell for replication and multiplication of virus. The mode of transmission and infection is illustrated in flow chart (Figure 3).

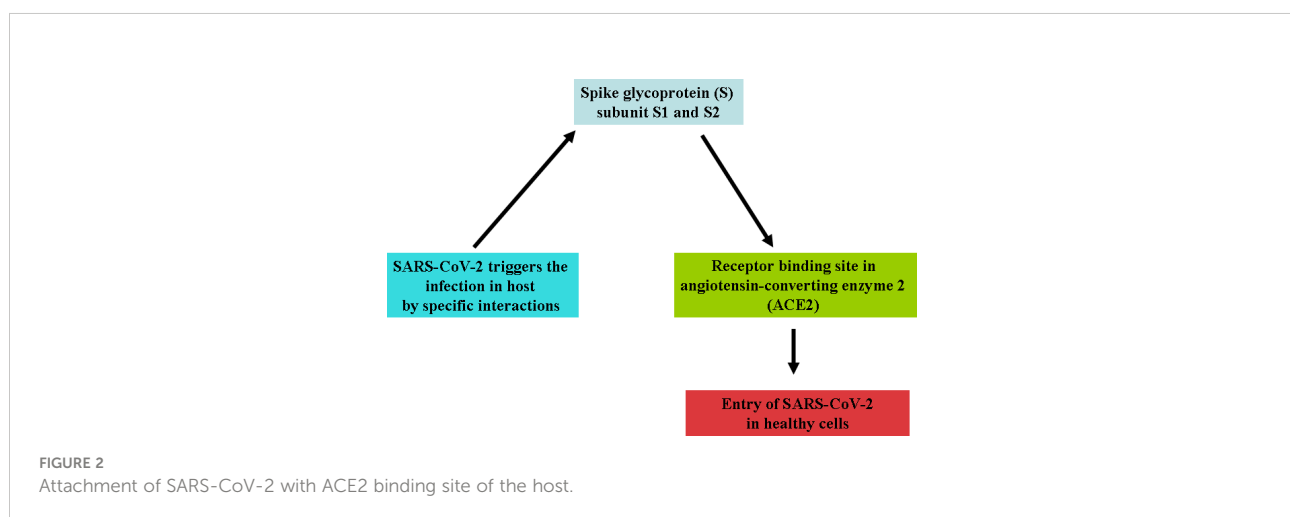
There is a specific attachment of SARS-CoV-2 with the receptor of the infected host cell. A cellular protein is expressed on the surface of cells of different organs, known as ACE2 receptors for the attachment of SARS-CoV-2 particles. SARS-CoV-2 has a spike protein that binds with a particular

receptor, facilitating the entry of the virus through fusion with membrane or ACE2 receptor. The virus genome is released in the cytoplasm of the host cell. The virus uses the host cell's ribosomes to translate essential proteins required for the multiplication of the virus. Then, the transcription and translation of different ORF1a/ORF1b and others ORF occur. The assembly and budding of mature virions occur during RNA replication and packaging. The virus particles are released from the infected cell by exocytosis and further infects to healthy cells (Figure 4).

4 Clinical symptoms and diagnosis of SARS-CoV-2

The major symptoms of SARS-CoV-2 infection are fever, cough, throat sore, slight dyspnoea, fatigueness, conjunctivitis, headache, and GI problems (Yang et al., 2020; Pascarella et al., 2020). Symptoms of the disease may help for the identification of SARS-CoV-2 infection from other respiratory viral infections, specifically in community and urgent care setting programs where rapid diagnosis of samples may be inadequate. The documentation of symptoms should be helpful and supportive for the detection of new cases. The Centers for Disease Control and Prevention (CDC) of the United States identified three main symptoms of SARS-CoV-2, which include cough, fever, and shortness of breath (CDC, 2020). The symptoms list was increased as the pandemic of COVID-19 progressed, which include shortness of breath, myalgias, chills, sore throat, headache, chest pain, ageusia (the loss of taste), anosmia (the loss of smell), diarrhea, delirium, abdominal pain, skipped meals, and hoarse voice (Menni et al., 2020).

The symptoms of infection may confirm by performing reliable diagnosis including real-time PCR (RT-PCR),



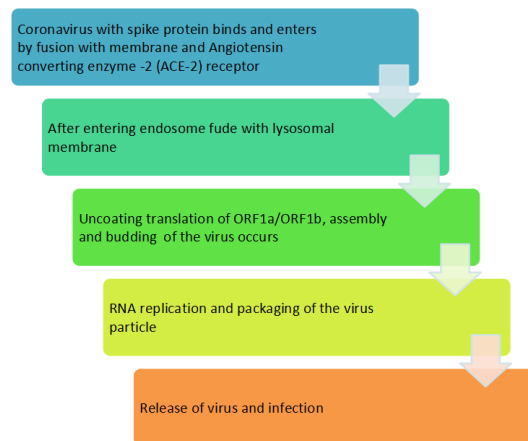


FIGURE 3
Schematic representation of transmission and infection of SARS-CoV-2 in the host cell.

computed tomography, and x-ray. Molecular diagnosis technique RT-PCR is implicated as a detection tool using samples of nasal swab, bronchoalveolar lavage or tracheal aspirate. Computed tomography and x-ray results are very imperative for both detection of SARC-CoV-2 infection and follow-up the disease (Pascarella et al., 2020). A study suggested that diagnostic reliability and accuracy may be enhanced by combining clinical symptoms with the result of CT and RT-PCR. Prior to final conclusion, specimens of upper and/or lower respiratory tract should be re-diagnosed in the patients of

negative RT-PCR report but has high suspicion or risk of infection (Lippi et al., 2020). This practice may minimize the possibility of error in diagnosis.

5 Strategies for the treatment of SARS-CoV-2

Various strategies have been implicated in the treatment and management of SARS-CoV-2 infection as follows.

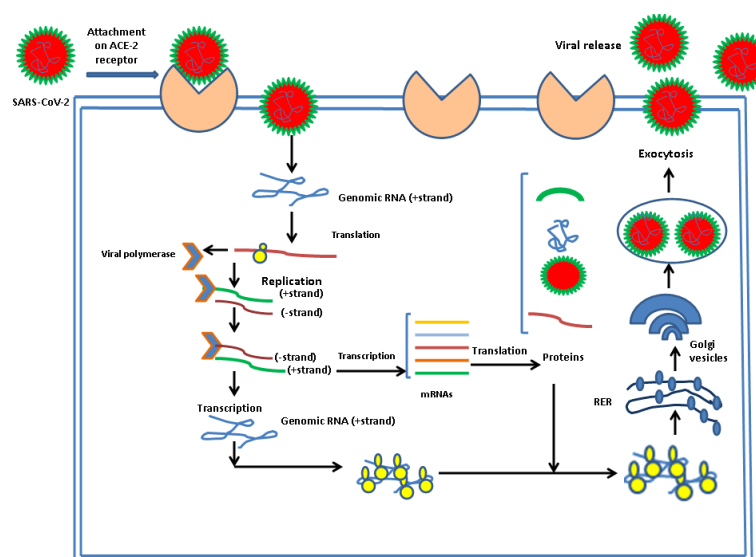


FIGURE 4
Entry, uncoating, and replication of SARS-CoV-2 in host.

5.1 Immunotherapeutic strategies to combat SARS-CoV-2

The four vital targets of SARS-CoV-2 include N protein surrounding the viral RNA, E protein covering the viral envelope, M protein emerging from the cell membrane, and S protein interacting with the ACE2 receptor on the host cell. The IgG antibodies can neutralize less vulnerable viruses' N and S protein and allow successful host immunity. These are also prospective targets for future vaccination approaches. The M and E proteins are frequently changed; hence, the potential of antibodies toward these proteins is not much more defensive during the infection of SARS-CoV-2. The cross-reactive antibody can provide a level of anti-SARS-CoV-2 protection that has developed during the treatment of measles and rubella viral infections through vaccination. Intravenous immunoglobulin and different antibodies that are neutral in convalescent serum may block the entry of the virus into the host cells and reduce the hyper-inflammation (Gold et al., 2020) (Figure 5).

Baricitinib, a known Janus kinase (JAK) as a hindrance permitted for medical care of rheumatoid arthritis, might obstruct ACE2-mediated endocytosis (Richardson et al., 2020). The second one JAK as a hindrance, ruxolitinib, would be examined in a clinical investigation to remedy COVID-19 end of this year. Another way is to provide an excessive mass of a solvable form of ACE2, potentially decreasing virus entry into target host cells. This concept is being examined with APNO1; APEIRON is developed by rejoining the form of ACE2. It was recently in a clinical test. S protein is targeted by the monoclonal antibodies that obstruct the virus entry or fusion with the receptor of host cells. Nafamostat mesylate (Wang et al.,

2020a) and camostat mesylate (Hoffman et al., 2020). The protease inhibitor camostat mesylate inhibits the entry of SARS-CoV-2 in lung cells. INO-4800 DNA vaccine showed 100% immunogenic potential with outstanding safety and tolerability for the treatment of SARS-CoV-2 infection (Tebas et al., 2021). Although no specific clinical trials are performed to examine the potential of drugs against COVID-19 at this time of writing the review article, this combination therapy might be efficient because nafamostat mesylate hampers intravascular coagulopathy, to directly target the entry of virus in epithelial cells of the host. The treatment of a patient with combinational therapy might be effective as it has the potential to prevent the access of virus into the respiratory part (Hoffman et al., 2020; Zhang et al., 2020). The inhibition of SMYD2 decreases the expression of TMPRSS2, which reduced the infection of SARS-CoV-2 by blocking the viral replication (Yu et al., 2022).

5.2 Inhibitors present in the host to prevent the spread of the virus

Our body reacts against the infection through various proteases like neutrophil elastase, mast cell tryptase, serine proteases, and others (Heutinck et al., 2010). The relation between the immune response and disease severity (immune-pathogenic reaction) led the idea to target proteases to control the threshold body's response. Neutrophil elastase found in bone marrow is known to affect the levels of growth factor-alpha and stimulates mucus secretion (Nakamura et al., 1992). TMPRSS2, HAT, TTSPs, TMPRSS11a, Cathepsin B/L, and Factor Xa are transmembrane proteins that initiate spike protein priming,

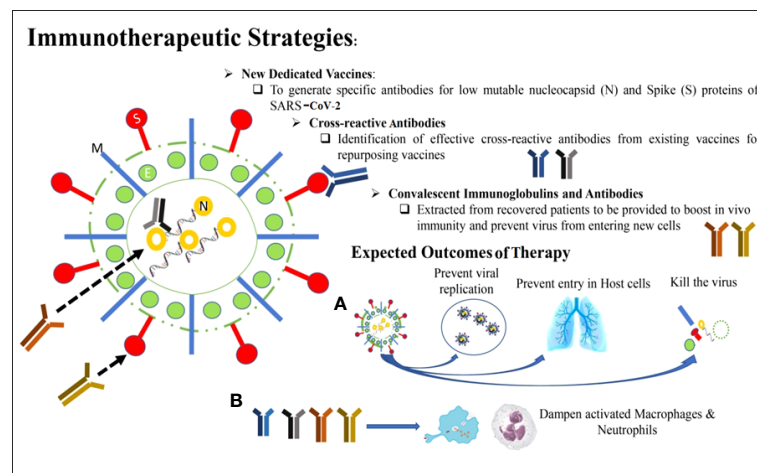


FIGURE 5

Immunotherapeutic strategies for the management and treatment of SARS-CoV-2.

leading to ACE2 receptor-dependent viral entry (Bertram et al., 2011; Seth et al., 2020). It has been found that expression of chymase and tryptase of mast cells are different in the pulmonary and gastrointestinal tract. Because of the absence of protease inhibitors in lungs, uncontrolled elevated expression of granzymes leads to degradation of extracellular matrix and induces the induction of pro-inflammatory cytokines (Pejler et al., 2007). There are other potential host proteases that inhibit the SARS-CoV-2 virus that has been mentioned in Table 1.

The virus enters the host and can be prohibited by protease inhibitors because SARS-CoV-2 enters the host cell either by serine protease TMPRSS2 at the cell surface or by cysteine protease cathepsin L in the endosome. Hence, a combination of cathepsin L and serine protease TMPRSS2 inhibitors is efficient for inhibiting viral entry inside the host cell. Total inhibition is achieved by a couple of camostat mesylate and Cathepsin B/L inhibitor E-64d (Hoffmann et al., 2020). SPINT2, another gene-encoded protease inhibitor, targets TMPRSS2 by restricting the cleavage activation and viral growth (Magnen et al., 2017; Reid et al., 2017). Recently, a unique discovery of a new furin-like cleavage site in SARS-CoV-2 and a new furin-like protease recognition is in progress. Till now, it has been decided that the enzymatic activity of furin protease might be restricted by adding a decanoyl group at the N terminus and chloromethyl ketone (CMK) group to the C terminus of a polybasic cleavage motif (dec-RVKR-cmk) (Coutard et al., 2020).

5.3 Drugs and compounds used to combat SARS-CoV-2 infection

During the pandemic, various phytochemicals and repurposing drugs have been identified to understand their efficacy against different modes of action of viruses including SARS-CoV-2. Therapeutic drugs such as arbidol, hydroxychloroquine, chloroquine, and lopinavir have shown *in vitro* anti-coronaviral properties by preventing multiple pathways in the virus life cycle (Devaux et al., 2020; Yao et al., 2020; Zhou et al., 2020; Rai et al., 2022). Some of the important therapeutic interventions of repurposing drugs against coronaviruses are mentioned as follows:

1. Baricitinib (JAK1 and JAK2 inhibitor): It is an anti-inflammatory molecule approved by the FDA to cure RA, blocking the cytokine signaling to inhibit JAK (Richardson et al., 2020). Apart from inhibition, they regulate the receptor-mediated endocytosis by binding with the cyclin G-assisted kinase (Stebbing et al., 2020; Favalli et al., 2020). These inhibitors are used to disrupt receptor-mediated endocytosis and prevent viral entry into the host cell. However, side effects of the COVID-19 infection may limit the application of the JAK inhibitors in the infected patients (Sunzini et al., 2020; Akbarzadeh-Khiavi et al., 2022).

TABLE 1 Potential host proteases that inhibit SARS-CoV-2 virus.

| Inhibitors | Location | Mechanism Involved | References |
|---------------------------------|---------------------|--|--|
| Neutrophil elastase | Bone marrow | Affects the levels of growth factor alpha and stimulates mucus secretion | Nakamura et al. (1992); Roghanian and Sallenne (2008) |
| TMPS2 | Transmembrane | Spike protein priming leading to ACE2 receptor-dependent viral entry. | Bertram et al. (2011); Seth et al. (2020) |
| HAT | Histone protein | | |
| TTSPs | Transmembrane | | |
| TMPS11a | Transmembrane | | |
| Cathepsin B/L | Endosome | | |
| Factor Xa | Liver | | |
| Chymase | Lining of intestine | Due to absence of protease inhibitors in lungs, uncontrolled elevated expression of granzymes lead to degradation of extracellular matrix and induce the induction of pro-inflammatory cytokines | Pejler et al. (2007) |
| Tryptase | Connective tissue | | |
| Kallikrein-related peptidase 13 | Chromosome | Involved in assisting human coronavirus entry by specific cleaving at S1/S2 site | Milewska et al. (2020) |
| KLK1 | Kidney, | Involved in cleavage of hemagglutinin, enhancing the viral production | Leu et al. (2015); Magnen et al. (2017) |
| KLK5 | pancreas | | |
| | Epidermis | | |
| Proteinase 3 | Neutrophils | Overexpression leads to uncontrolled degradation of extracellular matrix and inflammatory responses | Van der Geld et al. (2001) |
| Cathepsin C | Lysosome | Activation of several pro-inflammatory serine proteases | Méthot et al. (2007) |
| Granzymes A, B, H, K, and M | NK cells | Causative agent of NK cells, T cells | Morice et al. (2007); Zhu et al. (2009); Jahrsdorfer et al. (2010) |
| Cathepsin G | Neutrophils | | |

2. Remdesivir (nucleoside analog): Remdesivir is an analog of adenosine that inhibits the activity of viral RNA polymerase. It has two important targets including protease (Mpro) and RNA-dependent RNA polymerases (RdRp). It performed its action by interacting with RdRp through electrostatic force. On the other hand, it is interacted with protease Mpr by van der Waals interaction and formed Mpro-remdesivir complex. Thus, clinical trials show its efficacy against SARS-CoV-2 (Wang et al., 2020a; Elfiky, 2020). However, it shows hypersensitivity and infusion-related reactions. Remdesivir can cause elevated liver enzymes that can lead to liver injury (Thomas et al., 2020; Zampino et al., 2020).
3. Lopinavir/ritonavir and antiretrovirals (HIV protease inhibitor): An FDA-approved drug is useful against HIV; now, in the case of COVID-19, these are used for the hindrance of 3-chymotrypsin-like protease (Chu et al., 2004; de Wilde et al., 2014). They bind to the key enzyme, M^{pro}, to suppress coronavirus activity. Safety concerns: risk of cardiac arrhythmias, the possibility of bradycardia, and should be carefully used with patients with hepatic disease.
4. Ivermectin (antiparasitic): They inhibit the duplication of SARS-CoV-2 by restraining the intracellular transport process followed by the virus to suppress the host antiviral response to inhibit the host alpha/beta-1 nuclear transport proteins (Wulan et al., 2015; Caley et al., 2020). It is harmful to patients with hepatic disease or asthma.
5. Actinomycin D (antibiotic): They activate the p53 molecule degraded by the SARS-CoV-encoded papain-like protease (PLpro) and suppress the interferon signaling. Thus, they enhance the p53's expression by upregulating the interferon signaling/interferon production (Yuan et al., 2015; Krześniak et al., 2020).

5.3.1 Side effects of drugs

With the massive use of repurposed remedies to cure COVID-19, a new enigmatic concern of antimicrobial resistance prevails. The resistance to various tetracycline antibiotics occurs because of the tet and otr genes acquisition. The increased resistance in microbes due to the chromosomal mutations or long constant exposure to the drugs has generated several other dysfunctions in the host's body (Narendrakumar and Thomas, 2018; Narendrakumar et al., 2020; Singh et al., 2021). The central and peripheral nervous system gets affected by these drugs depending on the drug and its mode of action.

Protease inhibitors (Lopinavir, Ritonavir, and Darunavir) work against CYP450 by altering the blood plasma value of

various psychotropic drugs. Being inherently neurotoxic, they show perioral paresthesias (25%) and peripheral paresthesias (7%) with depressive symptoms after the first month of treatment (Abers et al., 2014).

Corticosteroids alter the immune system by modulating hyperinflammation. Memory deficits and cognitive impairment occur in up to 90% of the patients. Approximately 50% of the patients feel delirium and mood changes after having a light dose for three months. Apart from these, mania and hypomania are also being observed (Fardet et al., 2007).

A monoclonal antibody named Tocilizumab, when used with IL-6 receptor at the critical point of COVID-19, triggers enormous growth of pro-inflammatory cytokines, leading to a cytokine storm. The heterogeneity of IL-6 and IL-1 β increases the production of inflammatory cytokines (Mehta et al., 2020; WHO, 2020; Michot et al., 2020).

Patients treated with Bevacizumab head toward the vascular outburst that produces intrusion of inflammatory cells, due to which the already involved alveolar space becomes flooded with cells and other cytokines (Teuwen et al., 2020; Jacobi et al., 2020). The shoot of aerial levels of Vascular endothelial growth factor (VEGF) necessary for the vascular permeability causes serious issues [(USNLM, 2020) in serious patients with COVID-19 pneumonia].

The ACE2 effector drugs influence multiple vital organs through systemic inflammatory responses leading to disorders in the brain (encephalitis, necrotic hemorrhage, and epileptic seizures) (Carod Artal, 2020), disorders in the heart (cardiomyopathy and myocarditis) (Adão and Guzik, 2020), disorders in lungs (Varga et al., 2020), and disorders in the GI tract (Yang and Tu, 2020).

5.3.2 Other variants of SARS-CoV-2

On 14 April 2022, the U.S. government SARS-CoV-2 Interagency Group (SIG) downgraded Delta from a variant of concern (VOC) to a variant being monitored (VBM) [National Center for Immunization and Respiratory Diseases (NCIRD), Division of Viral Diseases, 2020]. This new classification was based on significant and sustained reductions in its national and regional proportions over time. Evidence suggests that Delta variant does not currently pose a significant risk to public health in the United States. The SIG variant classification scheme defines four classes of SARS-CoV-2 variants (Public Health England, 2020)

- I. Variant being monitored (VBM): This might include many variants of SARS-CoV-2, which were found to infect people in different countries and regions with severe transmission rates.
- II. Variant of interest (VOI): These are those variations that are anticipated to have an impact on the virus's ability to spread, the severity of the disease,

immunological escape, and diagnostic or therapeutic escape. In addition, these could significantly affect community transmission, increasing the risk to public health globally.

III. Variant of concern (VOC): These have been classified as the variants with a majority in epidemiological changes, causing the severe acute respiratory syndrome. These are known to be with increased virulence and lessen the effectiveness of the diagnostics and medical facilities. Some of them are listed as follows:

- a. Alpha (B.1.1.7 and Q lineages): This was the first time detected in the UK with a greater frequency of mutations. This variant has been found to spread faster at a very rapid rate of transmission (Bayarri-Olmos et al., 2021).
- b. Beta (B.1.351 and descendent lineages): This was for the first time detected in South Africa. This was the variant known to cause the second wave of the pandemic with higher transmission and severity levels (Roquebert et al., 2021). Later on, this variant spread to 23 states of the United States and 48 other countries. Its mutations were notable due to its enhanced ability to bind to ACE-3 receptor protein which brought serious concern internationally (Bayarri-Olmos et al., 2021).
- c. Gamma (P.1 and descendent lineages): SARS-CoV-2 lineage P.1 was first discovered in Brazil in November 2020. It comes from the lineage B.1.1.28. It has three problematic mutations—N501Y, E484K, and K417T—as well as 17 distinctive amino acid alterations, 10 of which are in the spike protein. With the same capacity to infect both adults and old persons, it demonstrated 2.2 times increased transmissibility. It was classified as a VOC by WHO on 11 January 2021. WHO gave it the name Gamma on 31 May 2021.
- d. Delta (B.1.617.2 and AY lineages): SARS-CoV-2 lineage B.1.617.2 was first discovered in India in October 2020. It was designated as a VOC on 11 May 2021, and, on 31 May 2021, it was given the name Delta. It carries the L452R, T478K, and P681R mutations and can spread approximately two times as quickly as the Alpha form. The “Delta plus” or “AY.1” variant is a further mutation of the extremely contagious Delta variant. Because of the newly added variant’s low occurrence in India, it is not yet a VOC.
- e. Epsilon (B.1.427 and B.1.429): SARS-CoV-2 of lineages B.1.427 and B.1.429 was first detected in the United States in March 2020. I4205V and D1183Y in the ORF1ab-gene, as well as S13I, W152C, and L452R in the spike protein’s S-gene, are two of the five unique mutations that characterize it. The WHO identified it as a VOI on 05 March 2021, and, on May 31, 2021, it was given the name Epsilon.
- f. Eta (B.1.525): In December 2020, reports of SARS-CoV-2 lineage B.1.525 were made in numerous nations. It is a variant under investigation according to Public Health England (VUI-21FEB-03). The E484K mutation and the novel F888L mutation set Eta apart from all previous forms. The WHO identified it as a VOI on 17 March 2021, and, on May 31, 2021, it was given the name Eta.
- g. Iota (B.1.526): In November 2020, the SARS-CoV-2 lineage B.1.526 was first discovered in the United States. Initial levels were rather high in some areas, but in the spring of 2021, the more transmissible Alpha version outcompeted it. The WHO identified it as a VOI on 24 March 2021, and, on May 31, 2021, it was given the name Iota.
- h. Kappa (B.1.617.1): SARS-CoV-2 lineage B.1.617.1 was first discovered in India in December 2020. Public Health England recognized it as a variant under investigation on 01 April 2021 (VUI-21APR-01). On 04 April 2021, WHO classified it as a VOI, and, on May 31, 2021, it was given the name Kappa.
- i. 1.617.3: A recently described SARS-CoV-2 variant under examination was first discovered in October 2020 in India and is also known as G/452R.V3 and is now designated by WHO with the Greek letters. Three sublineages identified as B.1.617.1 (), B.1.617.2 (), and B.1.617.3 as of May 2021 are being investigated for their potential effects on the ongoing epidemic. There are 13 amino acid alterations in this variation, three of which in the spike protein—E484Q, L452R, and P681R—are currently of considerable concern (Pascarella et al., 2021).
- j. Mu (B.1.621 and B.1.621.1): SARS-CoV-2 lineage B.1.621 was first detected in Colombia in January 2021. On 30 August 2021, the WHO classified it as a VOI and gave it the moniker Mu.
- k. Zeta (P.2): SARS-CoV-2 lineage P.2 was first discovered in Brazil in April 2020. The WHO identified it as a VOI on 17 March 2021, and, on May 31, 2021, it was given the name Zeta.
- l. Omicron (B.1.1.529, BA.1, BA.1.1, BA.2, BA.3, BA.4, and BA.5 lineages): In November 2021, South Africa received the first report of the B.1.1.529 lineage. On 26 November 2021, the WHO gave it the name Omicron and classified it as a VOC. According to reports, the Delta form of COVID-19, the earlier COVID-19 variation, is less deadly than the most recent SARS-CoV-2 variant. Omicron can spread swiftly, is infectious, and is not immune to the current vaccination.

IV. Variant of high consequence (VOHC): To date, no variants of high consequence have been identified in the United States.

5.4 Current status of vaccine and their issues

As of 08 April 2022, WHO has evaluated that the following vaccines against COVID-19 have met the necessary criteria for safety and efficacy: AstraZeneca/Oxford vaccine, Johnson and Johnson, Moderna, Pfizer/BioNTech, Sinopharm, Sinovac, COVAXIN, Covovax, Nuvaxovid, and CanSino. However, there were some adverse reactions reported in people due to prior allergies (Sumito et al., 2021). Although *Withania somnifera* cannot fully eradicate SARS-CoV-2, studies have shown that co-administration of Ashwagandha with the COVISHIELD™ vaccine enhanced the antibody titers, particularly after the first dose of the vaccine (Chopra et al., 2022).

6 Herbal medicine

Various herbal medicines have been used to treat and manage diseases, including microbial infections such as viral, bacterial, and fungal diseases. Extracts of the herbal plants have been found as broad-spectrum anti-coronaviral drugs shown with less or no side effects (Sharma et al., 2021). Wijayasinghe et al. have shown that most of the anti-coronaviral phytochemicals from different herbal plants are not only effective against viral proteases but also affected the other mechanisms such as viral protein synthesis, viral entry, and viral replication (Wijayasinghe et al., 2021). Therefore, to accomplish the strategy, *Withania somnifera* is one of the potential herbal medicines that can be used against various types of infections.

6.1 *Withania somnifera* works as a potent drug in combating COVID-19

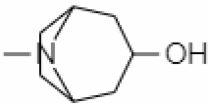
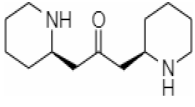
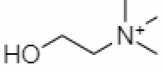
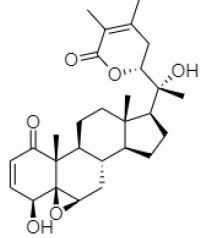
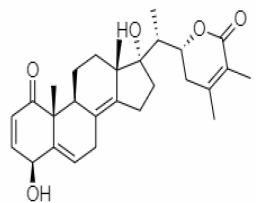
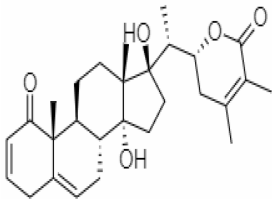
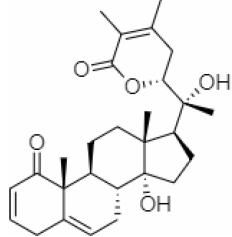
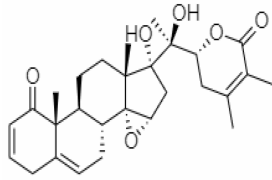
WHO's COVID-19 management techniques include infection prevention, detection of the cases, and supportive care. *Withania somnifera* belongs to the *Solanaceae* family that grows to 35–75 cm in the drier parts of India (Narinderpal et al., 2013). All aspects of this therapeutically important plant are used for treating osteoarthritis, gout, neurodegenerative diseases, and many more (Dar and MuzamilAhmad., 2020). The chemical constituents of the *Withania somnifera* genus include withanolides (class of naturally occurring C28 steroidal lactone triterpenoids along with, steroidal lactones, alkaloids, tropine,

and cuscohygrine) (Singh et al., 2016). The anti-inflammatory and analgesic attributes are supported by the inhibition property of cyclo-oxygenase-2 (Ryu et al., 2010).

Withanolides contribute to the pharmacological benefits of *Withania somnifera*. A bioactive steroidal lactone withaferin A reduces the secretion of various pro-inflammatory cytokines, for example, TNF α , IL-6, IL-8, and IL-18 (Straughn and Kakar, 2019), whereas withanone blocks the SARS-CoV entries by lowering the electrostatic component of ACE2-RBD complex (Mi-Sun et al., 2008), and it hinders the ventures and regulation of cell surface receptor protein TMPRSS2 and viral replicative protease M^{Pro} (Dhanjal et al., 2021; Markus et al., 2020). *In silico* studies represent that *Withania somnifera* can repress the replication of the COVID-19 virus through its capability to adjust T-cell separation NK-cell cytotoxicity (Maurya and Sharma, 2020). Several withanolides cause downregulation of viral envelope (E-gene) expression and nucleoplasmic sequences (N-gene). The organ preservative outcomes of *Withania somnifera* are used to reduce systemic inflammation, which protects the severity of inflammation-induced organ damage. Apart from these anti-viral actions, the Ministry of AYUSH has also confirmed the role of *Withania somnifera* for the maintenance of mental health, which may very helpful for the management and treatment of COVID-19 (Chopra et al., 2021).


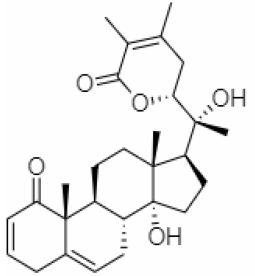
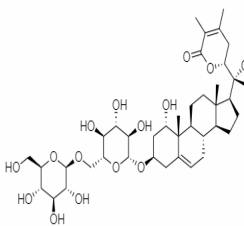
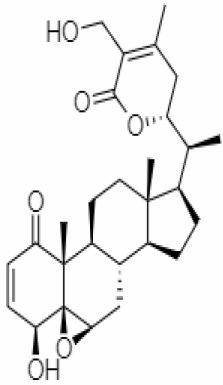
Withania somnifera has showed many benefits such as 1) maintaining the immune balance of the body, 2) regulation of the inflammation, 3) suppression of pro-inflammatory cytokines, 4) protection of multiple organs, and 5) anti-viral, anti-stress, and anti-hypertensive properties. The plant's phytochemicals, in combination with drugs or other clinical treatments, can be used in therapeutic purpose including management of infection of the SARS-CoV-2. Several docking and simulation (under clinical trial) experiments have removed the dust from the idea of obstructing the translation of viral protein. Some of the important bioactive metabolites extracted from *Withania somnifera* could be promising in combating SARS-CoV-2 (Trivedi and Choudhrey 2011). *In silico* studies revealed that the methanolic extract of *Withania somnifera* containing Anaferine, Cuscohygrine, and Hygrine has been found to that bind at the specified binding site for the agonists of $\alpha 7$ nAChR, thus avoiding dysregulation of the NCS (Nicotinic Cholinergic System) and moderating the symptoms and clinical manifestations of COVID-19 (Cardenas et al., 2012). Whereas Tropine, Choline, Withanolide D, and Withanisomniferol C were found to Inhibit PLpro and 3CLpro and bind to spike (S) protein (Chatterjee et al., 2010; Tomar et al., 2019). Mesoanaferine, Withanolide O, Withanolide P, Withanolide G, Withanolide F, Withanoside IV, Withanolide D, β -sitosterol, and Somniwithanolide have shown to inhibit main protease (M^{Pro}) of SARS-CoV-2. Apart from these, there are other several potent compounds that may be effective against the infection of SARS-CoV-2, which are also mentioned in Table 2.

TABLE 2 Important bioactive metabolites extracted from *Withania somnifera* may be used for the management of COVID-19.

| S.No. | Phytochemicals | Pubchem Id | Binding energy (kcal/mol) | Molecular weight (g/mol) | Part of Plant used | Structure of Phytochemical | Nature | References |
|-------|----------------|------------|---------------------------|--------------------------|--------------------|--|------------|---|
| 1. | Tropine | 449293 | -2.54 | 141.21 | Leaves |  | Methanolic | Chatterjee et al. (2010); Tomar et al. (2019) |
| 2. | Mesoanferine | 443143 | -3.42 | 224.34 | Leaves |  | Methanolic | Cardenas et al. (2012); Kumar and Singh (2020) |
| 3. | Choline | 305 | | 104.17 | Leaves |  | Methanolic | Ahlawat et al. (2017) |
| 4. | Withanolide D | 23266147 | -8.9 | 470.6 | Leaves |  | Methanolic | Ben Bakrim et al., 2018 |
| 5. | Withanolide O | 23266146 | -7.8 | 454.6 | Leaves |  | Methanolic | Khanal et al. (2020) |
| 6. | Withanolide P | 21679034 | -7.7 | 468.6 | Leaves |  | Methanolic | Khanal et al. (2020) |
| 7. | Withanolide G | 21679023 | -9.00 | 470.6 | Leaves |  | Alcoholic | Mousavi et al. (2021) |
| 8. | Withanolide M | 25090669 | -9.1 | 652.8 | Leaves |  | Alcoholic | Khanal et al. (2020) |

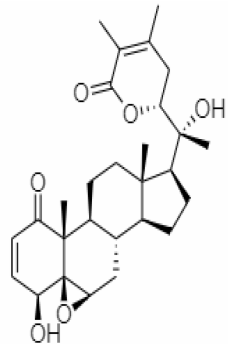
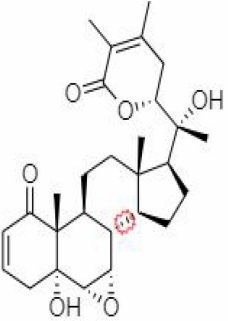
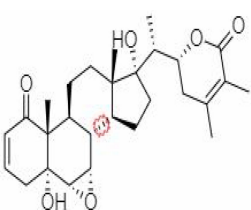
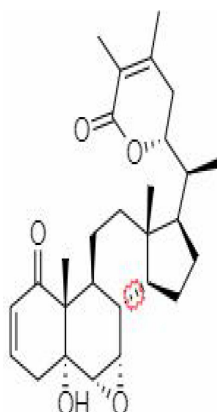
(Continued)

TABLE 2 Continued

| S.No. | Phytochemicals | Pubchem Id | Binding energy (kcal/mol) | Molecular weight (g/mol) | Part of Plant used | Structure of Phytochemical | Nature | References |
|-------|----------------|------------|---------------------------|--------------------------|--------------------|--|------------|---|
| 9. | Withanolide F | 44562999 | -7.8 | 488.6 | Leaves |  | Alcoholic | Khanal et al. (2020) |
| 10. | Withanoside IV | 71312551 | -11.02 | 782.9 | Leaves |  | Butanol | Ali et al. (2022) |
| 11. | Withanoside VI | 91827019 | 8.083 | 782.9 | Leaves |  | Methanolic | Patel et al. (2021) |
| 12. | Withaferin A | 265237 | -2.85 | 470.6 | Leaves and Roots |  | Methanolic | Balkrishna et al. (2020); Kumar and Singh (2020); Mohan et al. (2016); Kumar et al. (2022); Pandit and Latha (2020) |

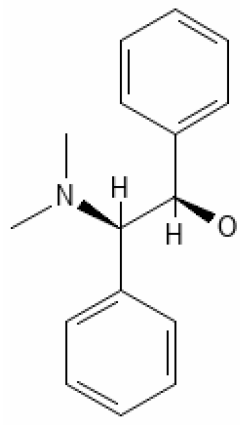
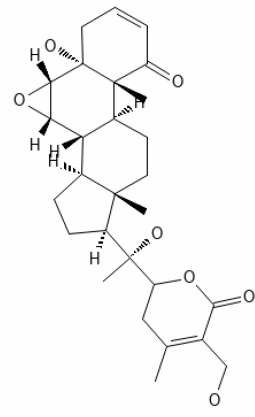
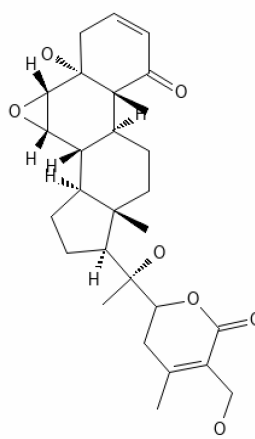
(Continued)

TABLE 2 Continued

| S.No. | Phytochemicals | Pubchem Id | Binding energy (kcal/mol) | Molecular weight (g/mol) | Part of Plant used | Structure of Phytochemical | Nature | References |
|-------|--------------------------|------------|---------------------------|--------------------------|--------------------|--|------------|---|
| 13. | Withanolide D | 118701104 | -5.55 | 470.6 | Leaves and Roots |  | Methanolic | Khanal et al. (2020) |
| 14. | Withanolide A | 11294368 | -5.26 | 470.6 | Leaves and Roots |  | Methanolic | Kour et al. (2009); Soman et al. (2013); Pandit and Latha (2020) |
| 15. | Withanone | 21679027 | -6.14 | 470.6 | Leaves and Roots |  | Methanolic | Wadegaonkar and Wadegaonkar (2013); Dar et al. (2017); Kumar and Singh (2020); Balkrishna et al. (2020) |
| 16. | 27-hydroxy withanolide B | 14236711 | -5.23 | 454.6 | Leaves and Roots |  | Methanolic | Turrini et al. (2016); Balkrishna et al. (2021) |

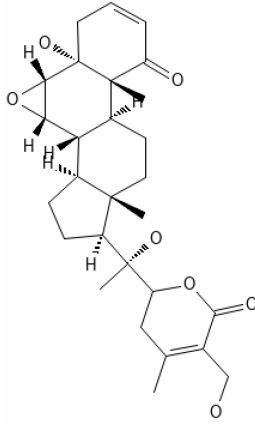
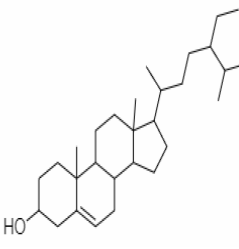
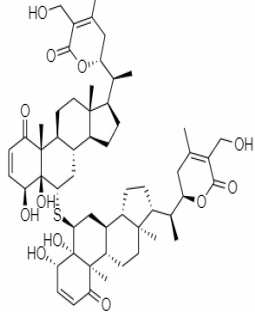
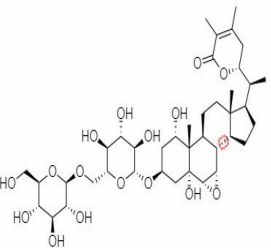
(Continued)

TABLE 2 Continued

| S.No. | Phytochemicals | Pubchem Id | Binding energy (kcal/mol) | Molecular weight (g/mol) | Part of Plant used | Structure of Phytochemical | Nature | References |
|-------|-------------------|------------|---------------------------|--------------------------|--------------------|--|------------|--|
| 17. | Pseudowithanine | 10955717 | -3.34 | 241.33 | Leaves and Roots |  | Methanolic | Turrini et al. (2016); Balkrishna et al. (2021) |
| 18. | Withasomniferol A | 101710595 | -3.35 | 486.6 | Leaves and Roots |  | Methanolic | Singh et al. (2020) |
| 19. | Withasomniferol B | 101710596 | -4.22 | 472.6 | Leaves and Roots |  | Methanolic | Singh et al. (2020) |

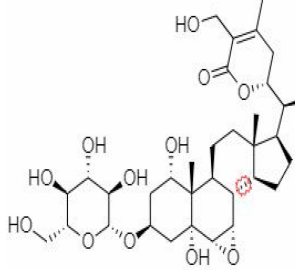
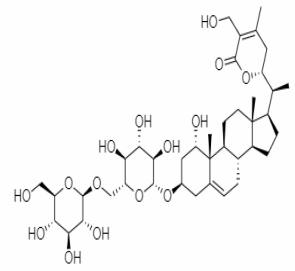
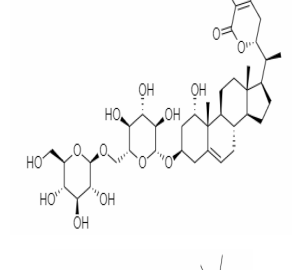
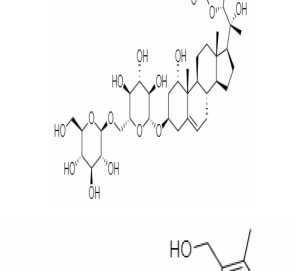
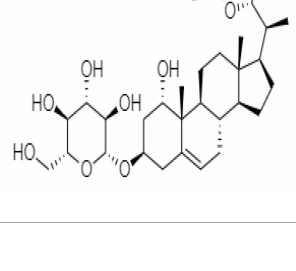
(Continued)

TABLE 2 Continued

| S.No. | Phytochemicals | Pubchem Id | Binding energy (kcal/mol) | Molecular weight (g/mol) | Part of Plant used | Structure of Phytochemical | Nature | References |
|-------|---------------------|------------|---------------------------|--------------------------|--------------------|--|------------|---|
| 20. | Withasomniferol C | 101710597 | -4.88 | 470.6 | Leaves and Roots |  | Methanolic | Kandagalla et al. (2022) |
| 21. | β -sitosterol | 348285530 | -5.44 | 414.71 | Leaves and Roots |  | Methanolic | Kandagalla et al. (2022) |
| 22. | Withanolide | 53477765 | -5.26 | 470.6 | Leaves and Roots |  | Methanolic | Kalra and Kandimalla (2021) |
| 23. | Withanosides II | 101168811 | -11.30 | 798.9 | Leaves and Roots |  | Methanolic | Kalra and Kandimalla (2021) |

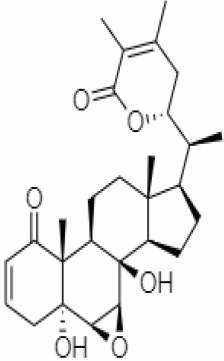
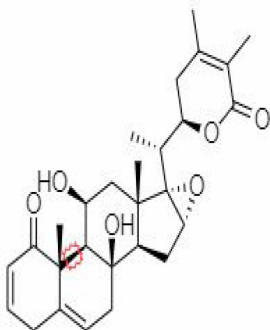
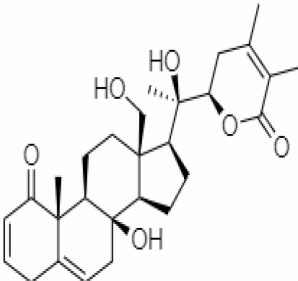
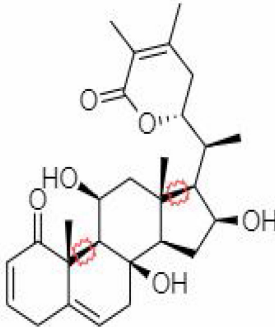
(Continued)

TABLE 2 Continued

| S.No. | Phytochemicals | Pubchem Id | Binding energy (kcal/mol) | Molecular weight (g/mol) | Part of Plant used | Structure of Phytochemical | Nature | References |
|-------|------------------|------------|---------------------------|--------------------------|--------------------|--|------------|--|
| 24. | Withanosides III | 101168810 | | 652.8 | Leaves and Roots |  | Methanolic | Ali et al. (1997); Jayaprakasam et al. (2004); Kalra and Kandimalla (2021) |
| 25. | Withanosides IV | 71312551 | -11.02 | 782.9 | Leaves and Roots |  | Methanolic | Kalra and Kandimalla (2021) |
| 26. | Withanosides V | 10700345 | -8.96 | 766.9 | Leaves and Roots |  | Methanolic | Kalra and Kandimalla (2021) |
| 27. | Withanosides VI | 91827019 | | 782.9 | Leaves and Roots |  | Methanolic | Kalra and Kandimalla (2021) |
| 28. | Physagulin D | 10100412 | -4.48 | 620.8 | Leaves and Roots |  | Methanolic | Kumar and Singh (2020) |

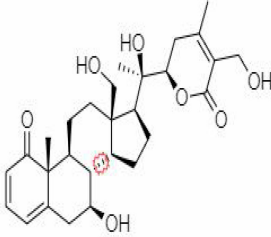
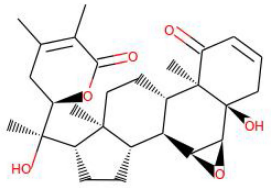
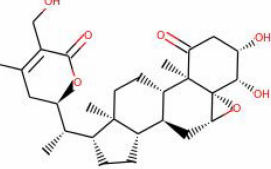
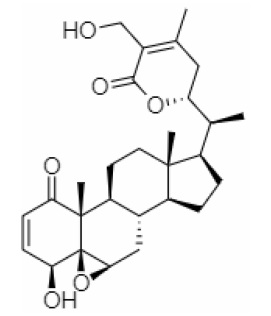
(Continued)

TABLE 2 Continued

| S.No. | Phytochemicals | Pubchem Id | Binding energy (kcal/mol) | Molecular weight (g/mol) | Part of Plant used | Structure of Phytochemical | Nature | References |
|-------|----------------------|---------------------------|---------------------------|--------------------------|--------------------|--|------------|--|
| 29. | Withasomnilide | 102066413 | -4.98 | 470.6 | Stem Bark |  | Ethanolic | Tong et al. (2011) |
| 30. | Somniferanolide | 102066415 | -7.89 | 468.6 | Stem Bark |  | Methanolic | Hasan et al, 2022; Ali et al, 1997 |
| 31. | Somniferine | 14106343 | 9.62 | 608.7 | Stem Bark |  | Methanolic | Hasan et al, 2022; Ali et al, 1997 |
| 32. | Withasomniferanolide | 102066414 | -3.53 | 470.6 | Stem Bark |  | Methanolic | Kalra and Kandimalla (2021) |

(Continued)

TABLE 2 Continued

| S.No. | Phytochemicals | Pubchem Id | Binding energy (kcal/mol) | Molecular weight (g/mol) | Part of Plant used | Structure of Phytochemical | Nature | References |
|-------|---|------------|---------------------------|--------------------------|--------------------|--|------------|--|
| 33. | Somniwithanolide | 102066417 | -5.42 | 486.6 | Stem Bark |  | Methanolic | Prajapati et al. (2022) |
| 34. | Withanolide | 9469353 | -5.81 | 370.4 | Whole plant |  | Methanolic | Kirson et al. (1971); Kirson et al. (1971); Matsuda et al. (2001); Jayaprakasam and Nair (2003); Choudhary et al. (2010) |
| 35. | Viscosalactone B | 57403080 | -11.1 | 488.6 | Whole plant |  | Methanolic | Borse et al., 2020 |
| 36. | 27-acetoxy -4β,6α - dihydroxy -5β-chloro -1-oxowitha -2,24- dienolide | 21044792 | -3.30 | 523.34 | Aerial parts |  | Methanolic | Kuboyama et al. (2006); Tong et al. (2011); Seth et al. (2020) |

7 Possible roles of *Withania somnifera* as immune homeostasis/therapeutics in the management of COVID-19

During the viral infection such as SARS-CoV-2, it has been seen that the secretions of inflammatory molecules at higher risk with elevated levels of (macrophages and neutrophils accompanied by lower levels of T cells and B cells) (Sadanandam et al., 2020). In this approach, a multicentric clinical investigation has been set up by the Ministry of AYUSH, Government of India to mitigate the deleterious effect of inflammatory cytokines in the management of COVID-19. Several studies have shown that administration of *Withania somnifera* solutions enhanced the immune system with the proliferation of immune response such as activation of T cells and

B cells, platelets, and NK cells accompanied by maintaining the Th1/Th2 response in different immunocompromised/infected animal models (Kushwaha et al., 2012a; Sun, 2019). In addition to that, administration of extracts of Withaferin A and *Withania somnifera* have suppressed the inflammatory cytokines such as IL-1β, IL-6, and TNF-α and modulated many inflammatory pathways including NLRP3 inflammasome, NF-κB pathway, and infection-induced TLR4 expression in macrophages through chaperone activity of peroxiredoxins as interventions of inflammatory response in different studies models (Noh et al., 2016; Khan et al., 2018; Wang et al., 2020b; Balkrishna et al., 2020; Aziz et al., 2020). Thus, *Withania somnifera* will be the potential herbal medicine to enhance immune system as a modulator of high-risk inflammatory response of COVID-19 infection (Parwe et al., 2020; Varma et al., 2020).

On the other hand, it has been demonstrated that systemic inflammatory response along with the COVID-19 infection

resulted in multi-organ failure due to the releasing of inflammatory mediators in the blood of several organ and this amplify the complication of the affected organs. In this regard, *Withania somnifera* has emerged as a potential candidate to protect organs against the side effects caused due to the inflammatory reactions of COVID-19. Several studies have reported that the extracts of *Withania somnifera* containing Withanolide A show neuroprotective candidate against hypoxia-induced and promote cerebral ischemia-induced apoptosis for curing the neurological disorders (Kuboyama et al., 2005; Mukherjee et al., 2020). Likewise, extracts of *Withania somnifera* have shown wonderful response in maintaining elevated levels of cardiac troponin I and IL-6 in the cardiomyopathy condition during the infection (Adão and Guzik, 2020; Ingawale et al., 2020). They have also shown the modulator of proliferating cell nuclear antigen (PCNA) by regulating the NF- κ B transcription factor against the pulmonary inflammation (Kaur et al., 2015b). In addition, extracts of *Withania somnifera* were found to restore the antioxidant enzyme expression in GI, kidney cells, and pancreas and to reduce the serum levels of urea and creatinine in kidney and muscles during the viral infections in the different study models. Withaferin A from *Withania somnifera* protects the cytotoxicity effect of bromobenzene in the liver and kidney cells (Jeyanthi and Subramanian, 2010; Vedi and Sabina, 2016; Tiruveedi et al., 2018). Thus, it can be proposed that extract of *Withania somnifera* can be the potential drug against the biological consequences of infections and inflammation and also decelerate the side effects in COVID-19 patients. The current therapeutic approaches in the management of COVID-19 are the use of several repurposing drugs such as chloroquine, azithromycin, remdesivir, and hydroxychloroquine. However, the beneficial effects of all the drugs in the therapy of COVID-19 are still inconclusive (Ferner et al., 2020). Several reports have shown that use of such repurposing drug might accelerate the conditions of heart and respiratory failure in the patients of COVID-19 (Lane et al., 2020). In such condition, *Withania somnifera* is acting as a miracle drug for cardiorespiratory protection and enhances the antibody titer in the immunocompromised model and thus acts as a synergistic effects in the management of COVID-19 (Davis and Kuttan, 2000; Davis and Kuttan, 2002). To circumvent the pandemic of COVID-19, there is an urgent need for effective vaccine and the efficacy of the vaccine can be enhanced by the co-formulation of the mixture of vaccine and herbal immunostimulants such as the extract of *Withania somnifera*, and this formula will lead to an additive adjuvant to boost vaccine immunogenicity. In this aspect, extract of *Withania somnifera* has been shown to recruit more NK cells against influenza infection, which led to the elimination of toxic cells in the infected model (Davis and Kuttan, 2002). All these previously beneficial effects of *Withania somnifera* prove that it will be the leading candidate to explore the vaccine development in the management of COVID-19.

8 Conclusion

We have tried to update the current knowledge and information of SARS-CoV-2 infection, mode of transmission, clinical symptoms diagnosis, and possible treatments through different approaches. With the era of different harmful after-effects from re-purposed drugs, we are now moving forward to find the herbal cure for the SARS-CoV-2 virus disease using traditional knowledge systems along with modern medicine. With this reference, the first choice may be *Withania somnifera* cocktail with other herbal medicines for better efficiency. We explored the various bioactive compounds of *Withania somnifera*, which have the potential to inhibit the interaction between RBD of SARS-CoV-2 S-protein and ACE2 receptor. Because the interaction of RBD of SARS-CoV-2 S-protein and ACE2 receptor is very important for the entry of virus into the host cells during infection, thus bioactive compound of *Withania somnifera* such as withanone and withaferin-A may be implicated for the management and treatment of COVID-19 (CMP, 2020). However, advanced research is required to understand molecular mechanism of bioactive compounds of *Withania somnifera* for improvement in clinical outcome of patients with COVID-19 (CMP, 2020). A deeper multidimensional understanding of *Withania somnifera*'s biological mechanisms will be an encouraging field for future research.

Author contributions

Conceptualization: MS, KJ, and DS; methodology: SB, MA, FK, and NKP; validation: AC, MA, AS, and MS; formal analysis: SB, and NKP; investigation: AC, FK, MA, AS, and data curation, FK, SK, MS, SB, and MA; writing—original draft preparation: MS, DS, and SK; writing—review and editing: DL, MA, SUDK, and SB; visualization: AS, AC, MA, and NKP; supervision: SK and DL; project administration: MA. All authors contributed to the article and approved the submitted version.

Funding

This work was supported by the Sichuan Science and Technology Program (No. 2021YFH0093) and the China Postdoctoral Science Foundation (No. 2020M673187).

Conflict of interest

The authors declare that the research was conducted in the absence of any commercial or financial relationships that could be construed as a potential conflict of interest.

Publisher's note

All claims expressed in this article are solely those of the authors and do not necessarily represent those of their affiliated

organizations, or those of the publisher, the editors and the reviewers. Any product that may be evaluated in this article, or claim that may be made by its manufacturer, is not guaranteed or endorsed by the publisher.

References

- Abers, M. S., Shandera, W. X., and Kass, J. S. (2014). Neurological and psychiatric adverse effects of antiretroviral drugs. *CNS Drug* 28 (2), 131–145. doi: 10.1007/s40263-013-0132-4
- Adão, R., and Guzik, T. (2020). Inside the heart of COVID-19. *Cardiovasc. Res.* 116, 1–3. doi: 10.1093/cvr/cvaa086
- Ahlawat, S., Saxena, P., Ali, A., Khan, S., and Abidin, M. Z. (2017). Comparative study of withanolide production and the related transcriptional responses of biosynthetic genes in fungi elicited cell suspension culture of withania somnifera in shake flask and bioreactor. *Plant Physiol. Biochem.* 114, 19–28. doi: 10.1016/j.plaphy.2017.02.013
- Akbarzadeh-Khiavi, M., Torabi, M., and Rahbarnia, L. (2022). Baricitinib combination therapy: a narrative review of repurposed Janus kinase inhibitor against severe SARS-CoV-2 infection. *Infection*. 50, 295–308. doi: 10.1007/s15010-021-01730-6
- Ali, A. A. M., Bugarcic, A., Naumovski, N., and Ghildyal, R. (2022). Ayurvedic formulations: Potential COVID-19 therapeutics? *Phytomed. Plus*, 2(3), 100286. doi: 10.1016/j.phyplu.2022.100286
- Ali, M., Shuaib, M., and Ansari, S. H. (1997). Withanolides from the stem bark of withania somnifera somnifera. *Phytochem* 44, 1163–1168. doi: 10.1016/S0031-9422(96)00656-5
- Aziz, M., Fatima, R., and Assaly, R. (2020). Elevated interleukin-6 and severe COVID-19: a meta-analysis. *J. Med. Virol.* 92 (11), 2283–2285. doi: 10.1002/jmv.25948
- Balkrishna, A., Nain, P., Chauhan, A., Sharma, N., Gupta, A., Ranjan, R., et al. (2020). Super critical fluid extracted fatty acids from withania somnifera seeds repair psoriasis-like skin lesions and attenuate pro-inflammatory cytokines (TNF- α and IL-6) release. *Biomolecules* 10 (2), 185. doi: 10.3390/biom10020185
- Balkrishna, A., Pokhrel, S., Singh, H., Joshi, M., Mulay, V. P., Haldar, S., et al. (2021). Withanone from withania somnifera attenuates SARS-CoV-2 RBD and host ACE2 interactions to rescue spike protein induced pathologies in humanized zebrafish model. *Drug Design Dev. Ther.* 15, 1111. doi: 10.2147/DDDT.S292805
- Balkrishna, A., Pokhrel, S., Singh, J., and Varshney, A. (2020). Withanone from withania somnifera may inhibit novel coronavirus (COVID-19) entry by disrupting interactions between viral s-protein receptor binding domain and host ACE2 receptor. *Virol. J.* doi: 10.21203/rs.3.rs-17806/v1
- Bayarri-Olmos, R., Johnsen, L. B., Idorn, M., Reinert, L. S., Rosbjerg, A., Vang, S., et al. (2021). The alpha/B.1.1.7 SARS-CoV-2 variant exhibits significantly higher affinity for ACE-2 and requires lower inoculation doses to cause disease in K18-hACE2 mice. *Elife* 10, e70002. doi: 10.7554/eLife.70002
- Ben Bakrim, W., El Bouzidi, L., Nuzillard, J. M., Cretton, S., Saraux, N., Monteillier, A., et al. (2018). Bioactive metabolites from the leaves of withania adpressa. *Pharm. Biol.* 56 (1), 505–510. doi: 10.1080/13880209.2018.1499781
- Bertram, S., Glowacka, I., Müller, M. A., Lavender, H., Gnirss, K., Nehlmeier, I., et al. (2011). Cleavage and activation of the severe acute respiratory syndrome coronavirus spike protein by human airway trypsin-like protease. *J. Virol.* 85, 13363–13372. doi: 10.1128/JVI.05300-11
- Borse, S., Joshi, M., Saggam, A., Bhat, V., Walia, S., Marathe, A., et al. (2020). Ayurveda botanicals in COVID-19 management: An in silico multi-target approach. *PLoS One* 16 (6), e0248479. doi: 10.21203/rs.3.rs-30361/v1
- Caly, L., Druce, J. D., Catton, M. G., Jans, D. A., and Wagstaff, K. M. (2020). A-approved drug ivermectin inhibits the replication of SARS-CoV-2 *in vitro*. *Antiviral Res.* 3, 104787. doi: 10.1016/j.antiviral.2020.104787
- Cardenas, J., Esquivel, B., Gupta, M., Rray, A. B., and Rodriguez-Hahn, L. (2012). *Fortschritte der chemie organischer Naturstoffe/Progress in the chemistry of organic natural products (Vol. 63)* (Wien New York: Springer Science & Business Media).
- Carod Artal, F. J. (2020). Complicaciones neurológicas por coronavirus y COVID-19. *Rev Neurol* 70 (9), 311–322. doi: 10.33588/rn.7009.2020179
- Centers for Disease Control and Prevention (CDC) US (2020) *Symptoms of coronavirus*. Available at: <https://www.cdc.gov/coronavirus/2019-ncov/symptoms-testing/symptoms.html>.
- Chatterjee, S., Srivastava, S., Khalid, A., Singh, N., Sangwan, R. S., Sidhu, O. P., et al. (2010). Comprehensive metabolic fingerprinting of withania somnifera somnifera leaf and root extracts. *Phytochemistry* 71 (10), 1085–1094. doi: 10.1016/j.phytochem.2010.04.001
- Cheng, Z. J., and Shan, J. (2019). Novel coronavirus: where we are and what we know. *Infection* 2020, 1–9. doi: 10.1007/s15010-020-01401-y
- Chopra, A., Chavan-Gautam, P., Tillu, G., Saluja, M., Borse, S., Sarmukaddam, S., et al. (2022). Randomized, double blind, placebo controlled, clinical trial to study ashwagandha administration in participants vaccinated against COVID-19 on safety, immunogenicity, and protection with COVID-19 vaccine—a study protocol. *Front. Med.* 9. doi: 10.3389/fmed.2022.761655
- Chopra, A., Srikanth, N., Patwardhan, B., AYUSH CCRAS Research Group (2021). Withania somnifera as a safer option to hydroxychloroquine in the chemoprophylaxis of COVID-19: Results of interim analysis. *Complement Ther. Med.* 102768. doi: 10.1016/j.ctim.2021.102768
- Choudhary, M. I., Hussain, S., Yousuf, S., Dar, A., Mudassar, and Atta-ur-Rahman, (2010). Chlorinated and diepoxy withanolides from withania somnifera somnifera and their cytotoxic effects against human lung cancer cell line. *Phytochemistry* 71 (17–18), 2205–2209. doi: 10.1016/j.phytochem.2010.08.019
- Chu, C. M., Cheng, V. C., Hung, I. F., et al. (2004). HKU/UCH SARS study group. role of lopinavir/ritonavir in the treatment of SARS: Initial virological and clinical findings. *Thorax* 59 (3), 252–256. doi: 10.1136/thorax.2003.012658
- CMP. (2020). *Clinical management protocol: COVID-19*. Available at: <https://www.mohfw.gov.in/pdf/ClinicalManagementProtocolforCOVID19.pdf>
- Coutard, B., Valle, C., de Lamballerie, X., Canard, B., Seidah, N. G., and Decroly, E. (2020). The spike glycoprotein of the new coronavirus 2019-nCoV contains a furin-like cleavage site absent in CoV of the same clade. *Antivir. Res.* 176, 104742. doi: 10.1016/j.antiviral.2020.104742
- Dar, N. J., Bhat, J. A., Satti, N. K., Sharma, P. R., Hamid, A., and Ahmad, M. (2017). Withanone, an active constituent from withania somnifera, affords protection against NMDA-induced excitotoxicity in neuron-like cells. *Mol. Neurobiol.* 54 (7), 5061–5073. doi: 10.1007/s12035-016-0044-7
- Dar, N. J., and Muzamil, A. (2020). Neurodegenerative diseases and Withania somnifera (L.): An update. *J. Ethnopharmacol.* 256, 112769. doi: 10.1016/j.jep.2020.112769
- Davis, L., and Kuttan, G. (2000). Immunomodulatory activity of withania somnifera. *J. Ethnopharmacol.* 71 (1–2), 193–200. doi: 10.1016/s0378-8741(99)00206-8
- Davis, L., and Kuttan, G. (2002). Effect of withania somnifera on cell mediated immune responses in mice. *J. Exp. Clin. Cancer Res.* 21 (4), 585–590.
- Devaux, C. A., Rolain, J. M., Colson, P., and Raoult, D. (2020). New insights on the antiviral effects of chloroquine against coronavirus: What to expect for COVID-19? *Int. J. Antimicrob. Agents* 55(5), 105938. doi: 10.1016/j.ijantimicag.2020.105938
- de Wilde, A. H., Jochmans, D., Posthuma, C. C., Zevenhoven-Dobbe, J. C., van Nieuwkoop, S., Bestebroer, T. M., et al. (2014). Screening of an FDA-approved compound library identifies four small-molecule inhibitors of middle East respiratory syndrome coronavirus replication in cell culture. *Antimicrob. Agents Chemother.* 58 (8), 4875–4884. doi: 10.1128/AAC.03011-14
- Dhanjal, J. K., Kumar, V., Garg, S., Subramani, C., Agarwal, S., Wang, J., et al. (2021). Molecular mechanism of anti-SARS-CoV2 activity of withania somnifera somnifera -derived withanolides. *Int. J. Biol. Macromol.* 1 (84), 297–312. doi: 10.1016/j.ijbiomac.2021.06.015
- Elfiky, A. A. (2020). Anti-HCV, nucleotide inhibitors, repurposing against COVID-19. *Life Sci.* 28, 117477. doi: 10.1016/j.lfs.2020.117477
- Fardet, L., Flahault, A., Kettaneh, A., Tiev, K. P., Gènereau, T., and Tolédano, C. (2007). Corticosteroid-induced clinical adverse events: frequency, risk factors and

- patient's opinion. *Br. J. Dermatol.* 157 (1), 142–148. doi: 10.1111/j.1365-2133.2007.07950.x
- Favalli, E. G., Biggioggero, M., Maioli, G., and Caporalia, R. (2020). Baricitinib for COVID-19: a suitable treatment. *Lancet Infect. Dis.* 20 (9), 1012–1013. doi: 10.1016/S1473-3099(20)30262-0
- Ferner, R. E., Aronson, J. K., and Aronson, J. K. (2020). Chloroquine and hydroxychloroquine in covid-19. *BMJ* 369, m1432. doi: 10.1136/bmj.m1432
- Gao, Y., Yan, L., Huang, Y., Liu, F., Zhao, Y., Cao, L., et al. (2020). Structure of the RNA-dependent RNA polymerase from COVID-19 virus. *Science* 368(6492), 779–782. doi: 10.1126/science.abb7498
- Gold, J. E., Baumgartl, W. H., Okyay, R. A., Licht, W. E., Fidel, P. L. Jr., Noverr, M. C., et al. (2020). Analysis of measles-Mumps-Rubella (MMR) titers of recovered COVID-19 patients. *mBio* 11 (6), e02628–e02620. doi: 10.1128/mBio.02628-20
- Guo, Y. R., Cao, Q. D., Hong, Z. S., Tan, Y. Y., Chen, S. D., Jin, H. J., et al. (2020). The origin, transmission and clinical therapies on coronavirus disease 2019 (COVID-19) outbreak—an update on the status. *Mil. Med. Res.* 11, 11. doi: 10.1186/s40779-020-00240-0
- Hasan, A. H., Hussien, N. H., Shakyia, S., Jamalis, J., Pratama, M. R. F., Chander, S., et al. (2022). In silico discovery of multi-targeting inhibitors for the COVID-19 treatment by molecular docking, molecular dynamics simulation studies, and ADMET predictions. *Structural Chemistry*, 1–21.
- Heutinck, K. M., ten Berge, I. J. M., Hack, C. E., Hamann, J., and Rowshani, A. T. (2010). Serine proteases of the human immune system in health and disease. *Mol. Immunol.* 47, 1943–1955. doi: 10.1016/j.molimm.2010.04.020. Withania somnifera somnifera hani.
- Hoffmann, M., Kleine-Weber, H., Schroeder, S., Krüger, N., Herrler, T., Erichsen, S., et al. (2020). SARS-CoV-2 cell entry depends on ACE2 and TMPRSS2 and is blocked by a clinically proven protease inhibitor. *Cell* 181 (2), 271–280.e8. doi: 10.1016/j.cell.2020.02.052
- Ingawale, M., Deepa, S., and Namdeo, A. G. (2020). Pharmacological evaluation of withania somnifera highlighting its healthcare claims, safety, and toxicity aspects. *J. Dietary Suppl.* 18 (2), 183–226. doi: 10.1080/19390211.2020.1741484
- Institute for Health Metrics and Evaluation (IHME) (2022) *COVID-19 projections*. Available at: <https://covid19.healthdata.org/global?view=cumulative-deaths&tab=trend>.
- Jackson, C. B., Farzan, M., Chen, B., and Choe, H. (2022). Mechanisms of SARS-CoV-2 entry into cells. *Nat. Rev. Mol. Cell Biol.* 23 (1), 3–20. doi: 10.1038/s41580-021-00418-x
- Jacobi, A., Chung, M., Bernheim, A., and Eber, C. (2020). Portable chest X-ray in coronavirus disease-19 (COVID-19): a pictorial review. *Clin. Imaging* 64, 35–42. doi: 10.1016/j.clinimag.2020.04.001
- Jahrsdörfer, B., Vollmer, A., Blackwell, S. E., Maier, J., Sontheimer, K., Beyer, T., et al. (2010). Granzyme b produced by human plasmacytoid dendritic cells suppresses T-cell expansion. *Blood* 115, 1156–1165. doi: 10.1182/blood-2009-07-235382
- Jayaprakasam, B., and Nair, M. G. (2003). Cyclooxygenase-2 enzyme inhibitory withanolides from withania somnifera somnifera leaves. *Tetrahedron* 59, 841–849. doi: 10.1016/S0040-4020(02)01601-0
- Jayaprakasam, B., Strasburg, G. A., and Nair, M. G. (2004). Potent lipid peroxidation inhibitors from withania somnifera somnifera fruits. *Tetrahedron* 60, 3109–3121. doi: 10.1016/j.tet.2004.01.016
- Jeyanthi, T., and Subramanian, P. (2010). Protective effect of withania somnifera root powder on lipid peroxidation and antioxidant status in gentamicin-induced nephrotoxic rats. *J. Basic Clin. Physiol. Pharmacol.* 21 (1), 61–78. doi: 10.1515/jbcp.2010.21.1.61
- Kalra, R. S., and Kandimalla, R. (2021). Engaging the spikes: Heparan sulfate facilitates SARS-CoV-2 spike protein binding to ACE2 and potentiates viral infection. *Signal Transduction Targeted Ther.* 6 (1), 1–2. doi: 10.1038/s41392-021-00470-1
- Kandagalla, S., Rimac, H., Gurushankar, K., Novak, J., Grishina, M., and Potemkin, V. (2022). Withasomniferol c, a new potential SARS-CoV-2 main protease inhibitor from the withania somnifera plant proposed by in silico approaches. *PeerJ* 10, e13374. doi: 10.7717/peerj.13374.eCollection2022
- Kaur, G., Singh, N., Samuel, S. S., Bora, H. K., Sharma, S., Pachauri, S. D., et al. (2015b). Withania somnifera shows a protective effect in monocrotaline induced pulmonary hypertension. *Pharm. Biol.* 53 (1), 147–157. doi: 10.3109/13880209.2014.912240
- Khan, M. A., Ahmed, R. S., Chandra, N., Arora, V. K., and Ali, A. (2018). In vivo, extract from withania somnifera root ameliorates arthritis via regulation of key immune mediators of inflammation in experimental model of arthritis. *Anti-Inflammatory Anti-Allergy Agents Med. Chem.* 18 (1), 55–70. doi: 10.2174/1871523017666181116092934
- Khanal, P., Chikhale, R., Dey, Y. N., Pasha, I., Chand, S., Gurav, N., et al. (2020). Withanolides from withania somnifera as an immunity booster and their therapeutic options against COVID-19. *J. Biomol. Structure Dynamics*, 1–14. doi: 10.1080/07391102.2020.1869588
- Kirson, I., Glotter, E., Lavis, D., and Abraham, A. (1971). Constituents of withania somnifera somnifera dunal XII the withanolides of an Indian chemotype. *J. Chem. Soc.* 52, 2032–2044. doi: 10.1039/j39710002032
- Kour, K., Pandey, A., Suri, K. A., Satti, N. K., Gupta, K. K., and Bani, S. (2009). Restoration of stress-induced altered T cell function and corresponding cytokines patterns by withanolide a. *Int. Immunopharmacol.* 9 (10), 1137–1144. doi: 10.1016/j.intimp.2009.05.011
- Krokhin, O., Li, Y., Andonov, A., Feldmann, H., Flick, R., Jones, S., et al. (2003). Mass spectrometric characterization of proteins from the SARS virus: a preliminary report. *Mol. Cell Proteomics* 2, 346–356. doi: 10.1074/mcp.M300048-MCP200
- Kręśniak, M., Zajkowicz, A., Gdowicz-Kłosok, A., Glowala-Kosińska, M., Łasut-Szyska, B., and Rusin, M. (2020). Synergistic activation of p53 by actinomycin d and nutlin-3a is associated with the upregulation of crucial regulators and effectors of innate immunity. *Cell Signal.* 1 (69), 109552. doi: 10.1016/j.cellsig.2020.109552
- Kuboyama, T., Tohda, C., and Komatsu, K. (2005). Neuritic regeneration and synaptic reconstruction induced by withanolide a. *Br. J. Pharmacol.* 144 (7), 961–971. doi: 10.1038/sj.bjp.0706122
- Kuboyama, T., Tohda, C., and Komatsu, K. (2006). Withanoid IV and its active metabolite, sominone, attenuate $\alpha\beta$ (25–35)-induced neurodegeneration. *Eur. J. Neurosci.* 23 (6), 1417–1426. doi: 10.1111/j.1460-9568.2006.04664.x
- Kumar, V., Dhanjal, J. K., Bhargava, P., Kaul, A., Wang, J., Zhang, H., et al. (2022). Withanone and Withaferin-A are predicted to interact with transmembrane protease serine 2 (TMPRSS2) and block entry of SARS-CoV-2 into cells. *Journal of Biomolecular Structure and Dynamics*, 40 (1), 1–13.
- Kumar, Y., and Singh, H. (2020). In silico identification and docking-based drug repurposing against the main protease of SARS-CoV-2, causative agent of COVID-19. *ChemRxiv*. Cambridge: Cambridge Open Engage; doi: 10.26434/chemrxiv.12049590.v1
- Kushwaha, S., Soni, V. K., Singh, P. K., Bano, N., Kumar, A., Sangwan, R. S., et al. (2012a). Withania somnifera chemotypes nmitli 101R, nmitli 118R, nmitli 128R and withaferin a protect mastomys coucha from bugria malayi infection. *Parasite Immunol.* 34 (4), 199–209. doi: 10.1111/j.1365-3024.2012.01352.x
- Lane, J. C. E., Weaver, J., Kostka, K., Duarte-Salles, T., Abrahao, M. T. F., Alghoul, H., et al. (2020). Risk of hydroxychloroquine alone and in combination with azithromycin in the treatment of rheumatoid arthritis: a multinational, retrospective study. *Lancet Rheumatol.* 2 (11), e698–e711. doi: 10.1016/S2665-9913(20)30276-9
- Leu, C.-H., Yang, M.-L., Chung, N.-H., Huang, Y.-J., Su, Y.-C., Chen, Y.-C., et al. (2015). Kallistatin ameliorates influenza virus pathogenesis by inhibition of kallikrein-related peptidase 1-mediated cleavage of viral hemagglutinin. *Antimicrob. Agents Chemother.* 59, 5619–5630. doi: 10.1128/AAC.00065-15
- Li, Q., Guan, X., Wu, P., Wang, X., Zhou, L., Tong, Y., et al. (2020). Early transmission din wuhan, China, of novel coronavirus-infected pneumonia. *N. Engl. J. Med.* 382 (13), 1199–1207. doi: 10.1056/NEJMoa2001316
- Lippi, G., Simundic, A. M., and Plebani, M. (2020). Potential preanalytical and analytical vulnerabilities in the laboratory diagnosis of coronavirus disease 2019 (COVID-19). *Clin. Chem. Lab. Med.* 58 (7), 1070–1076. doi: 10.1515/cclm-2020-0285
- Magnen, M., Gueugnon, F., Guillon, A., Baranek, T., Thibault, V. C., Petit-Courty, A., et al. (2017). Kallikrein-related peptidase 5 contributes to H3N2 influenza virus infection in human lungs. *J. Virol.* 91, 421–417. doi: 10.1128/JVI.00421-17
- Markus, H., Weber, H. K., Schroeder, S., Krüger, N., Herrler, T., Erichsen, S., et al. (2020). SARS-CoV-2 cell entry depends on ACE2 and TMPRSS2 and is blocked by a clinically proven protease inhibitor. *Cell* 181, (2), 271–280. doi: 10.1016/j.cell.2020.02.052
- Matsuda, H., Murakami, T., Kishi, A., and Yoshikawa, M. (2001). Structures of withanosides I, II, III, IV, V, VI, and VII, new withanolide glycosides, from the roots of Indian withania somnifera DUNAL. and inhibitory activity for tachyphylaxis to clonidine in isolated guinea-pig ileum. *Bioorg. Med. Chem.* 9 (6), 1499–1507. doi: 10.1016/S0968-0896(01)00024-4
- Maurya, K. D., and Sharma, D. (2020). Evaluation of traditional ayurvedic preparation for prevention and management of the novel coronavirus (SARS-CoV-2) Using Molecular docking approach. *ChemRxiv*. Cambridge: Cambridge Open Engage
- Mehta, P., McAuley, D. F., Brown, M., Sanchez, E., Tattersall, R. S., and Manson, J. J. (2020). COVID-19: consider cytokine storm syndromes and immunosuppression. *lancet* 395 (10229), 1033–1034. doi: 10.1016/S0140-6736(20)30628-0
- Menni, C., Valdes, A. M., Freidin, M. B., Sudre, C. H., Nguyen, L. H., Drew, D. A., et al. (2020). Real-time tracking of self-reported symptoms to predict potential COVID-19. *Nat. Med.* 26 (7), 1037–1040. doi: 10.1038/s41591-020-0916-2
- Méthot, N., Rubin, J., Guay, D., Beaulieu, C., Ethier, D., Reddy, T. J., et al. (2007). Inhibition of the activation of multiple serine proteases with a cathepsin c inhibitor

requires sustained exposure to prevent pro-enzyme processing. *J. Biol. Chem.* 282, 20836–20846. doi: 10.1074/jbc.M702615200

Michot, J. M., Albiges, L., Chaput, N., Saada, V., Pommeret, F., Griscelli, F., et al. (2020). Tocilizumab, an anti-IL6 receptor antibody, to treat covid-19-related respiratory failure: a case report. *Ann. Oncol.: Off. J. Eur. Soc. Med. Oncol.* 7, 961–964. doi: 10.1016/j.jannonc.2020.03.300

Milewska, A., Falkowski, K., Kalinska, M., Bielecka, E., Naskalska, A., Mak, P., et al. (2020). Kallikrein 13 serves as a priming protease during infection by the human coronavirus HKU1. *Sci. Signal.* 13 (659), 1–14. doi: 10.1126/scisignal.aba9902

Mi-Sun, Y., June, L., Jin Moo, L., Younggyu, K., Young-Won, C., Jun-Goo, J., et al. (2008). Identification of myricetin and scutellarein as novel chemical inhibitors of the SARS coronavirus helicase, nsP13. *J. Ethnopharmacol.* 118, 79–85. doi: 10.1016/j.bmcl.2012.04.081

Mohan, R., and Bargagna-Mohan, P. (2016). The use of withaferin A to study intermediate filaments. In *Methods in enzymology* (Vol. 568, pp. 187–218). Academic Press.

Morice, W. G., Jevremovic, D., and Hanson, C. A. (2007). The expression of the novel cytotoxic protein granzyme m by large granular lymphocytic leukaemias of both T-cell and NK-cell lineage: an unexpected finding with implications regarding the pathobiology of these disorders. *Br. J. Haematol.* 137, 237–239. doi: 10.1111/j.1365-2141.2007.06564.x

Mousavi, S. S., Karami, A., Haghighi, T. M., Tumilaar, S. G., Idroes, R., Mahmud, S., et al. (2021). In silico evaluation of Iranian medicinal plant phytoconstituents as inhibitors against main protease and the receptor-binding domain of SARS-CoV-2. *Molecules* 26 (18), 5724. doi: 10.3390/molecules26185724

Mukherjee, S., Kumar, G., and Patnaik, R. (2020). Withanolide A penetrates brain via intra-nasal administration and exerts neuroprotection in cerebral ischemia reperfusion injury in mice. *Xenobiotica* 50 (8), 957–966. doi: 10.1080/00498254.2019.1709228

Mulay, A., Konda, B., Garcia, G. Jr, Yao, C., Beil, S., Villalba, J. M., et al. (2021). SARS-CoV-2 infection of primary human lung epithelium for COVID-19 modeling and drug discovery. *Cell Rep.* 35 (5), 109055. doi: 10.1016/j.celrep.2021.109055

Murray, C. J. L. (2022). COVID-19 will continue but the end of the pandemic is near. *Lancet* 399 (10323), 417–419. doi: 10.1016/S0140-6736(22)00100-3

Nakamura, H., Yoshimura, K., McElvaney, N. G., and Crystal, R. G. (1992). Neutrophil elastase in respiratory epithelial lining fluid of individuals with cystic fibrosis induces interleukin-8 gene expression in a human bronchial epithelial cell line. *J. Clin. Invest.* 89, 1478–1484. doi: 10.1172/JCI115738

Narendrakumar, L., Chandrika, S. K., and Thomas, S. (2020). Adaptive resistance evolution of *V. cholerae* to doxycycline associated with spontaneous mutation. *Int. J. Antimicrob. Agents* 56 (3), 106097. doi: 10.1016/j.jantimicag.2020.106097

Narendrakumar, L., and Thomas, S. (2018). Vibrio cholerae O1 gaining reduced susceptibility to doxycycline, India. *J. Glob. Antimicrob. Resist.* 31 (12), 141–142. doi: 10.1016/j.jgar.2018.01.009

Narinderpal, K., Junaid, N., and Raman, B. (2013). A review on pharmacological profile of withania somnifera somnifera (Withania somnifera somnifera). *Res. Rev.: J. Bot. Sci.* 2, 6–14.

National Center for Immunization and Respiratory Diseases (NCIRD) and Division of Viral Diseases. (2020). Centers for Disease Control and Prevention Science Brief: Options to Reduce Quarantine for Contacts of Persons with SARS-CoV-2 Infection Using Symptom Monitoring and Diagnostic Testing [Internet]. Available at: <https://www.ncbi.nlm.nih.gov/books/NBK570434/>

Noh, E. J., Kang, M. J., Jeong, Y. J., Lee, J. Y., Park, J. H., Choi, H. J., et al. (2016). Withaferin A inhibits inflammatory responses induced by fusobacterium nucleatum and aggregatibacter actinomycetemcomitans in macrophages. *Mol. Med. Rep.* 14 (1), 983–988. doi: 10.3892/mmr.2016.5326

Pandit, M., and Latha, N. (2020). In silico studies reveal potential antiviral activity of phytochemicals from medicinal plants for the treatment of COVID-19 infection. doi: 10.21203/rs.3.rs-22687/v1

Parwe, S. D., Nisargandha, M. A., and Morey, D. T. (2020). Role of withania somnifera (Withania somnifera somnifera) as immunomodulator in coronavirus in a pandemic – a systemic review. doi: 10.26452/ijrps.v11iSPL1.4078

Pascarella, G., Ciccozzi, M., Zella, D., Bianchi, M., Benedetti, F., Benvenuto, D., et al. (2021). SARS-CoV-2 B.1.617 Indian variants: Are electrostatic potential changes responsible for a higher transmission rate? *J. Med. Virol.* 93 (12), 6551–6556. doi: 10.1002/jmv.27210

Pascarella, G., Strumia, A., Piliego, C., Bruno, F., Del Buono, R., Costa, F., et al. (2020). COVID-19 diagnosis and management: a comprehensive review. *J. Intern. Med.* 288 (2), 192–206. doi: 10.1111/joim.13091

Patel, C. N., Goswami, D., Jaiswal, D. G., Parmar, R. M., Solanki, H. A., and Pandya, H. A. (2021). Pinpointing the potential hits for hindering interaction of SARS-CoV-2 s-protein with ACE2 from the pool of antiviral phytochemicals

utilizing molecular docking and molecular dynamics (MD) simulations. *J. Mol. Graphics Model.* 105, 107874. doi: 10.1016/j.jmglm.2021.107874

Pejler, G., Åbrink, M., Ringvall, M., and Wernersson, S. (2007). Mast cell proteases. *Adv. Immunol.* 95, 167–255. doi: 10.1016/S0065-2776(07)95006-3

Prajapati, K. S., Singh, A. K., Kushwaha, P. P., Shuaib, M., Maurya, S. K., Gupta, S., et al. (2022). Withaniasomnifera phytochemicals possess SARS-CoV-2 RdRp and human TMPPRS2 protein binding potential. *Vegetos* 15, 1–20. doi: 10.1007/s42535-022-00404-4

Public Health England (2020). “Variant of concern 202012/01: Technical briefing 2,” in *Investigation of novel SARS-CoV-2 variant*.

Qin, A., and Hernández, J. C. (2020). China Reports first death from new virus (USA: The New York Times). ISSN 0362-4331. Archived from the original on 11 January 2020. Retrieved 11 January 2020.

Rai, P. K., Mueed, Z., Chowdhury, A., Deval, R., Kumar, D., Kamal, M. A., et al. (2022). Current overviews on COVID-19 management strategies. *Curr. Pharm. Biotechnol.* 23(3):361–387. doi: 10.2174/1389201022666210509022313

Raj, V. S., Mou, H., Smits, S. L., Dekkers, D. H., Müller, M. A., and Dijkman, R. (2013). Dipeptidyl peptidase 4 is a functional receptor for the emerging human coronavirus-EMC. *Nature* 495 (7440), 251–254. doi: 10.1038/nature12005

Reid, J. C., Matsika, A., Davies, C. M., He, Y., Broomfield, A., Bennett, N. C., et al. (2017). Pericellular regulation of prostate cancer expressed kallikrein-related peptidases and matrix metalloproteinases by cell surface serine proteases. *Am. J. Cancer Res.* 7, 2257–2274.

Richardson, P., Griffin, I., Tucker, C., Smith, D., Oechsle, O., and Phelan, A. (2020). Baricitinib as potential treatment for 2019-nCoV acute respiratory disease. *Lancet* 395 (10223), e30–e31. doi: 10.1016/S0140-6736(20)30304-4

Roghiani, A., and Sallenave, J. M. (2008). Neutrophil elastase (NE) and NE inhibitors canonical and noncanonical functions in lung chronic inflammatory diseases (Cystic fibrosis and chronic obstructive pulmonary disease). *J. Aerosol. Med. Pulm. Drug Deliv.* 21, 125–144. doi: 10.1089/jamp.2007.0653

Roquebert, B., Trombert-Paolantoni, S., Haim-Boukoba, S., Lecorche, E., Verdum, L., and Foulongne, V. (2021). The SARS-CoV-2 B.1.351 lineage (VOC b) is outgrowing the B.1.1.7 lineage (VOC a) in some French regions in April 2021. *Euro Surveill* 26 (23), 2100447. doi: 10.2807/1560-7917.ES.2021.26.23.2100447

Rota, P. A., Oberste, M. S., Monroe, S. S., Nix, W. A., Campagnoli, R., Icenogle, J. P., et al. (2003). Characterization of a novel coronavirus associated with severe acute respiratory syndrome. *Science* 300, 1394–1399. doi: 10.1126/science.1085952

Ryu, Y. B., Jeong, H. J., Kim, J. H., Kim, Y. M., Park, J. Y., Kim, D., et al. (2010). Biflavonoids from torreyanucifera displaying SARS-CoV 3CL (pro) inhibition. *Bioorg. Med. Chem.* 18, 7940–7947. doi: 10.1016/j.bmc.2010.09.035

Sadanandam, A., Bopp, T., Dixit, S., Knapp, D. J., Emperumal, C. P., Vergidis, P., et al. (2020). A blood transcriptome-based analysis of disease progression, immune regulation, and symptoms in coronavirus-infected patients. *Cell Death Discovery* 6 (1), 141. doi: 10.1038/s41420-020-00376-x

Seth, S., Batra, J., and Srinivasan, S. (2020). COVID-19: targeting proteases in viral invasion and host immune response. *Front. Mol. Biosci.* 7. doi: 10.3389/fmolb.2020.00215

Sharma, P., Tyagi, A., Bhansali, P., Pareek, S., Singh, V., Ilyas, A., et al. (2021). Saponins: Extraction, bio-medicinal properties and way forward to anti-viral representatives. *Food Chem. Toxicol.* 150, 112075. doi: 10.1016/j.fct.2021.112075

Singh, P., Hariprasad, V. R., Babu, U. V., Rafiq, M., and Rao, R. P. (2020). Potential phytochemical inhibitors of the coronavirus RNA dependent RNA polymerase: a molecular docking study. doi: 10.21203/rs.3.rs-35334/v1

Singh, M., Singh, D., Rai, P., Suyal, D. C., Saurabh, S., and Soni, R. (2021). “Fungi in remediation of hazardous wastes: current status and future,” in recent trends in mycological research, 195–224. *Fungal Biology*. doi: 10.1007/978-3-030-68260-6_8

Singh, G., Tiwari, M., Singh, S. P., Singh, S., Trivedi, P. K., and Misra, P. (2016). Silencing of sterol glycosyltransferases modulates the withanolide biosynthesis and leads to compromised basal immunity of withania somnifera. *Sci. Rep.* 6 (1), 1–13. doi: 10.1038/srep25562

Soman, S., Anju, T. R., Jayanarayanan, S., Antony, S., and Paulose, C. S. (2013). Impaired motor learning attributed to altered AMPA receptor function in the cerebellum of rats with temporal lobe epilepsy: ameliorating effects of withania somnifera and withanolide A. *Epilepsy Behav.* 27 (3), 484–491. doi: 10.1016/j.yebeh.2013.01.007

Stebbing, J., Phelan, A., Griffin, I., Tucker, C., Oechsle, O., et al. (2020). COVID-19: combining antiviral and anti-inflammatory treatments. *Lancet Infect. Dis.* 20 (4), 400–402. doi: 10.1016/S1473-3099(20)30132-8

Straughn, A. R., and Kakar, S. S. (2019). Withaferin A ameliorates ovarian cancer-induced cachexia and proinflammatory signaling. *J. Ovarian Res.* 12 (1), 115. doi: 10.1186/s13048-019-0586-1

Sumito, I., Igarashi, A., Morikane, K., Hachiya, O., Watanabe, M., Kakehata, S., et al. (2021). Adverse reactions to BNT162b2 mRNA COVID-19 vaccine in

- medical staffs with a history of allergy. S. Inoue, A. Igarashi, K. Morikane, et al. *Respir Investig*, 60(2), 248–255. doi: 10.1016/j.resinv.2021.11.007
- Sun, Q. S. (2019). Withaferin a attenuates ovalbumin induced airway inflammation. *Front. Biosci.* 24, 576–596. doi: 10.2741/4737
- Sunzini, F., McInnes, I., and Siebert, S. (2020). JAK inhibitors and infections risk: focus on herpes zoster. *Therapeutic Advances in Musculoskeletal Disease*, 12, 1759720X20936059
- Swelum, A. A., Shafi, M. E., Albaqami, N. M., El-Saadony, M. T., Elsify, A., Abdo, M., et al. (2020). COVID-19 in human, animal, and environment: A review. *Front. Vet. Sci.* 7. doi: 10.3389/fvets.2020.00578
- Tebas, P., Yang, S., Boyer, J. D., Reuschel, E. L., Patel, A., Christensen-Quick, A., et al. (2021). Safety and immunogenicity of INO-4800 DNA vaccine against SARS-CoV-2: A preliminary report of an open-label, phase 1 clinical trial. *EClinicalMedicine* 31, 100689. doi: 10.1016/j.eclinm.2020.100689
- Teuwen, L.-A., Geldhof, V., Pasut, A., and Carmeliet, P. (2020). COVID-19: the vasculature unleashed. *Nat. Rev. Immunol.* 20, 389–391. doi: 10.1038/s41577-020-0343-0
- Thomas, ZR., Leuppi-Taegtmeier, A., Jamiolkowski, D., Steveling-Klein, E., Bellutti-Enders, F., Hofmeier, KS., et al. (2020). Emerging treatments in COVID-19: Adverse drug reactions including drug hypersensitivities. *Journal of Allergy and Clinical Immunology*, 146 (4), 786–789.
- Tiruveedi, V. L., Bale, S., Khurana, A., Godugu, C., and Godugu, C. (2018). Withaferin a, a novel compound of Indian ginseng (*Withania somnifera*), ameliorates cerulein-induced acute pancreatitis: possible role of oxidative stress and inflammation. *Phytother. Res.* 32 (12), 2586–2596. doi: 10.1002/ptr.6200
- Tomar, V., Beuerle, T., and Sircar, D. J. (2019). A validated HPTLC method for the simultaneous quantifications of three phenolic acids and three withanolides from *withania somnifera* plants and its herbal products. *Chromatogr. B. Anal. Technol. BioMed. Life Sci.* 1124, 154–160. doi: 10.1016/j.jchromb.2019.06.009
- Tong, X., Zhang, H., and Timmermann, B. N. (2011). Chlorinated withanolides from *withania somnifera* *somnifera*. *Phytochem. Lett.* 4 (4), 411–414. doi: 10.1016/j.phytol.2011.04.016
- Trivedi, P. C., and Choudhrey, N. (2011). Isolation and characterization of bioactive compound sitosterol from *withania somnifera* *somnifera* L. *J. Pharma. Res.* 4, 4252–4253.
- Turrini, E., Calcabrini, C., Sestili, P., Catanzaro, E., De Gianni, E., Diaz, A. R., et al. (2016). *Withania somnifera* induces cytotoxic and cytostatic effects on human T leukemia cells. *Toxins* 8 (5), 147. doi: 10.3390/toxins8050147
- USNLM. (2020). *Bevacizumab in severe or critical patients with COVID-19 pneumonia (BEST-CP)*. Available at: <https://clinicaltrials.gov/ct2/show/NCT04275414>.
- Van der Geld, Y. M., Limburg, P. C., and Kallenberg, C. G. M. (2001). Proteinase 3, wegener's autoantigen: from gene to antigen. *J. Leukoc. Biol.* 69, 177–190. doi: 10.1189/jlb.69.2.177
- Varga, Z., Flammer, A. J., Steiger, P., Haberecker, M., Rea, A., Annelies, S., et al. (2020). Endothelial cell infection and endotheliitis in COVID-19. *Lancet* 395 (10234), 1417–1418. doi: 10.1016/S0140-6736(20)30937-5
- Varma, V., Parwe, S., and Nisargandha, M. (2020). Systematic review of anti-viral & immunomodulatory potential of *withania somnifera* (*Withania somnifera* Linn) in light of covid-19 pandemic. *Int. J. Bot. Stud.* 5 (5), 494–497.
- Vedi, M., and Sabina, E. P. (2016). Assessment of hepatoprotective and nephroprotective potential of withaferin a on bromobenzene-induced injury in Swiss albino mice: possible involvement of mitochondrial dysfunction and inflammation. *Cell Biol. Toxicol.* 32 (5), 373–390. doi: 10.1007/s10565-016-9340-2
- Wadegaonkar, V. P., and Wadegaonkar, P. A. (2013). Withanone as an inhibitor of survivin: A potential drug candidate for cancer therapy. *J. Biotechnol.* 168 (2), 229–233. doi: 10.1016/j.jbiotec.2013.08.028
- Wang, M., Cao, R., Zhang, L., Yang, X., Liu, J., Xu, M., et al. (2020a). Remdesivir and chloroquine effectively inhibit the recently emerged novel coronavirus, (2019-nCoV) *in vitro*. *Cell Res.* 30 (3), 269–271. doi: 10.1038/s41422-020-0282-0
- Wang, Z., Zhang, S., Xiao, Y., Zhang, W., Wu, S., Qin, T., et al. (2020b). NLRP3 inflammasome and inflammatory diseases. *Oxid. Med. Cell Longev.* 2020, 1–11. doi: 10.1155/2020/4063562
- Wijayasinghe, Y. S., Bhansali, P., Viola, R. E., Kamal, M. A., and Poddar, N. K. (2021). Natural products: A rich source of antiviral drug lead candidates for the management of COVID-19. *Curr. Pharm. Des.* 27 (33), 3526–3550. doi: 10.2174/138161282666201118111151
- WHO. (2020). *WHO R&D blueprint COVID-19 informal consultation on the potential role of IL-6/IL-1 antagonists in the clinical management of COVID 19 infection*.
- World Health Organization. (2020). *Report of the WHO-China joint mission on coronavirus disease 2019 (COVID-19)* (Geneva: WHO). Available at: <https://www.who.int/docs/default-source/coronaviruse/who-china-joint-mission-on-covid-19-final-report.pdf> (Accessed 14 April 2020).
- Wulan, W. N., Heydet, D., Walker, E. J., Gahan, M. E., and Ghildyal, R. (2015). Nucleocytoplasmic transport of nucleocapsid proteins of enveloped RNA viruses. *Front. Microbiol.* 6, 553. doi: 10.3389/fmicb.2015.00553
- Xu, J., Zhao, S., Teng, T., Abdalla, A. E., Zhu, W., Xie, L., et al. (2020). Systematic comparison of two animal-to-Human transmitted human coronaviruses: SARS-CoV-2 and SARS-CoV. *Viruses* 12, 1–17. doi: 10.3390/v12020244
- Yang, L., and Tu, L. (2020). Implications of gastrointestinal manifestations of COVID-19. *Lancet Gastroenterol. Hepatol.* 5 (7), 629–630. doi: 10.1016/s2468-1253(20)30132-1
- Yang, J., Zheng, Y., Gou, X., Pu, K., Chen, Z., Guo, Q., et al. (2020). Prevalence of comorbidities and its effects in coronavirus disease 2019 patients: A systematic review and meta-analysis. *Int. J. Infect. Dis. IJID Off. Publ. Int. Soc. Infect. Dis.* 94, 91–95. doi: 10.1016/j.ijid.2020.03.017
- Yao, X., Ye, F., Zhang, M., Cui, C., Huang, B., et al. (2020). *In vitro* antiviral activity and projection of optimized dosing design of hydroxychloroquine for the treatment of severe acute respiratory syndrome coronavirus 2 (SARS-CoV-2). *Clin. Infect. Dis.* doi: 10.1093/cid/ciaa237
- Yuan, L., Chen, Z., Song, S., et al. (2015). p53 degradation by a coronavirus papain-like protease suppresses type I interferon signaling. *J. Biol. Chem.* 290 (5), 3172–3182. doi: 10.1074/jbc.M114.619890
- Yu, Y. Q., Herrmann, A., Thonn, V., Cordsmeier, A., Neurath, M. F., and Ensser, A. (2022). SMYD2 inhibition downregulates TMPRSS2 and decreases SARS-CoV-2 infection in human intestinal and airway epithelial cells. *Cells* 11 (8), 1262. doi: 10.3390/cells11081262
- Zampino, R., Mele, F., Florio, L. L., Bertolino, L., Andini, R., Galdo, M., et al. (2020). Liver injury in remdesivir-treated COVID-19 patients. *Hepatology international*, 14 (5), 881–883.
- Zhang, H., Penninger, J. M., Li, Y., Zhong, N., and Slutsky, A. S. (2020). Angiotensin-converting enzyme 2 (ACE2) as a SARS-CoV-2 receptor: Molecular mechanisms and potential therapeutic target. *Intensive Care Med.* 46, 586–590. doi: 10.1007/s00134-020-05985-9
- Zhao, J., Cui, W., and Tian, B. P. (2020). The potential intermediate hosts for SARS-CoV-2. *Front. Microbiol.* 11. doi: 10.3389/fmicb.2020.580137
- Zhou, D., Dai, S. M., and Tong, Q. (2020). COVID-19: a recommendation to examine the effect of hydroxychloroquine in preventing infection and progression. *J. Antimicrob. Chemother.* 114, 1667–1670. doi: 10.1093/jac/dkaa114
- Zhu, P., Martinvalet, D., Chowdhury, D., Zhang, D., Schlesinger, A., and Lieberman, J. (2009). The cytotoxic T lymphocyte protease granzyme a cleaves and inactivates poly(adenosine 5'-diphosphate-ribose) polymerase-1. *Blood* 114, 1205–1216. doi: 10.1182/blood-2008-12-195768



OPEN ACCESS

EDITED BY

Vikas Sood,
Jamia Hamdard University, India

REVIEWED BY

Amal Rahmeh,
Universidad Pompeu Fabra (UPF),
Spain
Manish Sharma,
Emory University, United States

*CORRESPONDENCE

Brett E. Pickett
brett_pickett@byu.edu

SPECIALTY SECTION

This article was submitted to
Virus and Host,
a section of the journal
Frontiers in Cellular and
Infection Microbiology

RECEIVED 01 August 2022

ACCEPTED 26 August 2022

PUBLISHED 20 September 2022

CITATION

Scott TM, Solis-Leal A, Lopez JB,
Robison RA, Berges BK and Pickett BE
(2022) Comparison of Intracellular
Transcriptional Response of NHBE
Cells to Infection with SARS-CoV-2
Washington and New York Strains.
Front. Cell. Infect. Microbiol.
12:1009328.
doi: 10.3389/fcimb.2022.1009328

COPYRIGHT

© 2022 Scott, Solis-Leal, Lopez,
Robison, Berges and Pickett. This is an
open-access article distributed under
the terms of the [Creative Commons
Attribution License \(CC BY\)](#). The use,
distribution or reproduction in other
forums is permitted, provided the
original author(s) and the copyright
owner(s) are credited and that the
original publication in this journal is
cited, in accordance with accepted
academic practice. No use,
distribution or reproduction is
permitted which does not comply with
these terms.

Comparison of Intracellular Transcriptional Response of NHBE Cells to Infection with SARS-CoV-2 Washington and New York Strains

Tiana M. Scott¹, Antonio Solis-Leal^{1,2}, J. Brandon Lopez¹,
Richard A. Robison¹, Bradford K. Berges¹ and Brett E. Pickett^{1*}

¹Department of Microbiology and Molecular Biology, Brigham Young University, Provo, UT, United States, ²Population Health and Host-pathogen Interactions Programs, Texas Biomedical Research Institute, San Antonio, TX, United States

Severe acute respiratory syndrome coronavirus 2 (SARS-CoV-2) was first reported in Wuhan, China in December 2019 and caused a global pandemic resulting in millions of deaths and tens of millions of patients positive tests. While studies have shown a D614G mutation in the viral spike protein are more transmissible, the effects of this and other mutations on the host response, especially at the cellular level, are yet to be fully elucidated. In this experiment we infected normal human bronchial epithelial (NHBE) cells with the Washington (D614) strain or the New York (G614) strains of SARS-CoV-2. We generated RNA sequencing data at 6, 12, and 24 hours post-infection (hpi) to improve our understanding of how the intracellular host response differs between infections with these two strains. We analyzed these data with a bioinformatics pipeline that identifies differentially expressed genes (DEGs), enriched Gene Ontology (GO) terms and dysregulated signaling pathways. We detected over 2,000 DEGs, over 600 GO terms, and 29 affected pathways between the two infections. Many of these entities play a role in immune signaling and response. A comparison between strains and time points showed a higher similarity between matched time points than across different time points with the same strain in DEGs and affected pathways, but found more similarity between strains across different time points when looking at GO terms. A comparison of the affected pathways showed that the 24hpi samples of the New York strain were more similar to the 12hpi samples of the Washington strain, with a large number of pathways related to translation being inhibited in both strains. These results suggest that the various mutations contained in the genome of these two viral isolates may cause distinct effects on the host transcriptional response in infected host cells, especially relating to how quickly translation is dysregulated after infection. This comparison of the intracellular host response to infection with these two SARS-CoV-2 isolates suggest that some of the mechanisms associated with more severe disease from these viruses could include virus replication, metal ion usage, host translation shutdown, host transcript stability, and immune inhibition.

KEYWORDS

SARS-CoV-2, COVID-19, data mining, bioinformatics, mechanism, virology, host response, host-virus

Introduction

Near the end of 2019, a novel human coronavirus emerged in Wuhan, China (Zhou et al., 2020). This virus was subsequently named severe acute respiratory syndrome coronavirus 2 (SARS-CoV-2) and is the causative agent of coronavirus disease 2019 (COVID-19). Since its emergence, SARS-CoV-2 has caused a global pandemic that has cost millions of lives and disrupted many more (WHO, 2022). Even at early stages of the pandemic, it was noted that certain factors made individuals more susceptible to severe disease. Particularly, it was noted that the elderly and those with specific pre-existing conditions were more likely to develop severe symptoms than individuals of younger age groups (Sherwani and Khan, 2020; Lara et al., 2020). In addition, previous studies have observed that symptoms, severity of disease, and transmissibility can vary due to the viral strain or variant (Kim et al., 2020; Moghaddar et al., 2021; Radvak et al., 2021).

Mutations in the viral genome spontaneously occur during viral replication (Weber et al., 2021), which may result in viruses having an increase in overall fitness (Benedetti et al., 2020; Pachetti et al., 2020). If at least one of these mutations emerges in a viral genome, it could become a prominent strain in the host population until a new and more fit strain emerges (Baric, 2020; Plante et al., 2021). Coronaviruses have a proofreading mechanism, which results in a relatively low mutation rate for an RNA virus. Although the viral polymerase can fix many of the errors that occur during genome replication (Smith et al., 2013; Yan et al., 2021), mutations still occur, leading to the emergence of new SARS-CoV-2 strains, some of which have higher fitness than the original strain from 2019.

Recent studies have divided the different strains of SARS-CoV-2 into clades based on the presence of specific genetic mutations (Forster et al., 2020; Mercatelli and Giorgi, 2020). The D614G substitution in the viral spike protein has been the focus of many studies, and is characteristic of the G-clade (Volz et al.; Mercatelli and Giorgi, 2020; Zhang et al., 2020). This mutation has been linked to a higher transmissibility of

the virus due to the stabilizing effect it has on the spike protein which is crucial for viral entry into the cell (Volz et al.; Zhang et al., 2020). An analysis of the geographical prevalence of SARS-CoV-2 strains identified the G-clade in geographical regions that appeared to have higher levels of morbidity and mortality in the early stages of the pandemic. Specifically, areas such as the east coast of the United States, tended to have a higher percentage of G614 viruses than the west coast of the United States, which appeared to have lower mortality metrics (Brufsky, 2020). Since the first waves of infection, the G614 substitution spread rapidly and eventually became responsible for ~99% of the virus isolates collected from patients with severe or symptomatic disease (Mercatelli and Giorgi, 2020; Pandey et al., 2021; von Bartheld et al., 2021).

While there are many studies that have performed comparative genetic analyses on the different clades and strains of SARS-CoV-2 (Forster et al., 2020; Mercatelli and Giorgi, 2020), there are fewer studies that have looked at how these different strains affect the host intracellular transcriptional response. The aim of the current study was to use RNA sequencing and bioinformatics tools to analyze the transcriptome of normal human bronchial epithelial (NHBE) cells infected with two early isolates of SARS-CoV-2 that had differences in morbidity and mortality in human populations. The infected versus normal host transcriptomes of these cells were characterized at 6, 12, and 24 hours post-infection (hpi). Both strains were isolated from patient samples in early 2020. Our analysis found thousands of differentially expressed genes, hundreds of enriched gene ontology terms as well as dozens of affected signaling pathways. Overall, we found that the transcriptional changes in cells were similar at matched time points between cells infected with the different strains, but we also observed that the dysregulation of many pathways, particularly those involved in translation, were delayed in cells infected with the G614 strain. These differences in host response may at least partially account for some of the differences in the host response, and in the viral replication dynamics that were observed in geographical regions affected by early SARS-CoV-2 strains.

Methods

Three biological replicates were performed in biosafety level three containment by growing three sets of NHBE cells to near confluency and separating them into two infected cultures and one mock-infected culture. Cell cultures were incubated for one hour with either the Washington (USA-WA1/2020) or New York (New York 1-PV08001/2020) isolate of SARS-CoV-2, which were obtained from BEI Resources, at a multiplicity of infection (MOI) of two. The media containing unattached virions was then removed, cells were washed three times with PBS and incubated in complete media at 37°C with 5% CO₂. Cells were harvested at 6, 12, and 24 hours post-infection (hpi). Mock-infected cells were incubated using the same protocol and reagents, and only lacked the presence of virus.

RNA was extracted from all samples using Trizol reagent according to the manufacturer's protocol prior to quantification using a NanoDrop instrument. Reverse transcription of the RNA into cDNA was then performed prior to quantification, generation of Nextera XT sequencing libraries, and barcoding of samples for multiplexing. An Illumina NovaSeq instrument was then used to produce paired-end 150bp reads for each sample, with a mean of 27.2 million reads from each sample for downstream analysis.

The fastq files containing the RNA sequencing data were processed and analyzed using the existing Automated Reproducible MOdular Workflow for Preprocessing and Differential Analysis of RNA-seq Data (ARMOR) pipeline (Scott et al., 2021). Briefly, this software performs the following steps: generate read quality control metrics using fastQC (Website), trim sequencing adaptors and poor-quality regions of the reads with TrimGalore! (Babraham Bioinformatics, 2022), map and quantify reads to the human transcriptome using Salmon (Patro et al., 2017), calculate differentially expressed genes using edgeR (Robinson et al., 2010), predict differential transcript usage with DRIMseq (Nowicka and Robinson, 2016), and identify enriched Gene Ontology terms (The Gene Ontology Consortium, 2019) and Hallmark gene sets (Liberzon et al., 2015) using the Camera algorithm to adjust for inter-gene correlation (Durinck et al., 2005; Wu and Smyth, 2012).

The Ensembl identifiers for each of the differentially expressed genes, which were calculated with ARMOR, were then converted to the corresponding NCBI Entrez Gene identifiers through the BioMart database using R and Bioconductor (Huber et al., 2015) prior to calculating pathway enrichment with the Signaling Pathway Impact Analysis (SPIA) algorithm (Tarca et al., 2009). This pathway analysis algorithm applies a bootstrapping-based method to generate a null distribution that enables the calculation of robust statistics. The pathway information is derived from a combination of public databases including KEGG (Kanehisa and Goto, 2000),

Reactome (Jassal et al., 2020), Panther (Mi et al., 2017), NCI (Schaefer et al., 2009), and BioCarta.

Results

Differentially expressed genes

We began by constructing *in silico* transcriptomic comparisons between infections for each virus isolate at each time point and the appropriate mock-infected controls (Supplementary Tables S1-6). This consisted of subjecting the quantified read mappings to a differential expression analysis using the edgeR algorithm. This approach provided us with a list of calculated differentially expressed genes for each time point for both virus strains. We then analyzed these lists to identify genes that were significantly affected (adjusted p-value <0.05). This process produced a list of 8,617 Ensembl gene identifiers that were significantly affected in at least one of the six examined conditions (two viruses at three time points), which correspond to 8,499 unique genes. Of these significant differentially expressed genes, we analyzed the ten genes that had the highest and lowest fold-change values (i.e. up- and down-regulated genes) for each condition and compared them to the significant genes identified in the other conditions. We constructed a table containing these top genes and how they are affected in the different strains (Supplementary Table 7).

Overall, we found the most similarity existing between matched time points of the two strains. We observed that cells infected by either virus at 6hpi shared 4 genes that were significantly up-regulated, (*IFITM10*, *TSEN*, *BDP1*, and *PPP1R11*). Of these genes only *BDP1* is significantly affected in another condition and it is down regulated at 24hpi for the Washington strain. Additionally at 6hpi in both strains, we observed seven genes were significantly down-regulated (*AC270230.1*, *RING1*, *PPP1R3B*, *PPP1R18*, *AC120057.2*, and *MCCC2*). *PPP1R18* was also down-regulated at 12hpi for the Washington strain. A list of the dysregulated genes at 6hpi for both strains, along with their fold change values and adjusted p-values, can be found in Table 1.

The 12hpi conditions shared four genes (*DDX39B*, *AC139530.2*, *AC068533.4* and *GSDMC*) that were up-regulated and three genes (*NSF*, *GPANK1*, and *ZNF100*) that were down-regulated. Of the four up-regulated genes, one, *DDX39B*, was down-regulated at 6hpi for the Washington strain. Out of the three genes that were down-regulated, *NSF* was also down-regulated at 24hpi for the Washington strain, and *ZNF100* was up-regulated at 6hpi for the New York strain. This set of genes includes several that are thought to play roles in the immune response such as *GPANK1*, *DDX39B*, and *GSDMC*. A list of the dysregulated genes at 12hpi for both strains, along with their fold change values and adjusted p-values, can be found in Table 2.

TABLE 1 Fold-change (case vs. control) and adjusted p-values for dysregulated genes at 6hpi for both SARS-CoV-2 isolates.

| Gene | | Washington 6hpi | | New York 6hpi | |
|-----------------|-------------------|------------------|----------------------|------------------|----------------------|
| Ensembl ID | Gene Symbol | Log2 Fold-change | FDR adjusted p-value | Log2 Fold-change | FDR adjusted p-value |
| ENSG00000236560 | <i>PPP1R11</i> | 10.9 | 0.00236 | 10.5 | 0.00145 |
| ENSG00000145734 | <i>BDP1</i> | 10.5 | 0.0321 | 9.95 | 0.0198 |
| ENSG00000281618 | <i>IFITM10</i> | 8.49 | 0.0171 | 7.47 | 0.028 |
| ENSG00000274129 | <i>TSEN34</i> | 5.09 | 0.0268 | 5.02 | 0.012 |
| ENSG00000288461 | <i>AC270230.1</i> | -10 | 0.0113 | -10 | 0.00505 |
| ENSG00000206287 | <i>RING1</i> | -9.34 | 0.0157 | -9.34 | 0.00717 |
| ENSG00000285343 | <i>PPP1R3B</i> | -9.34 | 0.0172 | -9.34 | 0.00792 |
| ENSG00000236428 | <i>PPP1R18</i> | -9.27 | 0.0139 | -9.27 | 0.00655 |
| ENSG00000262526 | <i>AC120057.2</i> | -8.2 | 0.0369 | -8.2 | 0.0178 |
| ENSG00000275300 | <i>MCCC2</i> | -8.3 | 0.00485 | -8.3 | 0.00222 |

The 24hpi conditions shared eight up-regulated genes (*FAM189B*, *AGPAT1*, *PPP1R3B*, *PRR3*, *ZBED6*, *SLC43A2*, *MAML1* and *AC020907.6*) and nine down-regulated genes (*SLC30A8*, *AC022149.1*, *RSPH14*, *AGXT*, *MAP3K15*, *AL136295.4*, *AL691477.1*, *AL358113.1* and *ARHGAP23*). One of the up-regulated genes, *AGPAT1*, was significantly down-regulated during infection with the New York strain at 12hpi. Another of the up-regulated genes, *PPP1R3B* was up-regulated at both 6hpi and 12hpi during infection with the New York strain. While the gene *PPP1R3B* is also seen to be down-regulated at 6hpi, it is categorized under a different Ensembl ID number and is therefore analyzed separately. None of the down-regulated genes were significantly affected at any other time point. A list of the dysregulated genes at 24hpi for both strains, along with their fold change values and adjusted p-values, can be found in Table 3.

GO Terms

In order to make the analysis of the differentially expressed genes easier to interpret, we used the camera algorithm to analyze the significantly enriched Gene Ontology (GO) terms

and Hallmark gene sets for infection with each isolate and time point (Supplementary Tables S8-13; Supplementary Figure S1). These terms and gene sets enable us to better understand some of the mechanistic biological processes and molecular functions that were over-represented in the lists of differentially expressed genes. We identified 211 terms that were significantly enriched in at least one condition. While there were several terms that were significantly enriched at 6hpi and 12hpi with either strain, there were no significantly enriched terms at 24hpi for either virus. Of these 211 terms we analyzed the ten most significant positively- and negatively-regulated terms for each condition, or all available terms if there were less than ten, and compared these terms to those that were identified as significant in the other conditions. A list of these terms and their adjusted p-values can be found in Table 4.

This analysis produced a shorter list of 49 terms, with three being negatively regulated in all four conditions (both viruses, at 6hpi and 12hpi). These terms included the “detoxification of inorganic compound”, “metallothioneins bind metals”, and “response to metal ions”. Two additional terms, “cellular response to zinc ion” and “response to arsenite”, were negatively regulated in each condition except for 6hpi with the New York strain. Several terms were positively regulated in all

TABLE 2 Fold-change (case vs. control) and adjusted p-values for dysregulated genes at 12hpi for both SARS-CoV-2 isolates.

| Gene | | Washington 12hpi | | New York 12hpi | |
|-----------------|-------------------|------------------|----------------------|------------------|----------------------|
| Ensembl ID | Gene Symbol | Log2 Fold-change | FDR adjusted p-value | Log2 Fold-change | FDR adjusted p-value |
| ENSG00000230624 | <i>DDX39B</i> | 8.43 | 0.0256 | 7.24 | 0.0421 |
| ENSG00000262660 | <i>AC139530.2</i> | 8.47 | 0.0124 | 6.35 | 0.0377 |
| ENSG00000249319 | <i>AC068533.4</i> | 6.22 | 0.0131 | 5.23 | 0.0243 |
| ENSG00000147697 | <i>GSDMC</i> | 2.86 | 0.00148 | 2.24 | 0.00959 |
| ENSG00000274746 | <i>ZNF100</i> | -8.91 | 0.011 | -8.91 | 0.0076 |
| ENSG00000278174 | <i>NSF</i> | -9.49 | 0.00881 | -7.99 | 0.0117 |
| ENSG00000236011 | <i>GPANK1</i> | -8.44 | 0.00778 | -8.44 | 0.0062 |

TABLE 3 Fold-change (case vs. control) and adjusted p-values for dysregulated genes at 24hpi for both SARS-CoV-2 isolates.

| Gene | | Washington 24hpi | | New York 24hpi | |
|-----------------|-------------------|------------------|----------------------|------------------|----------------------|
| Ensembl ID | Gene Symbol | Log2 Fold-change | FDR adjusted p-value | Log2 Fold-change | FDR adjusted p-value |
| ENSG00000160767 | <i>FAM189B</i> | 11.2 | 0.00162 | 11.9 | 0.000179 |
| ENSG00000206324 | <i>AGPAT1</i> | 11.8 | 4.45E-07 | 11.9 | 2.46E-07 |
| ENSG00000229202 | <i>PRR3</i> | 11.6 | 1.62E-05 | 11.4 | 4.66E-05 |
| ENSG00000257315 | <i>ZBED6</i> | 10.9 | 0.0219 | 11.7 | 0.00321 |
| ENSG00000173281 | <i>PPP1R3B</i> | 12.8 | 2.87E-05 | 12.5 | 0.000109 |
| ENSG00000278550 | <i>SLC43A2</i> | 11 | 0.00538 | 11 | 0.00697 |
| ENSG00000283780 | <i>MAML1</i> | 11.5 | 0.0353 | 11.6 | 0.0357 |
| ENSG00000285526 | <i>AC020907.6</i> | 10.8 | 0.0365 | 10.9 | 0.0353 |
| ENSG00000100218 | <i>RSPH14</i> | -11.1 | 2.16E-05 | -6.3 | 0.000209 |
| ENSG00000164756 | <i>SLC30A8</i> | -11.7 | 9.07E-06 | -7.07 | 4.82E-05 |
| ENSG00000172482 | <i>AGXT</i> | -2.28 | 0.0456 | -9.37 | 0.000182 |
| ENSG00000180815 | <i>MAP3K15</i> | -10 | 0.000305 | -10 | 0.000222 |
| ENSG00000259522 | <i>AL136295.4</i> | -10.5 | 8.32E-05 | -10.5 | 4.28E-05 |
| ENSG00000273291 | <i>AC092042.3</i> | -10.8 | 0.00164 | -10.8 | 0.00158 |
| ENSG00000273780 | <i>ARHGAP23</i> | -11 | 0.0364 | -11 | 0.0408 |
| ENSG00000280249 | <i>AL691477.1</i> | -4.06 | 0.000224 | -10.5 | 4.51E-06 |
| ENSG00000285130 | <i>AL358113.1</i> | -11.5 | 0.0012 | -3.53 | 0.0357 |

conditions except at 12hpi in the Washington strain, which include “UV response cluster G28”, “serum response 120 MCF10A”, “lung vasculature development”, and “silenced by tumor microenvironment”. Additional terms that were positively regulated in all conditions besides 6hpi in the Washington strain include “tight junction interactions” and “calcium independent cell-cell adhesion *via* plasma membrane cell adhesion molecules”. Many of these terms are involved in how the body deals with and responds to metal ions. These terms, and their respective adjusted p-values, can be found in [Table 5](#). On further comparison of the dysregulated terms we also found that there were more similarities between different time points for the same strain than for matched time points of the two different strains.

At 6hpi and 12hpi with the New York strain there are seven shared terms that are negatively regulated. These terms include “farnesyl diphosphate metabolic process,” “cholesterol biosynthesis”, “mevalonate pathway”, “SREBF targets”, “POR targets in limb bud”, and “POR targets global.” Many of these negatively regulated terms play a role in metabolism, specifically involving cholesterol and its precursors. There are also seven terms that are positively regulated at 6hpi and 12hpi with the New York strain. This includes “CXCR chemokine receptor binding,” “IFNA response,” “IFNB1 targets,” “Upregulated in beta interferon treated bronchial epithelial cells,” “Upregulated in COVID19 bronchial epithelial cells,” “Upregulated in COVID19 SARS-CoV-2 infection CALU3 cells,” and “Upregulated in human parainfluenza virus 3 infection A594 cells.” These positively regulated terms are mainly related to the immune system or

represent groups of genes noted to be affected after viral infections. The adjusted p-values for these terms can be found in [Table 6](#).

Interestingly, there are no terms that are exclusively shared at 6hpi and 12hpi with the Washington strain and there are no terms exclusively shared at 12hpi with either virus. There are, however, five terms that are positively regulated at 6hpi with both the New York and the Washington strain. These terms include “UV response cluster G2,” “Positive regulation of immature T-cell proliferation,” “regulation of adiponectin secretion,” “CDH1 targets,” and “Interleukin 10 signaling.” Similar to the terms that were affected at 6hpi and 12hpi with the New York strain, these terms are mostly related to the immune system. A list of these terms and their respective adjusted p-values can be found in [Table 7](#).

Intracellular signaling pathways

To determine what intracellular pathways were significantly affected by the viral infection, we used the differentially expressed genes that we previously identified as input for the SPIA algorithm. This method generates a null distribution for each of over 1500 pathways that are present in five public pathway databases, which facilitates subsequent statistical calculations. These signaling pathways include manually curated protein-protein interactions, particularly those that convey signals from receptors on the cell surface to the nucleus. We performed this analysis for infections with each viral isolate and time point ([Supplementary Tables S14-19](#)).

TABLE 4 Directionality and adjusted p-values for enriched terms across multiple time points and SARS-CoV-2 isolates.

| Database | Term | New York 6hpi | | Washington 6hpi | | New York 12hpi | | Washington 12hpi | |
|----------|---|----------------------|-----------|----------------------|-----------|----------------------|-----------|----------------------|-----------|
| | | FDR adjusted p-value | Direction | FDR adjusted p-value | Direction | FDR adjusted p-value | Direction | FDR adjusted p-value | Direction |
| GO | Detoxification of inorganic compound | 0.00043 | Down | 0.000104 | Down | 0.000353 | Down | 2.05E-06 | Down |
| Reactome | Metallothioneins bind metal | 0.00126 | Down | 0.000104 | Down | 0.001844 | Down | 1.70E-05 | Down |
| Reactome | Response to metal ions | 0.0086 | Down | 0.000813 | Down | 0.00269 | Down | 6.25E-05 | Down |
| Hallmark | Amit serum response 120 MCF10A | 0.001 | Up | 0.018998 | Up | 0.01118 | Up | | |
| Hallmark | Dazard UV response cluster G28 | 0.00043 | Up | 0.000602 | Up | 0.042113 | Up | | |
| GO | Lung vasculature development | 0.00043 | Up | 0.000813 | Up | 0.033232 | Up | | |
| Hallmark | Lin silenced by tumor microenvironment | 0.00043 | Up | 0.003791 | Up | 0.0189 | Up | | |
| GO | Calcium independent cell-cell adhesion <i>via</i> plasma membrane cell adhesion molecules | 0.00341 | Up | | | 0.00403 | Up | 0.014062 | Up |
| Reactome | Tight junction interactions | 0.01483 | Up | | | 0.01118 | Up | 0.034701 | Up |
| GO | Cellular response to zinc ion | | | 0.009728 | Down | 0.033232 | Down | 0.009274 | Down |
| Hallmark | Zheng response to arsenite up | | | 0.049621 | Down | 0.013182 | Down | 0.000588 | Down |
| Hallmark | Blanco Melo Beta interferon treated bronchial epithelial cells up | 0.00341 | Up | | | 0.013182 | Up | | |
| Hallmark | Blanco Melo COVID-19 bronchial epithelial cells SARS-Cov-2 infection up | 0.00043 | Up | | | 0.033232 | Up | | |
| Hallmark | Blanco Melo COVID-19 SARS-CoV-2 infection Calu-3 cells up | 0.00643 | Up | | | 0.006878 | Up | | |
| Hallmark | Blanco Melo human parainfluenza virus 3 infection A549 cells up | 0.00045 | Up | | | 0.027899 | Up | | |
| GO | CXCR chemokine receptor binding | 0.01568 | Up | | | 0.013182 | Up | | |
| Hallmark | Hecker IFNB1 targets | 0.00043 | Up | | | 0.009306 | Up | | |
| Hallmark | Moserle IFNA response | 0.00341 | Up | | | 0.003021 | Up | | |
| Reactome | Cholesterol biosynthesis | 0.00318 | Down | | | 0.003408 | Down | | |
| GO | Farnesyl diphosphate metabolic process | 0.01853 | Down | | | 0.01118 | Down | | |
| Hallmark | Schmidt POR targets in limb bud up | 0.00064 | Down | | | 0.000353 | Down | | |
| Hallmark | Weng POR targets global up | 0.03123 | Down | | | 0.00687 | Down | | |
| WP | Cholesterol biosynthesis pathway | 0.00047 | Down | | | 0.000353 | Down | | |
| WP | Mevalonate pathway | 0.00142 | Down | | | 0.001967 | Down | | |
| Hallmark | Horton SREBF targets | 0.00085 | Down | | | 0.000618 | Down | | |
| Reactome | Interleukin 10 signaling | 0.00017 | Up | 0.000529 | Up | | | | |
| GO | Positive regulation of immature T-cell proliferation | 0.00081 | Up | 0.002769 | Up | | | | |
| GO | Regulation of adiponectin secretion | 0.00498 | Up | 0.010201 | Up | | | | |
| Hallmark | Onder CDH1 targets 3 down | 0.00028 | Up | 0.010201 | Up | | | | |
| Hallmark | Dazard UV response cluster G2 | 0.00251 | Up | 0.003791 | Up | | | | |
| Hallmark | Liang silenced by methylation down | 0.01779 | Down | | | | | 0.02866 | Up |
| Hallmark | Browne interferon responsive genes | 0.00043 | Up | | | | | | |
| Hallmark | Croonquist IL6 deprivation down | 0.00111 | Down | | | | | | |
| Hallmark | Blanco Melo bronchial epithelial cells Influenza A delNS1 infection down | 0.00043 | Down | | | | | | |
| Hallmark | Graham normal quiescent vs normal dividing down | 0.0012 | Down | | | | | | |
| Hallmark | Kang doxorubicin resistance up | 0.00142 | Down | | | | | | |
| Hallmark | Rosty cervical cancer proliferation cluster | 0.0012 | Down | | | | | | |
| GO | Gas transport | | | 0.009248 | Up | | | | |
| Hallmark | Shin B-cell lymphoma cluster 6 | | | 0.002769 | Up | | | | |

(Continued)

TABLE 4 Continued

| Database | Term | New York 6hpi | | Washington 6hpi | | New York 12hpi | | Washington 12hpi | |
|----------|--|----------------------|-----------|----------------------|-----------|----------------------|-----------|----------------------|-----------|
| | | FDR adjusted p-value | Direction | FDR adjusted p-value | Direction | FDR adjusted p-value | Direction | FDR adjusted p-value | Direction |
| Hallmark | Amit delayed early genes | | | | | 0.014027 | Up | | |
| Hallmark | Bowie response to tamoxifen | | | | | 0.011965 | Up | | |
| GO | Regulation of cellular pH reduction | | | | | | | 0.037071 | Up |
| HP | Orthokeratosis | | | | | | | 0.009274 | Up |
| Hallmark | Montero thyroid cancer poor survival up | | | | | | | 0.009274 | Up |
| Hallmark | Fung IL2 signaling 2 | | | | | | | 0.00375 | Down |
| GO | Box C/D snoRNP complex | | | | | | | 0.002785 | Down |
| GO | Small subunit processome | | | | | | | 0.013573 | Down |
| Hallmark | Nadella PRKAR1A targets down | | | | | | | 0.009274 | Down |
| Reactome | rRNA modification in the nucleus and cytosol | | | | | | | 0.021817 | Down |

This analysis yielded 29 significantly affected pathways that were present in at least one of the conditions. A list of these pathways and whether they were activated or inhibited in each condition is shown in [Table 8](#). This included many pathways that are involved in the process of translation as well as rRNA processing. We manually reviewed these pathways to determine those that were shared between time points and conditions. We found that the “plasminogen activating cascade” signaling pathway was shared between the 6hpi time points of infection with the New York and Washington strains. This pathway was

inhibited in both conditions and is involved in cell invasion, fibrin degradation, and matrix turnover ([Patrizia Stoppelli, 2013](#)). The 12hpi time points shared no significantly affected pathways and the 24hpi time points shared two significantly affected pathways. Infections with either virus inhibited the olfactory transduction pathway and activated the platelet derived growth factor (PDGFR)-beta signaling pathway.

We also compared the pathways that were dysregulated at different time points during infection with the same virus. We found that the 6hpi and 12hpi time points for infection with

TABLE 5 Directionality and adjusted p-values for enriched terms associated with metal ions across multiple time points and SARS-CoV-2 isolates.

| Database | Term | New York 6hpi | | Washington 6hpi | | New York 12hpi | | Washington 12hpi | |
|----------|---|----------------------|-----------|----------------------|-----------|----------------------|-----------|----------------------|-----------|
| | | FDR adjusted p-value | Direction | FDR adjusted p-value | Direction | FDR adjusted p-value | Direction | FDR adjusted p-value | Direction |
| GO | Detoxification of inorganic compound | 0.00043 | Down | 0.000104 | Down | 0.000353 | Down | 2.05E-06 | Down |
| Reactome | Metallothioneins bind metal | 0.00126 | Down | 0.000104 | Down | 0.001844 | Down | 1.70E-05 | Down |
| Reactome | Response to metal ions | 0.0086 | Down | 0.000813 | Down | 0.00269 | Down | 6.25E-05 | Down |
| Hallmark | Amit serum response 120 MCF10A | 0.001 | Up | 0.018998 | Up | 0.01118 | Up | | |
| Hallmark | Dazard UV response cluster G28 | 0.00043 | Up | 0.000602 | Up | 0.042113 | Up | | |
| GO | Lung vasculature development | 0.00043 | Up | 0.000813 | Up | 0.033232 | Up | | |
| Hallmark | Lin silenced by tumor microenvironment | 0.00043 | Up | 0.003791 | Up | 0.0189 | Up | | |
| GO | Calcium independent cell-cell adhesion <i>via</i> plasma membrane cell adhesion molecules | 0.00341 | Up | | | 0.00403 | Up | 0.014062 | Up |
| Reactome | Tight junction interactions | 0.01483 | Up | | | 0.01118 | Up | 0.034701 | Up |
| GO | Cellular response to zinc ion | | | 0.009728 | Down | 0.033232 | Down | 0.009274 | Down |
| Hallmark | Zheng response to arsenite up | | | 0.049621 | Down | 0.013182 | Down | 0.000588 | Down |

TABLE 6 Directionality and adjusted p-values for enriched terms associated with host immune response across multiple time points with the New York isolate of SARS-CoV-2.

| Database | Term | New York 6hpi | | New York 12hpi | |
|----------|---|----------------------|-----------|----------------------|-----------|
| | | FDR adjusted p-value | Direction | FDR adjusted p-value | Direction |
| Hallmark | Blanco Melo Beta interferon treated bronchial epithelial cells up | 0.00341 | Up | 0.013182 | Up |
| Hallmark | Blanco Melo COVID-19 bronchial epithelial cells SARS-Cov-2 infection up | 0.00043 | Up | 0.033232 | Up |
| Hallmark | Blanco Melo COVID-19 SARS-CoV-2 infection Calu-3 cells up | 0.00643 | Up | 0.006878 | Up |
| Hallmark | Blanco Melo human parainfluenza virus 3 infection A549 cells up | 0.00045 | Up | 0.027899 | Up |
| GO | CXCR chemokine receptor binding | 0.01568 | Up | 0.013182 | Up |
| Hallmark | Hecker IFNB1 targets | 0.00043 | Up | 0.009306 | Up |
| Hallmark | Moserle IFNA response | 0.00341 | Up | 0.003021 | Up |
| Reactome | Cholesterol biosynthesis | 0.00318 | Down | 0.003408 | Down |
| GO | Farnesyl diphosphate metabolic process | 0.01853 | Down | 0.01118 | Down |
| Hallmark | Schmidt POR targets in limb bud up | 0.00064 | Down | 0.000353 | Down |
| Hallmark | Weng POR targets global up | 0.03123 | Down | 0.00687 | Down |
| WP | Cholesterol biosynthesis pathway | 0.00047 | Down | 0.000353 | Down |
| WP | Mevalonate pathway | 0.00142 | Down | 0.001967 | Down |
| Hallmark | Horton SREBF targets | 0.00085 | Down | 0.000618 | Down |

the New York strain shared two dysregulated pathways including the activated “keratinization” pathway, and the inhibited “plasminogen activating cascade”. The 12hpi and 24hpi time points both showed dysregulation in the “actin cytoskeleton” pathway during infection with the NY strain; however, this pathway was affected in different directions—the 12hpi condition being inhibited and the 24hpi condition being activated. We observed no significantly dysregulated signaling pathways for the Washington strain at multiple time points.

The conditions that shared the most dysregulated pathways were the 24hpi New York condition and the 12hpi Washington condition. They shared a total of 10 dysregulated pathways which mainly dealt with translation. These 10 pathways were all inhibited in both conditions. Infection with either viral strain led to dysregulation in the “SRP-dependent cotranslational protein targeting to membrane” pathway but in different

directions with the New York condition being activated and the Washington condition being inhibited.

Discussion

The goal of the current study was to generate and analyze RNA-sequencing data to compare the underlying mechanism(s) associated with infection at three time points (6, 12, and 24 hpi) with two SARS-CoV-2 isolates that were collected during the early stages of the pandemic. We found thousands of differentially expressed genes, hundreds of enriched functional terms, and various signaling pathways that provide additional insight into why one of these strains may result in higher pathogenesis and mortality in the human population.

Our identification of differentially expressed genes included several genes that are subunits of protein phosphatase 1 (PP1),

TABLE 7 Directionality and adjusted p-values for enriched terms identified at 6hpi with either the New York or Washington isolate of SARS-CoV-2.

| Database | Term | New York 6hpi | | Washington 6hpi | |
|----------|--|----------------------|-----------|----------------------|-----------|
| | | FDR adjusted p-value | Direction | FDR adjusted p-value | Direction |
| Reactome | Interleukin 10 signaling | 0.00017 | Up | 0.000529 | Up |
| GO | Positive regulation of immature T-cell proliferation | 0.00081 | Up | 0.002769 | Up |
| GO | Regulation of adiponectin secretion | 0.00498 | Up | 0.010201 | Up |
| Hallmark | Onder CDH1 targets 3 down | 0.00028 | Up | 0.010201 | Up |
| Hallmark | Dazard UV response cluster G2 | 0.00251 | Up | 0.003791 | Up |

TABLE 8 All significant positively (+) or negatively (-) dysregulated intracellular signaling pathways across multiple time points with either SARS-CoV-2 isolate.

| Pathway name | NY 6hr | NY 12hr | NY 24hr | WA 6hr | WA 12hr | WA 24hr |
|---|--------------|--------------|--------------|--------------|--------------|--------------|
| Cell cycle | 0.022257 (-) | | | | | |
| Keratinization | 0.001558 (+) | 0.017467 (+) | | | | |
| Stabilization and expansion of the E-cadherin adherens junction | 0.017463 (+) | | | | | |
| Alzheimer disease-presenilin pathway | 0.004439 (+) | | | | | |
| Plasminogen activating cascade | 0.007253 (-) | 0.034549 (-) | | 0.036979 (-) | | |
| Integrin signalling pathway | 0.007253 (+) | | | | | |
| Regulation of actin cytoskeleton | | 0.035812 (-) | 0.010134 (+) | | | |
| Signaling by TGF-beta Receptor Complex | | 0.00051 (+) | | | | |
| mTOR signaling pathway | | 0.049417 (-) | | | | |
| Olfactory transduction | | | 0.000384 (-) | | | 1.58E-05 (-) |
| Peptide chain elongation | | | 4.76E-09 (-) | | 1.62E-08 (-) | |
| Nonsense-Mediated Decay (NMD) | | | 4.76E-09 (-) | | 1.39E-05 (-) | |
| Nonsense Mediated Decay (NMD) enhanced by the Exon Junction Complex (EJC) | | | 4.76E-09 (-) | | 1.39E-05 (-) | |
| Eukaryotic Translation Elongation | | | 4.76E-09 (-) | | 3.23E-09 (-) | |
| Eukaryotic Translation Termination | | | 1.63E-06 (-) | | 1.63E-06 (-) | |
| Translation | | | 7.03E-05 (-) | | 0.000295 (-) | |
| SRP-dependent cotranslational protein targeting to membrane | | | 0.000171 (+) | | 0.000204 (-) | |
| GTP hydrolysis and joining of the 60S ribosomal subunit | | | 0.000417 (-) | | 0.000238 (-) | |
| Eukaryotic Translation Initiation | | | 0.001691 (-) | | 0.000295 (-) | |
| Cap-dependent Translation Initiation | | | 0.001691 (-) | | 0.000295 (-) | |
| rRNA processing in the nucleus and cytosol | | | 0.004313 (-) | | 3.78E-13 (-) | |
| PDGFR-beta signaling pathway | | | 0.010419 (+) | | | 0.003059 (+) |
| Apoptosis | | | | 1.59E-05 (+) | | |
| Amyotrophic lateral sclerosis (ALS) | | | | 0.001498 (+) | | |
| MAPK signaling pathway | | | | 0.002158 (+) | | |
| Hippo signaling pathway | | | | | 0.006153 (+) | |
| Major pathway of rRNA processing in the nucleolus and cytosol | | | | | 3.32E-13 (-) | |
| rRNA processing | | | | | 4.45E-13 (-) | |
| Gene Expression | | | | | 0.000162 (-) | |

NY, New York; WA, Washington; "+", Activated; "-", Inhibited.

particularly *PPP1R11*, *PPP1R3B*, and *PPP1R18*. Previous studies have found that PP1 plays a role in dephosphorylating PP1 to reduce translation during some viral infections and recent studies have indicated a potential role in SARS-CoV-2 infections (He et al., 1997; Nekhai et al., 2007; Ilinykh et al., 2014; McDermott et al., 2016). Another gene found to be differentially expressed is *GSDMC*, whose protein product can be processed by caspase, which leads to pyroptosis (Liu et al., 2021). Pyroptosis has been observed in macrophages infected

with SARS-CoV-2, which may be a factor that promotes the large inflammatory response associated with severe COVID-19 (Yap et al., 2020; Ferreira et al., 2021). Another differentially expressed gene is *DDX39B*, which is a mRNA splicing factor that plays a role in the nuclear export of mRNA (Fleckner et al., 1997; Zhang et al., 2021). It has also been found to play a role in inhibiting NF-kappaB (Szymura et al., 2020). Our study found that *DDX39B* was up-regulated in many of the sample conditions, which could be one of the methods the virus uses

to avoid an inflammatory response after infection. Other studies have found that *DDX39B* can be targeted by the viral Nsp1 (Zhang et al., 2021) protein that serves to suppress the host immune response and decrease host gene expression so that cellular resources can be allocated to the translation of viral proteins (Yuan et al., 2021). A study of fatal COVID-19 patients found that *DDX39B* was significantly down regulated, which suggests this gene product may play a role in differentiating between mild and severe cases of COVID-19; particularly since the downregulation of *DDX39B* would be expected to trigger an inflammatory response that may get out of control in patients with severe COVID-19 (Wang et al., 2022).

We specifically chose our earliest time point to be 6hpi to give the virus sufficient time to affect the host cell. Although we were unable to directly quantify the presence of viral gene products in this study, it is known that viral proteins can affect the innate immune response (Shemesh et al., 2021; Vazquez et al., 2021; Cheemarla et al., 2021; Zhao et al., 2021) negatively impact the translation of host transcripts (Thoms et al., 2020; Simeoni et al., 2021). We assume the virus would produce relatively low levels of gene products prior to 6hpi, which would usually activate the interferon and other antiviral responses. However, the virus remains undetectable in alveolar macrophages (Dalskov et al., 2020), and may be only minimally detected in other cell types. This strategy enables the virus to produce its own components until the cell is overwhelmed and no longer able to contain the infection.

Our analysis of the GO enrichment results identified gene products associated with Zinc. Interestingly, recent work has shown that multiple host zinc metalloproteins interact with viral gene products including orf8 (Shemesh et al., 2021). In addition, Zinc has been shown to inhibit the viral protease so any decrease in host intracellular Zinc-related functions is likely biologically relevant (Vazquez et al., 2021; Cheemarla et al., 2021). Although the immune system component of infection has been well characterized (Thoms et al., 2020; Zhao et al., 2021), the modification of tight junctions and cell adhesion have also been associated with viral pathogenesis (Dalskov et al., 2020; Simeoni et al., 2021; Chasapis et al., 2021). In infections with the New York strain, we also see a negative regulation of terms that are involved in cholesterol biosynthesis. It has been shown that cholesterol plays an important role in many steps of the coronavirus life cycle and lower levels of cholesterol have been associated with increased COVID-19 severity and mortality (Panchariya et al., 2021; Grifagni et al., 2021; Ferrarini et al., 2021). We also see many GO terms that are related to the immune system and infection, which is to be expected. These include sets of genes that were observed to be affected in other experiments with SARS-CoV-2 in a few different cell types (Liang et al., 2020). Additional studies are needed to better

understand the cellular and viral components that play a role in these functions.

The statistical signaling pathway analysis identified the plasminogen activating cascade as being inhibited at 6hpi and 12hpi. Although this pathway has been identified previously in the hamster model (Rauti et al., 2021), its directionality was not reported. The PDGFR pathway has been identified previously as decreasing SARS-CoV-2 replication (Cao et al., 2021). However, our NHBE cell model showed evidence that this pathway was positively affected 24hpi. We found it interesting that a small number of pathways could be modulated in opposite directions at the 12hpi and 24hpi time points for the NY strain. This may be a contributor to the increased pathogenesis associated with infections occurring in NY early in the pandemic. We were not surprised that infection with either virus isolate would affect 10 translation-related processes, since viruses take control of the host cellular machinery to generate genetic material, produce new viral proteins, and reduce host immune-related defenses (Raghavan et al., 2021; Zinellu et al., 2021; Masana et al., 2021; Dai et al., 2022).

Our validation of the previous finding that SARS-CoV-2 infection has a statistically significant effect on the actin cytoskeleton pathway was also of interest (Blanco-Melo et al., 2020; Suresh et al., 2021). At least two explanations for this observation are possible. The first could be that infected cells reorganize their cytoskeleton either in an attempt to prevent virus replication or as a mechanism for the virus to assemble virions more efficiently inside of the cell. The second possible explanation may only be relevant in the context of an infected human, where this pathway has been suggested to play a role in vascular structure in aging mice (Klann et al., 2020). It is possible that actin could at least partially explain some of the cardiovascular, neurological, and other signs and symptoms that are observed in a subset of infected patients (Belhadjer et al., 2020; Liu et al., 2020; Yuan et al., 2020; Alexander et al., 2021; Khatoon et al., 2021; Kim et al., 2021).

We found the observation that the SRP-dependent Cotranslational Protein Targeting to Membrane pathway was activated (NY strain) or inhibited (WA strain) to be of interest. This pathway has been reported previously in human samples, although the lineage(s) of the SARS-CoV-2 viruses were not consistently reported in these studies (Banerjee et al., 2020; Rivera et al., 2020; Daamen et al., 2021; Ibrahim and Ellakwa, 2021; Mohan and Wollert, 2021; Messina et al., 2021). A separate computational analysis used a machine learning approach to identify members of this same pathway to have high accuracy as markers of SARS-CoV-2 infection (Rabaglino et al., 2021).

It is important to recognize that the present study specifically focused on comparing the intracellular host transcriptional response to two viral isolates collected early in the pandemic. Additional experiments will be needed to better characterize how subsequent emergent SARS-CoV-2 variants may interact with, and affect, the host response and disease severity.

Conclusion

This study provides additional insight into the intracellular host transcriptional response associated with either the New York or Washington SARS-CoV-2 isolates, which were collected in early 2020 when the pandemic was in its early stages. We identified genes, annotated functions, and signaling pathways that may be associated with the different pathogenicity profiles for these strains. We expect that these findings will be relevant to the development of improved prophylactics and/or therapeutics to minimize the underlying mechanistic effects of severe disease.

Data availability statement

The datasets presented in this study can be found in online repositories. The names of the repository/repositories and accession number(s) can be found below: <https://www.ncbi.nlm.nih.gov/geo/>, GSE207923.

Author contributions

TS contributed to data analysis, data interpretation, and manuscript preparation. AS-L and J.B.L. contributed laboratory experiments and manuscript review. RR and BB contributed experimental design, data interpretation and manuscript review. BP contributed inception, data analysis, data interpretation, code, and manuscript preparation. All authors contributed to the article and approved the submitted version.

Acknowledgments

The following reagent was deposited by the Centers for Disease Control and Prevention and obtained through BEI Resources, NIAID, NIH: SARS-Related Coronavirus 2, Isolate USA-WA1/2020, NR-52281. The following reagent was obtained through BEI Resources, NIAID, NIH: SARS-Related Coronavirus 2, Isolate New York 1-PV02001/2020, NR-52368. We are grateful to the BYU Office of Research Computing for providing the computational resources needed to complete this study.

Conflict of interest

The authors declare that the research was conducted in the absence of any commercial or financial relationships that could be construed as a potential conflict of interest.

Publisher's note

All claims expressed in this article are solely those of the authors and do not necessarily represent those of their affiliated organizations, or those of the publisher, the editors and the reviewers. Any product that may be evaluated in this article, or claim that may be made by its manufacturer, is not guaranteed or endorsed by the publisher.

Supplementary material

The Supplementary Material for this article can be found online at: <https://www.frontiersin.org/articles/10.3389/fcimb.2022.1009328/full#supplementary-material>

SUPPLEMENTARY FIGURE 1

Pie charts of significant Gene Ontology functional terms across both strains at 6hpi and 12hpi.

SUPPLEMENTARY TABLE 1

Significant differentially expressed genes in the NY isolate (infected vs mock-infected) at 6hpi.

SUPPLEMENTARY TABLE 2

Significant differentially expressed genes in the NY isolate (infected vs mock-infected) at 12hpi.

SUPPLEMENTARY TABLE 3

Significant differentially expressed genes in the NY isolate (infected vs mock-infected) at 24hpi.

SUPPLEMENTARY TABLE 4

Significant differentially expressed genes in the WA isolate (infected vs mock-infected) at 6hpi.

SUPPLEMENTARY TABLE 5

Significant differentially expressed genes in the WA isolate (infected vs mock-infected) at 12hpi.

SUPPLEMENTARY TABLE 6

Significant differentially expressed genes in the WA isolate (infected vs mock-infected) at 24hpi.

SUPPLEMENTARY TABLE 7

Combined set of most significant differentially expressed genes across viral isolates and time points.

SUPPLEMENTARY TABLE 8

Significant affected functional terms in the NY isolate (infected vs mock-infected) at 6hpi.

SUPPLEMENTARY TABLE 9

Significant affected functional terms in the NY isolate (infected vs mock-infected) at 12hpi.

SUPPLEMENTARY TABLE 10

Significant affected functional terms in the NY isolate (infected vs mock-infected) at 24hpi.

SUPPLEMENTARY TABLE 11

Significant affected functional terms in the WA isolate (infected vs mock-infected) at 6hpi.

SUPPLEMENTARY TABLE 12

Significant affected functional terms in the WA isolate (infected vs mock-infected) at 12hpi.

SUPPLEMENTARY TABLE 13

Significant affected functional terms in the WA isolate (infected vs mock-infected) at 24hpi.

SUPPLEMENTARY TABLE 14

Significant affected signaling pathways in the NY isolate (infected vs mock-infected) at 6hpi.

SUPPLEMENTARY TABLE 15

Significant affected signaling pathways in the NY isolate (infected vs mock-infected) at 12hpi.

SUPPLEMENTARY TABLE 16

Significant affected signaling pathways in the NY isolate (infected vs mock-infected) at 24hpi.

SUPPLEMENTARY TABLE 17

Significant affected signaling pathways in the WA isolate (infected vs mock-infected) at 6hpi.

SUPPLEMENTARY TABLE 18

Significant affected signaling pathways in the WA isolate (infected vs mock-infected) at 12hpi.

SUPPLEMENTARY TABLE 19

Significant affected signaling pathways in the WA isolate (infected vs mock-infected) at 24hpi.

References

- Alexander, M. R., Brice, A. M., Jansen van Vuren, P., Rootes, C. L., Tribolet, L., Cowled, C., et al. (2021). Ribosome-profiling reveals restricted post transcriptional expression of antiviral cytokines and transcription factors during SARS-CoV-2 infection. *Int. J. Mol. Sci.* 22 (7), 3392. doi: 10.3390/ijms22073392
- WHO. 2022. WHO coronavirus (COVID-19) dashboard. Available at: <https://covid19.who.int>.
- Babraham Bioinformatics. 2022. Babraham bioinformatics - trim galore!. Available at: https://www.bioinformatics.babraham.ac.uk/projects/trim_galore/.
- Banerjee, A. K., Blanco, M. R., Bruce, E. A., Honson, D. D., Chen, L. M., Chow, A., et al. (2020). SARS-CoV-2 disrupts splicing, translation, and protein trafficking to suppress host defenses. *Cell* 183 (5), 1325–39.e21. doi: 10.1016/j.cell.2020.10.004
- Baric, R. S. (2020). Emergence of a highly fit SARS-CoV-2 variant. *N Engl. J. Med.* 383 (27), 2684–2686. doi: 10.1056/NEJMcibr2032888
- Belhadj, Z., Méot, M., Bajolle, F., Khraiche, D., Legendre, A., Abakka, S., et al. (2020). Acute heart failure in multisystem inflammatory syndrome in children in the context of global SARS-CoV-2 pandemic. *Circulation* 142 (5), 429–436. doi: 10.1161/CIRCULATIONAHA.120.048360
- Benedetti, F., Pachetti, M., Marini, B., Ippodrino, R., Ciccozzi, M., and Zella, D. (2020). SARS-CoV-2: March toward adaptation. *J. Med. Virol.* 92 (11), 2274–2276. doi: 10.1002/jmv.26233
- Blanco-Melo, D., Nilsson-Payant, B. E., Liu, W. C., Uhl, S., Hoagland, D., Möller, R., et al. (2020). Imbalanced host response to SARS-CoV-2 drives development of COVID-19. *Cell* 181 (5), 1036–1045. doi: 10.1016/j.cell.2020.04.026
- Brufsky, A. (2020). Distinct viral clades of SARS-CoV-2: Implications for modeling of viral spread. *J. Med. Virol.* 92 (9), 1386–1390. doi: 10.1002/jmv.25902
- Cao, W., Feng, Q., and Wang, X. (2021). Computational analysis of TMPRSS2 expression in normal and SARS-CoV-2-infected human tissues. *Chem. Biol. Interact.* 346, 109583. doi: 10.1016/j.cb.2021.109583
- Chasapis, C. T., Georgiopolou, A. K., Perlepes, S. P., Björklund, G., and Peana, M. (2021). A SARS-CoV-2 -human metalloproteome interaction map. *J. Inorg Biochem.* 219, 111423. doi: 10.1016/j.jinorgbio.2021.111423
- Cheemarla, N. R., Watkins, T. A., Mihaylova, V. T., Wang, B., Zhao, D., Wang, G., et al. (2021). Dynamic innate immune response determines susceptibility to SARS-CoV-2 infection and early replication kinetics. *J. Exp. Med.* 218 (8), e20210583. doi: 10.1084/jem.20210583
- Daamen, A. R., Bachali, P., Owen, K. A., Kingsmore, K. M., Hubbard, E. L., Labonte, A. C., et al. (2021). Comprehensive transcriptomic analysis of COVID-19 blood, lung, and airway. *Sci. Rep.* 11 (1), 7052. doi: 10.1038/s41598-021-86002-x
- Dai, J., Wang, H., Liao, Y., Tan, L., Sun, Y., Song, C., et al. (2022). Coronavirus infection and cholesterol metabolism. *Front. Immunol.* 13, 791267. doi: 10.3389/fimmu.2022.791267
- Dalskov, L., Møhlenberg, M., Thyrted, J., Blay-Cadanet, J., Poulsen, E. T., Folkersen, B. H., et al. (2020). SARS-CoV-2 evades immune detection in alveolar macrophages. *EMBO Rep.* 21 (12), e51252. doi: 10.15252/embr.202051252
- Durinck, S., Moreau, Y., Kasprzyk, A., Davis, S., De Moor, B., Brazma, A., et al. (2005). BioMart and bioconductor: a powerful link between biological databases and microarray data analysis. *Bioinformatics* 21 (16), 3439–3440. doi: 10.1093/bioinformatics/bti525
- Ferrarini, M. G., Lal, A., Rebollo, R., Gruber, A. J., Guarracino, A., Gonzalez, I. M., et al. (2021). Genome-wide bioinformatic analyses predict key host and viral factors in SARS-CoV-2 pathogenesis. *Commun. Biol.* 4 (1), 590. doi: 10.1038/s42003-021-02095-0
- Ferreira, A. C., Soares, V. C., de Azevedo-Quintanilha, I. G., Dias S da, S. G., Fintelman-Rodrigues, N., Sacramento, C. Q., et al. (2021). SARS-CoV-2 engages inflammasome and pyroptosis in human primary monocytes. *Cell Death Discov.* 7 (1), 43. doi: 10.1038/s41420-021-00428-w
- Fleckner, J., Zhang, M., Valcárcel, J., and Green, M. R. (1997). U2AF65 recruits a novel human DEAD box protein required for the U2 snRNP-branchpoint interaction. *Genes Dev.* 11 (14), 1864–1872. doi: 10.1101/gad.11.14.1864
- Forster, P., Forster, L., Renfrew, C., and Forster, M. (2020). Phylogenetic network analysis of SARS-CoV-2 genomes. *Proc. Natl. Acad. Sci. U S A* 117 (17), 9241–9243. doi: 10.1073/pnas.2004999117
- Grifagni, D., Calderone, V., Giuntini, S., Cantini, F., Fragai, M., and Banci, L. (2021). SARS-CoV-2 m inhibition by a zinc ion: structural features and hints for drug design. *Chem. Commun.* 57 (64), 7910–7913. doi: 10.1039/D1CC02956H
- He, B., Gross, M., and Roizman, B. (1997). The gamma(1)34.5 protein of herpes simplex virus 1 complexes with protein phosphatase 1alpha to dephosphorylate the alpha subunit of the eukaryotic translation initiation factor 2 and preclude the shutoff of protein synthesis by double-stranded RNA-activated protein kinase. *Proc. Natl. Acad. Sci. U S A* 94 (3), 843–848. doi: 10.1073/pnas.94.3.843
- Huber, W., Carey, V. J., Gentleman, R., Anders, S., Carlson, M., Carvalho, B. S., et al. (2015). Orchestrating high-throughput genomic analysis with bioconductor. *Nat. Methods* 12 (2), 115–121. doi: 10.1038/nmeth.3252
- Ibrahim, I. H., and Ellakwa, D. E. S. (2021). SUMO pathway, blood coagulation and oxidative stress in SARS-CoV-2 infection. *Biochem. Biophys. Rep.* 26, 100938. doi: 10.1016/j.bbrep.2021.100938
- Illyukh, P. A., Tigabu, B., Ivanov, A., Ammosova, T., Obukhov, Y., Garron, T., et al. (2014). Role of protein phosphatase 1 in dephosphorylation of Ebola virus VP30 protein and its targeting for the inhibition of viral transcription. *J. Biol. Chem.* 289 (33), 22723–22738. doi: 10.1074/jbc.M114.575050
- Jassal, B., Matthews, L., Viteri, G., Gong, C., Lorente, P., Fabregat, A., et al. (2020). The reactome pathway knowledgebase. *Nucleic Acids Res.* 48 (D1), D498–D503. doi: 10.1093/nar/gkz1031
- Kanehisa, M., and Goto, S. (2000). KEGG: kyoto encyclopedia of genes and genomes. *Nucleic Acids Res.* 28 (1), 27–30. doi: 10.1093/nar/28.1.27
- Khatoun, F., Prasad, K., and Kumar, V. (2021). COVID-19 associated nervous system manifestations. *Sleep Med.* 91, 231–236. doi: 10.1016/j.sleep.2021.07.005
- Kim, J. S., Jang, J. H., Kim, J. M., Chung, Y. S., Yoo, C. K., and Han, M. G. (2020). Genome-wide identification and characterization of point mutations in the SARS-CoV-2 genome. *Osong Public Health Res. Perspect.* 11 (3), 101–111. doi: 10.24171/j.phrp.2020.11.3.05
- Kim, D., Kim, S., Park, J., Chang, H. R., Chang, J., Ahn, J., et al. (2021). A high-resolution temporal atlas of the SARS-CoV-2 transcriptome and transcriptome. *Nat. Commun.* 12 (1), 5120. doi: 10.1038/s41467-021-25361-5
- Klann, K., Bojkova, D., Tascher, G., Ciesek, S., Münch, C., and Cinatl, J. (2020). Growth factor receptor signaling inhibition prevents SARS-CoV-2 replication. *Mol. Cell.* 80 (1), 164–74.e4. doi: 10.1016/j.molcel.2020.08.006
- Lara, P. C., Macias-Verde, D., and Burgos-Burgos, J. (2020). Age-induced NLRP3 inflammasome over-activation increases lethality of SARS-CoV-2 pneumonia in elderly patients. *Aging Dis.* 11 (4), 756–762. doi: 10.14336/AD.2020.0601

- Liang, Y., Wang, M. L., Chien, C. S., Yarmishyn, A. A., Yang, Y. P., Lai, W. Y., et al. (2020). Highlight of immune pathogenic response and hematopathologic effect in SARS-CoV, MERS-CoV, and SARS-CoV-2 infection. *Front. Immunol.* 11, 1022. doi: 10.3389/fimmu.2020.01022
- Liberzon, A., Birger, C., Thorvaldsdóttir, H., Ghandi, M., Mesirov, J. P., and Tamayo, P. (2015). The molecular signatures database (MSigDB) hallmark gene set collection. *Cell Syst.* 1 (6), 417–425. doi: 10.1016/j.cels.2015.12.004
- Liu, H., Gai, S., Wang, X., Zeng, J., Sun, C., Zhao, Y., et al. (2020). Single-cell analysis of SARS-CoV-2 receptor ACE2 and spike protein priming expression of proteases in the human heart. *Cardiovasc. Res.* 116 (10), 1733–1741. doi: 10.1093/cvr/cvaa191
- Liu, X., Xia, S., Zhang, Z., Wu, H., and Lieberman, J. (2021). Channelling inflammation: gasdermins in physiology and disease. *Nat. Rev. Drug Discovery* 20 (5), 384–405. doi: 10.1038/s41573-021-00154-z
- Masana, L., Correig, E., Ibarretxe, D., Anoro, E., Arroyo, J. A., Jericó, C., et al. (2021). Low HDL and high triglycerides predict COVID-19 severity. *Sci. Rep.* 11 (1), 7217. doi: 10.1038/s41598-021-86747-5
- McDermott, J. E., Mitchell, H. D., Gralinski, L. E., Eisfeld, A. J., Josset, L., Bankhead, A. 3rd, et al. (2016). The effect of inhibition of PP1 and TNF α signaling on pathogenesis of SARS coronavirus. *BMC Syst. Biol.* 10 (1), 93. doi: 10.1186/s12918-016-0336-6
- Mercatelli, D., and Giorgi, F. M. (2020). Geographic and genomic distribution of SARS-CoV-2 mutations. *Front. Microbiol.* 11, 1800. doi: 10.3389/fmicb.2020.01800
- Messina, F., Giombini, E., Montaldo, C., Sharma, A. A., Zoccoli, A., Sekaly, R. P., et al. (2021). Looking for pathways related to COVID-19: confirmation of pathogenic mechanisms by SARS-CoV-2-host interactome. *Cell Death Dis.* 12 (8), 788. doi: 10.1038/s41419-021-03881-8
- Mi, H., Huang, X., Muruganujan, A., Tang, H., Mills, C., Kang, D., et al. (2017). PANTHER version 11: expanded annotation data from gene ontology and reactome pathways, and data analysis tool enhancements. *Nucleic Acids Res.* 45 (D1), D183–D189. doi: 10.1093/nar/gkx1138
- Moghaddar, M., Radman, R., and Macreadie, I. (2021). Severity, pathogenicity and transmissibility of delta and lambda variants of SARS-CoV-2, toxicity of spike protein and possibilities for future prevention of COVID-19. *Microorganisms* 9 (10), 2167. doi: 10.3390/microorganisms9102167
- Mohan, J., and Wollert, T. (2021). Membrane remodeling by SARS-CoV-2 - double-enveloped viral replication. *Fac Rev.* 10, 17. doi: 10.12703/r/10-17
- Nekhai, S., Jerebtsova, M., Jackson, A., and Southerland, W. (2007). Regulation of HIV-1 transcription by protein phosphatase 1. *Curr. HIV Res.* 5 (1), 3–9. doi: 10.1096/fasebj.21.6.A1033-b
- Nowicka, M., and Robinson, M. D. (2016). DRIMSeq: a dirichlet-multinomial framework for multivariate count outcomes in genomics. *F1000Res.* 5, 1356. doi: 10.12688/f1000research.8900.2
- Pachetti, M., Marini, B., Benedetti, F., Giudici, F., Mauro, E., Storici, P., et al. (2020). Emerging SARS-CoV-2 mutation hot spots include a novel RNA-dependent-RNA polymerase variant. *J. Transl. Med.* 18 (1), 179. doi: 10.1186/s12967-020-02344-6
- Panchariya, L., Khan, W. A., Kuila, S., Sonkar, K., Sahoo, S., Ghoshal, A., et al. (2021). Zinc ion inhibits SARS-CoV-2 main protease and viral replication. *Chem. Commun.* 57 (78), 10083–10086. doi: 10.1039/D1CC03563K
- Pandey, U., Yee, R., Shen, L., Judkins, A. R., Bootwalla, M., Ryutov, A., et al. (2021). High prevalence of SARS-CoV-2 genetic variation and D614G mutation in pediatric patients with COVID-19. *Open Forum Infect. Dis.* 8 (6), ofaa551. doi: 10.1093/ofid/ofaa551
- Patrizia Stoppelli, M. (2013). “The plasminogen activation system in cell invasion,” in *Madame curie bioscience database* (Austin, Texas: Landes Bioscience).
- Patro, R., Duggal, G., Love, M. I., Irizarry, R. A., and Kingsford, C. (2017). Salmon provides fast and bias-aware quantification of transcript expression. *Nat. Methods* 14 (4), 417–419. doi: 10.1038/nmeth.4197
- Plante, J. A., Liu, Y., Liu, J., Xia, H., Johnson, B. A., Lokugamage, K. G., et al. (2021). Spike mutation D614G alters SARS-CoV-2 fitness. *Nature.* 592 (7852), 116–121. doi: 10.1038/s41586-020-2895-3
- Rabaglino, M. B., Wakabayashi, M., Pearson, J. T., and Jensen, L. J. (2021). Effect of age on the vascular proteome in middle cerebral arteries and mesenteric resistance arteries in mice. *Mech. Ageing Dev.* 200, 111594. doi: 10.1016/j.mad.2021.111594
- Radvak, P., Kwon, H. J., Kosikova, M., Ortega-Rodriguez, U., Xiang, R., Phue, J. N., et al. (2021). SARS-CoV-2 B.1.1.7 (alpha) and B.1.351 (beta) variants induce pathogenic patterns in K18-hACE2 transgenic mice distinct from early strains. *Nat. Commun.* 12 (1), 6559. doi: 10.1038/s41467-021-26803-w
- Raghavan, S., Kenchappa, D. B., and Leo, M. D. (2021). SARS-CoV-2 spike protein induces degradation of junctional proteins that maintain endothelial barrier integrity. *Front. Cardiovasc. Med.* 8, 687783. doi: 10.3389/fcvm.2021.687783
- Rauti, R., Shahoha, M., Leichtmann-Bardoogo, Y., Nasser, R., Paz, E., Tamir, R., et al. (2021). Effect of SARS-CoV-2 proteins on vascular permeability. *Elife* 10, e69314. doi: 10.7554/eLife.69314
- Rivera, B., Leyva, A., Portela, M. M., Moratorio, G., Moreno, P., Durán, R., et al. (2020). Quantitative proteomic dataset from oro- and naso-pharyngeal swabs used for COVID-19 diagnosis: Detection of viral proteins and host's biological processes altered by the infection. *Data Brief* 32, 106121. doi: 10.1016/j.dib.2020.106121
- Robinson, M. D., McCarthy, D. J., and Smyth, G. K. (2010). edgeR: a bioconductor package for differential expression analysis of digital gene expression data. *Bioinformatics.* 26 (1), 139–140. doi: 10.1093/bioinformatics/btp616
- Schaefer, C. F., Anthony, K., Krupa, S., Buchoff, J., Day, M., Hannay, T., et al. (2009). PID: the pathway interaction database. *Nucleic Acids Res.* 37 (Database issue), D674–D679. doi: 10.1093/nar/gkn653
- Scott, T. M., Jensen, S., and Pickett, B. E. (2021). A signaling pathway-driven bioinformatics pipeline for predicting therapeutics against emerging infectious diseases. *F1000Res.* 10, 330. doi: 10.12688/f1000research.52412.2
- Shemesh, M., Aktepe, T. E., Deearin, J. M., McAuley, J. L., Audsley, M. D., David, C. T., et al. (2021). SARS-CoV-2 suppresses IFN β production mediated by NSP1, 5, 6, 15, ORF6 and ORF7b but does not suppress the effects of added interferon. *PLoS Pathog.* 17 (8), e1009800. doi: 10.1371/journal.ppat.1009800
- Sherwani, S., and Khan, M. W. A. (2020). Cytokine response in SARS-CoV-2 infection in the elderly. *J. Inflamm. Res.* 13, 737–747. doi: 10.2147/JIR.S276091
- Simeoni, M., Cavinato, T., Rodriguez, D., and Gatfield, D. (2021). [nspl]ecting SARS-CoV-2-ribosome interactions. *Commun. Biol.* 4 (1), 715. doi: 10.1038/s42003-021-02265-0
- Smith, E. C., Blanc, H., Surdel, M. C., Vignuzzi, M., and Denison, M. R. (2013). Coronaviruses lacking exoribonuclease activity are susceptible to lethal mutagenesis: evidence for proofreading and potential therapeutics. *PLoS Pathog.* 9 (8), e1003565. doi: 10.1371/journal.ppat.1003565
- Suresh, V., Mohanty, V., Avula, K., Ghosh, A., Singh, B., Reddy, R. K., et al. (2021). Quantitative proteomics of hamster lung tissues infected with SARS-CoV-2 reveal host factors having implication in the disease pathogenesis and severity. *FASEB J.* 35 (7), e21713. doi: 10.1096/fj.202100431R
- Szymura, S. J., Bernal, G. M., Wu, L., Zhang, Z., Crawley, C. D., Voce, D. J., et al. (2020). DDX39B interacts with the pattern recognition receptor pathway to inhibit NF- κ B and sensitize to alkylating chemotherapy. *BMC Biol.* 18 (1), 1–17. doi: 10.1186/s12915-020-0764-z
- Tarca, A. L., Draghici, S., Khatri, P., Hassan, S. S., Mittal, P., Kim, J. S., et al. (2009). A novel signaling pathway impact analysis. *Bioinformatics.* 25 (1), 75–82. doi: 10.1093/bioinformatics/btn577
- The Gene Ontology Consortium (2019). The gene ontology resource: 20 years and still GOing strong. *Nucleic Acids Res.* 47 (D1), D330–D338. doi: 10.1093/nar/gky1055
- Thoms, M., Buschauer, R., Ameismeier, M., Koepke, L., Denk, T., Hirschenberger, M., et al. (2020). Structural basis for translational shutdown and immune evasion by the Nsp1 protein of SARS-CoV-2. *Science.* 369 (6508), 1249–1255. doi: 10.1126/science.abc8665
- Vazquez, C., Swanson, S. E., Negatu, S. G., Dittmar, M., Miller, J., Ramage, H. R., et al. (2021). SARS-CoV-2 viral proteins NSP1 and NSP13 inhibit interferon activation through distinct mechanisms. *PLoS One* 16 (6), e0253089. doi: 10.1371/journal.pone.0253089
- Volz, E., Hill, V., McCrone, J. T., Price, A., Jorgensen, D., O'Toole, A., et al. (2021). Evaluating the effects of SARS-CoV-2 spike mutation D614G on transmissibility and pathogenicity. *Cell* 184 (1), 64–75.e11. doi: 10.1101/2020.07.31.20166082
- von Bartheld, C. S., Hagen, M. M., and Butowt, R. (2021). The D614G virus mutation enhances anosmia in COVID-19 patients: Evidence from a systematic review and meta-analysis of studies from south Asia. *ACS Chem. Neurosci.* 12 (19), 3535–3549. doi: 10.1021/acschemneuro.1c00542
- Wang, C., Chen, L., Chen, Y., Jia, W., Cai, X., Liu, Y., et al. (2022). Abnormal global alternative RNA splicing in COVID-19 patients. *PLoS Genet.* 18 (4), e1010137. doi: 10.1371/journal.pgen.1010137
- Weber, S., Ramirez, C. M., Weiser, B., Burger, H., and Doerfler, W. (2021). SARS-CoV-2 worldwide replication drives rapid rise and selection of mutations across the viral genome: a time-course study - potential challenge for vaccines and therapies. *EMBO Mol. Med.* 13 (6), e14062. doi: 10.15252/emmm.202114062
- Website. Available at: www.bioinformatics.babraham.ac.uk/projects/fastqc/.
- Wu, D., and Smyth, G. K. (2012). Camera: a competitive gene set test accounting for inter-gene correlation. *Nucleic Acids Res.* 40, e133–e133. doi: 10.1093/nar/gks461
- Yan, L., Yang, Y., Li, M., Zhang, Y., Zheng, L., Ge, J., et al. (2021). Coupling of N7-methyltransferase and 3'-5' exoribonuclease with SARS-CoV-2 polymerase

reveals mechanisms for capping and proofreading. *Cell*. 184 (13), 3474–85.e11. doi: 10.1016/j.cell.2021.05.033

Yap, J. K. Y., Moriyama, M., and Iwasaki, A. (2020). Inflammasomes and pyroptosis as therapeutic targets for COVID-19. *J. Immunol.* 205 (2), 307–312. doi: 10.4049/jimmunol.2000513

Yuan, S., Balaji, S., Lomakin, I. B., and Xiong, Y. (2021). Coronavirus Nsp1: Immune response suppression and protein expression inhibition. *Front. Microbiol.* 0. doi: 10.3389/fmicb.2021.752214

Yuan, S., Peng, L., Park, J. J., Hu, Y., Devarkar, S. C., Dong, M. B., et al. (2020). Nonstructural protein 1 of SARS-CoV-2 is a potent pathogenicity factor redirecting host protein synthesis machinery toward viral RNA. *Mol. Cell*. 80 (6), 1055–66.e6. doi: 10.1016/j.molcel.2020.10.034

Zhang, L., Jackson, C. B., Mou, H., Ojha, A., Rangarajan, E. S., Izard, T., et al. (2020). The D614G mutation in the SARS-CoV-2 spike protein reduces S1 shedding and increases infectivity. *bioRxiv*. 2020.06.12.148726. doi: 10.1101/2020.06.12.148726

Zhang, K., Miorin, L., Makio, T., Dehghan, I., Gao, S., Xie, Y., et al. (2021). Nsp1 protein of SARS-CoV-2 disrupts the mRNA export machinery to inhibit host gene expression. *Sci. Adv.* 7 (6), eabe7386. doi: 10.1126/sciadv.abe7386

Zhang, S., Qu, R., Wang, P., and Wang, S. (2021). Identification of novel COVID-19 biomarkers by multiple feature selection strategies. *Comput. Math Methods Med.* 2021, 2203636. doi: 10.1155/2021/2203636

Zhao, Y., Sui, L., Wu, P., Wang, W., Wang, Z., Yu, Y., et al. (2021). A dual-role of SARS-CoV-2 nucleocapsid protein in regulating innate immune response. *Signal Transduct Target Ther.* 6 (1), 331. doi: 10.1038/s41392-021-00742-w

Zhou, P., Yang, X. L., Wang, X. G., Hu, B., Zhang, L., Zhang, W., et al. (2020). A pneumonia outbreak associated with a new coronavirus of probable bat origin. *Nature*. 579 (7798), 270–273. doi: 10.1038/s41586-020-2012-7

Zinellu, A., Paliogiannis, P., Fois, A. G., Solidoro, P., Carru, C., and Mangoni, A. A. (2021). Cholesterol and triglyceride concentrations, COVID-19 severity, and mortality: A systematic review and meta-analysis with meta-regression. *Front. Public Health.* 9, 705916. doi: 10.3389/fpubh.2021.705916



OPEN ACCESS

EDITED BY

Vikas Sood,
Jamia Hamdard University, India

REVIEWED BY

Pranesh Padmanabhan,
University of Queensland, Australia
Alexander V. Ivanov,
Engelhardt Institute of Molecular
Biology (RAS), Russia

*CORRESPONDENCE

Bernard La Scola
bernard.la-scola@univ-amu.fr

SPECIALTY SECTION

This article was submitted to
Virus and Host,
a section of the journal
Frontiers in Cellular and
Infection Microbiology

RECEIVED 26 July 2022

ACCEPTED 03 October 2022

PUBLISHED 21 October 2022

CITATION

Pires De Souza GA, Le Bideau M,
Boschi C, Wurtz N, Colson P, Aherfi S,
Devaux C and La Scola B (2022)
Choosing a cellular model to
study SARS-CoV-2.
Front. Cell. Infect. Microbiol.
12:1003608.
doi: 10.3389/fcimb.2022.1003608

COPYRIGHT

© 2022 Pires De Souza, Le Bideau,
Boschi, Wurtz, Colson, Aherfi, Devaux
and La Scola. This is an open-access
article distributed under the terms of
the [Creative Commons Attribution
License \(CC BY\)](https://creativecommons.org/licenses/by/4.0/). The use, distribution
or reproduction in other forums is
permitted, provided the original
author(s) and the copyright owner(s)
are credited and that the original
publication in this journal is cited, in
accordance with accepted academic
practice. No use, distribution or
reproduction is permitted which does
not comply with these terms.

Choosing a cellular model to study SARS-CoV-2

Gabriel Augusto Pires De Souza^{1,2}, Marion Le Bideau^{1,2},
Céline Boschi^{1,2}, Nathalie Wurtz^{1,2}, Philippe Colson^{1,2},
Sarah Aherfi^{1,2}, Christian Devaux^{1,2,3} and Bernard La Scola^{1,2*}

¹Microbes, Evolution, Phylogeny and Infection (MEPHI), UM63, Institut de Recherche pour le Développement (IRD), Assistance Publique - Hôpitaux de Marseille (AP-HM), Aix-Marseille Université, Marseille, France, ²Institut Hospitalo-Universitaire Méditerranée Infection, Marseille, France, ³Department of Biological Sciences (INSB), Centre National de la Recherche Scientifique, Marseille, France

As new pathogens emerge, new challenges must be faced. This is no different in infectious disease research, where identifying the best tools available in laboratories to conduct an investigation can, at least initially, be particularly complicated. However, in the context of an emerging virus, such as SARS-CoV-2, which was recently detected in China and has become a global threat to healthcare systems, developing models of infection and pathogenesis is urgently required. Cell-based approaches are crucial to understanding coronavirus infection biology, growth kinetics, and tropism. Usually, laboratory cell lines are the first line in experimental models to study viral pathogenicity and perform assays aimed at screening antiviral compounds which are efficient at blocking the replication of emerging viruses, saving time and resources, reducing the use of experimental animals. However, determining the ideal cell type can be challenging, especially when several researchers have to adapt their studies to specific requirements. This review strives to guide scientists who are venturing into studying SARS-CoV-2 and help them choose the right cellular models. It revisits basic concepts of virology and presents the currently available *in vitro* models, their advantages and disadvantages, and the known consequences of each choice.

KEYWORDS

SARS-CoV-2, COVID-19, viral culture, *in vitro* approaches, susceptible cells, cell lines, organoids, cell model

Introduction

In order to study obligate intracellular parasites such as viruses, it is necessary to have the capacity to maintain the host upon which they reproduce in the laboratory. When virology was just in its infancy, at a time when viruses were still understood as filterable infectious agents, the study of viruses was limited to plant viruses and, later, to bacterial

viruses (bacteriophages), since cultivating their hosts was relatively easy (Simon, 1912; Bos, 1981; Van Helvoort, 1994; Clokie et al., 2011).

This was a particular limitation for animal viruses, however, since initially experimental animals were the only available means of isolating and multiplying viruses (e.g. the rabies virus was multiplied in rabbits) (Gorman, 1991; Faisst, 1999). One alternative was to inoculate virus samples into the cavities (such as the allantois) of embryonated eggs, where there are tissues which are susceptible to infection by certain viruses (such as measles, influenza, polio, and herpes viruses) (Faisst, 1999).

It was only in the 1940s, with the improvement of cell culture techniques, that the study of animal viruses made significant advances (Faisst, 1999; Leland and Ginocchio, 2007). In 1953, HeLa cells were found to be an effective tool for growing large quantities of poliovirus (Scherer et al., 1953), and this knowledge laid important groundwork for the later development of the polio vaccine (Weller et al., 1949; Sabin and Boulger, 1973). Later, the growth of T lymphocytes from normal human bone marrow and the discovery of interleukin 2 made it possible to characterize the first human retrovirus in the early 1980s (Morgan et al., 1976; Mier and Gallo, 1980; Poiesz et al., 1980). It is now easy to manipulate and clean flasks, grow thousands of cells (in the form of immortalized human and animal cell lines) which are susceptible to virus isolation, generate viruses in high titers, and, in the case of antibiotics, control contamination (Leland and Ginocchio, 2007).

Coronaviruses (CoV) were identified by electron microscopy in the mid-1960s precisely because of the difficulty of multiplying the infectious agent, which was hitherto unknown, in routine cell culture at that time, even though it multiplied *in vitro* in organ cultures. The researchers Tyrrell and Bynoe decided to try to visualise the particles through electron microscopy, a piece of equipment handled by June Almeida (Tyrrell et al., 1965; Almeida and Tyrrell, 1967). As a result, they identified the characteristic particle of coronaviruses with the prominent spikes forming a kind of crown, hence the name of the virus.

Coronaviruses are enveloped viruses with a positive single-stranded RNA genome that infect various animal hosts, including humans. The family *Coronaviridae* comprises subfamily *Orthocoronavirinae* that is divided into four genera: *Alphacoronavirus*, *Betacoronavirus*, *Gammacoronavirus*, and *Deltacoronavirus* (Cui et al., 2019; Murgolo et al., 2021; Zhou et al., 2021c). However, only seven coronaviruses of the *Alpha* and *Beta* genera are known to infect humans (Chu et al., 2020), triggering pathologies that range from typical symptoms of the common cold to life-threatening respiratory illnesses in the lower respiratory tract (Murgolo et al., 2021).

Two of these coronaviruses are considered as being historically relevant, due to the outbreaks they caused in the past, of namely Severe Acute Respiratory Syndrome (SARS) and Middle East Respiratory Syndrome (MERS). SARS was first

reported in Asia in February 2003, though cases were subsequently tracked back to November 2002. SARS quickly spread to 26 countries until the epidemic subsided after about four months, with no new cases being no longer detected since 2004. (Li et al., 2005; Graham and Baric, 2010). More than 8,000 people were infected with SARS-CoV, and 774 died (a fatality rate of about 10%) (Ooi and Phua, 2009). MERS-CoV was first reported in Saudi Arabia in September 2012 and has since spread to 27 countries (Ramadan and Shaib, 2019; Al-Tawfiq et al., 2021). The fatality rate of MERS-CoV was much higher (estimated at about 38%), with more than 400 deaths mainly in the Middle East.

In December 2019, a new betacoronavirus named Severe Acute Respiratory Syndrome Coronavirus 2 (SARS-CoV-2) (Gorbalenya et al., 2020; Hui et al., 2020) was detected in patients presenting with viral pneumonia in Wuhan, China (Zhu et al., 2020). SARS-CoV-2 was notable for its rapid spread and quickly became a threat to global public health, and was recognised as potentially leading to the risk of global healthcare system collapse (WHO, 2021). However, unlike previous SARS-CoV and MERS-CoV outbreaks, the new coronavirus outbreak expanded tremendously worldwide. As a result, in March 2020, the World Health Organization (WHO) declared the new coronavirus disease, Coronavirus Disease 2019 (COVID-19), as a pandemic (Murgolo et al., 2021).

After SARS-CoV-2 broke through the borders of Asia and became a global threat, coronaviruses started attracting dramatically increased attention of the scientific community and governments alike. Although much could be inferred from what had been discovered for SARS-CoV and MERS-CoV (Boni et al., 2020; Zhou et al., 2021b), significant doubts remained about the particularities of SARS-CoV-2, including the most suitable cellular models for studying the new coronavirus.

Developing models of infection and pathogenesis was considered an urgent requirement by the scientific community. In order to combat SARS-CoV-2, cell-based approaches are crucial for understanding coronavirus infection biology, growth kinetics, and tropism (Leist et al., 2020). The commonly used laboratory cell lines were the first line of experimental models used to study the viral pathogenicity and to perform assays aimed at screening antiviral compound which were efficient for blocking the replication of emerging viruses (Saccon et al., 2021).

For example, selecting optimal cell line(s) for compound evaluation and screening is imperative for understanding the antiviral mechanisms of action beyond the inhibition of viral non-structural proteins (Murgolo et al., 2021). While assays to determine the neutralizing antibodies titers are performed in virus-specific permissive cells and understood as strong correlate of vaccine efficacies in humans (Earle et al., 2021; Padmanabhan et al., 2022).

However, determining the ideal cell type can be challenging when it comes to studying a new virus, especially in scenarios

where several researchers are adapting their studies to meet a specific need. This review aims to guide scientists who are venturing into the study of SARS-CoV-2 and to help them choose cellular models. It revisits basic concepts of virology and presents the currently available *in vitro* models, their advantages and disadvantages, and the known consequences of each choice.

General concepts involved in choosing cells to study viruses

One of the characteristics of most viruses is that they are host-specific and have a specific tropism. In other words, viruses only can attach to and infect certain cells of certain organisms (known as “susceptible hosts”) which express the appropriate viral receptor(s). This is also why research is conducted into the cell line that will best support the replication of the virus in question and facilitate observation of the phenomena being investigated by the researcher (Lednicky and Wyatt, 2012). Choosing a cellular model to study viruses requires an understanding of certain basic concepts of virus-host interaction. These concepts often become essential to identify a suitable cell model, although many can be established empirically. These are general requirements when it comes to choosing a cell model to study any virus and should also guide the choice of cells for studying SARS-CoV-2.

Host and cellular tropisms

Understanding that viruses have a specific host range, being species-specific, and a specific cellular tropism is the first step towards finding a cell to study. The most rational way is to look for cells from the same host species from which the virus has been isolated or from a phylogenetically close species. In the case of human viruses, in addition to the wide variety of isolated cells derived from this species, many viruses are produced in non-human primate cells (Kiesslich and Kamen, 2020). Obviously, cells isolated from other animals allow the replication of human viruses (Tuffereau and Flamand, 1983; Lee et al., 2020a). The capability of a virus to infect a distinct group of cells in the host is defined as tropism, which is often associated with a variety of cellular devices available on the surface of the host cell (Chappell and Dermody, 2015).

For example, the oncolytic myxoma virus (MYXV), a member of the *Leporipoxvirus* genus, typically infects rabbits but not humans (McFadden et al., 2009; Rahman and McFadden, 2020). This is understood as a host tropism. As an example of tissue tropism, the influenza virus typically infects lung tissues, while HIV presents cellular tropism for CD4+ T lymphocytes (Weiss, 2002; McFadden et al., 2009; Reperant et al., 2012). The main cell models for studying the hepatitis B

and D viruses are carried out in cell lines initially derived from liver tissue or hepatoma cell lines (Hu et al., 2019; Heuschkel et al., 2021). When it comes to antiviral assays for HIV inhibition studies, primary *in vitro* cell culture, particularly monocytes or cells derived therefrom, are usually used as relevant and robust infection models (Wong et al., 2021). Considering viral tropism is essential, therefore, for the development of cellular models for studying viruses.

Although the main manifestations of COVID-19 are observed in the respiratory tract, current evidence points to a multiple organ and cell tropism of SARS-CoV-2 infection. By detecting SARS-CoV-2 antigens in post-mortem samples, SARS-CoV-2 has been found to infect the respiratory system (i.e., the lungs and trachea) but also the kidneys, small intestines, pancreas, blood vessels, and other tissues (Liu et al., 2021). In addition, it has been suggested that SARS-CoV-2 also targets even the sweat glands and vascular endothelial cells in the skin (Liu et al., 2020). The consequences of this broad spectrum of viral tropisms may contribute to multi-organ damage, which is a concern in the pathophysiology of COVID-19.

With the spread of SARS-CoV-2 and the emergence of new variants, there are strong indications that there has been a shift in tropism in these variants, such as Omicron (B.1.1.529) (Meng et al., 2022). This, associated with the viral tropism of SARS-CoV-2 for various cell types, reflects a differential expression of the key host factors involved in viral attachment and entry (Murgolo et al., 2021). A study using the SARS-CoV-2 Wuhan 1 strain (B lineage), which estimated the relative usage of entry pathways in different cell lines, demonstrated that each cell lineage has a relative percentage of entry preferential pathway mediated by host proteases to be used by the virus (Padmanabhan et al., 2020). While another study suggests that the Omicron variant (B.1.1.529) shows increased Cathepsin B/L mediated entry compared to other strains (Padmanabhan & Dixit, 2022 - Preprint). Unravelling the cellular factors that determine viral tropism is, therefore, an important step for predicting viral pathogenesis and for choosing cellular models to study the virus.

Cellular receptors and viral entry

The adhesion step must be well orchestrated to overcome cellular barriers. Once it reaches the intracellular environment, the virus can establish the infection and take possession of the cellular machinery. Therefore, virus-receptor interaction is the key to cell invasion (Dimitrov, 2004; Maginnis, 2018; de Souza et al., 2021). For many viruses, the availability of virus receptors on the surface of a host cell determines the tropism (Chappell and Dermody, 2015), and studies on viral receptors have established certain generalities: (1) some viruses (such as lentiviruses) use not only a receptor, but also a coreceptor, and both determine tropism (for example, the human

immunodeficiency virus binds to CD4 and uses CCR5, CXCR4 or both as co-receptors); (2) many viruses can use more than one molecule as a receptor (e.g. HIV can enter cells through the DC-sign); (3) viruses are constantly adapting and a single virus can change its receptor usage after successive passages in cell culture or animal models; and (4) the expression pattern of receptors *in vitro* and *in vivo* can be different, which can mislead researchers (Dimitrov, 2004; Neal, 2014; Bhella, 2015).

After the adhesion of the viral particle to the cell receptor, the virus begins the process of entering the cell which will potentially be infected. This process of viral entry can occur in different ways. For animal viruses, this is commonly through endocytosis pathways, especially clathrin-mediated pathways. This is an effective process that transports incoming viruses together with their receptor into endosomes (Marsh and Helenius, 2006). Indeed, other pathways, such as the micropinocytosis pathway (an action-driven process) (Canton, 2018), the clathrin-independent pathway, the caveolar pathway, and the cholesterol-dependent endocytic pathway which is devoid of clathrin and caveolin, have also been identified as an entry mechanism for the viruses (Dimitrov, 2004; Marsh and Helenius, 2006; Sobhy, 2017). In addition, viruses can fuse their membrane to the host membrane, as has been observed for HIV, the measles virus and some poxviruses (Buchholz et al., 1996; Sobhy, 2017).

SARS-CoV-2 uses its surface envelope Spike glycoprotein (S-protein) to interact and gain access to host cells by binding to the Angiotensin-I converting enzyme-2 (ACE2) receptor. The S-protein-ACE2 interaction is the primary key to virus entry (Figure 1) (Shang et al., 2020; Jackson et al., 2022). The receptor binding domain located in the surface unit, S1, of the S protein of SARS-CoV-2, exhibits sequence homology with SARS-CoV (the agent of the SARS outbreak in 2003), which also uses ACE2 (Hoffmann et al., 2020; Zhou et al., 2020b; Hoffmann and Pöhlmann, 2022). Therefore, much of the knowledge about the S-protein adhesion process has been acquired throughout studies on SARS-CoV. However, alternative receptors have been identified for SARS-CoV-2.

One study identified the cellular proteins asialoglycoprotein receptor-1 (ASGR1) and Kringle Containing Transmembrane Protein 1 (KREMEN1) as alternative receptors for the S-protein from SARS-CoV-2 (Gu et al., 2022; Hoffmann and Pöhlmann, 2022). In that study, ASGR1 and KREMEN1 were expressed in an ACE2-deficient cell line resulting in SARS-CoV-2 but not SARS-CoV entry (Gu et al., 2022). This result was also supported in a mouse model infected with SARS-CoV-2, although this did reveal that entry *via* ASGR1 and KREMEN1 was generally less efficient than ACE2-dependent entry.

Blocking the CD147 receptor with a monoclonal antibody (Meplazumab) has been shown to inhibit SARS-CoV-2 from invading Vero E6 cells (Wang et al., 2020; Masre et al., 2021; Jackson et al., 2022). Also, human T cells with natural deficiency of ACE2 are infected by a SARS-CoV-2

pseudovirus, this infection can be inhibited explicitly by the Meplazumab anti-CD147 antibody (Wang et al., 2020). In murine models, viral loads were detectable in the lung of transgenic animals, which express human CD147, but not in wild-type mice (Wang et al., 2020). Establishing it as an alternative receptor for SARS-CoV-2.

Some other receptors have been presented as alternative receptors of SARS-CoV-2, such as Neuropilin-1 (NRP1) and Dipeptidyl peptidase 4 (DPP4). NRP1 was understood as another docking receptor to facilitate SARS-CoV-2 entry, and presents increased expression in biological samples from COVID-19 patients (Cantuti-Castelvetri et al., 2020; Masre et al., 2021; Jackson et al., 2022). The furin-cleaved S1 fragment from SARS-CoV-2 S-protein binds directly to NRP1, and blockage of this interaction by RNA interference or selective inhibitors reduces viral infection in cell culture (Daly et al., 2020). Regarding DPP4 (also known as CD26), it binds to the SARS-CoV-2 spike glycoprotein (Vankadari and Wilce, 2020), suggesting that SARS-CoV-2 may share the mode of entry through DPP4 with MERS-CoV.

However, it is not just the availability of receptors which determines the success of viral entry. For example, for SARS-CoV-2, a series of host factors also influence this process which is triggered by the virus, including interaction between the N-terminal domain (NTD) of the spike and lipid rafts, the affinity for ACE2, and some proteases involved in viral fusion and entry, namely furin, Transmembrane proteases serine 2 (TMPRSS2) and 4 (TMPRSS4), Cathepsin L1 (CTSL1) (Zang et al., 2020; Murgolo et al., 2021). Cleavage of the multibasic site (Arg-Arg-Ala-Arg) between the S1-S2 portions of the Spike protein is a prerequisite for cleavage of the S2' site, and both cleavage events are essential to initiate the membrane-fusion process (Belouzard et al., 2012; Peacock et al., 2021; Zhang et al., 2021).

TMPRSS2 is present on the cell surface, and TMPRSS2-mediated S protein activation takes place at the plasma membrane, whereas cathepsin-mediated activation takes place in the endolysosome (Figure 1) (Shulla et al., 2011; Gomes et al., 2020; Shang et al., 2020; Zhang et al., 2021; Zhao et al., 2021). Therefore, depending on the entry route taken by SARS-CoV-2, the S2' site is cleaved by different proteases. SARS-CoV-2 has two known entry pathways and can target either of them according to the cell type expression of TMPRSS2 (Koch et al., 2021). When the expression of TMPRSS2 is insufficient, the virus-ACE2 complex is internalised *via* clathrin-mediated endocytosis (Bayati et al., 2021). In the endolysosomes, cleavage by cathepsins occurs after acidification of the endolysosome environment, which triggers the fusion of the viral membrane with the endolysosome membrane (Jackson et al., 2022). In contrast, when entry occurs in the presence of TMPRSS2, cleavage occurs on the cell surface, triggering the fusion of the viral membrane with the plasma membrane (Jackson et al., 2022).

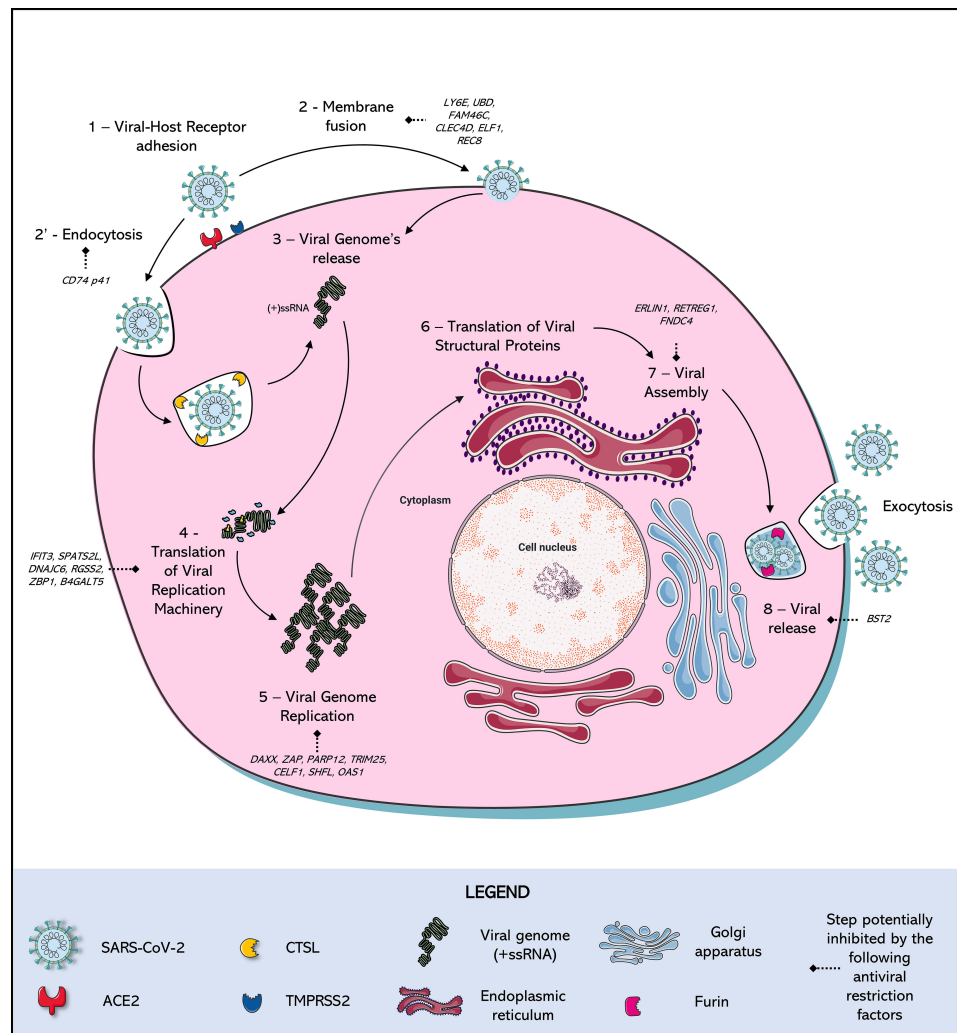


FIGURE 1

SARS-CoV-2 Replication Cycle and antiviral restriction factors in each step of viral replication. (1) Adhesion: SARS-CoV-2 Spike (S) protein binds to a cellular receptor, which is mostly Angiotensin-Converting Enzyme 2 (ACE2), although alternative receptors are described (Ex: ASGR1, KREMEN1). (2) Entry: When there is expression of transmembrane protease serine 2 (TMPRSS2), this protease cleaves the viral Spike protein mediating entry by fusion of the viral membrane to the host cell membrane. In parallel, in the absence of expression of this protease, entry occurs by (2') endocytosis mediated by the receptor, triggering the formation of endo-lysosomes in which Cathepsin L (CTSL) will be responsible for the cleavage of the Spike protein. A new conformational arrangement is induced by this cleavage, triggering (3) the viral genome (+ssRNA) release (via uncoating) into the cell cytoplasm. After the viral RNA is delivered into the host cell, the (4) translation of the viral replication machinery begins: the coronavirus genomic RNA encodes nonstructural proteins (NSPs) that have a critical role in (5) Viral Genome replication: process in which the virus induces the synthesis its RNA, mediated by NSPs. (6) Translation of Viral Structural Protein: the structural proteins S, Envelope (E), and Membrane (M) are translated by ribosomes that are bound to the endoplasmic reticulum (ER). The nucleocapsid proteins (N) remain in the cytoplasm and are assembled from genomic RNA. They fuse with the precursor virion, which is then transported from the ER through the Golgi Apparatus. The Spike cleavage at the S1/S2 furin site probably takes place when virions are released through the Golgi apparatus, responsible for the (7) Viral release: transporting virions to the cell surface via small vesicles, finally released by (8) Exocytosis: the viral progeny is released by exocytosis to the extracellular medium, ready to find and infect new cells. Many of these steps are antagonized by intact cell defense mechanisms, known as restriction factors, which stop viral replication in response to infection.

The expression of receptors in cell lines directly impacts the usage of entry pathways by SARS-CoV-2 and a main advantage of cell culture systems is that it allows direct visualization and quantification of the SARS-CoV-2 entry and replication processes. A study using the SARS-CoV-2 Wuhan 1 strain (B

lineage) estimated the relative usage of entry pathways in different cell lines: in 293T cells expressing ACE2, the virus used nearly exclusively the Cathepsin B/L pathway, and in Vero expressing TMPRSS2 at approximately 65% of the time entry occurred via the TMPRSS2-mediated pathway (Padmanabhan

et al., 2020). Similar results to those obtained in this Vero cell model were found in HeLa cells that expressed both ACE2 and TMPRSS2. In Caco-2 cells, usage of the TMPRSS2 pathway hit around 85% and nearly 100% for Calu-3 cells (Padmanabhan et al., 2020).

However, it is not just the expression of receptors and proteases that dictate this dominant profile of entry pathway in each cell type. The emergence of new variants of SARS-CoV-2 showed that the mutations accumulated by the virus also influence the virus's preferred entry pathway. For example, in an analysis performed by Padmanabhan and Dixit (2022 - Preprint) from the results of Hoffmann et al. (2022), who measured the extent of infection of cells *in vitro* by the Omicron variant (BA.1 sub-lineage) relative to other variants in different cell types, found that the Omicron pseudotyped virus entry was less efficient than the Wuhan 1 strain (B lineage) and Delta variant strains in Calu-3 and Caco-2 cell lines where the TMPRSS2 entry pathway is dominant for the Wuhan 1 strain. In parallel, the entry of the Omicron variant would be more efficient in HEK 293T and Vero E6 cells where the Cathepsin B/L entry pathway is dominant by the original B lineage (Hoffmann et al., 2022; Padmanabhan & Dixit, 2022 - Preprint). Entering the host cell alone is no guarantee of taking control of the cellular machinery, since cell susceptibility and permissibility to any given virus may vary from cell to cell, even when the cells are derived from the same tissue.

Resistance, susceptibility, and permissibility

There are many cellular functions upon which viruses depend on when it comes to successfully infecting a cell. For a productive infection to be successful, cellular structures and molecular pathways must ensure all essential viral replication events, including adhesion, entry, uncoating, replication, assembly, and the release of new infective particles (Louten, 2016). For example, a cell without the specific receptor for a given virus is considered resistant to this virus. However, genetic engineering can reverse these misfortunes, and the gene encoding the cell receptor can be inserted into the cell's genome that allows to express it on the cell surface (Ramirez et al., 2021).

In this context, a cell that allows the adhesion and entry of the virus is understood as being susceptible to the virus (Faisst, 1999). The presence of the functional receptor on the cell surface alone does not guarantee that this cell will support viral replication. Cells have developed certain defense mechanisms against viral infection, producing antiviral restriction factors which make the cell less permissive to viruses. Antiviral restriction factors are proteins produced by the host cell, which constitute a first line strategy to block viral replication

and propagation, by interfering at critical steps of the viral replication cycle or triggering innate responses (Colomer-Lluch et al., 2018). This is well-exemplified in HIV-resistant cells due to the expression of numerous robust antiviral factors, such as the apolipoprotein B mRNA editing enzyme, catalytic subunit 3G (APOBEC3G) and the tripartite motif-containing protein 5 (TRIM5 α). TRIM5 α for example, binds to sensitive, incoming retroviruses *via* its C-terminal domain and recruits them to the proteasome where it is degraded (Huthoff and Towers, 2008).

Most antiviral resistance factors are Interferon Stimulated Genes (ISGs), in other words, genes that activate their expression after detecting interferons by cellular receptors (Schneider et al., 2014; Danziger et al., 2022). Binding interferon to their receptors triggers a series of signaling cascade in the cell to protect against an infection. ISGs encode functionally diverse gene products, including the antiviral effectors that antagonise distinct steps of viral life cycles (Schoggins, 2019; Danziger et al., 2022). As they depend on an interferon stimulus, induced resistance usually is not a concern for *in vitro* virology studies, as most cell lines used for viral production do not produce endogenous interferons. However, studies often use cells that express interferons or stimulate cells with interferon to better understand the mechanisms of resistance to viral infections.

Multiple studies have reported evidence implicating interferon as a key component in the host response to SARS-CoV-2. Several *in vitro* reports have highlighted that it effectively blocks SARS-CoV-2 infection when added to cell culture prior to the infection (Felgenhauer et al., 2020; Lokugamage et al., 2020). In parallel, transcriptome analyses of interferon-stimulated cell lines make it possible to identify ISGs and the resistance factors that restrict SARS-CoV-2 replication at different stages of the replication cycle (Supplementary Table 1 and Figure 1) (Bruchez et al., 2020; Nchioua et al., 2020; Lee et al., 2021; Martin-Sancho et al., 2021; Danziger et al., 2022; Mac Kain et al., 2022). Lymphocyte Antigen 6 Family Member E (LY6E) has been identified as a restriction factor for SARS-CoV-2 entry, inhibiting viral Spike protein-mediated membrane fusion (Pfaender et al., 2020; Zhao et al., 2020b; Martin-Sancho et al., 2021).

Other factors have been identified as inhibiting SARS-CoV-2 RNA translation or replication. The Interferon Induced Protein with Tetratricopeptide Repeats 3 (IFIT3), Spermatogenesis Associated Serine Rich 2 Like (SPATS2L), DnaJ Heat Shock Protein Family (Hsp40) and Member C6 (DNAJC6) expression on HEK 293T cells leads to a significant decrease in SARS-CoV-2 RNA levels (Martin-Sancho et al., 2021). IFIT3 is known to prevent active viral RNA replication by detecting and sequestering single-stranded 50-ppp or 20 O-unmethylated RNA (Metz et al., 2013), while SPAT2SL is recruited to cytoplasmic stress granules sequestering viral RNA and reducing viral genome synthesis (Zhu et al., 2008; Miller, 2011).

Restriction factors that prevent viral release, such as the Bone Marrow Stromal Cell Antigen 2 (BST2), have been identified as potent inhibitors of SARS-CoV-2 release in HEK 293T cells (Martin-Sancho et al., 2021). BST2 inhibits the release of several enveloped viruses, such as HIV-1 and other CoVs, by tethering the virions to the cell surface or intracellular membranes (Neil et al., 2008; Van Damme et al., 2008; Wang et al., 2014; Taylor et al., 2015). The effect of this restriction factor is antagonized by SARS-CoV-2 Orf7 (Martin-Sancho et al., 2021).

Antagonizing innate host cell responses is a common strategy among viruses. The interferon pathway itself has been described as being antagonized by various mechanisms involving the SARS-CoV-2 proteins ORF3b, ORF8, ORF9b, ORF6, Nsp15 and Spike (Ribero et al., 2020; Zinzula, 2021; Freitas et al., 2022). In conclusion, viral replication in an infected cell is the result of complex interactions between the host and viral proteins. Conversely, cells that allow post-entry steps, such as uncoating, replication, assembly, and release, are then understood to be virus-permissive cells (Faisst, 1999). Therefore, in most virus assays, the aim is to find cell models that are both susceptible and permissive to the virus being studied.

Types of infection

When choosing to work with cells that are both susceptible and permissive to a virus, what is being sought is a complete infection, where the virus infects, takes control of the cellular machinery, expresses its structural and non-structural components, and ensures the assembly and release of infectious particles at the end of the cycle. However, infected cells can also undergo abortive infections. Thus, although the cells are infected with a virus, they do not produce any progeny virus due to this infection (Cohen et al., 2019). Abortive viral infections are frequently observed even during the infection of susceptible and permissive cell types, however, some single-cell studies of viral infections have suggested that even in permissive cells, around 40% of the infected cells do not produce progeny viruses (Combe et al., 2015; Heldt et al., 2015). This suggests that abortive infection is a common outcome for many viral infections.

Abortive SARS-CoV-2 infections have been described for different cells. In primary cell culture, such as the primary human umbilical vein endothelial cells (HUVECs), human microvascular endothelial cells from the lung (HMVEC-L), and human primary lung microvascular endothelial cells (HLMECs), increased nucleocapsid protein expression of SARS-CoV-2 has been detected, but without generating infectious progeny (Caccuri et al., 2020; Schimmel et al., 2021). Abortive SARS-CoV-2 in T cells (Flemming, 2021; Swadling et al., 2021) and brain endothelial cells (Bauer et al., 2022). However, the

consequences of abortive infections on the pathophysiology of SARS-CoV-2 are still uncertain. Therefore, here we will focus on cells that allow effective SARS-CoV-2 infection, characterized by the production of infectious viral particles.

Cytopathic effect

The observation of cytopathic effects (CPE) is crucial in virology. CPE refers to structural changes in the host cells due to viral invasion and replication. Some viruses cause characteristic morphological alterations in the infected cells, such as rounding and detaching, fusion with adjacent cells to form syncytia, and the appearance of nuclear or cytoplasmic inclusion bodies (Faisst, 1999; De Souza et al., 2020). Observing the CPE is essential for virologists who isolate and identify viruses.

Combining a virus with a permissive cell that presents CPE is desired, since the presence of CPE can provide the researcher with indications about the course of infection. Usually a peak in visualizing CPE on the cell monolayer indicates the best time to collect viral production, although it may be desired to determine the protection of these cells in the antiviral assays and serological evaluation (Faisst, 1999), for example. A cytopathic effect also enables relatively simple assays for quantifying infectious particles, known as viral titration assays, which can be based on, for example, counting plaque forming units (PFU) or observing CPEs to determine Median Tissue Culture Infectious Dose (TCID₅₀) (Faisst, 1999; Payne, 2017). Although these previously mentioned viral quantification methods are widely used, other methods have been developed for viruses that cannot find the virus-cell pair that results in CPE, such as focus-forming and hemagglutination assays or even enzyme-linked immunosorbent assays (ELISA), a cell-based indirect immunofluorescence assay, which involves antibody-based approaches (Payne, 2017).

The lighter CPE typically seen for SARS-CoV-2 is present in cells derived from the kidneys of the African green monkey (*Chlorocebus sabaeus*) and rhesus macaque (*Macaca mulatta*). In Vero/Vero E6, MA1040, and BGM cells, cell rounding can be observed 48 hours after the infection is initiated in an asynchronous infection cycle (Wurtz et al., 2021). However, other cell lines can present high SARS-CoV-2 production levels, without presenting evident CPE, as do Caco-2 cells.

Isolating and producing SARS-CoV-2

Isolating viruses is still a sensitive and essential method for virologic diagnosis and has long served as the “gold standard” for virus detection (Hosoya et al., 1998; Mizuta et al., 2003; Leland and Ginocchio, 2007). Currently, the isolation of viruses has lost ground to molecular detection methods, although especially in the field of virus research having a viral strain isolated allows

researchers to study the biological aspects of a specific virus, such as the replication cycles, the entry process, and the receptors used by the virus, for example.

This isolated virus can also enable the production of antigens or can be employed in antiviral susceptibility screening tests (Leland and Ginocchio, 2007). However, this posterior assay requires a well-characterised viral stock produced in cell culture, ideally with minimal passaging to reduce the rise of genetic sub-populations and heterogeneity of phenotypes of the virus stock (Baczenas et al., 2021). Therefore, this virus stock will serve as a seed stock which will be propagated to make more extensive stocks.

When isolating a virus in cell culture, the experimenter often looks for permissive cells that present CPE, since the aspect of the CPE is often characteristic of certain viruses in each cell and indicates a successful infection (Faisst, 1999). In addition, when producing a sizeable viral stock, high viral titers are often sought (Leland and Ginocchio, 2007), in other words, a cell with a high production of infective viral particles.

Verda reno E6 cells (Vero E6)

Vero cells were established from kidney tissue sampled from an African green monkey (*C. sabaues*) (Ammerman et al., 2008; Naoki et al., 2014). They originated from a primary culture initiated in March 1962 by a group from Chiba University in Japan. Over the months of serial passages of these cells, the researchers obtained a series of sub-lines, one of which was chosen as the standard Vero cell line (Ammerman et al., 2008; Naoki et al., 2014).

This cell lineage was widely distributed among research laboratories and has become one of the most common mammalian immortalized cell lines used in research (Ammerman et al., 2008). In the field of virology, these cells have gained prominence for being susceptible to a wide range of viruses, such as simian polyomavirus SV-40, rubella virus, arboviruses, adenoviruses, H5N1 influenza virus, Ebola hemorrhagic fever virus 19, SARS-CoV, and MERS-CoV (Ellis et al., 1979; Horimoto and Kawaoka, 2006; Zaki et al., 2012; Kiesslich and Kamen, 2020). Vero cells are also widely used in vaccine production as safe cell substrates for antigen production (Barrett et al., 2009).

The Vero E6 clone was obtained by using the dilution method into microtiter plates in 1979 by PJ Price (Yamate et al., 2005). The main characteristic of Vero E6 is that it E6 exhibits contact inhibition after forming a monolayer; therefore, it helps growing slow-replicating viruses. Since 2003, Vero E6 cells have also been used extensively for SARS-CoV-like virus research and cell-culture-based infection models by many laboratories as it supports viral replication to high titers. This high susceptibility could be related to the high expression level of the ACE-2 receptor (Gillim-Ross et al., 2004), which is used by

both SARS-CoV-2 and SARS-CoV (Hoffmann et al., 2020) and/or their lack of ability to produce interferon (De Clercq et al., 1973; Emeny and Morgan, 1979).

Vero E6 cells are, therefore, highly susceptible, and permissive cells to SARS-CoV-2, being able to be used both in the isolation and production of viral stocks due to the abundance of receptors and because they present characteristic CPE (cell rounding, detaching and lysis) as well as allow the recovery of high titers of SARS-CoV-2 (Figure 2). Furthermore, studies also point to these cells as a suitable basis for performing the initial screening of antiviral compounds, which makes it possible to select the most promising hits for in-depth mechanistic studies in other cells (Ogando et al., 2020). The high viral titers obtained in Vero E6 cells can also be influenced by the medium in which the cells are grown, as demonstrated by cultivating these cells in Physiological Plasmax Medium, which, when infected by different RNA viruses, including SARS-CoV-2, had lower viral release rates compared to the cells cultivated under Dulbecco's Modified Eagle Medium (DMEM) (Golikov et al., 2022).

However, studies have shown that SARS-CoV-2 adapts rapidly to passages in Vero E6 cells (Lamers et al., 2021; Pyke et al., 2021). For example, SARS-CoV-2 exhibited remarkable phenotypic variation in the plate assays within a few passages after its isolation from the clinical samples (Ogando et al., 2020). This change in phenotype has been associated with the emergence of mutations near the so-called furin-like S1/S2 cleavage site, which triggers its inactivation and provides a selective advantage over SARS-CoV-2 passages in Vero E6 (Ogando et al., 2020; Peacock et al., 2021; Sasaki et al., 2021). This, in turn, leads to favoring an entry pathway in that cell with low expression of TMPRSS2. It was also reported that the conversion of procathepsin L to cathepsin L (CTSL) is significantly higher in Vero cells than in other susceptible cell lines, such as Calu-3, Caco-2, and Huh-7 (Figure 2) (Koch et al., 2021; Zhao et al., 2021).

This information raises issues around the number of passages that are made in that cell, as they can lead to attenuation of the virus, mainly if later experiments are to be carried out in other cells and if they require a TMPRSS2-dependent entry route. This attenuation can be easily avoided by adopting an engineered VeroE6/TMPRSS2 cell line, understood as highly susceptible to SARS-CoV-2 (Matsuyama et al., 2020). Although most studies using SARS-CoV-2 employ the Vero E6 sub-lineage, other Vero lineages have also been shown to be permissive to the virus, such as VERO 81 and VERO SLAM, this last one transfected with a plasmid encoding the gene for the human signaling lymphocytic activation molecule (SLAM) molecule (Wurtz et al., 2021).

It must, however, be considered that Vero cells are cells derived from African green monkey tissue and, therefore, a non-human primate (NHP). Although it is a species phylogenetically close to humans, with low ACE2 polymorphism compared to human ACE2, this may represent a limitation for studying a

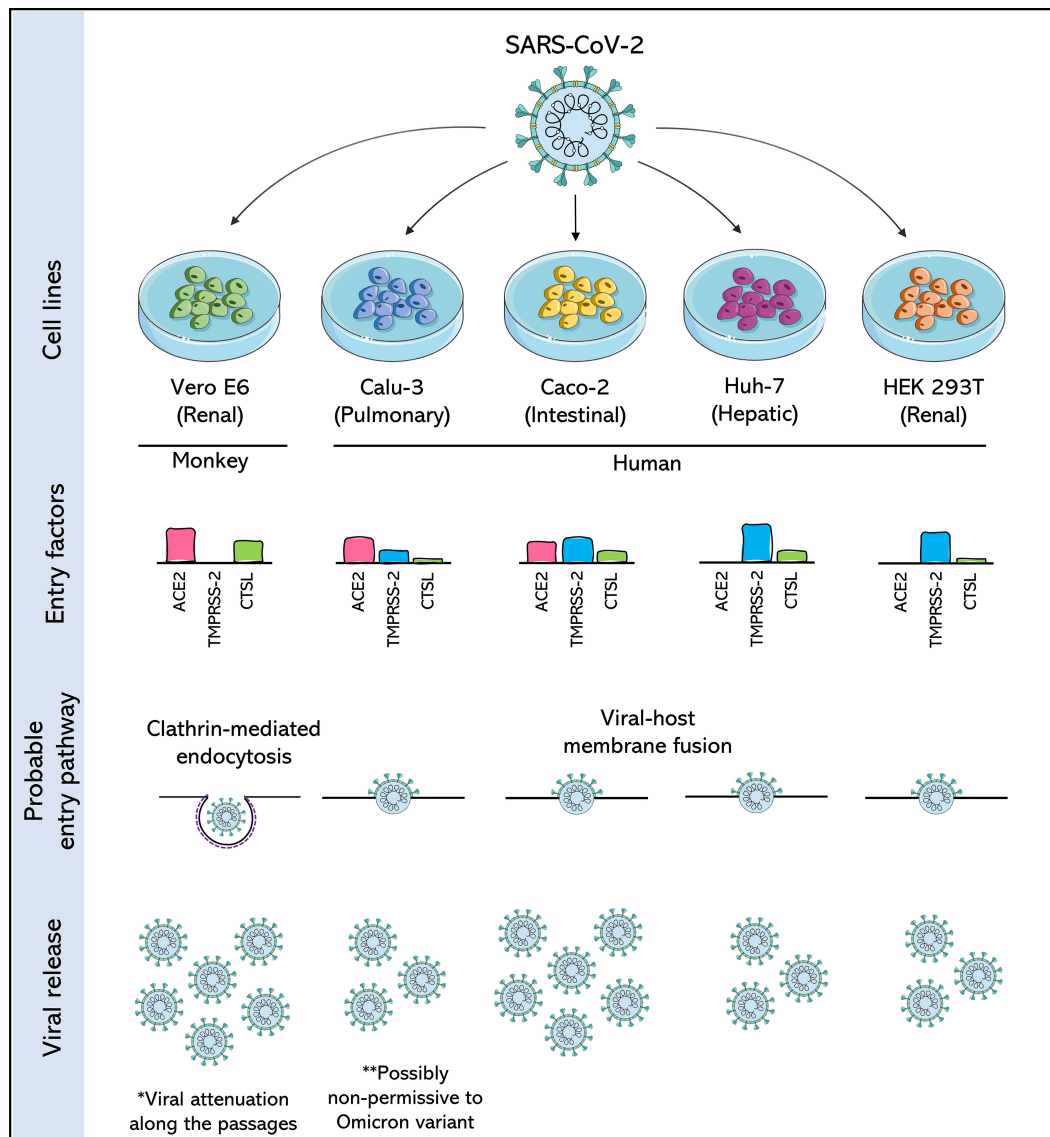


FIGURE 2

Comparison of SARS-CoV-2 permissive cell lines. Four human cell lines: Calu-3 (Pulmonary), Caco-2 (Intestinal), Huh-7 (Hepatic) and HEK 293T (Renal), are compared with each other and with the Vero E6 cell, a cell derived from the African green monkey kidney, and widely used in the isolation and production of SARS-CoV-2. Cells are compared for the expression of three important entry factors used by SARS-CoV-2: angiotensin-converting enzyme 2 receptor (ACE2), transmembrane protease serine 2 (TMPRSS2) and the lysosomal protease cathepsin L (CTSL), based on data from [Murgolo et al., 2021](#), [Saccon et al., 2021](#) and [Shuai et al., 2020](#). The expression of these factors dictates the entry pathway used by SARS-CoV-2. The release of SARS-CoV-2 viral particles is also compared. The asterisks draw attention to likely consequences of producing SARS-CoV-2 in these cells.

human virus such as SARS-CoV-2. This means a restriction on the information recovered during drug screening, especially if the drugs are designed to be metabolised in human cells ([Pruijssers et al., 2020](#); [Ramirez et al., 2021](#)). Therefore, many assays seek to employ cells derived from human tissues to prevent the isolates from suffering attenuation in cells of other species and especially for drug screening.

Human cell lines

Cultured human airway epithelial cells (Calu-3)

As SARS-CoV-2 was initially understood to be a virus that triggers diseases in the lower respiratory tract ([Murgolo et al.,](#)

2021), the search for a human cell derived from lung tissue that was permissive to this virus became essential for the *in vitro* study of the disease, its pathogenicity and especially anti-SARS-CoV-2 drug screening.

Calu-3 cells are a human lung adenocarcinoma cell line isolated in 1975 from the pleural effusion of a 25-year-old Caucasian male (Fogh et al., 1977). Calu-3 is commonly used in cancer research and drug development (Zhu et al., 2010) and was understood as a highly permissive cell to SARS-CoV (Tseng et al., 2005). However, during the previous epidemic in 2003, when it was initially challenging to establish infection models in cells derived from human lungs, this compromised studies on the pathogenesis of the SARS-CoV, which, as is the case in SARS-CoV-2, mainly causes manifestations in the respiratory tract (Tseng et al., 2005; Grossegessse et al., 2022).

The knowledge already established from the 2003 SARS-CoV outbreak was revisited with the emergence of SARS-CoV-2 in 2019, and Calu-3 cells were perceived as permissive cells for both viruses. SARS-CoV-2 grew faster and at a higher titer than SARS-CoV in Calu3 cells (Chu et al., 2020). However, comparative studies demonstrate that the production of SARS-CoV-2 by Calu-3 is usually lower than that obtained in Vero E6 cells (Figure 2), and, unlike these latter cells, Calu-3 cells do not show CPE when infected with SARS-CoV-2 (Chu et al., 2020; Park et al., 2021; Wurtz et al., 2021; de Souza et al., 2022).

In addition to these two disadvantages of using Calu-3 Cells, a third can also be mentioned. Calu-3 cells grow more slowly than Vero cells (Baczenas et al., 2021), but this does not mean they are inferior to Vero cells. Instead, this is because, unlike in Vero cells, the furin cleavage site appears to be preserved in SARS-CoV-2 produced in Calu-3 cells, rather than promoting the attenuation typically observed during passages in Vero cells (Baczenas et al., 2021; Lamers et al., 2021; Mykytyn et al., 2021a).

This type of feature makes Calu-3 cells interesting for SARS-CoV-2 studies, particularly if this stock is being produced for infections in animal models, as Calu-3-derived virus stocks remained pathogenic in hamsters, and the Calu-3-specific variants were maintained (Baczenas et al., 2021). In addition, these cells are also widely used in drug screening studies against SARS-CoV-2 (Dittmar et al., 2021; Tao et al., 2021; Coimbra et al., 2022).

However, with the emergence of many variants of SARS-CoV-2, several of them being classified as variants of concern by the WHO, it is unclear whether mutations acquired by the virus within the population can impact viral fitness (Harvey et al., 2021). For example, for the Omicron (B.1.1.529) variant of concern, mounting evidence, mainly from animal studies, suggests that Omicron BA.1 sub-lineage does not readily multiply in lung tissue (Abdelnabi et al., 2022; Halfmann et al., 2022; McMahan et al., 2022). This could impact the production of this and other new variants by Calu-3 cells, which would require a new adaptation of the isolates to the cells through different passages, which consequently would

distance them from the original isolate and the circulating variant.

Cancer coli 2 cells (Caco-2)

Although SARS-CoV-2 primarily affects the respiratory system, increasing evidence suggests that this virus may have gastrointestinal manifestations. The SARS-CoV-2 genome was previously found in gastric, rectal, and duodenal mucosa samples, suggesting that the digestive system is a potential source of viral transmission (Arslan et al., 2020; Kipkorir et al., 2020; Zhang et al., 2020). SARS-CoV-2 replicates in gastrointestinal cells *in vivo* and is frequently detected in faeces (Chen et al., 2020; Cheung et al., 2020; Lee et al., 2020b; Wu et al., 2020; Xiao et al., 2020), providing evidence that SARS-CoV-2 can also infect intestinal cells.

Caco-2 cells were established in 1977 from a colorectal adenocarcinoma taken from a 72-year-old Caucasian man using the explant culture technique (Fogh et al., 1977). The Caco-2 cell line demonstrated morphological and biochemical characteristics of small intestine enterocytes (Hidalgo et al., 1989) and has been widely used to study infection first with SARS-CoV and now with SARS-CoV-2 (Cinatl et al., 2004; Bojkova et al., 2020). These cells have become, along with Calu-3 cells, the main human cell lines explored in the *in vitro* studies of SARS-CoV-2.

Compared to Calu-3 cells, Caco-2 cells are suggested to have lower expression of the ACE2 receptor but higher expression of TMPRSS2 (Figure 2) (Shuai et al., 2020; Saccon et al., 2021). Although no assays have demonstrated that the furin cleavage site is maintained in SARS-CoV-2 produced in Caco-2, as is observed for the viral stocks produced in Calu-3, the high expression of TMPRSS2 is a strong indication that the attenuation observed by passages in Vero cells would not occur in this cell line.

Continuing with the comparison of Caco-2 cells and Calu-3 cells, one proteomics study pointed out that Caco-2 cells have 177 proteins which are differentially expressed during SARS-CoV-2 infection, while Calu-3 has more the 6,000 such proteins (Saccon et al., 2021). Yet another study showed that among the five cytokines/chemokines evaluated, SARS-CoV-2 infection leads to increased expression only of Interferon gamma-induced protein 10 (IP-10), but not of Tumor Necrosis Factor-alpha, RANTES (regulated on activation, normal T cell expressed and secreted), Interleukin 6, or Interleukin 8 in Caco-2 cells (Shuai et al., 2020). No relative increase in these cytokines/chemokines was observed in Calu-3 cells infected with SARS-CoV-2 (Shuai et al., 2020). Other authors suggest that the absence of CPE in Caco-2 could be due to the weak pro-inflammatory response triggered by SARS-CoV-2 (Zupin et al., 2022).

The absence of CPE in Caco-2 cells is suggested at least for low multiplicity of infections (MOIs) (Chu et al., 2020; Saccon et al., 2021; Wurtz et al., 2021; Mautner et al., 2022; Zupin et al., 2022) and this is its main disadvantage compared to Vero E6 cells. Furthermore, unlike Calu-3 cells, SARS-CoV-2 viral production by Caco-2 cells typically reaches levels similar to or higher than those seen in Vero E6 cells (Figure 2) (Chu et al., 2020; Koch et al., 2021; Saccon et al., 2021; de Souza et al., 2022). These characteristics make Caco-2 cells a good choice of human cells for SARS-CoV-2 assays.

Human hepatoma 7 cells (HuH-7)

The HuH-7 cell line was established from an already well-differentiated hepatocyte derived from a cellular carcinoma cell line originally collected from a liver tumour from a 57-year-old Japanese man. The line was established by Nakabayashi et al. (1982), who found that this epithelial-like cell replicated continuously in a chemically defined medium when the medium was supplemented with Na₂SeO₃ (Kawamoto et al., 2020). Huh-7 is highly susceptible to the hepatitis C virus (HCV) and is, therefore, often used for the *in vitro* production of infectious HCV particles and in anti-HCV drug assays in a replicon-based system (Liu et al., 2014).

Huh-7 cells are permissive to different coronaviruses, such as CoV 229E, CoV OC43, MERS-CoV, and SARS-CoV (Ois Freymuth et al., 2005; de Wilde et al., 2013). This cell also exemplifies how different viruses, even if they belong to the same family, can have different patterns of cytopathic effect in the same cell. For example, using Huh-7 as an infection model, MERS-CoV was highly cytopathic. At the same time, SARS-CoV presented a delayed CPE, and no CPE was observed for SARS-CoV-2 using the same infectious dose for the three viruses (Chen et al., 2021).

Unlike other cells, despite Huh-7 is permissive to SARS-CoV-2, co-expression analyses of ACE2 and TMPRSS2 revealed that Huh-7 cells strongly expressed TMPRSS2 but lacked ACE2 expression (Figure 2), which was understood as an indication that each receptor plays an individual role in aiding the infection (Saccon et al., 2021). A post-infection proteomics study pointed out that there is no change in the global protein abundance in Huh-7 infected with SARS-CoV-2, with only four proteins being differentially expressed (Saccon et al., 2021). In this same cellular model, a type I interferon signature induced by SARS-CoV-2 infection distinct from that with other coronaviruses such as SARS-CoV and MERS-CoV, was also observed (Chen et al., 2021).

Although Huh-7 cells are permissive to SARS-CoV-2, viral replication in these cells is considered to be moderate (Figure 2) (Chu et al., 2020), possibly due to the aforementioned factors regarding receptor expression, interferon signature, and protein expression. However, retaining a cell of liver origin in culture for

SARS-CoV-2 studies is particularly interesting, as the liver has been identified as one of the main target organs in cases of COVID-19, and the rate of incidence of liver injury in these patients is 14%–53% (Zhou et al., 2021a; Wanner et al., 2022). Furthermore, Huh7, like many previously cited cell lines, is an immortalised cancer cell line that may not be physiologically representative of human tissue.

Human embryonic kidney 293T cells (HEK 293T)

The HEK 293T is an important sub-lineage of the HEK 293 cell line, differing from it in that it contains the temperature-sensitive mutant Simian Vacuolating Virus 40 (SV40) T-antigen that allows episomal replication of transfected plasmids containing the SV40 origin of replication. It was introduced by Michele Calos's lab at Stanford in 1987 (Rio et al., 1985; Dubridge et al., 1987). This modification made these cells particularly popular for producing recombinant proteins and retroviruses (Pear et al., 1993).

Like Vero cells, HEK 293 cells, from which HEK 293T cells were derived, are kidney-derived epithelial cells. They were established by Graham et al. (1977) for the transformation of primary human embryonic kidney (HEK) cells obtained from a spontaneously miscarried or aborted female following exposure to sheared fragments of human adenovirus type 5 DNA (Graham et al., 1977; Shaw et al., 2002).

The HEK 293T cells strongly expresses TMPRSS2 but lack ACE2 expression (Figure 2). At the same time, the post-infection proteomics studies have not found any change in the global protein abundance in HEK 293T infected with SARS-CoV-2, results that are similar to those obtained for Huh-7 cells (Saccon et al., 2021). The results of these two cells are also similar for the production of SARS-CoV-2 in that both are understood as low-level virus production compared with Caco-2 (Figure 2) (Chu et al., 2020; Saccon et al., 2021). As with the other human cells mentioned above, there is no cytopathic effect on HEK 293T cells after SARS-CoV-2 infection (Chu et al., 2020).

HEK 293 cells appear to produce only abortive SARS-CoV-2 infections; therefore, only HEK 293T cells should be used in SARS-CoV-2 studies (Harcourt et al., 2020; Modrof et al., 2020). HEK 293T cells are embryo cells and, due to differences in receptor expression and viral production, it is difficult to compare these human kidney cells with monkey kidney cells (Vero cells). Moreover, there are doubts as to whether they can be minimally representative in studies of the renal pathology of SARS-CoV-2.

Nevertheless, HEK 293T cells appear to be valuable tools for studies evaluating the impact of specific protein expression on viral replication once these cells can be transfected with high efficiency and support productive replication of SARS-CoV-2. One study that evaluated antiviral restriction factors at various

stages in the SARS-CoV-2 replication cycle was conducted in HEK 293T cells transduced with lentiviruses carrying the gene previously identified as a potential restriction factor (Supplementary Table 1) (Martin-Sancho et al., 2021). This type of approach is essential for understanding virus-host interactions.

Other permissive mammalian cell lines

With the emergence of SARS-CoV-2, some studies were dedicated to testing the susceptibility of commonly used laboratory cell lines, and therefore, immortalized cells, to the new coronavirus (Chu et al., 2020; Saccon et al., 2021; Wang et al., 2021; Wurtz et al., 2021). This was a way to quickly present cells that could be used for the isolation and propagation of SARS-CoV-2 and to define the first line of experimental models to study the pathogenicity and perform antiviral assays on the emerging virus (Saccon et al., 2021). In addition to the human cells presented above, many mammalian cells were identified as at least susceptible to SARS-CoV-2 infection (Table 1).

Cells derived from non-human primate kidneys are often thought to be cells which are susceptible to SARS-CoV-2 infection. Buffalo green monkey kidney cells (BGMK) and Cellosaurus cell line MA-104, both epithelial cells, and Cellosaurus cell line 1 (CV-1), with fibroblast morphology, are all derived from African green monkey kidneys (*C. sabaeus*) and appear to support the SARS-CoV-2 replication cycle (Wang et al., 2021; Wurtz et al., 2021). Rhesus macaque kidney epithelial LLC-MK2 and RhMK cells are also suggested to be permissive cells for SARS-CoV-2 (Wang et al., 2021; Wurtz et al., 2021).

In addition to cells from non-human primates, cell lines derived from cats, rabbits and pig kidneys has also been identified with a limited permissibility to SARS-CoV-2 infection (Table 1) (Chu et al., 2020; Wang et al., 2021). The Crandell-Rees Feline Kidney Cell (CRFK), isolated in 1973 and generally used in the production of viruses used in vaccines for felines, was recently identified as having a mesenchymal phenotype, in contrast to the previous characterisation of epithelial cells (Lawsan 2019; Lappin 2005; Crandell, 1973). In addition, the transmission of SARS-CoV-2 between cat owners and felines and from an infected cat to naive felines has been

TABLE 1 SARS-CoV-2 permissive mammalian cells lines. Commonly used laboratory mammalian cell lines that can support SARS-CoV-2 replication with infective particles release at the end of the cycle.

| Cell Line | Organism | Tissue | Morphology | Cytopathic Effects | References |
|-----------|--|---------------------------|-------------------------|------------------------------------|---|
| Caco-2 | Human (<i>Homo sapiens</i>) | Colorectal adenocarcinoma | Epithelial | Absent | Chu et al., 2020; Saccon et al., 2021; Wurtz et al., 2021 |
| Calu-3 | | Lung adenocarcinoma | Epithelial | Absent | Chu et al., 2020; Saccon et al., 2021 |
| HEK 293T | | Kidney | Epithelial | Absent | Chu et al., 2020; Saccon et al., 2021 |
| Huh-7 | | Liver tumour | Epithelial | Absent | Chu et al., 2020; Saccon et al., 2021 |
| U251 | | Glioblastoma | Pleomorphic/astrocytoid | Absent | Chu et al., 2020 |
| BGMK | African green monkey (<i>Chlorocebus sabaeus</i>) | Kidney | Epithelial | Cell rounding and detaching | Wang et al., 2021; Wurtz et al., 2021 |
| MA-104 | | | Epithelial | Cell rounding and detaching | Wurtz et al., 2021 |
| Vero E6 | | | Epithelial | Cell rounding, detaching and lysis | Wang et al., 2021; Wurtz et al., 2021 |
| CV-1 | | | Fibroblast | Cell rounding and detaching | Wurtz et al., 2021 |
| LLC-MK2 | Rhesus macaque (<i>Macaca mulatta</i>) | Kidney | Epithelial | Absent | Wang et al., 2021; Wurtz et al., 2021 |
| RhMK | | | Epithelial | Cell rounding and detaching | Wang et al., 2021; Wurtz et al., 2021 |
| CRFK | Cat (<i>Felis catus</i>) | Kidney | Epithelial | Absent | Wang et al., 2021. Chu et al., 2020 |
| PK-15 | Pig (<i>Sus scrofa</i>) | Kidney | Epithelial | Cell rounding and detaching | Chu et al., 2020; Meekins et al., 2020; Lee et al., 2020b |
| ST | | Testicle | Fibroblast | Cell rounding and detaching | Meekins et al., 2020 |
| RK-13 | Rabbit (<i>Oryctolagus cuniculus</i>) | Kidney | Epithelial | Absent | Chu et al., 2020 |

previously presented and may explain the susceptibility of cat cells to the virus (Bosco-Lauth, 2020; Patterson, 2020).

The RK13 cell line was obtained from the kidney of a five-week-old rabbit and is commonly used for viral isolation, as the RK13 cells have proven to be permissive to infection by the herpes simplex virus, pseudorabies virus, vaccinia virus, rabbitpox virus, simian adenoviruses, rubella virus and SARS-CoV (Coombs et al., 1961; Fogel and Plotkin, 1969; Kaye et al., 2006). Susceptibility to SARS-CoV-2 was suggested by Chu et al. (2020). Rabbits are widely used as experimental animals in the laboratory (Thomas et al., 2012). The susceptibility of rabbits to SARS-CoV-2 has been previously demonstrated with the detection of infectious viruses from the nose and throat upon experimental viral inoculation (Mykytyn et al., 2021b). They may, therefore, represent precious models for the study of SARS-CoV-2.

In contrast, pigs inoculated with SARS-CoV-2 by a broader number of viral inoculation routes, did not show any productive infection (Meekins et al., 2020; Vergara-Alert et al., 2021), even though they presented seroconversion and the presence of neutralising antibodies 22 days post-infection when inoculated by parenteral routes (Vergara-Alert et al., 2021). The immune response of these animals was indicated as a key factor for the protection of these animals against COVID-19. In porcine primary respiratory epithelial cells, self-limiting SARS-CoV-2 replication was associated with higher rates of apoptosis in infected cells (Nelli et al., 2021). However, in swine testicle (ST) and kidney (PK-15) cell lines, it was possible to establish SARS-CoV-2 infections in which CPE was visualised after two and four passages, respectively (Chu et al., 2020; Lee et al., 2020b; Meekins et al., 2020; Schlottau et al., 2020).

Unfortunately, neither the non-human primate cells nor the other mammals cell lines have been thoroughly characterized from the perspective of use for studies with SARS-CoV-2. There is no information about the abundance of its receptors, and little is known about the virus replication rates in these cells compared to human cells or even Vero cells. Wurtz et al. (2021) presented viral titers measured by TCID₅₀ that indicate that those obtained with BGMK and MA-104 cells are between three and ten times higher than those obtained by Vero E6 cells approaches for two distinct isolates of SARS-CoV-2 at seven days post-infection, and they observed evident CPE 48 hours post-infection (Table 1). The TCID₅₀/mL results published by Wang et al. (2021) also point out viral productions which are higher or similar to Vero E6 cells for BGMK and CV-1 cells, while those with rhesus macaque (*M. mulatta*) kidney epithelial cells LLC-MK2 and RhMK are usually lower than those with Vero E6.

These studies employing SARS-CoV-2 against a range of cell lines commonly used in research laboratories (Wurtz et al., 2021 and Wang et al., 2021) also generate a great deal of information about cells that are not susceptible to SARS-CoV-2. These data

are presented in [Supplementary Table 2](#) to prevent strains from being repeatedly tested against this virus or being erroneously used in studies.

Overcoming SARS-CoV-2 culture restrictions

This SARS-CoV-2 not-permissive range of immortalized cells has become a challenge for developing these virus studies. In addition to many cells not allowing the virus to replicate, many of the established human cell culture lines have low-level SARS-CoV-2 production levels (Takayama, 2020). However, these drawbacks can be overcome by applying biotechnology tools to design cells that can, conveniently, be explicitly used for SARS-CoV-2.

Regarding cell susceptibility, cells were widely developed that expressed or overexpressed the receptors used by the virus for adhesion and penetration. For example, the lung adenocarcinoma cell line A549 was previously understood to be a cell which was not susceptible to SARS-CoV-2 (Chu et al., 2020; Wurtz et al., 2021), but the overexpression of human ACE2 in this cell line makes infection with SARS-CoV-2 possible (Figure 3) (Weston et al., 2020; Xie et al., 2020). The A549 cells overexpressing ACE2 has been shown to be valuable tools in anti-SARS-CoV-2 drug screening (Plaze et al., 2021; Pyrc et al., 2021; Napolitano et al., 2022). A new report of transduced A549 subclones selected to express more ACE2, and TMPRSS2 transcripts than existing commercial A549 cells engineered to express ACE2 and TMPRSS2 highlights its increased susceptibility, including to the Delta and Omicron variants, and its potential as a drug-inhibition cellular model (Chang et al., 2022).

Commercial HeLa-bases (derived from cervical cancer cells (Scherer et al., 1953)) and HEK 293T-based cell lines that are genetically modified to express ACE2, TMPRSS2, or both are currently available (Figure 3) (Vectorbuilder). HeLa-based cell lines have zero expression of endogenous TMPRSS2, and both HeLa and 293T-based cell lines do not express endogenous ACE2 (Vectorbuilder; Hoffmann et al., 2020). Combining cells that usually are not susceptible to a virus but that now express one or the other receptor, or both, is a valuable tool for understanding the role of each receptor in the viral entry process.

In addition to non-susceptible cells, the expression of additional receptors/co-receptors in cells known to be permissive to SARS-CoV-2 may represent a strategy to increase susceptibility and the rate of isolation. It has been well reported in TMPRSS2-expressing Vero E6 Cells, which were highly permissive to SARS-CoV-2 and other coronaviruses after this modification (Matsuyama et al., 2020). This leads not only to an increase in viral isolation rates but may also represent

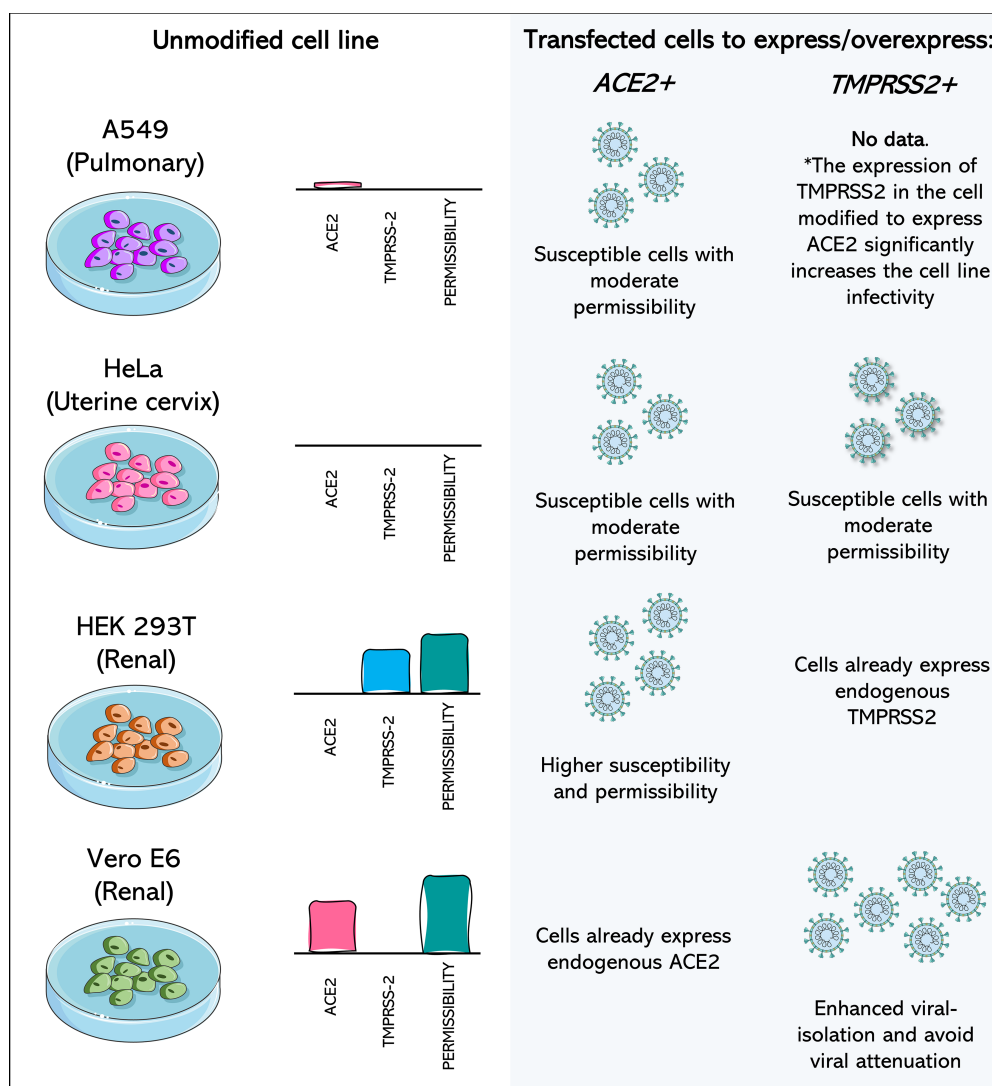


FIGURE 3

Cell lines transfected to express or overexpress ACE2 and TMPRSS2 show increased isolation of, susceptibility to, and permissibility for SARS-CoV-2. A549 (Pulmonary) cell line has poor expression of ACE2 and no expression of TMPRSS2, being considered a non-permissive cell to SARS-CoV-2. When ACE2 or both components are expressed after transfection of the cell, it becomes moderately permissive and susceptible to SARS-CoV-2. HeLa cells (Uterine cervix) are not susceptible to SARS-CoV-2 infection, as they do not express the viral receptors. Transfection of ACE2 and TMPRSS2 leads to susceptibility and moderate permissibility. In susceptible cells, such as Vero E6 monkey cells and HEK 293T and human renal cells, transfection with the receptor which they do not express endogenously leads to greater cell permeability. Vero E6/TMPRSS2 + cells have higher rates of SARS-CoV-2 isolation and potentially prevent attenuation of the virus. Data concerning the expression profile of each cell were recovered from Vectorbuilder; Murgolo et al., 2021; Saccon et al., 2021; Shuai et al., 2020 and Hoffmann et al., 2020. The asterisk (*) draws attention to the fact that no data was found about the impact of the expression of only TMPRSS2 in A549 cells, but the combination of TMPRSS2 expression in A549 cells already modified to overexpress ACE2 leads to increased infectivity.

a way of overcoming the main limitation of these cells (Figure 3), which is the rapid attenuation of the virus (Sasaki et al., 2021).

With the emergence/selection of new variants and subvariants, this approach using the same cell modified to express one or more receptors becomes particularly interesting for investigating the impact of the accumulated mutations in the

new variants/subvariants in viral invasion and pathogenesis. For example, the Omicron (B.1.1.529) BA.1 variant first identified in South Africa and Botswana rapidly spread globally, being classified as a variant of concern (VOC) by the WHO on 26 November 2021 (Burki, 2022; Fan et al., 2022). Attenuated replication and pathogenicity were identified and potentially

associated with the altered TMPRSS2-usage by this variant, impacting its infectivity (Goutam Mukherjee et al., 2022; Guo et al., 2022; McCallum et al., 2022; Meng et al., 2022; Shuai et al., 2022). When compared to the Delta variant, which preceded Omicron BA.1, the omicron variant presented higher affinity for ACE2, preferentially taking the endocytic pathway. This represents a concern about previously established cellular models becoming less efficient with the emergence of new variants and, in this way, the scientific community must remain vigilant.

It has also been shown that serial passage of a SARS-CoV-2 isolate in human cell lines can lead to a selection of clones that significantly improve infectivity in the human liver (Huh7 and Huh7.5) and lung cancer cells (Calu-1 and A549) (Ramirez et al., 2021). However, this selection does not take place without substantial mutations of the viral genome occurring, including spike protein mutations such as 9-amino-acid deletion and 3-amino acid changes (E484D, P812R, and Q954H) that exhibited significantly less dependence on ACE2 (Ramirez et al., 2021). Finding the balance between adaptations and the isolates closest to circulating variants is challenging for researchers.

Other *in vitro* approaches

Cell lines are not the only *in vitro* tools for studying viruses. Although these platforms have certain strengths, especially as they can be stored indefinitely in the laboratory, are fast growing, and are usually well characterised, cell lines often differ genetically and phenotypically from their tissue of origin (Pan et al., 2009; Geraghty et al., 2014; Lorsch et al., 2014). Therefore, their results may be relatively distant from what is observed in the original tissues, and inferences must be cautiously made.

To come to more consistent conclusions, it is desirable that the researcher can combine different *in vitro* approaches in order to later complement them with *in vivo* approaches. Therefore, in addition to searching for cell lineage models for the study of SARS-CoV-2, we also sought to evaluate and develop alternative *in vitro* tools against this virus, such as assays in primary cells and cellular organoids.

Primary cells

The primary cell culture is established from growing cells from the mechanical or enzymatic breakdown of tissue, from the moment of isolation until the first subculture (Lednický and Wyatt, 2012; Alves and Guimarães, 2010). After disaggregation, the cells will be selected and maintained in culture, and they will be considered as cells which have been isolated from a given

tissue. Although these cells have a short life span, their main advantage is the presence of their genotypic and phenotypic characteristics. That may reflect *in vitro* more faithfully than in the cell lines, as what happens in infected human airways.

For example, primary cell lines have been mainly used for SARS-CoV-2 culture in the aim to study the host transcriptional profiles, especially cytokines expression have been exhaustively analyzed aiming to better understand the immune phase and cytokine storm of COVID-19 (Blanco-Melo et al., 2020; Gamage et al., 2020). SARS-CoV-2 infection of primary neuronal cultures from transgenic mice expressing human ACE2 under the cytokeratin 18 promoter pointed for an activation of the ZBP1/pMLKL-regulated necroptosis pathway on this SARS-CoV-2 infected cells (Rothan et al., 2022). Proposing insights into the neuropathogenesis of SARS-CoV-2 infection in mice models.

Since the beginning of the SARS-CoV-2 outbreak, primary cells from the human airway epithelium (HAE) have been employed, since they had already been proposed for other coronaviruses. Primary HAE cells were used to isolate and discover SARS-CoV-2 just after its emergence in Wuhan, China. Bronchoalveolar lavage samples from three patients with unknown pneumonia were inoculated into the primary culture of HAE expanded in an air-liquid interface (ALI) system (Zhu et al., 2020). The virus was detected by transmission electron microscopy and molecular techniques for detecting the coronavirus genome. In addition, the culture presented CPE, the absence of ciliary movement, 96 hours post-infection (Zhu et al., 2020).

In Primary Human Nasal Epithelial Cells (HNECs) and human bronchial epithelial cells (HBECs), significant expression of ACE2 and TMPRSS2 was demonstrated (Gamage et al., 2020; Lukassen et al., 2020). The HNECs were permissive to SARS-CoV-2 strain harbouring a 382-nt deletion in ORF8, but revealed similar viral kinetics and host transcriptional profiles, as well as secretion of IP-10 (Gamage et al., 2020). Electron microscopy also sought to characterise the replication cycle, especially the assembly in viral factories of SARS-CoV-2 in HNEC (Morrison et al., 2022; Pinto et al., 2022). The infection of HBECs by SARS-CoV-2 led to the downregulation of tight junction molecules, the loss of cilia (Hao et al., 2020; Ryu and Shin, 2021), and the induction of many pro-inflammatory cytokines/chemokines (Blanco-Melo et al., 2020).

Primary human tracheal airway epithelial cells (HtAECs) and human small airway epithelial cells (HsAECs) also grow in ALI, showed themselves to be SARS-CoV-2 permissive cells, and presented robust viral release through the apical side for over 14 days post-infection (Nguyen et al., 2021). Both cells have been suggested to be useful for drug screening in antiviral trials (Nguyen et al., 2021).

The primary HAE cells are essential for understanding the pathophysiological mechanisms of SARS-CoV-2 infection and a large volume of information is generated by studies that use primary cells. However, it is challenging to reach general conclusions since the expression level of the evaluated molecules, which includes the receptors for SARS-CoV-2, vary by type, function, and location of the airway epithelial cells. They also differ from host to host depending on age, sex, and comorbid diseases (Ryu and Shin, 2021).

Although primary HAE cells have gained prominence in studies of SARS-CoV-2, which is a respiratory virus, other primary cultures, such as primary human renal epithelial cells (Kohli et al., 2022), primary ocular cells (Eriksen et al., 2021 - preprint; Eriksen et al., 2022), human peripheral blood mononuclear cells (PBMCs) (Pontelli et al., 2022) and human pancreatic progenitors (Szlachcic et al., 2022) are permissive to SARS-CoV-2. The range of primary cells permissive to SARS-CoV-2 opens the way for *in vitro* studies of more complex cellular organizations, such as organoids.

Organoid culture

An organoid is a three-dimensional multicellular *in vitro* tissue construct grown from stem cells on an extracellular matrix-like scaffold with specific niche factors (Ranga et al., 2014; Clevers, 2016; Sridhar et al., 2020; Hautefort et al., 2022). They can self-renew and aim to mimics their corresponding *in vivo* organ, generating *in vitro* functional structures containing the cell types present in the tissue they model (Hautefort et al., 2022). Therefore, organoids represent a valuable tool for studying aspects of an organ in the tissue culture dish.

Organoid technology was quickly embraced as a powerful tool for human virus studies, as it promised to provide a more accurate picture of the host factors essential for establishing viral infection and the mechanisms of viral pathogenesis (Clevers, 2020; Sridhar et al., 2020). With the emergence of COVID-19, multiple research groups turned to organoid approaches, especially to understand the tissue tropism of SARS-CoV-2 (Tran et al., 2022).

As for the study of primary cells, many approaches aimed to establish a respiratory model for SARS-CoV-2. The multipotent adult tissue stem cells (ASCs) approach allowed the elaboration of human distal lung organoids with apical-out polarity to present ACE2 on the exposed external surface, producing SARS-CoV-2 infective particles that were tested in Vero E6 cells, recovering from the organoid supernatant titers of less than 100 PFU/mL (Salahudeen et al., 2020). Meanwhile, bronchial infection rarely shows positive cells for the SARS-CoV-2 Spike protein, according to immunohistochemical analysis (Sano et al., 2022).

When the infection is successful, the main advantage presented by ALI cultures of airway organoid systems is that

the viral progeny recovered from them do not present culture-adaptive mutations in the multibasic cleavage site of the Spike protein of SARS-CoV-2 (Lamers et al., 2021; van der Vaart et al., 2021), suggesting that the organoid culture accurately models viral target cells *in vivo*.

As is the case for the cell lines derived from renal (HEK 293T), hepatic (Huh-7), and intestinal (Caco-2) tissues, kidney organoids established from human-induced pluripotent stem cells (iPSCs) (Monteil et al., 2020), ASCs-derived intestinal (Lamers et al., 2020; Zang et al., 2020; Zhou et al., 2020a) and liver organoids (Zhao et al., 2020a), were shown to be permissive to SARS-CoV-2. Infection of the liver organoids led to the formation of large syncytia such as CPE (Zhao et al., 2020a).

Established organoids from non-respiratory tissues play an essential role in understanding the viral pathophysiology and spread in the human body (Clevers, 2020). This can be further explored if organoids permissive to SARS-CoV-2 are developed from organs of which no cell lines permissive to the virus are known but which are affected in the infection process promoted by the emerging virus.

This is the case of eye cells. Cell lines have not been established which are derived from the tissues that make up the eyes, such as the cornea, sclera, and limbus. ACE2 and TMPRSS2 are expressed in the eyes, and in professional breeder cultures, SARS-CoV-2 has successfully infected limbus cells in particular (Eriksen et al., 2021; Tran et al., 2022). A similar result was obtained with retinal organoids and eye organoids, confirming endogenous receptors and SARS-CoV-2 infection mainly in limbus-like cells (Eriksen et al., 2021; Eriksen et al., 2022).

The issue of neurological complications of SARS-CoV-2 has also been addressed. It is proposed that the SARS-CoV-2 can enter the central nervous system by promoting damage to the epithelium and loss of barrier function or even by crossing the neural-mucosal interface in olfactory mucosa (Meinhardt et al., 2020). This may explain the loss of smell and taste experienced by some individuals with COVID-19.

The cell line U251 (derived from human glioblastoma) was previously suggested as a permissive cell for SARS-CoV-2 (Chu et al., 2020) but appears to have been little explored. In contrast, brain organoids have been well investigated, aiming to confirm or deny SARS-CoV-2 infection and identify target cell types in the brain. The results, however, have been conflicting, detecting the SARS-CoV-2 virus in the neurons but not producing infection (Ramani et al., 2020). Furthermore, effective infections were only confirmed in subsequent studies with brain organoids that contained choroid plexus epithelium and only in this choroid region (Jacob et al., 2020; Pellegrini et al., 2020).

Even though they are promising tools for studying SARS-CoV-2 or viruses in general, these cultures are still far from perfect (De Souza, 2018). Although more complex than the other *in vitro* models usually available in research laboratories,

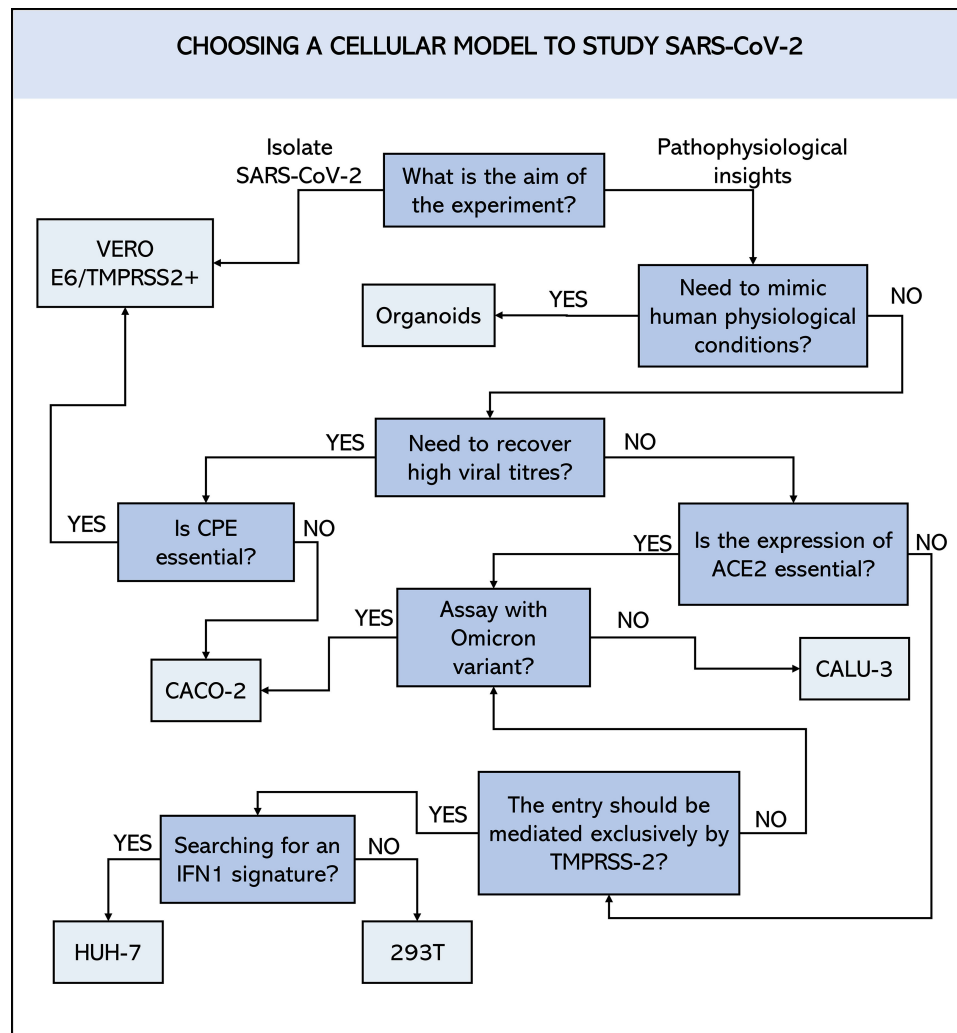


FIGURE 4

Schematic representation of a decision flowchart to choose which cell line to employ in SARS-CoV-2 studies. ACE2, angiotensin-converting enzyme 2 receptor; CPE, cytopathic effect; TMPRSS2, transmembrane protease serine 2; IFN1, Interferon type I.

they are still not complex enough, typically lacking vasculature and immune cells, for example. This approach is not easy to set up, it can take some time to develop the technology, and the final material is sometimes quantitatively limited and hard to handle. Thus, it is unlikely to be used for routine screening and has only been developed to address some very precise questions. Some types of organoids also do not fully replicate the structure of the organ they model. Taking brain organoids as an example, anatomical markers are not possible as they occur in the *in vivo* brain. Finally, the cells in the hPSC-derived organoids are relatively immature, with expression profiles similar to foetal tissues (De Souza, 2018). These limitations, therefore, should be considered when choosing organoids to study SARS-CoV-2.

Conclusions

There is currently no perfect cellular model for studying SARS-CoV-2. Each of the cells or approaches mentioned above has advantages over the others but also presents limitations in given setting. It is up to the researcher to find the balance between them and sometimes to consider overcoming these limitations through other resources. To this end, researchers must establish clear objectives and identify, within the current possibilities, the best model for the *in vitro* tests that will best serve their objective (Figure 4). This includes considering any financial and/or structural limitations. Given all the possibilities presented above, we hope that this study will contribute to making this choice easier.

Author contributions

Conceptualisation: GAPS and BLS; writing—original draft preparation, GAPS, MLB, SA, CD and BLS; writing—review and editing: GAPS, CB, NW, SA, PC, CD and BLS; supervision: BLS; project administration, BLS. All authors have read and agreed to the published version of the manuscript.

Funding

Agence Nationale de la Recherche (“Investments for the Future” program Méditerranée-Infection 10-IAHU-03).

Acknowledgments

Special thanks to my laboratory colleagues, Julie Dergham, Rita Jaafar, and Wahiba Bader, for all their support and for helping me conceptualize the figures with their advice.

References

- Abdelnabi, R., Foo, C. S., Zhang, X., Lemmens, V., Maes, P., Slechten, B., et al. (2022). The omicron (B.1.1.529) SARS-CoV-2 variant of concern does not readily infect Syrian hamsters. *Antiviral Res.* 198, 105253. doi: 10.1016/j.antiviral.2022.105253
- Almeida, J. D., and Tyrrell, D. A. J. (1967). The morphology of three previously uncharacterized human respiratory viruses that grow in organ culture. *J. Gen. Virol.* 1, 175–178. doi: 10.1099/0022-1317-1-2-175
- Al-Tawfiq, J. A., Azhar, E. I., Memish, Z. A., and Zumla, A. (2021). Middle East respiratory syndrome coronavirus. *Semin. Respir. Crit. Care Med.* 42, 828–838. doi: 10.1055/s-0041-1733804
- Alves, E. A., and Guimarães, A. C. R. (2010). “Cultivo celular,” in *Conceitos e métodos para a formação de profissionais em laboratórios de saúde*, vol. 2 (Rio de Janeiro: EPSJV), 215–252. Available at: http://www.epsjv.fiocruz.br/upload/d/capitulo_5_vol2.pdf.
- Ammerman, N., Beier-Sexton, M., and Azad, A. (2008). Vero cell line maintenance. *Curr. Protoc. Microbiol.* 4, 1–10. doi: 10.1002/9780471729259.mca04es11.Growth
- Arslan, M., Xu, B., and Gamal El-Din, M. (2020). Transmission of SARS-CoV-2 via fecal-oral and aerosols-borne routes: Environmental dynamics and implications for wastewater management in underprivileged societies. *Sci. Total Environ.* 743. doi: 10.1016/j.scitotenv.2020.140709
- Baczenas, J. J., Andersen, H., Rashid, S., Yarmosh, D., Puthuvelil, N., Parker, M., et al. (2021). Propagation of SARS-CoV-2 in calu-3 cells to eliminate mutations in the furin cleavage site of spike. *Viruses* 13. doi: 10.3390/V13122434
- Barrett, P. N., Mundt, W., Kistner, O., and Howard, M. K. (2009). Vero cell platform in vaccine production: moving towards cell culture-based viral vaccines. *Expert Rev. Vaccines* 8, 607–618. doi: 10.1586/ERV.09.19
- Bauer, L., Laksono, B. M., de Vrij, F. M. S., Kushner, S. A., Harschnitz, O., and van Riel, D. (2022). The neuroinvasiveness, neurotropism, and neurovirulence of SARS-CoV-2. *Trends Neurosci.* 45, 358–368. doi: 10.1016/j.tins.2022.02.006
- Bayati, A., Kumar, R., Francis, V., and McPherson, P. S. (2021). SARS-CoV-2 infects cells after viral entry via clathrin-mediated endocytosis. *J. Biol. Chem.* 296. doi: 10.1016/j.jbc.2021.100306
- Belouzard, S., Millet, J. K., Licita, B. N., and Whittaker, G. R. (2012). Mechanisms of coronavirus cell entry mediated by the viral spike protein. *Viruses* 4, 1011–1033. doi: 10.3390/v4061011
- Bhella, D. (2015). The role of cellular adhesion molecules in virus attachment and entry. *Philos. Trans. R. Soc. B Biol. Sci.* 370. doi: 10.1098/rstb.2014.0035
- Blanco-Melo, D., Nilsson-Payant, B. E., Liu, W. C., Uhl, S., Hoagland, D., Møller, R., et al. (2020). Imbalanced host response to SARS-CoV-2 drives development of COVID-19. *Cell* 181, 1036–1045.e9. doi: 10.1016/j.cell.2020.04.026
- Bojkova, D., Klann, K., Koch, B., Widera, M., Krause, D., Ciesek, S., et al. (2020). Proteomics of SARS-CoV-2-infected host cells reveals therapy targets. *Nature* 583, 469–472. doi: 10.1038/s41586-020-2332-7
- Boni, M. F., Lemey, P., Jiang, X., Lam, T. T. Y., Perry, B. W., Castoe, T. A., et al. (2020). Evolutionary origins of the SARS-CoV-2 sarbecovirus lineage responsible for the COVID-19 pandemic. *Nat. Microbiol.* 5, 1408–1417. doi: 10.1038/s41564-020-0771-4
- Bosco-Lauth, A. M., Hartwig, A. E., Porter, S. M., Gordy, P. W., Nehring, M., Byas, A. D., et al. (2020). Experimental infection of domestic dogs and cats with SARS-CoV-2: Pathogenesis, transmission, and response to reexposure in cats. *Proc. Natl. Acad. Sci. USA* 117, 26382–26388. doi: 10.1073/pnas.2013102117
- Bos, L. (1981). Hundred years of Koch's postulates and the history of etiology in plant virus research. *Netherlands J. Plant Pathol.* 87, 91–110. doi: 10.1007/BF01976645
- Bruchez, A., Sha, K., Johnson, J., Chen, L., Stefani, C., McConnell, H., et al. (2020). MHC class II transactivator CIITA induces cell resistance to ebola virus and SARS-like coronaviruses. *Science* 370, 241–247. doi: 10.1126/SCIENCE.ABB3753/SUPPL_FILE/ABB3753_BRUCHEZ_SM.PDF
- Buchholz, C. J., Schneider, U., Devaux, P., Gerlier, D., and Cattaneo, R. (1996). Cell entry by measles virus: long hybrid receptors uncouple binding from membrane fusion. *J. Virol.* 70, 3716–3723. doi: 10.1128/jvi.70.6.3716-3723.1996
- Burki, T. K. (2022). Omicron variant and booster COVID-19 vaccines on. *Lancet Respir. Med.* 10, e17. doi: 10.1016/S2213-2600(21)00559-2
- Caccuri, F., Zani, A., Messali, S., Giovanetti, M., Bugatti, A., Campisi, G., et al. (2020). A persistently replicating SARS-CoV-2 variant derived from an asymptomatic individual. *J. Transl. Med.* 18, 1–12. doi: 10.1186/s12967-020-02535-1
- Canton, J. (2018). Macropinocytosis: New insights into its underappreciated role in innate immune cell surveillance. *Front. Immunol.* 9. doi: 10.3389/fimmu.2018.02286

Conflict of interest

The authors declare that the research was conducted in the absence of any commercial or financial relationships that could be construed as a potential conflict of interest.

Publisher's note

All claims expressed in this article are solely those of the authors and do not necessarily represent those of their affiliated organizations, or those of the publisher, the editors and the reviewers. Any product that may be evaluated in this article, or claim that may be made by its manufacturer, is not guaranteed or endorsed by the publisher.

Supplementary material

The Supplementary Material for this article can be found online at: <https://www.frontiersin.org/articles/10.3389/fcimb.2022.1003608/full#supplementary-material>

- Cantuti-Castelvetri, L., Ojha, R., Pedro, L. D., Djannatian, M., Franz, J., Kuivainen, S., et al. (2020). Neuropilin-1 facilitates SARS-CoV-2 cell entry and infectivity. *Science* 370, 856–860. doi: 10.1126/science.abd2985
- Chang, C. W., Parsi, K. M., Somasundaran, M., Vanderleeden, E., Liu, P., Cruz, J., et al. (2022). A newly engineered A549 cell line expressing ACE2 and TMPRSS2 is highly permissive to SARS-CoV-2, including the delta and omicron variants. *Viruses* 14. doi: 10.3390/v14071369
- Chappell, J. D., and Dermody, T. S. (2015). Biology of viruses and viral diseases. *Mand. Douglas Bennett's Princ. Pract. Infect. Dis.* 2, 1681. doi: 10.1016/B978-1-4557-4801-3.00134-X
- Chen, Y., Chen, L., Deng, Q., Zhang, G., Wu, K., Ni, L., et al. (2020). The presence of SARS-CoV-2 RNA in the feces of COVID-19 patients. *J. Med. Virol.* 92, 833–840. doi: 10.1002/jmv.25825
- Chen, X., Saccon, E., Appelberg, K. S., Mikaeloff, F., Rodriguez, J. E., Vinhas, B. S., et al. (2021). Type-1 interferon signatures in SARS-CoV-2 infected Huh7 cells. *Cell Death Discovery* 7. doi: 10.1038/s41420-021-00487-z
- Cheung, K. S., Hung, I. F. N., Chan, P. P. Y., Lung, K. C., Tso, E., Liu, R., et al. (2020). Gastrointestinal manifestations of SARS-CoV-2 infection and virus load in fecal samples from a Hong Kong cohort: Systematic review and meta-analysis. *Gastroenterology* 159, 81–95. doi: 10.1053/j.gastro.2020.03.065
- Chu, H., Chan, J. F.-W., Yuen, T. T.-T., Shuai, H., Yuan, S., Wang, Y., et al. (2020). Comparative tropism, replication kinetics, and cell damage profiling of SARS-CoV-2 and SARS-CoV with implications for clinical manifestations, transmissibility, and laboratory studies of COVID-19: an observational study. *Lancet Microbe* 1, e14–e23. doi: 10.1016/s2666-5247(20)30004-5
- Cinat, J., Hoefer, G., Morgenstern, B., Preiser, W., Vogel, J. U., Hofmann, W. K., et al. (2004). Infection of cultured intestinal epithelial cells with severe acute respiratory syndrome coronavirus. *Cell. Mol. Life Sci.* 61, 2100–2112. doi: 10.1007/s00018-004-4222-9
- Clevers, H. (2016). Modeling development and disease with organoids. *Cell* 165, 1586–1597. doi: 10.1016/j.cell.2016.05.082
- Clevers, H. (2020). COVID-19: organoids go viral. *Nat. Rev. Mol. Cell Biol.* 21, 355–356. doi: 10.1038/s41580-020-0258-4
- Clok, M. R. J., Millard, A. D., Letarov, A. V., and Heaphy, S. (2011). Phages in nature. *Bacteriophage* 1, 31. doi: 10.4161/BACT.1.1.14942
- Cohen, E. M., Avital, N., Shamay, M., and Kobiler, O. (2019). Abortive herpes simplex virus infection of nonneuronal cells results in quiescent viral genomes that can reactivate. *Proc. Natl. Acad. Sci. U. S. A.* 117, 635–640. doi: 10.1073/pnas.1910537117
- Coimbra, L. D., Borin, A., Fontoura, M., Gravina, H. D., Nagai, A., Shimizu, J. F., et al. (2022). Identification of compounds with antiviral activity against SARS-CoV-2 in the MMV pathogen box using a phenotypic high-throughput screening assay. *Front. Virol.* 0. doi: 10.3389/FVIR.2022.854363
- Colomer-Lluch, M., Ruiz, A., Moris, A., and Prado, J. G. (2018). Restriction factors: From intrinsic viral restriction to shaping cellular immunity against HIV-1. *Front. Immunol.* 9. doi: 10.3389/fimmu.2018.02876
- Combe, M., Garijo, R., Geller, R., Cuevas, J. M., and Sanjuán, R. (2015). Single-cell analysis of RNA virus infection identifies multiple genetically diverse viral genomes within single infectious units. *Cell Host Microbe* 18, 424–432. doi: 10.1016/j.chom.2015.09.009
- Coombs, R. R. A., Gurner, B. W., Beale, A. J., Christofinis, G., and Page, Z. (1961). The identity of three strains of cells derived from pig or rabbit kidney tissue, checked by means of the mixed agglutination reaction. *Exp. Cell Res.* 24, 604–605. doi: 10.1016/0014-4827(61)90464-5
- Crandell, R. A., Fabricant, C. G., and Nelson-Rees, W. A. (1973). Development, characterization, and viral susceptibility of a feline (*Felis catus*) renal cell line (CRFK). *Vitr* 9, 176–185. doi: 10.1007/BF02618435
- Cui, J., Li, F., and Shi, Z. L. (2019). Origin and evolution of pathogenic coronaviruses. *Nat. Rev. Microbiol.* 17, 181–192. doi: 10.1038/s41579-018-0118-9
- Daly, J. L., Simonetti, B., Klein, K., Chen, K. E., Williamson, M. K., Antón-Plágaro, C., et al. (2020). Neuropilin-1 is a host factor for SARS-CoV-2 infection. *Science* 370, 861–865. doi: 10.1126/science.abd3072
- Danziger, O., Patel, R. S., DeGrace, E. J., Rosen, M. R., and Rosenberg, B. R. (2022). Inducible CRISPR activation screen for interferon-stimulated genes identifies OAS1 as a SARS-CoV-2 restriction factor. *PLoS Pathog.* 18, e1010464. doi: 10.1371/JOURNAL.PPAT.1010464
- De Clercq, E., Stewart, W. E., and De Somer, P. (1973). Studies on the mechanism of the priming effect of interferon on interferon production by cell cultures exposed to Poly(rI) · Poly(rC). *Infect. Immun.* 8, 309. doi: 10.1128/IAI.8.3.309-316.1973
- De Souza, N. (2018). Organoids. *Nat. Methods* 15, 23. doi: 10.1038/nmeth.4576
- de Souza, G. A. P., Bideau, M., Boschi, C., Ferreira, L., Wurtz, N., Devaux, C., et al. (2022). Emerging sars-cov-2 genotypes show different replication patterns in human pulmonary and intestinal epithelial cells. *Viruses* 14, 23. doi: 10.3390/v14010023
- de Souza, G. A. P., Queiroz, V. F., Coelho, L. F. L., and Abrahão, J. S. (2021). Alohomora! what the entry mechanisms tell us about the evolution and diversification of giant viruses and their hosts. *Curr. Opin. Virol.* 47, 79–85. doi: 10.1016/j.coviro.2021.02.003
- De Souza, G. A. P., Queiroz, V. F., Lima, M. T., De Sousa Reis, E. V., Coelho, L. F. L., and Abrahão, J. S. (2020). Virus goes viral: An educational kit for virology classes. *Virol. J.* 17, 1–8. doi: 10.1186/s12985-020-1291-9
- de Wilde, A. H., Raj, V. S., Oudshoorn, D., Bestebroer, T. M., van Nieuwkoop, S., Limpens, R. W. A. L., et al. (2013). MERS-coronavirus replication induces severe *in vitro* cytopathology and is strongly inhibited by cyclosporin A or interferon- α treatment. *J. Gen. Virol.* 94, 1749. doi: 10.1099/VIR.0.052910-0
- Dimitrov, D. S. (2004). Virus entry: Molecular mechanisms and biomedical applications. *Nat. Rev. Microbiol.* 2, 109–122. doi: 10.1038/nrmicro817
- Dittmar, M., Seung Lee, J., Whig, K., Segrist, E., Li, M., Kamalia, B., et al. (2021). Drug repurposing screens reveal cell-type-specific entry pathways and FDA-approved drugs active against SARS-CoV-2 graphical abstract. *Cell Rep.* 35, 108959. doi: 10.1016/j.celrep.2021.108959
- Dubridge, R. B., Tang, P., Chao Hsia, H., Leong, P.-M., Miller, J. H., and Calos, M. P. (1987). Analysis of mutation in human cells by using an Epstein-Barr virus shuttle system. *Mol. Cell. Biol.* 7, 379. doi: 10.1128/MCB.7.1.379
- Earle, K. A., Ambrosino, D. M., Fiore-Gartland, A., Goldblatt, D., Gilbert, P. B., Siber, G. R., et al. (2021). Evidence for antibody as a protective correlate for COVID-19 vaccines. *Vaccine* 39, 4423–4428. doi: 10.1016/j.vaccine.2021.05.063
- Ellis, D. S., Stamford, S., Tovey, D. G., Lloyd, G., Bowen, E. T. W., Platt, G. S., et al. (1979). Ebola And marburg viruses: II. thier development within vero cells and the extra-cellular formation of branched and torus forms. *J. Med. Virol.* 4, 213–225. doi: 10.1002/JMV.1890040307
- Emeny, J. M., and Morgan, M. J. (1979). Regulation of the interferon system: Evidence that vero cells have a genetic defect in interferon production. *J. Gen. Virol.* 43, 247–252. doi: 10.1099/0022-1317-43-1-247/CITE/NETWORKS
- Eriksen, A. Z., Möller, R., Makovoz, B., tenOever, B. R., and Blenkinsop, T. A. (2022). Protocols for SARS-CoV-2 infection in primary ocular cells and eye organoids. *STAR Protoc.* 3, 101383. doi: 10.1016/J.XPRO.2022.101383
- Eriksen, A. Z., Möller, R., Makovoz, B., Uhl, S. A., tenOever, B. R., and Blenkinsop, T. A. (2021). SARS-CoV-2 infects human adult donor eyes and hESC-derived ocular epithelium. *Cell Stem Cell* 28, 1205–1220.e7. doi: 10.1016/j.stem.2021.04.028
- Faist, S. (1999). “PROPAGATION OF VIRUSES | animal,” in *Encyclopedia of virology* (Cambridge:Massachusetts: Academic Press), 1408–1413. doi: 10.1006/rwvi.1999.0236
- Fan, Y., Li, X., Zhang, L., Wan, S., Zhang, L., and Zhou, F. (2022). SARS-CoV-2 omicron variant: recent progress and future perspectives. *Signal Transduction Targeting Ther.* 7, 141. doi: 10.1038/S41392-022-00997-X
- Felgenhauer, U., Schoen, A., Gad, H. H., Hartmann, R., Schaubmar, A. R., Failing, K., et al. (2020). Inhibition of SARS-CoV-2 by type I and type III interferons. *J. Biol. Chem.* 295, 13958–13964. doi: 10.1074/JBC.AC120.013788
- Flemming, A. (2021). Cross-reactive memory T cells abort SARS-CoV-2 infection. *Nat. Rev. Immunol.* 2021 221 22, 5–5. doi: 10.1038/s41577-021-00667-z
- Fogel, A., and Plotkin, S. A. (1969). Markers of rubella virus strains in RK 13 cell culture. *J. Virol.* 3, 157–163. doi: 10.1128/jvi.3.2.157-163.1969
- Fogh, J., Fogh, J. M., and Orfeo, T. (1977). One hundred and twenty seven cultured human tumor cell lines producing tumors in nude mice. *J. Natl. Cancer Inst.* 59, 221–226. doi: 10.1093/jnci/59.1.221
- Freitas, R. S., Crum, T. F., and Parvatiyar, K. (2022). SARS-CoV-2 spike antagonizes innate antiviral immunity by targeting interferon regulatory factor 3. *Front. Cell. Infect. Microbiol.* 11. doi: 10.3389/fcimb.2021.789462/BIBTEX
- Game, A. M., Sen, K., Chan, W. O. Y., Liu, J., Tan, C. W., Ong, Y. K., et al. (2020). Infection of human nasal epithelial cells with SARS-CoV-2 and a 382-nt deletion isolate lacking ORF8 reveals similar viral kinetics and host transcriptional profiles. *PLoS Pathog.* 16, e1009130. doi: 10.1371/JOURNAL.PPAT.1009130
- Geraghty, R. J., Capes-Davis, A., Davis, J. M., Downward, J., Freshney, R. I., Knezevic, I., et al. (2014). Guidelines for the use of cell lines in biomedical research. *Br. J. Cancer* 111. doi: 10.1038/bjc.2014.166
- Gillim-Ross, L., Taylor, J., Scholl, D. R., Ridenour, J., Masters, P. S., and Wentworth, D. E. (2004). Discovery of novel human and animal cells infected by the severe acute respiratory syndrome coronavirus by replication-specific multiplex reverse transcription-PCR. *J. Clin. Microbiol.* 42, 3196–3206. doi: 10.1128/JCM.42.7.3196-3206.2004
- Golikov, M. V., Karpenko, I. L., Lipatova, A. V., Ivanova, O. N., Fedyakina, I. T., Larichev, V. F., et al. (2022). Cultivation of cells in a physiological plasmex medium increases mitochondrial respiratory capacity and reduces replication levels of RNA viruses. *Antioxidants* 11. doi: 10.3390/antiox11010097

- Gomes, C. P., Fernandes, D. E., Casimiro, F., da Mata, G. F., Passos, M. T., Varela, P., et al. (2020). Cathepsin I in COVID-19: From pharmacological evidences to genetics. *Front. Cell. Infect. Microbiol.* 10. doi: 10.3389/fcimb.2020.589505
- Gorbalenya, A. E., Baker, S. C., Baric, R. S., de Groot, R. J., Drosten, C., Gulyaeva, A. A., et al. (2020). The species severe acute respiratory syndrome-related coronavirus: classifying 2019-nCoV and naming it SARS-CoV-2. *Nat. Microbiol.* 5, 536–544. doi: 10.1038/s41564-020-0695-z
- Gorman, B. (1991). The natural history of rabies: 2nd edn Editor: George m. baer. CRC press, Boca raton, FL. ISBN 0-8493-6760-3, US\$295. *Virus Res.* 21, 163. doi: 10.1016/0168-1702(91)90006-H
- Goutam Mukherjee, A., Ramesh Wanjari, U., Murali, R., Chaudhary, U., Renu, K., Madhyastha, H., et al. (2022). Omicron variant infection and the associated immunological scenario. *Immunobiology* 227, 152222. doi: 10.1016/J.IMBIO.2022.152222
- Graham, R. L., and Baric, R. S. (2010). Recombination, reservoirs, and the modular spike: mechanisms of coronavirus cross-species transmission. *J. Virol.* 84, 3134–3146. doi: 10.1128/JVI.01394-09
- Graham, F. L., Smiley, J., Russell, W. C., and Nairn, R. (1977). Characteristics of a human cell line transformed by DNA from human adenovirus type 5. *J. Gen. Virol.* 36, 59–72. doi: 10.1099/0022-1317-36-1-59/CITE/REFWORKS
- Grossegess, M., Bourquain, D., Neumann, M., Schaade, L., Schulze, J., Mache, C., et al. (2022). Deep time course proteomics of SARS-CoV-2 and SARS-CoV-2-Infected human lung epithelial cells (Calu-3) reveals strong induction of interferon-stimulated gene expression by SARS-CoV-2 in contrast to SARS-CoV. *Cite This J. Proteome Res.* 21, 459–469. doi: 10.1021/acs.jproteome.1c00783
- Gu, Y., Cao, J., Zhang, X., Gao, H., Wang, Y., Wang, J., et al. (2022). Receptome profiling identifies KREMEN1 and ASGR1 as alternative functional receptors of SARS-CoV-2. *Cell Res.* 32, 24–37. doi: 10.1038/s41422-021-00595-6
- Guo, Y., Han, J., Zhang, Y., He, J., Yu, W., Zhang, X., et al. (2022). SARS-CoV-2 omicron variant: Epidemiological features, biological characteristics, and clinical significance. *Front. Immunol.* 13. doi: 10.3389/fimmu.2022.877101
- Halfmann, P. J., Iida, S., Iwatsuki-Horimoto, K., Maemura, T., Kiso, M., Scheaffer, S. M., et al. (2022). SARS-CoV-2 omicron virus causes attenuated disease in mice and hamsters. *Nature* 603, 687–692. doi: 10.1038/s41586-022-04441-6
- Hao, S., Ning, K., Kuz, C. A., Vorhies, K., Yan, Z., and Qiu, J. (2020). Long-term modeling of SARS-CoV-2 infection of *In vitro* cultured polarized human airway epithelium. *MBio* 11, 1–17. doi: 10.1128/mBio.02852-20
- Harcourt, J., Tamin, A., Lu, X., Kamili, S., Sakthivel, S. K., Murray, J., et al. (2020). Severe acute respiratory syndrome coronavirus 2 from patient with coronavirus disease, united states. *Emerg. Infect. Dis.* 26, 1266–1273. doi: 10.3201/EID2606.200516
- Harvey, W. T., Carabelli, A. M., Jackson, B., Gupta, R. K., Thomson, E. C., Harrison, E. M., et al. (2021). SARS-CoV-2 variants, spike mutations and immune escape. *Nat. Rev. Microbiol.* 19, 409–424. doi: 10.1038/s41579-021-00573-0
- Hautefort, I., Poletti, M., Papp, D., and Korcsmaros, T. (2022). Everything you always wanted to know about organoid-based models (and never dared to ask). *Cell. Mol. Gastroenterol. Hepatol* 14, 311–331 doi: 10.1016/j.jcmgh.2022.04.012
- Heldt, F. S., Kupke, S. Y., Dorl, S., Reichl, U., and Frensing, T. (2015). Single-cell analysis and stochastic modelling unveil large cell-to-cell variability in influenza A virus infection. *Nat. Commun.* 2015 61 6, 1–12. doi: 10.1038/ncomms9938
- Heuschkel, M. J., Baumert, T. F., and Verrier, E. R. (2021). Cell culture models for the study of hepatitis d virus entry and infection. *Viruses* 13. doi: 10.3390/v13081532
- Hidalgo, I. J., Raub, T. J., and Borchardt, R. T. (1989). Characterization of the human colon carcinoma cell line (Caco-2) as a model system for intestinal epithelial permeability. *Gastroenterology* 96, 736–749. doi: 10.1016/S0016-5085(89)80072-1
- Hoffmann, M., Kleine-Weber, H., Schroeder, S., Krüger, N., Herrler, T., Erichsen, S., et al. (2020). SARS-CoV-2 cell entry depends on ACE2 and TMPRSS2 and is blocked by a clinically proven protease inhibitor. *Cell* 181, 271–280.e8. doi: 10.1016/j.cell.2020.02.052
- Hoffmann, M., Krüger, N., Schulz, S., Cossmann, A., Rocha, C., Kempf, A., et al. (2022). The omicron variant is highly resistant against antibody-mediated neutralization: Implications for control of the COVID-19 pandemic. *Cell* 185, 447–456.e11. doi: 10.1016/j.cell.2021.12.032
- Hoffmann, M., and Pöhlmann, S. (2022). Novel SARS-CoV-2 receptors: ASGR1 and KREMEN1. *Cell Res.* 32, 1. doi: 10.1038/s41422-021-00603-9
- Horimoto, T., and Kawaoka, Y. (2006). Strategies for developing vaccines against H5N1 influenza A viruses. *Trends Mol. Med.* 12, 506–514. doi: 10.1016/J.MOLMED.2006.09.003
- Hosoya, M., Honzumi, K., Sato, M., Katayose, M., Kato, K., and Suzuki, H. (1998). Application of PCR for various neurotropic viruses on the diagnosis of viral meningitis. *J. Clin. Virol.* 11, 117–124. doi: 10.1016/S1386-6532(98)00048-8
- Hui, D. S., Azhar, I., Madani, T. A., Ntoumi, F., Kock, R., Dar, O., et al. (2020). The continuing 2019-nCoV epidemic threat of novel coronaviruses to global health - the latest 2019 novel coronavirus outbreak in wuhan, China. *Int. J. Infect. Dis.* 91, 264–266. doi: 10.1016/j.ijid.2020.01.009
- Hu, J., Lin, Y. Y., Chen, P. J., Watashi, K., and Wakita, T. (2019). Cell and animal models for studying hepatitis b virus infection and drug development. *Gastroenterology* 156, 338–354. doi: 10.1053/j.gastro.2018.06.093
- Huthoff, H., and Towers, G. J. (2008). Restriction of retroviral replication by APOBEC3G/F and TRIM5α. *Trends Microbiol.* 16, 612–619. doi: 10.1016/j.tim.2008.08.013
- Jackson, C. B., Farzan, M., Chen, B., and Choe, H. (2022). Mechanisms of SARS-CoV-2 entry into cells. *Nat. Rev. Mol. Cell Biol.* 23, 3–20. doi: 10.1038/s41580-021-00418-x
- Jacob, F., Pather, S. R., Huang, W. K., Zhang, F., Wong, S. Z. H., Zhou, H., et al. (2020). Human pluripotent stem cell-derived neural cells and brain organoids reveal SARS-CoV-2 neurotropism predominates in choroid plexus epithelium. *Cell Stem Cell* 27, 937–950.e9. doi: 10.1016/j.stem.2020.09.016
- Kawamoto, M., Yamaji, T., Saito, K., Shirasago, Y., Satomura, K., Endo, T., et al. (2020). Identification of characteristic genomic markers in human hepatoma HuH-7 and Huh7.5.1-8 cell lines. *Front. Genet.* 11. doi: 10.3389/FGENE.2020.546106/BIBTEX
- Kaye, M., Druce, J., Tran, T., Kostecki, R., Chibo, D., Morris, J., et al. (2006). SARS-associated coronavirus replication in cell lines. *Emerg. Infect. Dis.* 12, 128–133. doi: 10.3201/eid1201.050496
- Kiesslich, S., and Kamen, A. A. (2020). Vero cell upstream bioprocess development for the production of viral vectors and vaccines. *Biotechnol. Adv.* 44, 107608. doi: 10.1016/j.biotechadv.2020.107608
- Kipkorir, V., Cheruiyot, I., Ngure, B., Misiani, M., and Munguti, J. (2020). Prolonged SARS-CoV-2 RNA detection in anal/rectal swabs and stool specimens in COVID-19 patients after negative conversion in nasopharyngeal RT-PCR test. *J. Med. Virol.* 92, 2328–2331. doi: 10.1002/jmv.26007
- Koch, J., Uckelely, Z. M., Doldan, P., Stanifer, M., Boulant, S., and Lozach, P. (2021). TMPRSS2 expression dictates the entry route used by SARS-CoV-2 to infect host cells. *EMBO J.* 40, 1–20. doi: 10.15252/emboj.2021107821
- Kohli, A., Sauerhering, L., Fehling, S. K., Klann, K., Geiger, H., Becker, S., et al. (2022). Proteomic landscape of SARS-CoV-2- and MERS-CoV-infected primary human renal epithelial cells. *Life Sci. Alliance* 5. doi: 10.26508/LSA.202201371
- Lamers, M. M., Beumer, J., Vaart, J., Knoop, K., Puschhof, J., Breugem, T. I., et al. (2020). SARS-CoV-2 productively infects human gut enterocytes. *Science* 369, 50–54. doi: 10.1126/SCIENCE.ABC1669/SUPPL_FILE/ABC1669_REPRODUCIBILITY_CHECKLIST.PDF
- Lamers, M. M., Mykytyn, A. Z., Breugem, T. I., Wang, Y., Wu, D. C., Riesebosch, S., et al. (2021). Human airway cells prevent sars-cov-2 multibasic cleavage site cell culture adaptation. *Elife* 10, 1–22. doi: 10.7554/ELIFE.66815
- Lappin, M. R., Jensen, W. A., Jensen, T. D., Basaraba, R. J., Brown, C. A., Radecki, S. V., et al. (2005). Investigation of the induction of antibodies against Crandell-Rees feline kidney cell lysates and feline renal cell lysates after parenteral administration of vaccines against feline viral rhinotracheitis, calicivirus, and panleukopenia in cats. *Am. J. Vet. Res.* 66, 506–511. doi: 10.2460/AJVR.2005.66.506
- Lawson, J. S., Syme, H. M., Wheeler-Jones, C. P.D., and Elliott, J. (2019). Characterisation of Crandell-Rees Feline Kidney (CRFK) cells as mesenchymal in phenotype. *Res. Vet. Sci.* 127, 99–102. doi: 10.1016/j.rvsc.2019.10.01
- Lednický, J. A., and Wyatt, D. E. (2012). The art of animal cell culture for virus isolation. *Biomed. Tissue Cult (Rijeka, Croatia: IntechOpen)*, 151–178. doi: 10.5772/51215
- Lee, S., Lee, Y., Choi, Y., Son, A., Park, Y., Lee, K. M., et al. (2021). The SARS-CoV-2 RNA interactome. *Mol. Cell* 81, 2838–2850.e6. doi: 10.1016/J.MOLCEL.2021.04.022
- Lee, D. K., Park, J., and Seo, D. W. (2020a). Suspension culture of vero cells for the production of adenovirus type 5. *Clin. Exp. Vaccine Res.* 9, 48. doi: 10.7774/CEVR.2020.9.1.48
- Lee, S., Yoon, G. Y., Myoung, J., Kim, S. J., and Ahn, D. G. (2020b). Robust and persistent SARS-CoV-2 infection in the human intestinal brush border expressing cells. *Emerg. Microbes Infect.* 9, 2169–2179. doi: 10.1080/22221751.2020.1827985
- Leist, S. R., Schäu, A., and Martinez, D. R. (2020). Cell and animal models of SARS-CoV-2 pathogenesis and immunity. *DMM Dis. Model. Mech.* 13, 1–6. doi: 10.1242/dmm.046581
- Leland, D. S., and Ginocchio, C. C. (2007). Role of cell culture for virus detection in the age of technology. *Clin. Microbiol. Rev.* 20, 49. doi: 10.1128/CMR.00002-06
- Li, W., Shi, Z., Yu, M., Ren, W., Smith, C., Epstein, J. H., et al. (2005). Bats are natural reservoirs of SARS-like coronaviruses. *Science* 310, 676–679. doi: 10.1126/SCIENCE.1118391

- Liu, S., Chen, R., and Hagedorn, C. H. (2014). Direct visualization of hepatitis c virus-infected Huh7.5 cells with a high titre of infectious chimeric JFH1-EGFP reporter virus in three-dimensional matrigel cell cultures. *J. Gen. Virol.* 95, 423. doi: 10.1099/VIR.0.055772-0
- Liu, J., Li, Y., Liu, L., Hu, X., Wang, X., Hu, H., et al. (2020). Infection of human sweat glands by SARS-CoV-2. *Cell Discovery* 6, 1–3. doi: 10.1038/s41421-020-00229-y
- Liu, J., Li, Y., Liu, Q., Yao, Q., Wang, X., Zhang, H., et al. (2021). SARS-CoV-2 cell tropism and multiorgan infection. *Cell Discovery* 7, 1–4. doi: 10.1038/s41421-021-00249-2
- Lokugamage, K. G., Hage, A., de Vries, M., Valero-Jimenez, A. M., Schindewolf, C., Dittmann, M., et al. (2020). Type I interferon susceptibility distinguishes SARS-CoV-2 from SARS-CoV. *J. Virol.* 94. doi: 10.1128/jvi.01410-20
- Lorsch, J. R., Collins, F. S., and Lippincott-Schwartz, J. (2014). Fixing problems with cell lines: Technologies and policies can improve authentication. *Science* 346, 1452. doi: 10.1126/SCIENCE.1259110
- Louten, J. (2016). "Virus replication," in *Essential human virology* (Cambridge: Massachusetts: Academic Press), 49–70. doi: 10.1016/b978-0-12-800947-5.00004-1
- Lukassen, S., Chua, R. L., Trefzer, T., Kahn, N. C., Schneider, M. A., Muley, T., et al. (2020). SARS-CoV-2 receptor ACE 2 and TMPRSS 2 are primarily expressed in bronchial transient secretory cells. *EMBO J.* 39. doi: 10.15252/embj.20105114
- Mac Kain, A., Maarifi, G., Aicher, S. M., Arhel, N., Baidaliuk, A., Munier, S., et al. (2022). Identification of DAXX as a restriction factor of SARS-CoV-2 through a CRISPR/Cas9 screen. *Nat. Commun.* 2022 131 13, 1–13. doi: 10.1038/s41467-022-30134-9
- Maginnis, M. S. (2018). Virus-receptor interactions: The key to cellular invasion. *J. Mol. Biol.* 430, 2590–2611. doi: 10.1016/j.jmb.2018.06.024
- Marsh, M., and Helenius, A. (2006). Virus entry: Open sesame. *Cell* 124, 729–740. doi: 10.1016/j.cell.2006.02.007
- Martin-Sancho, L., Lewinski, M. K., Pache, L., Stoneham, C. A., Yin, X., Becker, M. E., et al. (2021). Functional landscape of SARS-CoV-2 cellular restriction. *Mol. Cell* 81, 2656–2668.e8. doi: 10.1016/j.molcel.2021.04.008
- Masre, S. F., Jufri, N. F., Ibrahim, F. W., and Abdul Raub, S. H. (2021). Classical and alternative receptors for SARS-CoV-2 therapeutic strategy. *Rev. Med. Virol.* 31, 1–9. doi: 10.1002/rmv.2207
- Matsuyama, S., Nao, N., Shirato, K., Kawase, M., Saito, S., Takayama, I., et al. (2020). Enhanced isolation of SARS-CoV-2 by TMPRSS2-expressing cells. *Proc. Natl. Acad. Sci. U. S. A.* 117, 7001–7003. doi: 10.1073/PNAS.2002589117
- Mautner, L., Hoyos, M., Dangel, A., Berger, C., Ehrhardt, A., and Baiker, A. (2022). Replication kinetics and infectivity of SARS-CoV-2 variants of concern in common cell culture models. *Virol. J.* 19, 1–11. doi: 10.1186/S12985-022-01802-5/TABLES/1
- McCallum, M., Czudnochowski, N., Rosen, L. E., Zepeda, S. K., Bowen, J. E., Walls, A. C., et al. (2022). Structural basis of SARS-CoV-2 omicron immune evasion and receptor engagement. *Science* 375, 894–898. doi: 10.1126/science.abn8652
- McFadden, G., Mohamed, M. R., Rahman, M. M., and Barte, E. (2009). Cytokine determinants of viral tropism. *Nat. Rev. Immunol.* 9, 645. doi: 10.1038/NRI2623
- McMahan, K., Giffin, V., Tostanoski, L. H., Chung, B., Siamatu, M., Suthar, M. S., et al. (2022). Reduced pathogenicity of the SARS-CoV-2 omicron variant in hamsters. *Med* 3, 262–268.e4. doi: 10.1016/J.MEDJ.2022.03.004
- Meekins, D. A., Morozov, I., Trujillo, J. D., Gaudreault, N. N., Bold, D., Carosino, M., et al. (2020). Susceptibility of swine cells and domestic pigs to SARS-CoV-2. *Emerg. Microbes Infect.* 9, 2278–2288. doi: 10.1080/22221751.2020.1831405/SUPPL_FILE/TEMI_A_1831405_SM8625.DOCX
- Meinhardt, J., Radke, J., Dittmayer, C., Franz, J., Thomas, C., Mothes, R., et al. (2020). Olfactory transmucosal SARS-CoV-2 invasion as a port of central nervous system entry in individuals with COVID-19. *Nat. Neurosci.* 24, 168–175. doi: 10.1038/s41593-020-00758-5
- Meng, B., Abdullahi, A., Ferreira, I. A. T. M., Goonawardane, N., Saito, A., Kimura, I., et al. (2022). Altered TMPRSS2 usage by SARS-CoV-2 omicron impacts infectivity and fusogenicity. *Nature* 603, 706–714. doi: 10.1038/s41586-022-04474-x
- Metz, P., Reuter, A., Bender, S., and Bartenschlager, R. (2013). Interferon-stimulated genes and their role in controlling hepatitis c virus. *J. Hepatol.* 59, 1331–1341. doi: 10.1016/j.jhep.2013.07.033
- Mier, J. W., and Gallo, R. C. (1980). Purification and some characteristics of human T-cell growth factor from phytohemagglutinin-stimulated lymphocyte-conditioned media. *Proc. Natl. Acad. Sci. U. S. A.* 77, 6134–6138. doi: 10.1073/pnas.77.10.6134
- Miller, C. L. (2011). Stress granules and virus replication. *Future Virol.* 6, 1329–1338. doi: 10.2217/fvl.11.108
- Mizuta, K., Abiko, C., Goto, H., Murata, T., and Murayama, S. (2003). Enterovirus isolation from children with acute respiratory infections and presumptive identification by a modified microplate method. *Int. J. Infect. Dis.* 7, 138–142. doi: 10.1016/S1201-9712(03)90010-5
- Modrof, J., Kerschbaum, A., Farcet, M. R., Niemeyer, D., Corman, V. M., and Kriel, T. R. (2020). SARS-CoV-2 and the safety margins of cell-based biological medicinal products. *Biologicals* 68, 122–124. doi: 10.1016/J.BIOLOGICALS.2020.08.010
- Monteil, V., Kwon, H., Prado, P., Hagelkrüys, A., Wimmer, R. A., Stahl, M., et al. (2020). Inhibition of SARS-CoV-2 infections in engineered human tissues using clinical-grade soluble human ACE2. *Cell* 181, 905–913.e7. doi: 10.1016/j.cell.2020.04.004
- Morgan, D. A., Ruscetti, F. W., and Gallo, R. (1976). Selective *in vitro* growth of T lymphocytes from normal human bone marrows. *Science* 193, 1007–1008. doi: 10.1126/science.181845
- Morrison, C. B., Edwards, C. E., Shaffer, K. M., Araba, K. C., Wykoff, J. A., Williams, D. R., et al. (2022). SARS-CoV-2 infection of airway cells causes intense viral and cell shedding, two spreading mechanisms affected by IL-13. *Proc. Natl. Acad. Sci. U. S. A.* 119. doi: 10.1073/PNAS.2119680119/SUPPL_FILE/PNAS.2119680119.SAPP.PDF
- Murgolo, N., Therien, A. G., Howell, B., Klein, D., Koeplinger, K., Lieberman, L. A., et al. (2021). SARS-CoV-2 tropism, entry, replication, and propagation: Considerations for drug discovery and development. *PLoS Pathog.* 17, 1–18. doi: 10.1371/JOURNAL.PPAT.1009225
- Mykityn, A. Z., Breugem, T. I., Riesebosch, S., Schipper, D., van den Doel, P. B., Rottier, R. J., et al. (2021a). SARS-CoV-2 entry into human airway organoids is serine protease-mediated and facilitated by the multibasic cleavage site. *Elife* 10, 1–23. doi: 10.7554/ELIFE.64508
- Mykityn, A. Z., Lamers, M. M., Okba, N. M. A., Breugem, T. I., Schipper, D., van den Doel, P. B., et al. (2021b). Susceptibility of rabbits to SARS-CoV-2. *Emerg. Microbes Infect.* 10, 1–7. doi: 10.1080/22221751.2020.1868951
- Nakabayashi, H., Miyano, K., Sato, J., Yamane, T., and Taketa, K. (1982). Growth of human hepatoma cell lines with differentiated functions in chemically defined medium. *Cancer Res.* 42, 3858–3863.
- Naoki, O., Arihiro, K., Toshiyuki, Y., Noriko, H., Fumio, K., Suyoshi, S., et al. (2014). The genome landscape of the African green monkey kidney-derived vero cell line. *DNA Res.* 21, 673–683. doi: 10.1093/dnares/dsu029
- Napolitano, V., Dabrowska, A., Schorpp, K., Mourão, A., Barreto-Duran, E., Benedyk, M., et al. (2022). Acridlavine, a clinically approved drug, inhibits SARS-CoV-2 and other betacoronaviruses. *Cell Chem. Biol.* 29, 774–784.e8. doi: 10.1016/j.chembiol.2021.11.006
- Nchioua, R., Kmiec, D., Müller, J. A., Conzelmann, C., Groß, R., Swanson, C. M., et al. (2020). Sars-cov-2 is restricted by zinc finger antiviral protein despite preadaptation to the low-cpg environment in humans. *MBio* 11, 1–19. doi: 10.1128/MBIO.01930-20/ASSET/6BC64666-63E5-4AFB-98F8-723C2723A942/ASSETS/GRAPHIC/MBIO.01930-20-F0007.JPEG
- Neal, J. W. (2014). Flaviviruses are neurotropic, but how do they invade the CNS? *J. Infect.* 69, 203–215. doi: 10.1016/j.jinf.2014.05.010
- Neil, S. J. D., Zang, T., and Bieniasz, P. D. (2008). Tetherin inhibits retrovirus release and is antagonized by HIV-1 vpr. *Nature* 451, 425–430. doi: 10.1038/NATURE06553
- Nelli, R. K., Phadke, K. S., Castillo, G., Yen, L., Saunders, A., Rauh, R., et al. (2021). Enhanced apoptosis as a possible mechanism to self-limit SARS-CoV-2 replication in porcine primary respiratory epithelial cells in contrast to human cells. *Cell Death Discovery* 7, 1–10. doi: 10.1038/s41420-021-00781-w
- Nguyen, T., Do, D., Donckers, K., Vangeel, L., Chatterjee, A. K., Gally, P. A., et al. (2021). A robust SARS-CoV-2 replication model in primary human epithelial cells at the air liquid interface to assess antiviral agents. *Antiviral Res.* 192, 105122. doi: 10.1016/j.antiviral.2021.105122
- Ogando, N. S., Dalebout, T. J., Zevenhoven-Dobbe, J. C., Limpens, R. W. A. L., van der Meer, Y., Caly, L., et al. (2020). SARS-coronavirus-2 replication in vero E6 cells: Replication kinetics, rapid adaptation and cytopathology. *J. Gen. Virol.* 101, 925–940. doi: 10.1099/jgv.0.001453
- Ois Freymuth, F., Vabret, A., Rozenberg, F., Dina, J., Lle Petitjean, J., Phanie Gouarin, S., et al. (2005). Replication of respiratory viruses, particularly influenza virus, rhinovirus, and coronavirus in Huh7 hepatocarcinoma cell line. *J. Med. Virol.* 77, 295–301. doi: 10.1002/jmv.20449
- Ooi, G. L., and Phua, K. H. (2009). SARS in Singapore - challenges of a global health threat to local institutions. *Nat. Hazards* 48, 317–327. doi: 10.1007/s11069-007-9194-2
- Padmanabhan, P. (2022). Modelling how the altered usage of cell entry pathways by the SARS-CoV-2 omicron variant may affect the efficacy and synergy of TMPRSS2 and cathepsin B/L inhibitors. *bioRxiv Prepr.*, 1–29. doi: 10.1101/2022.01.13.476267

- Padmanabhan, P., Desikan, R., and Dixit, N. M. (2020). Targeting TMPRSS2 and cathepsin B/L together may be synergistic against SARS-CoV-2 infection. *PLoS Comput. Biol.* 16. doi: 10.1371/journal.pcbi.1008461
- Padmanabhan, P., Desikan, R., and Dixit, N. M. (2022). Modeling how antibody responses may determine the efficacy of COVID-19 vaccines. *Nat. Comput. Sci.* 2, 123–131. doi: 10.1038/s43588-022-00198-0
- Padmanabhan, P., and Dixit, N. M. (2022). Evidence of increased cathepsin B/L and decreased TMPRSS2 usage for cell entry by the SARS-CoV-2 omicron variant. *bioRxiv* 2022, 1.13.476267. doi: 10.1101/2022.01.13.476267
- Pan, C., Kumar, C., Bohl, S., Klingmueller, U., and Mann, M. (2009). Comparative proteomic phenotyping of cell lines and primary cells to assess preservation of cell type-specific functions. *Mol. Cell. Proteomics* 8, 443. doi: 10.1074/MCP.M800258-MCP200
- Park, B. K., Kim, D., Park, S., Maharjan, S., Kim, J., Choi, J. K., et al. (2021). Differential signaling and virus production in calu-3 cells and vero cells upon SARS-CoV-2 infection. *Biomol. Ther. (Seoul)* 29, 273–281. doi: 10.4062/BiomolTher.2020.226
- Patterson, E. I., Elia, G., Grassi, G. A., Giordano, A., Desario, C., Medardo, M., et al. (2020). Evidence of exposure to SARS-CoV-2 in cats and dogs from households in Italy. *Nat. Commun.* 11, 1–5. doi: 10.1038/s41467-020-20097-0
- Payne, S. (2017). “Methods to study viruses,” in *Viruses* (Cambridge: Massachusetts: Academic Press), 37–52. doi: 10.1016/b978-0-12-803109-4.00004-0
- Peacock, T. P., Goldhill, D. H., Zhou, J., Baillon, L., Frise, R., Swann, O. C., et al. (2021). The furin cleavage site in the SARS-CoV-2 spike protein is required for transmission in ferrets. *Nat. Microbiol.* 6, 899–909. doi: 10.1038/s41564-021-00908-w
- Pear, W. S., Nolan, G. P., Scott, M. L., and Baltimore, D. (1993). Production of high-titer helper-free retroviruses by transient transfection. *Proc. Natl. Acad. Sci. U. S. A.* 90, 8392–8396. doi: 10.1073/PNAS.90.18.8392
- Pellegrini, L., Albecka, A., Mallery, D. L., Kellner, M. J., Paul, D., Carter, A. P., et al. (2020). SARS-CoV-2 infects the brain choroid plexus and disrupts the blood-CSF barrier in human brain organoids. *Cell Stem Cell* 27, 951–961.e5. doi: 10.1016/j.stem.2020.10.001
- Pfaender, S., Mar, K. B., Michailidis, E., Kratzel, A., Boys, I. N., V'kovski, P., et al. (2020). LY6E impairs coronavirus fusion and confers immune control of viral disease. *Nat. Microbiol.* 5, 1330–1339. doi: 10.1038/s41564-020-0769-y
- Pinto, A. L., Rai, R. K., Brown, J. C., Griffin, P., Edgar, J. R., Shah, A., et al. (2022). Ultrastructural insight into SARS-CoV-2 entry and budding in human airway epithelium. *Nat. Commun.* 13, 1–14. doi: 10.1038/s41467-022-29255-y
- Plaze, M., Attali, D., Prot, M., Petit, A. C., Blatzer, M., Vinckier, F., et al. (2021). Inhibition of the replication of SARS-CoV-2 in human cells by the FDA-approved drug chlorpromazine. *Int. J. Antimicrob. Agents* 57, 106274. doi: 10.1016/j.ijantimicag.2020.106274
- Poiesz, B. J., Ruscetti, F. W., Gazdar, A. F., Bunn, P. A., Minna, J. D., and Gallo, R. C. (1980). Detection and isolation of type c retrovirus particles from fresh and cultured lymphocytes of a patient with cutaneous T-cell lymphoma. *Proc. Natl. Acad. Sci. U. S. A.* 77, 7415–7419. doi: 10.1073/PNAS.77.12.7415/ASSET/A1ED1572-9D3A-46AD-A656-4BA774001B33/ASSETS/GRAPHIC/PNAS.7415FIG04.JPEG
- Pontelli, M. C., Castro, I. A., Martins, R. B., La Serra, L., Veras, F. P., Nascimento, D. C., et al. (2022). SARS-CoV-2 productively infects primary human immune system cells *in vitro* and in COVID-19 patients. *J. Mol. Cell Biol.* 14, 1–14. doi: 10.1093/JMCM/JAC021
- Pruijssers, A. J., George, A. S., Schäfer, A., Leist, S. R., Gralinski, L. E., Dinno, K. H., et al. (2020). Remdesivir inhibits SARS-CoV-2 in human lung cells and chimeric SARS-CoV expressing the SARS-CoV-2 RNA polymerase in mice. *Cell Rep.* 32, 107940. doi: 10.1016/j.celrep.2020.107940
- Pyke, A. T., Nair, N., Van Den Hurk, A. F., Burtonclay, P., Nguyen, S., Barcelon, J., et al. (2021). Replication kinetics of B.1.351 and B.1.1.7 SARS-CoV-2 variants of concern including assessment of a B.1.1.7 mutant carrying a defective ORF7a gene. *Viruses* 13, 1–10. doi: 10.3390/v13061087
- Pyrć, K., Milewska, A., Duran, E. B., Botwina, P., Dabrowska, A., Jedrysk, M., et al. (2021). SARS-CoV-2 inhibition using a mucoadhesive, amphiphilic chitosan that may serve as an anti-viral nasal spray. *Sci. Rep.* 11, 1–11. doi: 10.1038/s41598-021-99404-8
- Rahman, M. M., and McFadden, G. (2020). Oncolytic virotherapy with myxoma virus. *J. Clin. Med.* 9. doi: 10.3390/JCM9010171
- Ramadan, N., and Shaib, H. (2019). Middle east respiratory syndrome coronavirus (MERS-COV): A review. *GERMS* 9, 35–42. doi: 10.18683/germs.2019.1155
- Ramani, A., Müller, L., Ostermann, P. N., Gabriel, E., Abida-Islam, P., Müller-Schiffmann, A., et al. (2020). SARS-CoV-2 targets neurons of 3D human brain organoids. *EMBO J.* 39, e106230. doi: 10.15252/EMBJ.2020106230
- Ramirez, S., Fernandez-Antunez, C., Galli, A., Underwood, A., Pham, L. V., Ryberg, L. A., et al. (2021). Overcoming culture restriction for SARS-CoV-2 in human cells facilitates the screening of compounds inhibiting viral replication. *Antimicrob. Agents Chemother.* 65. doi: 10.1128/AAC.00097-21
- Ranga, A., Gjorevski, N., and Lutolf, M. P. (2014). Drug discovery through stem cell-based organoid models. *Adv. Drug Deliv. Rev.* 69–70, 19–28. doi: 10.1016/J.ADDR.2014.02.006
- Reperant, L. A., Kuiken, T., Grenfell, B. T., Osterhaus, A. D. M. E., and Dobson, A. P. (2012). Linking influenza virus tissue tropism to population-level reproductive fitness. *PLoS One* 7, e43115. doi: 10.1371/journal.pone.0043115
- Ribero, M. S., Jouvenet, N., Dreux, M., and Nisole, S. (2020). Interplay between SARS-CoV-2 and the type I interferon response. *PLoS Pathog.* 16, e1008737. doi: 10.1371/journal.ppat.1008737
- Rio, D. C., Clark, S. G., and Tjian, R. (1985). A mammalian host-vector system that regulates expression and amplification of transfected genes by temperature induction. *Science* 227, 23–28. doi: 10.1126/SCIENCE.2981116
- Rothan, H. A., Kumari, P., Stone, S., Natekar, J. P., Arora, K., Aironi, T. T., et al. (2022). SARS-CoV-2 infects primary neurons from human ACE2 expressing mice and upregulates genes involved in the inflammatory and necroptotic pathways. *Pathogens* 11, 1–12. doi: 10.3390/pathogens11020257
- Ryu, G., and Shin, H. W. (2021). SARS-CoV-2 infection of airway epithelial cells. *Immune Netw.* 21, 1–16. doi: 10.4110/IN.2021.21.E3
- Sabin, A. B., and Boulger, L. R. (1973). History of Sabin attenuated poliovirus oral live vaccine strains. *J. Biol. Stand.* 1, 115–118. doi: 10.1016/0092-1157(73)90048-6
- Saccon, E., Chen, X., Mikaeloff, F., Rodriguez, J. E., Szekely, L., Vinhas, B. S., et al. (2021). Cell-type-resolved quantitative proteomics map of interferon response against SARS-CoV-2. *iScience* 24, 102420. doi: 10.1016/j.isci.2021.102420
- Salahudeen, A. A., Choi, S. S., Rustagi, A., Zhu, J., van Unen, V., de la, O., S. M., et al. (2020). Progenitor identification and SARS-CoV-2 infection in human distal lung organoids. *Nature* 588, 670–675. doi: 10.1038/s41586-020-3014-1
- Sano, E., Suzuki, T., Hashimoto, R., Itoh, Y., Sakamoto, A., Sakai, Y., et al. (2022). Cell response analysis in SARS-CoV-2 infected bronchial organoids. *Commun. Biol.* 5, 1–9. doi: 10.1038/s42003-022-03499-2
- Sasaki, M., Uemura, K., Sato, A., Toba, S., Sanaki, T., Maenaka, K., et al. (2021). SARS-CoV-2 variants with mutations at the S1/ S2 cleavage site are generated *in vitro* during propagation in TMPRSS2-deficient cells. *PLoS Pathog.* 17. doi: 10.1371/journal.ppat.1009233
- Scherer, W. F., Syverton, J. T., and Gey, G. O. (1953). Studies on the propagation *in vitro* of poliomyelitis viruses: IV. viral multiplication in a stable strain of human malignant epithelial cells (strain hela) derived from an epidermoid carcinoma of the cervix. *J. Exp. Med.* 97, 695–710. doi: 10.1084/jem.97.5.695
- Schimmel, L., Chew, K. Y., Stocks, C. J., Yordanov, T. E., Essebier, P., Kulasinghe, A., et al. (2021). Endothelial cells are not productively infected by SARS-CoV-2. *Clin. Transl. Immunol.* 10, 1–18. doi: 10.1002/cti2.1350
- Schlottau, K., Rissmann, M., Graaf, A., Schön, J., Sehl, J., Wylezich, C., et al. (2020). SARS-CoV-2 in fruit bats, ferrets, pigs, and chickens: an experimental transmission study. *Lancet Microbe* 1, e218–e225. doi: 10.1016/S2666-5247(20)30089-6
- Schneider, W. M., Chevillotte, M. D., and Rice, C. M. (2014). Interferon-stimulated genes: A complex web of host defenses. *Annu. Rev. Immunol.* 32, 513–545. doi: 10.1146/ANNUREV-IMMUNOL-032713-120231
- Schoggins, J. W. (2019). Interferon-stimulated genes: What do they all do? *Annu. Rev. Virol.* 6, 567–584. doi: 10.1146/annurev-virology-092818-015756
- Shang, J., Wan, Y., Luo, C., Ye, G., Geng, Q., Auerbach, A., et al. (2020). Cell entry mechanisms of SARS-CoV-2. *Proc. Natl. Acad. Sci. U. S. A.* 117. doi: 10.1073/pnas.2003138117
- Shaw, G., Morse, S., Ararat, M., and Graham, F. L. (2002). Preferential transformation of human neuronal cells by human adenoviruses and the origin of HEK 293 cells. *FASEB J.* 16, 869–871. doi: 10.1096/FJ.01-0995FJE
- Shuai, H., Chan, J. F. W., Hu, B., Chai, Y., Yuen, T. T. T., Yin, F., et al. (2022). Attenuated replication and pathogenicity of SARS-CoV-2 B.1.1.529 omicron. *Nature* 603, 693–699. doi: 10.1038/s41586-022-04442-5
- Shuai, H., Chu, H., Hou, Y., Yang, D., Wang, Y., Hu, B., et al. (2020). Differential immune activation profile of SARS-CoV-2 and SARS-CoV infection in human lung and intestinal cells: Implications for treatment with IFN-β and IFN inducer. *J. Infect.* 81, e1. doi: 10.1016/j.jinf.2020.07.016
- Shulla, A., Heald-Sargent, T., Subramanya, G., Zhao, J., Perlman, S., and Gallagher, T. (2011). A transmembrane serine protease is linked to the severe acute respiratory syndrome coronavirus receptor and activates virus entry. *J. Virol.* 85, 873–882. doi: 10.1128/jvi.02062-10
- Simon, C. E. (1912). THE FILTERABLE VIRUSES. *Lancet* 180, 1450–1451. doi: 10.1016/S0140-6736(01)41061-0
- Sobhy, H. (2017). A comparative review of viral entry and attachment during large and giant dsDNA virus infections. *Arch. Virol.* 162, 3567–3585. doi: 10.1007/s00705-017-3497-8

- Sridhar, A., Simmini, S., Ribeiro, C. M. S., Tapparel, C., Evers, M. M., Pakrtd, D., et al. (2020). A perspective on organoids for virology research. *Viruses* 12. doi: 10.3390/V12111341
- Swadling, L., Diniz, M. O., Schmidt, N. M., Amin, O. E., Chandran, A., Shaw, E., et al. (2021). Pre-existing polymerase-specific T cells expand in abortive seronegative SARS-CoV-2. *Nature* 601, 110–117. doi: 10.1038/s41586-021-04186-8
- Szlachcic, W. J., Dabrowska, A., Milewska, A., Ziojla, N., Blaszczyk, K., Barreto-Duran, E., et al. (2022). SARS-CoV-2 infects an *in vitro* model of the human developing pancreas through endocytosis. *iScience* 25, 104594. doi: 10.1016/j.isci.2022.104594
- Takayama, K. (2020). *In vitro* and animal models for SARS-CoV-2 research. *Trends Pharmacol. Sci.* 41, 513–517. doi: 10.1016/j.tips.2020.05.005
- Tao, S., Zandi, K., Bassit, L., Ong, Y. T., Verma, K., Liu, P., et al. (2021). Comparison of anti-SARS-CoV-2 activity and intracellular metabolism of remdesivir and its parent nucleoside. *Curr. Res. Pharmacol. Drug Discovery* 2. doi: 10.1016/j.CRP.HAR.2021.100045
- Taylor, J. K., Coleman, C. M., Postel, S., Sisk, J. M., Bernbaum, J. G., Venkataraman, T., et al. (2015). Severe acute respiratory syndrome coronavirus ORF7a inhibits bone marrow stromal antigen 2 virion tethering through a novel mechanism of glycosylation interference. *J. Virol.* 89, 11820–11833. doi: 10.1128/JVI.02274-15
- Thomas, B., Bhat, K., and Mapara, M. (2012). Rabbit as an animal model for experimental research. *Dent. Res. J. (Isfahan)* 9, 111. doi: 10.4103/1735-3327.92960
- Tran, B. M., Deliyannis, G., Hachani, A., Earnest, L., Torresi, J., and Vincan, E. (2022). Organoid models of SARS-CoV-2 infection: What have we learned about COVID-19? *Organoids* 2022 Vol. 1 Pages 2-27 1, 2–27. doi: 10.3390/ORGANOIDS1010002
- Tseng, C.-T. K., Tseng, J., Perrone, L., Worthy, M., Popov, V., and Peters, C. J. (2005). Apical entry and release of severe acute respiratory syndrome-associated coronavirus in polarized calu-3 lung epithelial cells. *J. Virol.* 79, 9470–9479. doi: 10.1128/jvi.79.15.9470-9479.2005
- Tuffereau, C., and Flamand, A. (1983). Characterization of rabies virus production by five persistently infected BHK-21 cell lines. *Ann. l'Institut Pasteur / Virol.* 134, 507–522. doi: 10.1016/S0769-2617(83)80023-9
- Tyrell, D. A. J., Bynoe, M. L., and Brit, M. (1965). Cultivation of a novel type of common-cold virus in organ cultures. *Med. J. 1467 J. 1*, 1467–1470. doi: 10.1136/bmj.1.5448.1467
- Van Damme, N., Goff, D., Katsura, C., Jorgenson, R. L., Mitchell, R., Johnson, M. C., et al. (2008). The interferon-induced protein BST-2 restricts HIV-1 release and is downregulated from the cell surface by the viral vpu protein. *Cell Host Microbe* 3, 245–252. doi: 10.1016/J.CHOM.2008.03.001
- van der Vaart, J., Lamers, M. M., Haagmans, B. L., and Clevers, H. (2021). Advancing lung organoids for COVID-19 research. *Dis. Model. Mech.* 14. doi: 10.1242/DMM.049060
- Van Helvoort, T. (1994). The construction of bacteriophage as bacterial virus: Linking endogenous and exogenous thought styles. *J. Hist. Biol.* 27, 91–139. doi: 10.1007/BF01058628
- Vankadari, N., and Wilce, J. A. (2020). Emerging Wuhan (COVID-19) coronavirus: glycan shield and structure prediction of spike glycoprotein and its interaction with human CD26. *Emerg. Microbes Infect.* 9, 601–604. doi: 10.1080/22221751.2020.1739565
- Vectorbuilder Cell Line Models for Coronavirus Research (2022) *VectorBuilder*. Available at: <https://en.vectorbuilder.com/products-services/service/cell-line-models-for-coronavirus-research.html> (Accessed June 19, 2022).
- Vergara-Alert, J., Rodon, J., Carrillo, J., Te, N., Izquierdo-Useros, N., Rodriguez de la Concepción, M. L., et al. (2021). Pigs are not susceptible to SARS-CoV-2 infection but are a model for viral immunogenicity studies. *Transbound Emerg. Dis.* 68, 1721–1725. doi: 10.1111/TBED.13861
- Wang, K., Chen, W., Zhang, Z., Deng, Y., Lian, J. Q., Du, P., et al. (2020). CD147-spike protein is a novel route for SARS-CoV-2 infection to host cells. *Signal Transduction Targeting Ther.* 5, 1–10. doi: 10.1038/s41392-020-00426-x
- Wang, L., Fan, X., Bonenfant, G., Cui, D., Hossain, J., Jiang, N., et al. (2021). Susceptibility to SARS-CoV-2 of cell lines and substrates commonly used to diagnose and isolate influenza and other viruses. *Emerg. Infect. Dis.* 27, 1380. doi: 10.3201/EID2705.210023
- Wang, S. M., Huang, K. J., and Wang, C. T. (2014). BST2/CD317 counteracts human coronavirus 229E productive infection by tethering virions at the cell surface. *Virology* 449, 287. doi: 10.1016/J.VIROL.2013.11.030
- Wanner, N., Andrieux, G., Badia-i-Mompel, P., Edler, C., Pfefferle, S., Lindenmeyer, M. T., et al. (2022). Molecular consequences of SARS-CoV-2 liver tropism. *Nat. Metab.* 2022 43 4, 310–319. doi: 10.1038/s42255-022-00552-6
- Weiss, R. A. (2002). Critical review HIV receptors and cellular tropism. *IUBMB Life* 53, 201–205. doi: 10.1080/15216540290098927
- Weller, T. H., Robbins, F. C., and Enders, J. F. (1949). Cultivation of poliomyelitis virus in cultures of human foreskin and embryonic tissues. *Proc. Soc. Exp. Biol. Med.* 72, 153–155. doi: 10.3181/00379727-72-17359
- Weston, S., Coleman, C. M., Haupt, R., Logue, J., Matthews, K., Li, Y., et al. (2020). Broad anti-coronavirus activity of food and drug administration-approved drugs against SARS-CoV-2 *In vitro* and SARS-CoV *In vivo*. *J. Virol.* 94. doi: 10.1128/JVI.01218-20/ASSET/CFF10AA4-2472-4CEB-9B8B-CE5A1C2E15C2/ASSETS/GRAPHIC/JVI.01218-20-F0006.JPEG
- WHO (2021) *WHO coronavirus (COVID-19) dashboard*. WHO coronavirus (COVID-19) dashboard with vaccination data (Who). Available at: <https://covid19.who.int/> (Accessed June 26, 2021).
- Wong, M. E., Johnson, C. J., Hearn, A. C., and Jaworowski, A. (2021). Development of a novel *In vitro* primary human monocyte-derived macrophage model to study reactivation of HIV-1 transcription. *J. Virol.* 95. doi: 10.1128/JVI.00227-21/FORMAT/EPUB
- Wu, Y., Guo, C., Tang, L., Hong, Z., Zhou, J., Dong, X., et al. (2020). Prolonged presence of SARS-CoV-2 viral RNA in faecal samples. *Lancet Gastroenterol. Hepatol.* 5, 434–435. doi: 10.1016/S2468-1253(20)30083-2
- Wurtz, N., Penant, G., Jardot, P., Duclos, N., and La Scola, B. (2021). Culture of SARS-CoV-2 in a panel of laboratory cell lines, permissivity, and differences in growth profile. *Eur. J. Clin. Microbiol. Infect. Dis.* 40, 477–484. doi: 10.1007/s10096-020-04106-0
- Xiao, F., Tang, M., Zheng, X., Liu, Y., Li, X., and Shan, H. (2020). Evidence for gastrointestinal infection of SARS-CoV-2. *Gastroenterology* 158, 1831–1833. doi: 10.1053/j.gastro.2020.02.055
- Xie, X., Muruato, A. E., Zhang, X., Lokugamage, K. G., Fontes-Garfias, C. R., Zou, J., et al. (2020). A nanoluciferase SARS-CoV-2 for rapid neutralization testing and screening of anti-infective drugs for COVID-19. *Nat. Commun.* 11111, 1–11. doi: 10.1038/s41467-020-19055-7
- Yamane, M., Yamashita, M., Goto, T., Tsuji, S., Li, Y. G., Warachit, J., et al. (2005). Establishment of vero E6 cell clones persistently infected with severe acute respiratory syndrome coronavirus. *Microbes Infect.* 7, 1530. doi: 10.1016/J.MICINF.2005.05.013
- Zaki, A. M., Van Boheemen, S., Bestebroer, T. M., Osterhaus, A. D. M. E., and Fouchier, R. A. M. (2012). Isolation of a novel coronavirus from a man with pneumonia in Saudi Arabia. *N. Engl. J. Med.* 367, 1814–1820. doi: 10.1056/NEJMoa1211721
- Zang, R., Castro, M. F. G., McCune, B. T., Zeng, Q., Rothlauf, P. W., Sonnek, N. M., et al. (2020). TMPSR2 and TMPSR4 promote SARS-CoV-2 infection of human small intestinal enterocytes. *Sci. Immunol.* 5, 3582. doi: 10.1126/SCIIMMUNOL.ABC3582/SUPPL_FILE/ABC3582_TABLE_S3.XLSX
- Zhang, H., Kang, Z., Gong, H., Xu, D., Wang, J., Li, Z., et al. (2020). Digestive system is a potential route of COVID-19: An analysis of single-cell coexpression pattern of key proteins in viral entry process. *Gut* 69, 1010–1018. doi: 10.1136/gutjnl-2020-320953
- Zhang, L., Mann, M., Syed, Z. A., Reynolds, H. M., Tian, E., Samara, N. L., et al. (2021). Furin cleavage of the SARS-CoV-2 spike is modulated by O-glycosylation. *Proc. Natl. Acad. Sci. U. S. A.* 118. doi: 10.1073/pnas.2109905118
- Zhao, B., Ni, C., Gao, R., Wang, Y., Yang, L., Wei, J., et al. (2020a). Recapitulation of SARS-CoV-2 infection and cholangiocyte damage with human liver ductal organoids. *Protein Cell* 11, 771–775. doi: 10.1007/s13238-020-00718-6
- Zhao, M. M., Yang, W. L., Yang, F. Y., Zhang, L., Huang, W. J., Hou, W., et al. (2021). Cathepsin L plays a key role in SARS-CoV-2 infection in humans and humanized mice and is a promising target for new drug development. *Signal Transduction Targeting Ther.* 6. doi: 10.1038/s41392-021-00558-8
- Zhao, X., Zheng, S., Chen, D., Zheng, M., Li, X., Li, G., et al. (2020b). LY6E restricts entry of human coronaviruses, including currently pandemic SARS-CoV-2. *J. Virol.* 94. doi: 10.1128/JVI.00562-20/ASSET/75291B2B-0ED8-415A-B1BB-3F68949984FB/ASSETS/GRAPHIC/JVI.00562-20-F0008.JPEG
- Zhou, J., Li, C., Liu, X., Chiu, M. C., Zhao, X., Wang, D., et al. (2020a). Infection of bat and human intestinal organoids by SARS-CoV-2. *Nat. Med.* 2020 267 26, 1077–1083. doi: 10.1038/s41591-020-0912-6
- Zhou, Z., Qiu, Y., and Ge, X. (2021c). The taxonomy, host range and pathogenicity of coronaviruses and other viruses in the nidovirales order. *Anim. Dis.* 1, 1–28. doi: 10.1186/s44149-021-00005-9
- Zhou, F., Xia, J., Yuan, H. X., Sun, Y., and Zhang, Y. (2021a). Liver injury in COVID-19: Known and unknown. *World J. Clin. cases* 9, 4980. doi: 10.12998/WJCC.V9.I19.4980
- Zhou, P., Yang, X., Wang, X. G., Hu, B., Zhang, L., Zhang, W., et al. (2020b). A pneumonia outbreak associated with a new coronavirus of probable bat origin. *Nature* 579, 270–273. doi: 10.1038/s41586-020-2012-7

Zhou, H., Yang, J., Zhou, C., Chen, B., Fang, H., Chen, S., et al. (2021b). A review of SARS-CoV2: Compared with SARS-CoV and MERS-CoV. *Front. Med.* 8. doi: 10.3389/FMED.2021.628370/BIBTEX

Zhu, Y., Chidekel, A., and Shaffer, T. H. (2010). Cultured human airway epithelial cells (Calu-3): A model of human respiratory function, structure, and inflammatory responses. *Crit. Care Res. Pract.* 2010, 1–8. doi: 10.1155/2010/394578

Zhu, C. H., Kim, J., Shay, J. W., and Wright, W. E. (2008) SGNP: An essential stress Granule/Nucleolar protein potentially involved in 5.8s rRNA Processing/Transport *PloS One* 3, e3716. doi: 10.1371/JOURNAL.PONE.0003716

Zhu, N., Zhang, D., Wang, W., Li, X., Yang, B., Song, J., et al. (2020). A novel coronavirus from patients with pneumonia in chin. *N. Engl. J. Med.* 382, 727–733. doi: 10.1056/nejmoa2001017

Zinzula, L. (2021). Lost in deletion: The enigmatic ORF8 protein of SARS-CoV-2. *Biochem. Biophys. Res. Commun.* 538, 116–124. doi: 10.1016/j.bbrc.2020.10.045

Zupin, L., Fontana, F., Clemente, L., Ruscio, M., Ricci, G., and Crovella, S. (2022). Effect of short time of SARS-CoV-2 infection in caco-2 cells. *Viruses* 14. doi: 10.3390/v14040704



OPEN ACCESS

EDITED BY
Rashed Noor,
Independent University, Bangladesh

REVIEWED BY
Daniela Toro-Ascuy,
Autonomous University of Chile, Chile
Thuy Linh Hoang,
Institut Pasteur in Ho Chi
Minh City, Vietnam

*CORRESPONDENCE
Vikas Sood
vikas1101@gmail.com

SPECIALTY SECTION
This article was submitted to
Virus and Host,
a section of the journal
Frontiers in Cellular and
Infection Microbiology

RECEIVED 11 June 2022
ACCEPTED 05 October 2022
PUBLISHED 28 November 2022

CITATION
Periwal N, Bhardwaj U, Sarma S,
Arora P and Sood V (2022) *In silico*
analysis of SARS-CoV-2 genomes:
Insights from SARS encoded
non-coding RNAs.
Front. Cell. Infect. Microbiol. 12:966870.
doi: 10.3389/fcimb.2022.966870

COPYRIGHT
© 2022 Periwal, Bhardwaj, Sarma, Arora
and Sood. This is an open-access article
distributed under the terms of the
[Creative Commons Attribution License](https://creativecommons.org/licenses/by/4.0/)
(CC BY). The use, distribution or
reproduction in other forums is
permitted, provided the original
author(s) and the copyright owner(s)
are credited and that the original
publication in this journal is cited, in
accordance with accepted academic
practice. No use, distribution or
reproduction is permitted which does
not comply with these terms.

In silico analysis of SARS-CoV-2 genomes: Insights from SARS encoded non-coding RNAs

Neha Periwal¹, Urvashi Bhardwaj¹, Sankritya Sarma²,
Pooja Arora² and Vikas Sood^{1*}

¹Department of Biochemistry, Jamia Hamdard, New Delhi, India, ²Department of Zoology, Hansraj College, University of Delhi, Delhi, India

The recent pandemic caused by Severe Acute Respiratory Syndrome Coronavirus-2 has resulted in enormous deaths around the world. Clues from genomic sequences of parent and their mutants can be obtained to understand the evolving pathogenesis of this virus. Apart from the viral proteins, virus-encoded microRNAs (miRNAs) have been shown to play a vital role in regulating viral pathogenesis. Thus we sought to investigate the miRNAs encoded by SARS-CoV-2, its mutants, and the host. Here, we present the results obtained using a dual approach i.e (i) identifying host-encoded miRNAs that might regulate viral pathogenesis and (ii) identifying viral-encoded miRNAs that might regulate host cell signaling pathways and aid in viral pathogenesis. Analysis utilizing the first approach resulted in the identification of ten host-encoded miRNAs that could target the SARS, SARS-CoV-2, and its mutants. Interestingly our analysis revealed that there is a significantly higher number of host miRNAs that could target the SARS-CoV-2 genome as compared to the SARS reference genome. Results from the second approach resulted in the identification of a set of virus-encoded miRNAs which might regulate host signaling pathways. Our analysis further identified a similar "GA" rich motif in the SARS-CoV-2 and its mutant genomes that was shown to play a vital role in lung pathogenesis during severe SARS infections. In summary, we have identified human and virus-encoded miRNAs that might regulate the pathogenesis of SARS coronaviruses and describe similar non-coding RNA sequences in SARS-CoV-2 that were shown to regulate SARS-induced lung pathology in mice.

KEYWORDS

coronavirus, SARS-CoV-2, miRNAs, non-coding RNAs, SARS

Introduction

Coronaviruses are a group of enveloped viruses with positive-sense single-stranded RNA as the genetic material. These viruses cause mild to severe respiratory and intestinal infections in immune-compromised individuals. They were not considered to be pathogenic until the outbreak of Severe Acute Respiratory Syndrome (SARS) in China and the Middle East Respiratory Syndrome Coronavirus (MERS-CoV) in Middle East countries in 2002 and 2012 respectively when the viral infection led to significant deaths among the infected individual's (Song et al., 2019). As on 24 September 2022, the SARS-CoV-2 pandemic has resulted in more than 611 million infections resulting in 6.5 million deaths globally (<https://covid19.who.int/>). Data from the ongoing pandemic suggest that mortality caused by this virus has already surpassed that of combined mortality caused by both SARS and MERS coronaviruses. Though SARS-CoV-2 has caused significant mortality and morbidity, its evolution trajectory points towards an increased transmissibility (Volz et al., 2021). SARS-CoV-2 has a slow evolutionary rate i.e. 1 or 2 nucleotide alterations/month/lineage in the viral genome which consists of around 30,000 base pairs (Boehm et al., 2021). Despite this slow mutation rate, SARS-CoV-2 has evolved into around sixteen lineages in a short time since the onset of the pandemic (Tegally et al., 2021). The underlying mutations in these lineages allow the virus to transmit efficiently thereby enhancing the viral fitness. The random mutations in the viral genomes have led to changes in the viral proteins resulting in improved functions (Korber et al., 2020). However, apart from modulating the functions of the viral proteins, the mutations in the viral genomes can lead to changes in the microRNA binding sites thereby resulting in the appearance of the escape mutants (Hosseini Rad and McLellan, 2020).

MicroRNAs (miRNAs) are non-coding RNA molecules that are ~21 nucleotides long and can regulate gene expression primarily *via* imperfect base pairing with the 3' untranslated regions of the target RNA molecules (Duchaine and Fabian, 2019; Liu and Wang, 2019). Apart from regulating the biological pathways, miRNAs have been shown to modulate viral infections (Mishra et al., 2020). Following viral infections, innate immune responses are induced leading to the generation of antiviral responses. This arm of antiviral signaling constitutes several potential antiviral factors including antiviral miRNAs. These miRNA molecules can lead to the inhibition of viral replication. For instance, miR-196, miR-351, and miR-448 have been shown to inhibit the Hepatitis C Virus infection (Pedersen et al., 2007). The miR-155 has been shown to regulate type I interferon signaling thereby modulating the replication of several viruses including HIV-1 (Swaminathan et al., 2012), Epstein-Barr virus (Jiang et al., 2006), reticuloendotheliosis virus (Bolisetty et al., 2009), Dengue virus (Su et al., 2020), West-Nile virus (Natekar et al., 2019), Japanese encephalitis virus (Thounaojam

et al., 2014; Pareek et al., 2014) and Herpes Simplex Virus 1 (Wang et al., 2019). Conversely, viruses have also been shown to encode small non-coding RNA molecules to facilitate viral replication. It has been shown that several miRNAs encoded by Kaposi's Sarcoma-associated Herpesvirus help in maintaining the viral latency (Lei et al., 2012). Several RNA viruses including Influenza virus (Li et al., 2018), HIV-1 (Zhang et al., 2014; Li et al., 2016), Dengue virus (Hussain and Asgari, 2014), and Ebola virus (Prasad et al., 2020) are also shown to encode small non-coding RNAs which can modulate the viral infection. Additionally, a complex cross-talk among miRNA and host factors further contributes to the replication of the viruses in their host (Bruscella et al., 2017; Mishra et al., 2020).

The ongoing SARS-CoV-2 pandemic has driven several studies to identify miRNAs as alternative therapeutics against the virus (Panda et al., 2022). Studying miRNAs has become crucial for the development of possible diagnostics, prognostics and therapeutics that could help in treatment strategies in the COVID-19 (Fani et al., 2021; Ying et al., 2021; Ahmed et al., 2022). Several studies aiming to predict miRNAs regulating SARS-CoV-2 pathogenesis were published and various miRNAs are identified that might have an impact on the replication of SARS-CoV-2 (Chen and Zhong, 2020; Marchi et al., 2021; Kucher et al., 2022; Morales et al., 2022; Yang et al., 2022). Apart from directly targeting the viral genomes, the miRNAs can indirectly regulate viral replication *via* regulating host factors that are critical for viral replication. The expression of proteins implicated in the SARS-CoV-2 life cycle, including ACE2, TMPRSS2, Spike proteins, and Nsp12, can be inhibited by miRNAs (Yang et al., 2022; Paul et al., 2022). The type I Interferon pathway is inhibited by SARS-CoV-2 encoded miRNAs, which also regulate the allelic differential expression of vulnerable genes (Zhu et al., 2021). Additionally, it has been shown that miRNAs can regulate SARS-CoV-2 replication *via* modulating certain receptors including ACE2, AXL, ADAM17, HAT1, NR1, VMP1, Cyclophilin A, and Cathepsin B (Zhang et al., 2021; Zeng et al., 2022).

Numerous host- and virus-specific indicators linked to SARS CoV-2 infection have recently emerged (Sevgin and Sevgin, 2021). Host miRNAs were found to target ACE2 and TMPRSS2 genes which regulate SARS-Cov-2 cellular entry (Kaur et al., 2021; Bellae Papannarao et al., 2022) and can also be modified to act in a pro-viral manner by blocking host immune systems (Sevgin and Sevgin, 2021). Recently several host-encoded miRNAs were found to regulate ORF1a/b which is necessary for viral replication and translation (Argghiani et al., 2021). A study on SARS coronavirus successfully characterized the role of viral encoded non-coding RNAs in the virus-induced lung pathology (Morales et al., 2017). Furthermore, phylogenetic and taxonomy studies have confirmed that SARS-CoV-2 forms a sister clade with SARS coronavirus suggesting that rich information on SARS coronavirus can be leveraged to gain insights into SARS-CoV-2 (The species *Severe acute*

respiratory syndrome-related coronavirus, 2020). It was observed that inhibiting viral encoded non-coding RNAs led to a reduction in the lung pathology of virus-infected mice. Taking into consideration the significant similarity between SARS and SARS-CoV-2 and the role of non-coding RNAs in virus pathogenesis and cell signaling pathways, we aimed to study host and viruses encoded miRNAs and compare them among SARS, SARS-CoV-2, and the mutants to understand the pathogenesis of these viruses.

In this study, we utilized a suite of highly popular algorithms to identify host and virus-encoded miRNAs that might have the potential to regulate SARS-CoV-2 pathogenesis. Moreover, we compared our results along with data from other published studies to identify a common set of miRNA candidates. These high-confidence candidates can then be validated in the wet lab as well as provide us with the opportunity to design broadly acting drug molecules against SARS-CoV-2 and its mutants.

Methods

Identification of host miRNAs targeting several SARS-CoV-2 and SARS reference genomes

MicroRNAs are known to regulate diverse biological pathways including various steps in viral replication (Bernier and Sagan, 2018). Hence, we studied the role of host miRNAs in regulating viral replication by predicting the host miRNA binding sites among the genome of these viruses. In order to gain an in-depth understanding of the pathogenesis of SARS-CoV-2, we analyzed the reference genome of SARS-CoV-2 along with its variants namely Alpha (B.1.1.7), Delta (B.1.617.2, AY.4.2), Beta (B.1.351), Omicron (B.1.1529, BA.1, BA.3, BA.1.1), Gamma lineage, Epsilon (B.1.27), Eta (B.1.525), Kappa (B.1.525), Lambda (C.37), Mu (B.1.627) and Theta (P.3) that were obtained from NCBI (Brister et al., 2015) and GISAID (Khare et al., 2021) (Supplementary table 1). The SARS reference genome was used for the comparison and the analysis was performed on both the forward and reverse sequences of viral genomes. For the prediction of host miRNAs that could bind to viral genomes, the miRDB algorithm was used (Chen and Wang, 2020). The analysis was performed in the custom mode where the user-defined sequences could be uploaded and processed. All the analyses were done on default settings and only those miRNAs were studied further that had a target score ≥ 80 so as to follow stringent selection criteria. Thus we obtained a list of miRNAs that could potentially target SARS-CoV-2 and its mutants. Recently, several studies were published to predict host-encoded miRNAs that might regulate SARS-CoV-2. Hence, we present the common miRNAs that are predicted by multiple studies involving diverse set of prediction algorithms.

Identification of SARS-CoV-2 and SARS encoded miRNAs

Several viruses have been shown to regulate host signaling pathways by encoding miRNAs in their genomes. However, there have been debates as to whether RNA viruses could encode miRNAs or not. Recent studies have successfully identified several miRNAs that are encoded by various RNA viruses including HIV-1 (Bennasser et al., 2004), West Nile Virus (Hussain et al., 2012), Dengue (Hussain and Asgari, 2014), Influenza (Li et al., 2018) and Ebola virus (Prasad et al., 2020). It was also observed that genomic sequences of these viruses could fold into stem-loop structures which gave rise to miRNAs (Klaver and Berkhout, 1994). Hence, in order to gain insights into various miRNAs possibly encoded by genomes of SARS coronavirus, SARS-CoV-2, and its variants, a set of computational tools was used to predict miRNAs encoded by these viruses. Since hairpin loops have been shown to produce miRNAs in RNA viruses, we used the miRNAfold algorithm to predict hairpin loops in viral genomes (Tempel and Tahi, 2012). As all hairpin loops do not result in functional miRNAs, hence output file from the miRNAfold algorithm was further processed using miRBoost algorithm to identify whether the predicted hairpin structures could form microRNAs or not (Tran et al., 2015). Once the viral encoded miRNAs were identified, the results were then processed using miRBase to find any similarities among the virus-encoded miRNAs and human miRNAs (Kozomara et al., 2019).

Comparison of SARS encoded non-coding RNA sequences with SARS-CoV-2 genomes

Recently, deep sequencing based approaches identified SARS encoded non-coding RNAs which played a critical role in virus-induced lung pathology (Morales et al., 2017). In order to gain an understanding of the genomic regions responsible for the generation of non-coding RNAs, we aligned SARS-CoV-2 sequences along with the mutants SARS reference sequence using the Clustal omega (Sievers et al., 2011). Aligned SARS genomic sequences that were shown to encode non-coding RNAs were then further studied to identify the percentage homology with that of SARS-CoV-2 and its mutants.

Results

Identification of host miRNAs targeting several SARS, SARS-CoV-2 and its variants

We used miRDB algorithm to gain insights into host encoded miRNAs (*Homo sapiens*) that could target viral

genomes. The analysis was performed on both the forward and reverse genomic sequences of all the genomes that were being studied. Our analysis identified several host miRNAs that could target each of the forward and reverse genomic sequences of SARS, SARS-CoV-2 and its variants (Supplementary Table 2). Figure 1A illustrates the common host miRNAs (n=354) that were predicted in 45% of the genomes used in this study. Similar analysis of common host miRNAs targeting 80% of the genomes identified 54 miRNAs (Figure 1B). A comparison of all the forward and reverse sequences of SARS, SARS-CoV-2 and its variants revealed 10 host miRNAs that could target all the genomes being studied and hence could be potentially used as broad-acting antivirals (Figure 1C). Out of these 10 miRNAs, three of them including hsa-miR-4282, hsa-miR-33a-3p and hsa-miR-4775 were found in several other studies. The hsa-miR-4282 has been shown to target ATF2 gene (Vadivalagan et al., 2022) that arrests the viral infection, hsa-miR-33a-3p targets SMAD4 which is involved in the Wnt signalling pathway (Yousefi et al., 2020), similarly hsa-miR-4775 targets SMAD7 and it plays role in TGF-beta signaling pathway (Yousefi et al., 2020). The hsa-miR-497-3p, inhibits vascular endothelial growth factor A, suppresses angiogenesis, and is found to be involved in the body's defense mechanisms (Van Laar et al., 2018). Another miRNA, hsa-miR-196a-1-3p was predicted to be able to bind to SARS-CoV, MERS-CoV, and SARS-CoV-2 genomes (Kim et al., 2020). The hsa-miR-548t-3p was found to be down-regulated in

the ischemic stroke (Li et al., 2022) whereas hsa-miR-33a-3p was shown to have ~90% sequence identity with VARV and VACV viral genomes. It was observed that hsa-miR-33a-3p targets A46L and A41L genes respectively thereby modulating the host defense mechanisms (Hasan et al., 2016). Recently, other groups have also utilized a diverse set of algorithms to identify the miRNAs that could target SARS-CoV-2 genomes (Mosharaf et al., 2022; Samy et al., 2022; Shirvani et al., 2022; Zeng et al., 2022). In order to further advance our understanding of host miRNAs targeting SARS-CoV-2 genomes, we compared our data with other studies. We observed several host-encoded miRNAs including hsa-miR-3529-3p, hsa-miR-516b-5p, and hsa-miR-155-5p that were common in many studies pointing toward the potential miRNAs that might be the strong candidates for further wet-lab validation and further understanding how these miRNAs are contributing towards the pathogenesis of SARS-CoV-2.

Identification of miRNAs encoded by SARS, SARS-CoV-2 and its variants

Viral encoded miRNAs have been shown to regulate cellular signaling pathways. RNA viruses are known to produce miRNAs that are critical for their replication cycle (Li and Zou, 2019). In order to identify miRNAs encoded by SARS, SARS-CoV-2, and

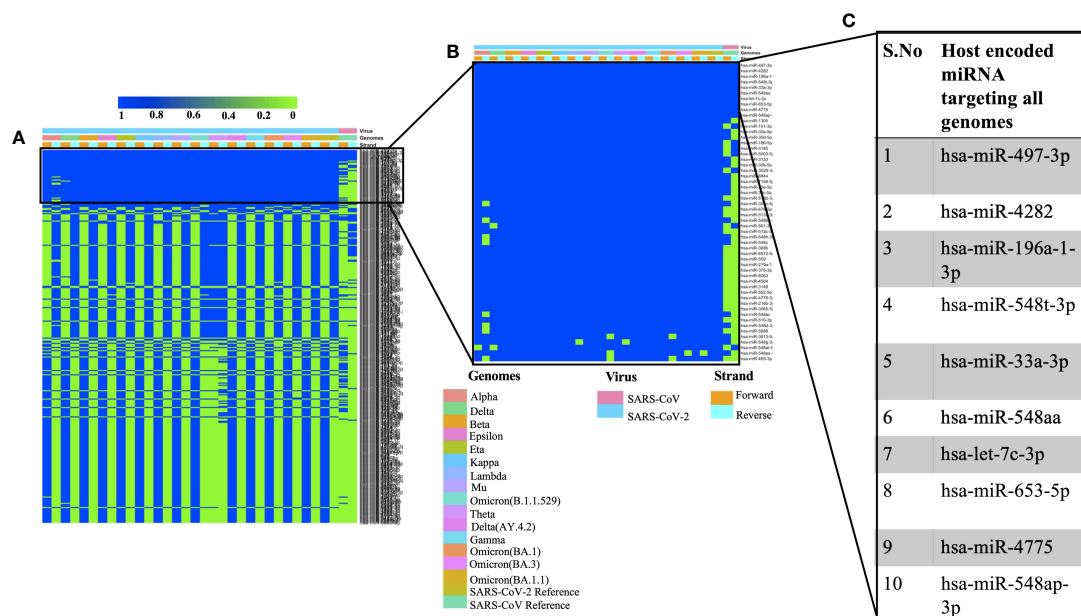


FIGURE 1

Shows the host-encoded miRNAs that could target SARS, SARS-CoV-2, and its variants. (A) Common miRNAs that could target 45% of genomes from the study. (B) Host miRNAs that could target 80% of the genomes from the study and (C) Top 10 miRNAs targeting all the forward and reverse genomes used in this study.

its mutants, we utilized a suite of algorithms that could identify stem-loop structures in the viral genomes. This was followed by the prediction of miRNAs among these stem-loop structures and finally comparing the predicted miRNAs with that of human-encoded miRNAs. As mentioned earlier, the miRNAfold algorithm was used to predict the stem loop structures in the viral genomes. The algorithm predicted various hairpin loops in genomes of SARS, SARS-CoV-2, and its variants. We used both the forward and the reverse strand of viral RNA to predict the stem-loop structures. Since all the predicted stem-loop structures do not form miRNAs, we used the miRBoost algorithm to identify potential stem-loop structures that could form miRNAs. The results thus obtained were then processed with the miRBase algorithm to investigate any similarity among virus and host-encoded miRNAs. We used this step with the rationale that any similarity among viral and host-encoded miRNAs will lead to the modulation of similar signaling pathways. The miRbase algorithm identified several viral encoded miRNAs that had similarities with human encoded miRNAs (Supplementary Table 3). Figure 2A represents the miRNAs that were predicted in 45% of the genomes used in this study. Figure 2B presents the top 10 miRNAs that can target various coronavirus genomes used in this study. Comparative analysis of miRNAs predicted from all the genomes used in this

study revealed that hsa-miR-4471 was present in 33 out of 34 genomes. This miRNA was predicted to be encoded by SARS-CoV-2 and all its mutants including the forward and the reverse genomic sequences. It was further observed that hsa-miR-4471 was encoded by only the reverse sequence of SARS coronavirus but not by the forward sequence.

A literature survey for the top ten miRNAs targeting SARS, SARS-CoV-2, and its mutants revealed that some of the miRNAs have been shown to play a key role in coronavirus pathogenesis. For instance, hsa-miR-3529-5p could modulate SARS-CoV-2 by targeting NF-kb pathway whereas hsa-miR-7-5p was shown to modulate cellular apoptosis *via* mTOR pathway (Abedi et al., 2021), hsa-miR-145-3p could regulate SARS-CoV-2 *via* interfering with SMAD3 levels and can also target 5' end of the Ebola virus genome (Golkar et al., 2016) and hsa-582-5p could target ACE-2 which is an important receptor of SARS-CoV-2 (Kim et al., 2020). Comparative analysis of miRNAs targeting all the forward and reverse genomic sequences led us to the identification of hsa-miR-4502 as a miRNA common in all the forward genomic sequences of SARS, SARS-CoV-2, and its mutants. Since these miRNAs are encoded by viral genomes, the prediction of a single miRNA in all the forward genomes of SARS-SARS-CoV-2 and its mutants points toward the importance of the putative miRNA. Our results are in

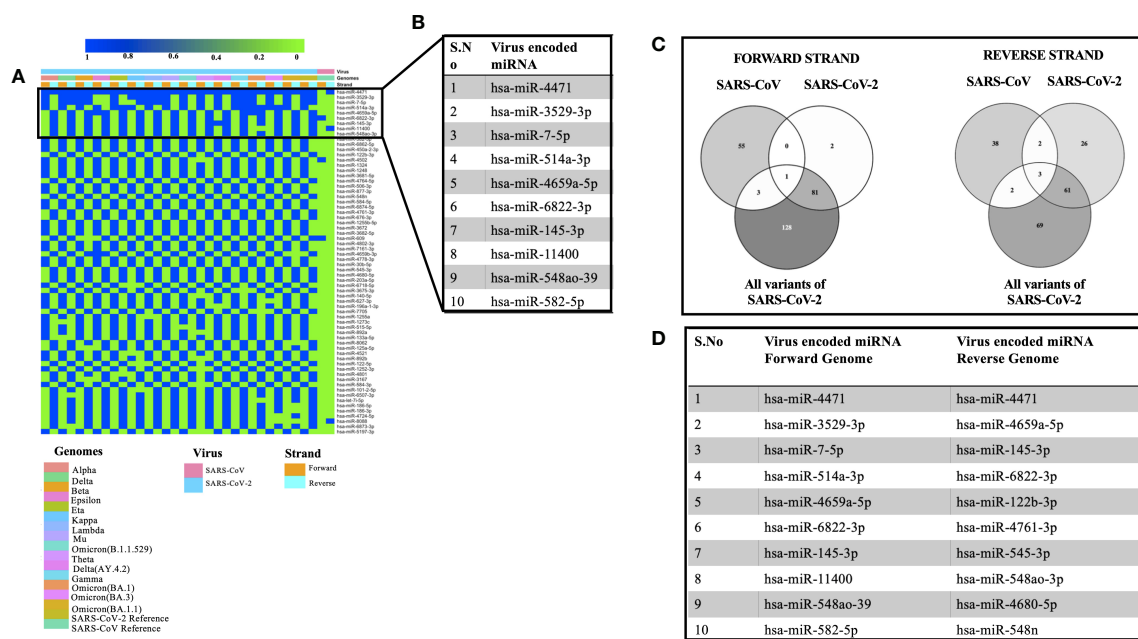


FIGURE 2 Showing the viral encoded miRNAs that had similarity with that of miRNAs encoded by the *H sapiens*. (A) Heatmap showing miRNAs encoded by 45% of the genomes under study. (B) Top 10 miRNAs that could target various genomes used in the study. (C) Common miRNAs among the forward and the reverse genomic sequences of SARS, SARS-CoV-2 and its variants. (D) Top 10 miRNAs targeting forward and the reverse genomes used in the study.

agreement with the previous study that identified similarities among SARS-CoV-2 encoded pre-miRNAs and human encoded hsa-miR-4502 (Aydemir et al., 2021). Analysis of all the reverse genomic sequences of SARS, SARS-CoV-2 and its mutants led us to the identification of three miRNAs (hsa-miR-8088, hsa-miR-11400, hsa-miR-4471) were found common in all reverse sequences (Figure 2C). The presence of these miRNAs in the reverse sequences of all the viral genomes under study points toward their importance in the viral life cycle.

Then we compared the miRNAs targeting forward and reverse genomes of all the SARS-CoV-2 variants used in the study (Figure 2D). It was observed that some of the predicted miRNAs could target cellular host factors thereby facilitating the replication of SARS-CoV-2. Some of the miRNAs targeting forward genomes of SARS-CoV-2 variants included hsa-miR-3672, hsa-miR-7161-5p, hsa-miR-30b-5p and hsa-miR-3682-5p were have been shown to regulate host factors including ICOSLG, G3BP1/P2, CREB1 respectively (Vastrad et al., 2020; Almutairy et al., 2021; Vadivalagan et al., 2022). Analysis of reverse sequences of SARS-CoV-2 mutants revealed that hsa-miR-548 could regulate G3BP1/P2 thereby contributing to viral replication (Almutairy et al., 2021).

Comparison of SARS encoded non-coding RNA sequences with SARS-CoV-2 and its mutants

A recent study had identified SARS encoded non-coding RNAs that contributed towards the pathology of the virus (Morales et al., 2017). In an attempt to understand the pathogenesis of SARS-CoV-2 and its variants, we compared its genomic sequence with that of SARS to estimate the sequence similarity among both the viruses in genomic regions that resulted in non-coding RNAs. We observed a very similar “GA” rich region SARS-CoV-2 including its variants that was reported to be enriched in several SARS encoded non-coding RNAs. This region was found to be highly conserved in all the variants except the omicron variant (BA.1, BA.3, BA.1.1, B.1.1.529) which had a deletion in N-9b domain from position 28038-28047 [Figure 3A (ix)]. Furthermore, comparative analysis for other non-coding RNAs revealed that SARS-CoV-2 also had similar stretches albeit with some nucleotide changes (Figure 3A). Figures 3B, C represents the SARS-CoV-2 variants that were used for the comparison. Interestingly genomic regions of SARS-CoV-2 had more than 85% similarity with SARS encoded scRNA-N whose

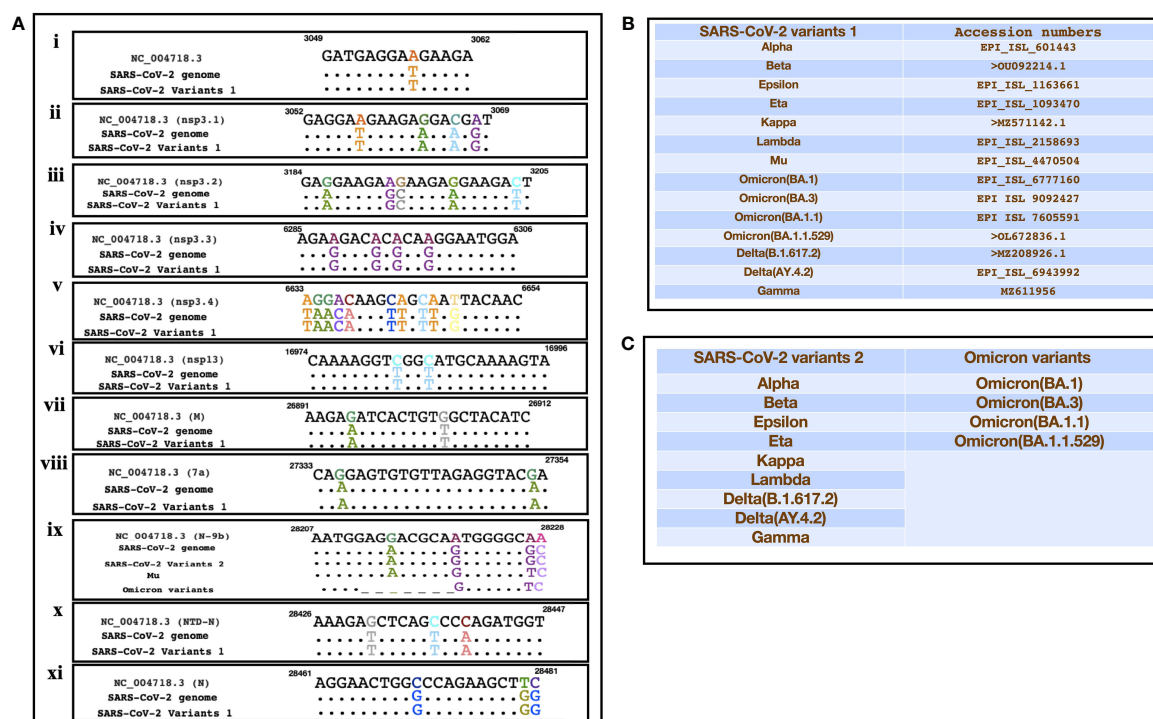


FIGURE 3

Showing the alignment of genomic regions of SARS-CoV-2 and its mutants with those regions of SARS that were shown to produce non-coding RNAs. (A) (i–xi) represents the genomic regions where SARS encoded ncRNAs were identified (Morales et al., 2017). (B, C) Represent the sequences of SARS-CoV-2 variants that were used for the comparison.

inhibition led to a reduction in SARS-induced lung pathology. Apart from scRNA-N, SARS-CoV-2 showed a high degree of similarity (>80-90%) with several SARS encoded non-coding RNAs from regions Nsp3.3, Nsp13, Membrane protein, 7a, N-9b, N-TDN, and Nucleocapsid protein. This high level of similarity among SARS coronavirus encoded non-coding RNAs with that of SARS-CoV-2 genomes suggest that the virus might also encode similar non-coding RNAs that have been shown to contribute towards lung pathology.

Discussion

The recent pandemic of COVID-19 has caused significant mortality around the world. Since its origin in Wuhan, China SARS-CoV-2 has been able to spread throughout the world in a very short duration. The efforts of the scientific community to design effective drugs against the virus are hindered by the emergence of SARS-CoV-2 mutants. The virus has evolved into more than sixteen lineages in a very short span of time. Therefore, understanding the evolution of the virus is of utmost importance. Scientists are racing against the time to find an effective cure for the virus. Apart from regulating vital cellular processes (Andergassen and Rinn, 2022), non-coding RNA has been shown to regulate viral pathogenesis (Liu et al., 2019) and they act as a negative regulator and inhibit antiviral responses (Kesheh et al., 2022). It has also been stipulated that the SARS-CoV-2 genome has sequence similarity with the host non-coding RNAs thereby resulting in the possible epigenetic crosstalk among the virus and its host (Talotta et al., 2022). lncRNAs that were found to be functionally linked and implicated in the innate immune response are upregulated as a result of SARS-CoV-2 infection (Enguita et al., 2022). They were found to alter the host's immune response (Paul et al., 2022). Therefore, the present study was designed to understand the dynamics of non-coding RNA among SARS, SARS-CoV-2, and its mutants. We used a suite of highly popular algorithms to identify host and viral encoded miRNAs that might affect viral replication in host cells. Owing to the significant similarity of SARS-CoV-2 with that of SARS, we sought to leverage the knowledge generated on SARS genomic sequences and apply it to SARS-CoV-2 and its mutant sequences to identify possible overlaps among both the viruses as well as understand ncRNA dynamics as the virus evolves. We compared several SARS-CoV-2 viral genomic sequences and their mutants with that of the SARS reference sequence in order to understand how they might be targeted by host-encoded miRNAs. Interestingly our data suggested that SARS-CoV-2 genomic sequences were targeted by significantly more numbers of host-encoded miRNAs as compared to the SARS reference genome. This might provide a possible explanation as to why the virus causes mild disease in healthy individuals. Moreover, our

comparative analysis of our candidates with that of other published candidates led to the identification of ten host-encoded miRNAs that were identified in many studies. Further wet lab validations are required for the proper validation of these potential candidates. These viral encoded miRNAs have been shown to arrest the transition of phases in cell cycle by preventing the replication of specific genes thereby contributing towards the viral replication. For instance, Let-7c-3p which is one of the top ten miRNAs from our study has been shown to be associated with SARS-CoV-2 infection and pathogenesis (Jafarinejad-Farsangi et al., 2020).

Viruses are known to encode miRNAs to dampen the host responses. We utilized a suite of algorithms to identify possible stem-loop structures in viral genomes which could have the potential to be converted into viral encoded miRNAs. Our tools successfully identified several virus-encoded miRNAs that had significant similarities with host miRNAs. Viral encoded miRNAs having very similar sequences to host-encoded miRNAs might be an excellent strategy to regulate cell signaling pathways. Though we identified several miRNAs encoded by SARS and SARS-CoV-2, despite the high degree of genomic similarity among SARS and SARS-CoV-2, we could not identify common miRNAs among both of them.

Recently, SARS-encoded non-coding RNAs were identified in the lungs of infected mice. These non-coding RNAs were distributed along the entire viral genome and antagomir-based inhibition of these viral encoded RNAs resulted in reduced lung pathology. This data indicate an important role of these viral encoded RNAs during viral pathogenesis. Therefore, we aligned all the SARS-CoV-2 and mutant genomic sequences with the SARS reference genome to investigate whether non-coding RNA sequences among both the viruses are conserved or not. We observed that there was a very similar "GA" rich region in all SARS-CoV-2 genomes including the mutants, that was identified as a part of SARS encoded non-coding RNAs. We also found a very high similarity among SARS encoded non-coding RNAs and all SARS-CoV-2 and mutant genomic sequences suggesting a possible role of these non-coding RNAs in SARS-CoV-2 pathogenesis.

To conclude, we have identified potential host encoded miRNAs that could target genomic sequences of SARS, SARS-CoV-2 and its mutants. We have also identified virus-encoded non-coding RNAs that might modulate the pathogenesis of SARS-CoV-2 thereby identifying new molecular targets against the virus.

Data availability statement

The original contributions presented in the study are included in the article/[Supplementary Material](#). Further inquiries can be directed to the corresponding author.

Author contributions

VS and PA conceived the idea, designed the experiments, supervised the study wrote and finalized the manuscript. NP, UB, and SS performed the analysis. All authors contributed to the article and approved the submitted version.

Funding

NP is supported by UGC fellowship. VS is supported by UGC under FRP programme. The study was funded by startup grant to VS by UGS and DST PURSE grant.

Acknowledgments

We are thankful to all those scientists who contributed to SARS-CoV-2 genomic sequences.

References

- Abedi, F., Rezaee, R., Hayes, A.W., Nasiripour, S., and Karimi, G. (2021). MicroRNAs and SARS-CoV-2 life cycle, pathogenesis, and mutations: biomarkers or therapeutic agents? *Cell Cycle* 20, 143–153. doi: 10.1080/15384101.2020.1867792
- Ahmed, J. Q., Maulud, S. Q., Dhawan, M., Priyanka, , Choudhary, P. O., Jalal, J. P., et al. (2022). MicroRNAs in the development of potential therapeutic targets against COVID-19: A narrative review. *J. Infection Public Health* 15 (7), 788–799. doi: 10.1016/j.jiph.2022.06.012
- Almutairy, B. K., Alshetali, A., and Anwer Khalid, M. N. A. (2021). In silico identification of MicroRNAs targeting the key nucleator of stress granules, G3BP: Promising therapeutics for SARS-CoV-2 infection. *Saudi J. Biol. Sci.* 28, 7499–7504. doi: 10.1016/j.sjbs.2021.08.056
- Andergassen, D., and Rinn, J. L. (2022). From genotype to phenotype: genetics of mammalian long non-coding RNAs in vivo. *Nat. Rev. Genet.* 23, 229–243. doi: 10.1038/s41576-021-00427-8
- Arghiani, N., Nissán, T., and Matin, M. M. (2021). Role of microRNAs in COVID-19 with implications for therapeutics. *Biomed. Pharmacother.* 144, 112247. doi: 10.1016/j.biopha.2021.112247
- Aydemir, M. N., Aydemir, H. B., Korkmaz, E. M., Budak, M., Cekin, N., Pinarbasi, E., et al. (2021). Computationally predicted SARS-COV-2 encoded microRNAs target NFKB, JAK/STAT and TGFB signaling pathways. *Gene Rep.* 22, 101012. doi: 10.1016/j.genrep.2020.101012
- Bellae Papannarao, J., Schwenke, D. O., Manning, P., Manning, P., and Katare, R. (2022). Upregulated miR-200c is associated with downregulation of the functional receptor for severe acute respiratory syndrome coronavirus 2 ACE2 in individuals with obesity. *Int. J. Obes.* 46, 238–241. doi: 10.1038/s41366-021-00984-2
- Bennasser, Y., Le, S.-Y., Yeung, M. L., and Jeang, K. T. (2004). HIV-1 encoded candidate micro-RNAs and their cellular targets. *Retrovirology* 1, 1–5. doi: 10.1186/1742-4690-1-43
- Bernier, A., and Sagan, S. M. (2018). The diverse roles of microRNAs at the host–virus interface. *Viruses* 10, 440. doi: 10.3390/v10080440
- Boehm, E., Kronig, I., Neher, R. A., Isabella, E., Vetter, P., Kaiser, L., et al. (2021). Novel SARS-CoV-2 variants: The pandemics within the pandemic. *Clin. Microbiol. Infection* 27, 1109–1117. doi: 10.1016/j.cmi.2021.05.022
- Bolisetty, M. T., Dy, G., Tam, W., and Beemon, K. L. (2009). Reticuloendotheliosis virus strain T induces miR-155, which targets JARID2 and promotes cell survival. *J. Virol.* 83, 12009–12017. doi: 10.1128/JVI.01182-09
- Briser, J. R., Ako-Adjei, D., Bao, Y., and Blinkova, O. (2015). NCBI viral genomes resource. *Nucleic Acids Res.* 43, D571–D577. doi: 10.1093/nar/gku1207
- Bruscella, P., Bottini, S., Baudesson, C., Pawlotsky, J. M., Feray, C., and Trabucchi, M. (2017). Viruses and miRNAs: more friends than foes. *Front. Microbiol.* 8, 824. doi: 10.3389/fmicb.2017.00824
- Chen, Y., and Wang, X. (2020). miRDB: an online database for prediction of functional microRNA targets. *Nucleic Acids Res.* 48, D127–D131. doi: 10.1093/nar/gkz757
- Chen, L., and Zhong, L. (2020). Genomics functional analysis and drug screening of SARS-CoV-2. *Genes Dis.* 7, 542–550. doi: 10.1016/j.gendis.2020.04.002
- Duchaine, T. F., and Fabian, M. R. (2019). Mechanistic insights into microRNA-mediated gene silencing. *Cold Spring Harbor Perspect. Biol.* 11, a032771. doi: 10.1101/cshperspect.a032771
- Enguita, F. J., Leitão, A. L., McDonald, J. T., Zaksas, V., Das, S., Galeano, D., et al. (2022). The interplay between lncRNAs, RNA-binding proteins and viral genome during SARS-CoV-2 infection reveals strong connections with regulatory events involved in RNA metabolism and immune response. *Theranostics* 12, 3946. doi: 10.7150/thno.73268
- Fani, M., Zandi, M., Ebrahimi, S., Soltani, S., and Abbasi, S. (2021). The role of miRNAs in COVID-19 disease. *Future Virol.* 16, 301–306. doi: 10.2217/fvl-2020-0389
- Golkar, Z., Battaria, R., Pace, D. G., and Bagasra, O. (2016). Inhibition of Ebola virus by anti-Ebola miRNAs in silico. *J. Infection Developing Countries* 10, 626–634. doi: 10.3855/jidc.7127
- Hassan, M., McLean, E., and Bagasra, O. (2016). A computational analysis to construct a potential post-exposure therapy against pox epidemic using miRNAs in silico. *J. Bioterror Biodef.* 7:140. doi: 10.4172/2157-2526.1000140
- Hosseini Rad, S. M. A., and McLellan, A. D. (2020). Implications of SARS-CoV-2 mutations for genomic RNA structure and host microRNA targeting. *Int. J. Mol. Sci.* 21, 4807. doi: 10.3390/ijms21134807
- Hussain, M., and Asgari, S. (2014). MicroRNA-like viral small RNA from dengue virus 2 autoregulates its replication in mosquito cells. *Proc. Natl. Acad. Sci.* 111, 2746–2751. doi: 10.1073/pnas.1320123111
- Hussain, M., Torres, S., Schnettler, E., Funk, A., Grundhoff, A., Pijlman, G. P., et al. (2012). West Nile Virus encodes a microRNA-like small RNA in the 3' untranslated region which up-regulates GATA4 mRNA and facilitates virus replication in mosquito cells. *Nucleic Acids Res.* 40, 2210–2223. doi: 10.1093/nar/gkr848

Conflict of interest

The authors declare that the research was conducted in the absence of any commercial or financial relationships that could be construed as a potential conflict of interest.

Publisher's note

All claims expressed in this article are solely those of the authors and do not necessarily represent those of their affiliated organizations, or those of the publisher, the editors and the reviewers. Any product that may be evaluated in this article, or claim that may be made by its manufacturer, is not guaranteed or endorsed by the publisher.

Supplementary material

The Supplementary Material for this article can be found online at: <https://www.frontiersin.org/articles/10.3389/fcimb.2022.966870/full#supplementary-material>

- Jafarinejad-Farsangi, S., Jazi, M. M., Rostamzadeh, F., and Hadizadeh, M. (2020). High affinity of host human microRNAs to SARS-CoV-2 genome: An in silico analysis. *Non-coding RNA Res.* 5, 222–231. doi: 10.1016/j.ncrna.2020.11.005
- Jiang, J., Lee, E. J., and Schmittgen, T. D. (2006). Increased expression of microRNA-155 in Epstein-Barr virus transformed lymphoblastoid cell lines. *Genes Chromosomes Cancer* 45, 103–106. doi: 10.1002/gcc.20264
- Kaur, T., Kapila, S., Kapila, R., Upadhyay, D., Kaur, M., Sharma, C., et al. (2021). Tmprss2 specific miRNAs as promising regulators for SARS-CoV-2 entry checkpoint. *Virus Res.* 294, 198275. doi: 10.1016/j.virusres.2020.198275
- Kesheh, M. M., Mahmoudvand, S., and Shokri, S. (2022). Long noncoding RNAs in respiratory viruses: A review. *Rev. Med. Virol.* 32, e2275. doi: 10.1002/rmv.2275
- Khare, S., Gurry, C., Freitas, L., Schultz, M. B., Bach, G., Diallo, A., et al. (2021). GISAID's role in pandemic response. *China CDC Weekly* 3, 1049. doi: 10.46234/ccdcw2021.255
- Kim, W. R., Park, E. G., Kang, K.-W., Lee, S. M., Kim, B., Kim, H. S., et al. (2020). Expression analyses of microRNAs in hamster lung tissues infected by SARS-CoV-2. *Molecules Cells* 43, 953. doi: 10.14348/molcells.2020.0177
- Klaver, B., and Berkhout, B. (1994). Evolution of a disrupted TAR RNA hairpin structure in the HIV-1 virus. *EMBO J.* 13, 2650–2659. doi: 10.1002/j.1460-2075.1994.tb06555.x
- Korber, B., Fischer, W. M., Gnanakaran, S., Yoon, H., Theiler, J., Abfalterer, W., et al. (2020). Tracking changes in SARS-CoV-2 spike: evidence that D614G increases infectivity of the COVID-19 virus. *Cell* 182, 812–827. doi: 10.1016/j.cell.2020.06.043
- Kozomara, A., Birgaoanu, M., and Griffiths-Jones, S. (2019). miRBase: From microRNA sequences to function. *Nucleic Acids Res.* 47, D155–D162. doi: 10.1093/nar/gky1141
- Kucher, A., Koroleva, I. A., Zarubin, A., and Nazarenko, M. S. (2022). MicroRNAs as the potential regulators of SARS-CoV-2 infection and modifiers of the COVID-19 clinical features. *Mol. Biol.* 56, 29–45. doi: 10.1134/S0026893322010034
- Lei, X., Zhu, Y., Jones, T., Bai, Z., Huang, Y., Gao, S. J., et al. (2012). A kaposi's sarcoma-associated herpesvirus microRNA and its variants target the transforming growth factor β pathway to promote cell survival. *J. Virol.* 86, 11698–11711. doi: 10.1128/JVI.06855-11
- Li, L., Feng, H., Da, Q., Jiang, H., Chen, L., Xie, L., et al. (2016). Expression of HIV-encoded microRNA-TAR and its inhibitory effect on viral replication in human primary macrophages. *Arch. Virol.* 161, 1115–1123. doi: 10.1007/s00705-016-2755-5
- Li, X., Fu, Z., Liang, H., Wang, Y., Qi, X., Ding, M., et al. (2018). H5N1 influenza virus-specific miRNA-like small RNA increases cytokine production and mouse mortality via targeting poly (rC)-binding protein 2. *Cell Res.* 28, 157–171. doi: 10.1038/cr.2018.3
- Li, K., Shen, L., Zheng, P., Wang, Y., Wang, L., Meng, X., et al. (2022). Identification of MicroRNAs as potential biomarkers for detecting ischemic stroke. *Genes Genomics* 44, 9–17. doi: 10.1007/s13258-021-01060-9
- Liu, S., Liu, X., Li, J., Zhou, H., Carr, M. J., Zhang, Z., et al. (2019). Long noncoding RNAs: novel regulators of virus-host interactions. *Rev. Med. Virol.* 29, e2046. doi: 10.1002/rmv.2046
- Liu, W., and Wang, X. (2019). Prediction of functional microRNA targets by integrative modeling of microRNA binding and target expression data. *Genome Biol.* 20, 1–10. doi: 10.1186/s13059-019-1629-z
- Li, X., and Zou, X. (2019). An overview of RNA virus-encoded microRNAs. *ExRNA* 1, 1–5. doi: 10.1186/s41544-019-0037-6
- Marchi, R., Sugita, B., Centa, A., Fonseca, A. S., Bortoletto, S., Fiorentin, K., et al. (2021). The role of microRNAs in modulating SARS-CoV-2 infection in human cells: a systematic review. *Infection Genet. Evol.* 91, 104832. doi: 10.1016/j.meegid.2021.104832
- Mishra, R., Kumar, A., Ingle, H., and Kumar, H. (2020). The interplay between viral-derived miRNAs and host immunity during infection. *Front. Immunol.* 10, 3079. doi: 10.3389/fimmu.2019.03079
- Morales, L., Oliveros, J. C., Enjuanes, L., and Sola, I. (2022). Contribution of host miRNA-223-3p to SARS-CoV-2-induced lung inflammatory pathology. *Mbio* 13, e03135-21. doi: 10.1128/mbio.03135-21
- Morales, L., Oliveros, J. C., Fernandez-Delgado, R., Robert tenOever, B., Enjuanes, L., Sola, I., et al. (2017). SARS-CoV-2-encoded small RNAs contribute to infection-associated lung pathology. *Cell Host Microbe* 21, 344–355. doi: 10.1016/j.chom.2017.01.015
- Mosharaf, M., Reza, M., Kibria, M., Ahmed, F.F., Kabir, M.H., Hasan, S., et al. (2022). Computational identification of host genomic biomarkers highlighting their functions, pathways and regulators that influence SARS-CoV-2 infections and drug repurposing. *Sci. Rep.* 12, 1–22. doi: 10.1038/s41598-022-08073-8
- Natekar, J. P., Rothan, H. A., Arora, K., Strate, P.G., and Kumar, M. (2019). Cellular microRNA-155 regulates virus-induced inflammatory response and protects against lethal West Nile virus infection. *Viruses* 12, 9. doi: 10.3390/v12010009
- Panda, M., Kalita, E., Singh, S., Kumar, K., Roa, A., Prajapati, V. K., et al. (2022). MiRNA-SARS-CoV-2 dialogue and prospective anti-COVID-19 therapies. *Life Sci.* 305, 120761. doi: 10.1016/j.lfs.2022.120761
- Pareek, S., Roy, S., Kumari, B., Jain, P., Banerjee, A., Vrtati, S., et al. (2014). MiR-155 induction in microglial cells suppresses Japanese encephalitis virus replication and negatively modulates innate immune responses. *J. Neuroinflamm.* 11, 1–13. doi: 10.1186/1742-2094-11-97
- Paul, S., Vázquez, L. A. B., Reyes-Pérez, P. R., Estrada-Meza, C., Albuquerque, R. A. A., Pathak, S., et al. (2022). The role of microRNAs in solving COVID-19 puzzle from infection to therapeutics: A mini-review. *Virus Res.* 308, 198631. doi: 10.1016/j.virusres.2021.198631
- Pedersen, I. M., Cheng, G., Wieland, S., Volinia, S., Croce, C.M., Chisari, F.V., et al. (2007). Interferon modulation of cellular microRNAs as an antiviral mechanism. *Nature* 449, 919–922. doi: 10.1038/nature06205
- Prasad, A. N., Ronk, A. J., Widen, S. G., Wood, T.G., Basler, C.F., Bukreyev, A., et al. (2020). Ebola Virus produces discrete small noncoding RNAs independently of the host microRNA pathway which lack RNA interference activity in bat and human cells. *J. Virol.* 94, e01441–e01441. doi: 10.1128/JVI.01441-19
- Samy, A., Maher, M. A., Abdelsalam, N. A., and Badr, E. (2022). SARS-CoV-2 potential drugs, drug targets, and biomarkers: a viral-host interaction network-based analysis. *Sci. Rep.* 12, 1–14. doi: 10.1038/s41598-022-15898-w
- Sevgin, O., and Sevgin, K. (2021). Systematic review of microRNAs in the SARS-CoV-2 infection: Are microRNAs potential therapy for COVID-19. *J. Genet. Genome Res.* 8, 053. doi: 10.23937/2378-3648/1410053
- Shirvani, H., Jafari, H., Moravveji, S. S., Faranghizadeh, F. A., Talebi, M., Ghanavi, J., et al. (2022). Non-coding RNA in SARS-CoV-2: Progress toward therapeutic significance. *Int. J. Biol. Macromolecules* 222 (Pt A):1538–1550. doi: 10.1016/j.ijbiomac.2022.09.105
- Sievers, F., Wilm, A., Dineen, D., Gibson, T.J., Karplus, K., Li, W., et al. (2011). Fast, scalable generation of high-quality protein multiple sequence alignments using clustal omega. *Mol. Syst. Biol.* 7, 539. doi: 10.1038/msb.2011.75
- Song, Z., Xu, Y., Bao, L., Zhang, L., Pin, Y., Yajin, Q., et al. (2019). From SARS to MERS, thrusting coronaviruses into the spotlight. *viruses* 11, 59. doi: 10.3390/v11010059
- Su, Y., Huang, Y., Wu, Y., Chen, H. F., Wu, Y. H., Hsu, C. C., et al. (2020). MicroRNA-155 inhibits dengue virus replication by inducing heme oxygenase-1-mediated antiviral interferon responses. *FASEB J.* 34, 7283–7294. doi: 10.1096/fj.201902878R
- Swaminathan, G., Rossi, F., Sierra, L.-J., Gupta, A., Navas-Martin, S., Martin-Garcia, J., et al. (2012). A role for microRNA-155 modulation in the anti-HIV-1 effects of toll-like receptor 3 stimulation in macrophages. *PLoS Pathog.* 8 (9), e1002937. doi: 10.1371/journal.ppat.1002937
- Talotta, R., Bahrami, S., and Laska, M. J. (2022). Sequence complementarity between human noncoding RNAs and SARS-CoV-2 genes: What are the implications for human health? *Biochim. Biophys. Acta (BBA)-Molecular Basis Dis.* 1868, 166291. doi: 10.1016/j.bbdis.2021.166291
- Tegally, H., Wilkinson, E., Lessells, R. J., Giandhari, J., Pillay, S., Msomi, N., et al. (2021). Sixteen novel lineages of SARS-CoV-2 in south Africa. *Nat. Med.* 27, 440–446. doi: 10.1038/s41591-021-01255-3
- Tempel, S., and Tahii, F. (2012). A fast ab-initio method for predicting miRNA precursors in genomes. *Nucleic Acids Res.* 40, e80–e80. doi: 10.1093/nar/gks146
- Tran, V. D., Tempel, S., Zerath, B., Zehraoui, F., and Tahii, F. (2015). miRBoost: boosting support vector machines for microRNA precursor classification. *RNA* 21, 775–785. doi: 10.1261/rna.043612.113
- Coronaviridae Study Group of the International Committee on Taxonomy of Viruses (2020). The species Severe acute respiratory syndrome-related coronavirus: Classifying 2019-nCoV and naming it SARS-CoV-2. *Nat. Microbiol.* 5, 536–544. doi: 10.1038/s41564-020-0695-z
- Thounaojam, M. C., Kundu, K., Kaushik, D. K., Swaroop, S., Mahadevan, A., Shankar, S.K., et al. (2014). MicroRNA 155 regulates Japanese encephalitis virus-induced inflammatory response by targeting src homology 2-containing inositol phosphatase 1. *J. Virol.* 88, 4798–4810. doi: 10.1128/JVI.02979-13
- Vadivalagan, C., Shitut, A., Kamalakannan, S., Chen, R.M., Serrano-Aroca, A., Mishra, V., et al. (2022). Exosomal mediated signal transduction through artificial microRNA (amiRNA): A potential target for inhibition of SARS-CoV-2. *Cell. Signalling* 95, 110334. doi: 10.1016/j.cellsig.2022.110334
- Van Laar, R., Lincoln, M., and Van Laar, B. (2018). Development and validation of a plasma-based melanoma biomarker suitable for clinical use. *Br. J. Cancer* 118, 857–866. doi: 10.1038/bjc.2017.477
- Vastrad, B., Vastrad, C., and Tengli, A. (2020). Identification of potential mRNA panels for severe acute respiratory syndrome coronavirus 2 (COVID-19) diagnosis and treatment using microarray dataset and bioinformatics methods. *3 Biotech.* 10, 1–65. doi: 10.1007/s13205-020-02406-y

- Volz, E., Mishra, S., Chand, M., Johnson, R., Geidelberg, L., Hinsley, W.R., et al. (2021). Assessing transmissibility of SARS-CoV-2 lineage b. 1.1.7 *England Nat.* 593, 266–269. doi: 10.1038/s41586-021-03470-x
- Wang, Z., Li, K., Wang, X., Huang, W., et al. (2019). MiR-155-5p modulates HSV-1 replication via the epigenetic regulation of SRSF2 gene expression. *Epigenetics* 14, 494–503. doi: 10.1080/15592294.2019.1600388
- Yang, C. -Y., Chen, Y. -H., Liu, P. -J., Hu, W. -C., and Tsai, K. W. (2022). The emerging role of miRNAs in the pathogenesis of COVID-19: Protective effects of nutraceutical polyphenolic compounds against SARS-CoV-2 infection. *Int. J. Med. Sci.* 19, 1340. doi: 10.7150/ijms.76168
- Ying, H., Ebrahimi, M., Keivan, M., Khoshnam, S. E., Salahi, S., Farzaneh, M., et al. (2021). miRNAs; a novel strategy for the treatment of COVID-19. *Cell Biol. Int.* 45, 2045–2053. doi: 10.1002/cbin.11653
- Yousefi, H., Poursheikhani, A., Bahmanpour, Z., Vatanmakanian, M., Taheri, M., Mashouri, L., et al. (2020). SARS-CoV infection crosstalk with human host cell noncoding-RNA machinery: An in-silico approach. *Biomed. Pharmacother.* 130, 110548. doi: 10.1016/j.biopha.2020.110548
- Zeng, Q., Qi, X., Ma, J., Hu, F., Wang, X., Qin, H., et al. (2022). Distinct miRNAs associated with various clinical presentations of SARS-CoV-2 infection. *Iscience* 25, 104309. doi: 10.1016/j.isci.2022.104309
- Zhang, S., Amahong, K., Sun, X., Lian, X., Liu, J., Sun, H., et al. (2021). The miRNA: a small but powerful RNA for COVID-19. *Briefings Bioinf.* 22, 1137–1149. doi: 10.1093/bib/bbab062
- Zhang, Y., Fan, M., Geng, G., Liu, B., Huang, Z., Luo, H., et al. (2014). A novel HIV-1-encoded microRNA enhances its viral replication by targeting the TATA box region. *Retrovirology* 11, 1–15. doi: 10.1186/1742-4690-11-23
- Zhu, Y., Zhang, Z., Song, J., Qian, W., Gu, X., Yang, C., et al. (2021). SARS-CoV-2-encoded MiRNAs inhibit host type I interferon pathway and mediate allelic differential expression of susceptible gene. *Front. Immunol.* 12. doi: 10.3389/fimmu.2021.767726

Frontiers in Cellular and Infection Microbiology

Investigates how microorganisms interact with their hosts

Explores bacteria, fungi, parasites, viruses, endosymbionts, prions and all microbial pathogens as well as the microbiota and its effect on health and disease in various hosts.

Discover the latest Research Topics

[See more →](#)

Frontiers

Avenue du Tribunal-Fédéral 34
1005 Lausanne, Switzerland
frontiersin.org

Contact us

+41 (0)21 510 17 00
frontiersin.org/about/contact

